POTENCY AND SPECIES SPECIFICITY OF ARYL HYDROCARBON RECEPTOR LIGANDS

Richard J. Wall, BSc. MRes.

Thesis submitted to the University of Nottingham

for the degree of Doctor of Philosophy

July 2012

The University of Nottingham

The Food and Environment Research Agency

FOOD STANDARDS AGENCY

Richard Wall

Abstract

The aryl hydrocarbon receptor (AhR) binds a wide range of structurally diverse compounds such as halogenated dibenzo-*p*-dioxins, dibenzofurans and biphenyls which are abundant in the environment. Activation of AhR leads to the regulation of a battery of xenobiotic enzymes including cytochrome P4501A1 (CYP1A1). The purely chlorinated compounds feature in the World Health Organisation's (WHO) evaluation of dioxin-like compounds derived from a meta-analysis of previous potency data (toxic equivalency factors; TEFs), which is used to calculate the total toxic equivalence (TEQ).

The first aim of this work was to fully characterise the three most environmentally abundant mono-*ortho*-substituted polychlorinated biphenyls (PCBs; PCB 105, 118 and 156) including a re-evaluation of their putative antagonistic effects on AhR. Secondly, the effects of mixed halogenated compounds, currently not included in the TEQ estimation, were investigated as AhR agonists based on their environmental exposure and potency. Quantitative real-time PCR (qRT-PCR) was used to measure the AhR mediated induction of CYP1A1 mRNA in rat H4IIE and human MCF-7 cells. The three mono-*ortho*-substituted PCBs were shown to be antagonists of rat and human AhRs, an effect which is not currently included in the TEQ calculation. 2-bromo-3,7,8-trichlorodibenzo-*p*-dioxin (2-B-3,7,8-TriCDD) was found to be an AhR agonist that was 2-fold more potent than 2,3,7,8-tetrachlorodibenzo-*p*-dioxin (TCDD; considered one of the most potent in the environment). The majority of the other tested compounds were found to be within 10-fold less potent than TCDD and could therefore have a significant impact on the TEQ. A family of putative AhR agonists from AstraZencea were investigated and one of the compounds was shown to be a highly potent AhR agonist, 5-fold more potent than TCDD at inducing CYP1A1.

The results indicate approximately a 15-fold higher sensitivity of the rat cell line to the AhR agonists compared with the human cell line. It is not currently understood what confers these differences whether it is a difference in the mechanism of activation or purely as a result of differences in the AhR sequence. The mechanism of action is thought to be the same in both species and the associated proteins are both comparable. The amino acid sequences of the AhR, in both human and rat are quite similar but may play a significant role in the differences observed between species. Therefore in order to directly compare the rat and human AhRs, two novel cell line models were created using an inducible expression system to infect an AhR-deficient mouse cell line with a replication-defective virus containing either the rat or human AhR. The AhRs were activated with various compounds to induce mouse CYP1A1. The CYP1A1 mRNA was measured using qRT-PCR but showed that the two AhR genes were not expressed enough to produce a response detectable above the background CYP1A1 induction by the low levels of mouse AhR.

This research has shown that these dioxin-like compounds can have very different potencies at AhRs in different species so it is not always possible to predict the potency in humans from *in vitro* or rat *in vivo* toxicity data. Furthermore, it has identified compounds, such as 5F-203, which are significantly more potent in human compared to rat. This thesis provides information on the AhR species differences between human and rat that can be applied to risk assessment.

Acknowledgements

Firstly, I would like to thank Dr. Ian Mellor for his advice, patience and humour, without that I'm not sure I would have survived. I'm sure Ian will be very sad that he no longer has to read through my manuscript drafts, hide in his office when he can see me coming (and at one point changing offices completely), answer simple questions and become an expert in AhR research purely to assist me with my work. For this I am eternally grateful. I would also like to thank Dr. David Bell for accepting me into this PhD and providing me with an interesting project. Despite being in another country, he has still taken the time to answer my questions, give me advice and make corrections.

I would like to thank my FERA supervisors, Dr. Alwyn Fernandes and Dr. Martin Rose. They have been an excellent source of advice, and were very welcoming when I visited FERA or when I have attended conferences with them. Thanks also to Dr. J. Craig Rowlands for his advice and corrections for my manuscripts, and to the FSA for their financial and intellectual support. Thanks also to my two examiners, Dr. Nick Plant and Dr. Ian Duce, for actually allowing me to pass with only a few corrections!

I would like to thank Declan Brady for his technical advice and conversation. He was always available if I had a problem (unless it was Friday night). I would like to thank all of the Bell Lab during my PhD, particularly Himanshu for his molecular biology knowledge, but also: Abeer, Ahmad, Cristina, Fikry, Hamad, Hao, Ning, Vroni, Wail, as well as Archana, Rakesh, Rosie who shared our office. I would also like to thank everyone at the School of Biology especially Mark, who was always around for a chat (or a moan) about life and has over the years, become a very good friend. I'd like to thank the Mellor/Duce Lab, especially young David, and for my office mate Charu, a lovely person and a great laugh (even if she was always late).

I would also like to thank the many fantastic people I have met over the last 4 years; starting at Raleigh Park and finishing at Derby Hall. Without you all... well... I'd still of passed my PhD, probably even done better than I have... but I would not have enjoyed the last few years so much. Thank you for being such great distractions.

Finally, as always, a huge thanks to my parents. They have always been there for me and I am very lucky to have such great family. They have supported me mentally (and sometimes financially) all the way through my earlier studies that allowed me to do this PhD. Thank you so much.

Abbreviations

7-ER	7-Ethoxyresorufin
95% CI	95% Confidence Interval
aā	Amino acid residue
AHH	Aryl Hydrocarbon Hydroxylase (CYP1A1)
AhR	Aryl Hydrocarbon Receptor
AIP	Aryl hydrocarbon receptor interacting protein (see XAP2)
α-NF	Alpha-naphthoflavone
Arnt	Aryl Hydrocarbon Receptor Nuclear Translocator
bHLH	Basic Helix-Loop-Helix
β-NF	Beta-naphthoflavone
BpRc1	Taoc1BP^{r}c1 AhR-defective cell line
cDMEM	Complete Dulbecco's modified Eagle's medium
cDNA	Complementary DNA
cMEM	Complete minimum essential medium
Chr	2-amino-isoflavones
CYP1A1	Cytochrome P450 1A1
CYP1A2	Cytochrome P450 1A2
CYP1B1	Cytochrome P450 1B1
DMSO	Dimethyl Sulfoxide
Dox	Doxycycline
DR-CALUX	Dioxin-Responsive-Chemical Activated LUciferase gene eXpression
DRE	Dioxin Response Element
EC$_{50}$	Concentration that gives 50% of maximal response
EROD	Ethoxyresorufin-O-deethylation
GC/MS	Gas chromatography/Mass spectrometry
H4IIE	Rat liver cell line
HAH	Halogenated aromatic hydrocarbon
HepG2	Human hepatocellular carcinoma cell line
Hepa1c1c7	Mouse hepatoma cell line
Hsp90	90 kDa Heat shock protein
IC$_{50}$	Half maximal inhibitory concentration
K$_d$	Equilibrium dissociation constant
K$_i$	Equilibrium inhibition constant

LBD	Ligand binding domain
Max	Max Speed (centrifuge)
MCF-7	Human breast carcinoma cell line
mRNA	Messenger RNA
MMTV	Mouse mammary tumour virus
MOI	Multiplicity of infection
MoMuLV	Moloney murine leukemia virus
NIH/3T3	mouse embryonic fibroblast cell line
p23	Prostaglandin E synthase 3 (Hsp90 accessory protein)
PAH	Polycyclic Aromatic Hydrocarbon
PAS	Per, Arnt, AhR, Sim
PBS	Dulbecco's phosphate buffered saline
PCB	Polychlorinated biphenyl
PCDD	Polychlorinated dibenzo-p-dioxin
PCDF	Polychlorinated dibenzofuran
PeCDF	2,3,4,7,8- Pentachlorodibenzofuran
Per	Drosophila circadian rhythm protein
PXB	Polyhalogenated biphenyl
PXDD	Polyhalogenated dibenzo-p-dioxin
PXDF	Polyhalogenated dibenzofuran
REP	Relative potency value
RevT	Reverse Transcriptase
RT	Room temperature ($20 - 25^{o}$C; centrifuge)
qRT-PCR	Quantitative Real-Time Polymerase Chain Reaction
Sim	Drosophila neurogenic protein
SYBR	SYBR green
Tc	Tetracycline
TCDD	2,3,7,8-Tetracholordibenzo-p-dioxin
TCDF	2,3,7,8-Tetrachlorodibenzofuran
TEF	Toxic equivalency factor
TEQ	Total toxic equivalency
TRE	Tet-response element
WHO	World Health Organisation
XRE	Xenobiotic Response Element
XAP2	Immunophilin-like associated protein 2 (X-associated protein 2; see AIP)

Table of Contents

List of Figures

List of Tables

List of Equations

1. Introduction

1.1 Activation of the Aryl hydrocarbon receptor (AhR)

1.1.1 Aryl hydrocarbon receptor (AhR)

The aryl hydrocarbon receptor (AhR) is a ligand activated transcription factor (Okey *et al.,* 1994) located in the cytosol first identified by Dr Alan Poland (Poland *et al.,* 1976). Nebert and co-workers first recognised a link between 3-methylchloranthrene (3-MC) and aryl hydrocarbon hydroxylase (AHH) induction (Nebert and Gelboin, 1969). Previous work by Poland and co-workers showed a correlation between some chlorinated dibenzo-*p*-dioxins (PCDDs) and the subsequent induction of AHH, showing that several of the compounds were potent inducers of AHH (Poland and Glover, 1972). The paper also highlighted that 2,3,7,8-tetrachlorodibenzo-*p*-dioxin (TCDD) was the most potent of the compounds tested. Further work showed that TCDD bound to high affinity sites in the cytosol which was later shown to be the AhR (Poland *et al.,* 1976). AHH was subsequently referred to as cytochrome P450 1A1 (CYP1A1).
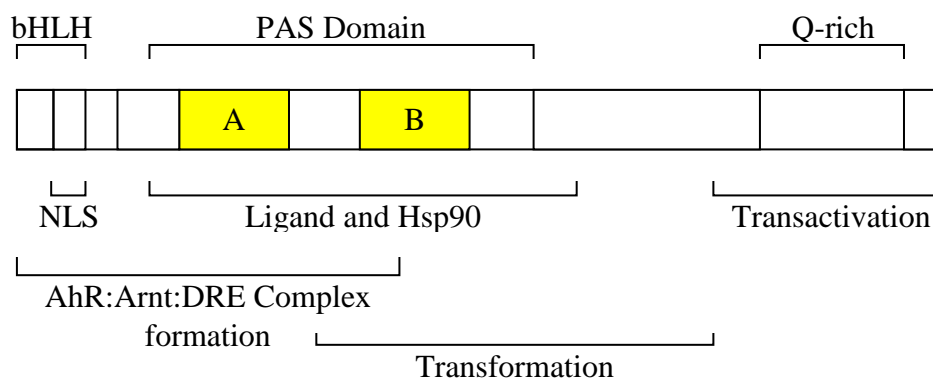
Figure 1.1: Structure of AhR - Adapted model of AhR structure from Denison *et al.* (2002). bHLH: basic helix-loop-helix, NLS: Nuclear localization sequence, PAS: Per-Arnt-Sim; A: Per A; B: Per B, hsp90: heat shock protein-90KDa, AhR: Aryl hydrocarbon receptor, Arnt: Aryl hydrocarbon Receptor Nuclear Translocator, DRE: Dioxin responsive element.

The structure of the AhR, which is shown in Figure 1.1, comprises of a basic-helix-loop-helix domain (bHLH) located at the n-terminus of the protein. This is followed by the Per-Arnt-

Sim protein domain (PAS). The PAS domain is made up of three protein domains, known as Per (period circadian protein), Arnt (aryl hydrocarbon receptor nuclear translocator protein) and Sim (single-minded protein). A protein domain is a part of a protein sequence that can form and fold independently of the main protein sequence. The three domains which make up PAS have been individually identified in a variety of other proteins in several different organisms but together they function as a RedOx signal sensor (Taylor and Zhulin, 1999). AhR is part of the (bHLH/PAS) family of transcription factors (Gu *et al.,* 2000). The bHLH and PAS domains are associated with ligand binding, binding to the chaperone proteins and formation of the transcription binding complex with Aryl hydrocarbon Receptor Nuclear Translocator (Arnt).

	Rat	Human	Mouse
Chromosome location	6q16	7p15	12a3
mRNA length	2538 bp	2547 bp	2418 bp
Amino acid length	845 aā	848 aā	805 aā
Location of LBD	234 – 401 aā[2]	236 – 403 aā[2]	230 – 397 aā[1]

Table 1.1: Comparison of the three AhR proteins of rat, human and mouse – Data was taken from the NCBI website (www.ncbi.nlm.nih.gov), accessed on 28/06/2012. [1]location based on research by Fukunaga *et al.,* 1995. [2]Theroetical position based on comparison with the mouse AhR LBD location. aā: amino acid residue (stop codon not included).

Table 1.1 shows some of the basic comparisons between rat, human and mouse AhR proteins (a more detailed AhR comparison is shown in section 1.1.2 and comparison of the homology of AhR and its chaperone proteins is shown in Table 4.6). The data shows that all of the proteins are similar size with binding domains in similar locations demonstrating the high homology between the three species. In rats, the AhR has been found in most tissues with the highest concentrations found in the thymus, liver, lung and kidney (Carlstedt-Duke, 1979; Carver *et al.,* 1994a). In humans, high concentrations of AhR can be found in the placenta, lung, spleen and heart, with limited levels in liver, pancreas and kidney (Dolwick *et al.,* 1993;

Yamamoto *et al.,* 2004). The AhR has been found in a wide range of mammalian and non-mammalian species and is highly conserved (section 1.1.2; Reviewed by Hahn, 1998). Several attempts have been made to ascertain the structure of the AhR ligand binding domain (LBD) either practically (Helaly, 2011), with limited success, by computer modelling of the binding domain (Bisson *et al.,* 2009; Denison *et al.,* 2002; Jacobs *et al.,* 2003; Pandini *et al.,* 2007; Procopio *et al.,* 2002) or by ligand binding prediction studies (Lo Piparo *et al.,* 2006; Petkov *et al.,* 2010; Waller and McKinney, 1995) to estimate binding affinity and/or efficacy of compounds based on their structure. Helaly (2011) attempted to express the *Caenorhabditis elegans* (*C. elegans)* AhR LBD in several expression systems such as yeast and bacteria, but was either unable to obtain enough protein in its ligand-bound form or produced soluble protein yields too low for structural studies. Lo Piparo *et al.* (2006) did a virtual screening to predict AhR binding and produced a model, based on the dibenzo-*p*-dioxin structure, of which parts of the ligand are important for receptor binding. They wrongly identified 2,3,7-tribromodibenzo-*p*-dioxin as the most toxic compound, as the experimental data set was based on binding affinity not actual potency. However the model did show that positions 4, 6 and 7 had an important role in the potency of the compound (Figure 1.2A). They also showed that the dibenzo-*p*-dioxin structure of TCDD was strongly related to the toxicity of the compound. The mouse AhR LBD has been identified as located approximately between amino acid residues 230-421 (Coumailleau *et al.,* 1995) or 230-397 (Fukunaga *et al.,* 1995) which is just less than 25% of the total size of the AhR protein (Coumailleau *et al.,* 1995). Denison *et al.* (2002) and Procopio *et al.* (2002) developed theoretical models of the mouse AhR LBD based on the structures of other proteins belonging to the PAS family. This theoretical mouse AhR LBD is shown in Figure 1.2B (Denison *et al.,* 2002).
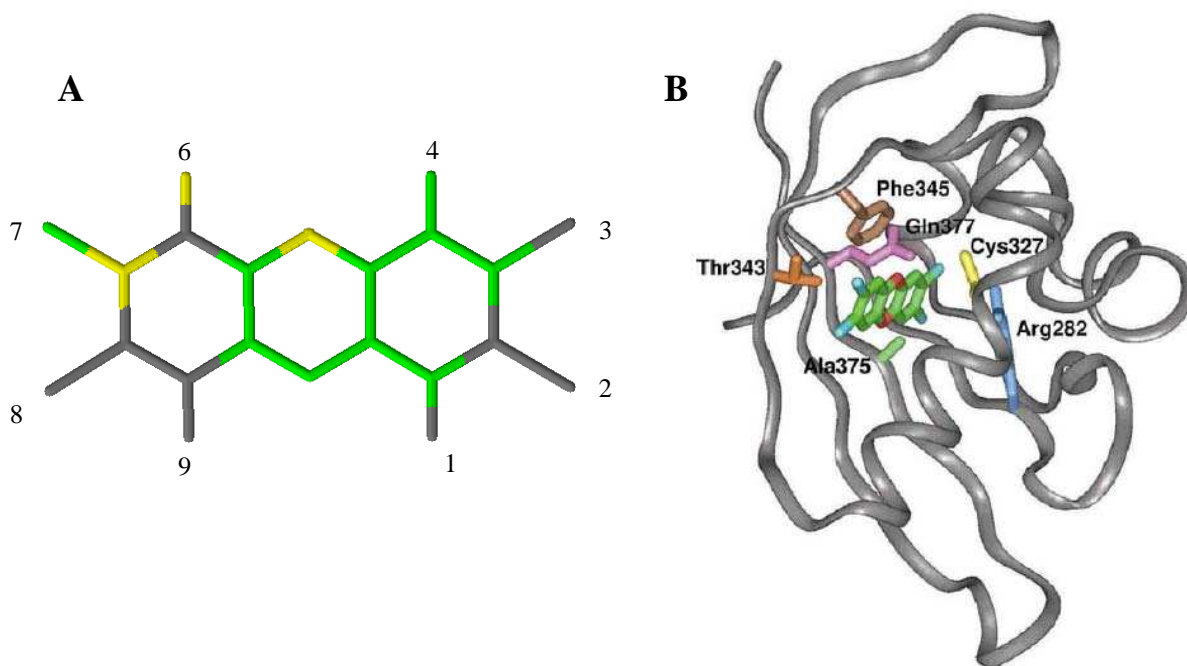
Figure 1.2: Computer generated prediction of ligand interaction and the AhR – (A) The putative individual contributions of one of the more toxic compounds, 2,3,7-tribromodibenzo-*p*-dioxin. Simplified figure taken from Lo Piparo *et al.* (2006). The colours at the red end of the spectrum reflect poor contributions whereas those at the green end (yellow, green-blue, and green) reflect favourable contributions (grey has no effect). (B) The predicted LBD of mouse AhR (with TCDD interaction) based on the structures of various PAS related proteins taken directly from Denison *et al.* (2002).

The AhR has been shown to exist in ancient *invertebrate* evolution demonstrating its importance for the immune system, further established by its effect on the liver and immunity when removed from the animal system (Fernandez-Salguervo *et al.,* 1995; Hahn *et al.,* 1997; Schmidt *et al.,* 1996).

1.1.2 Species differences in the AhR

Ligands tend to interact with the AhR in the same way regardless of the species with only a few exceptions. The most significant difference is the level of potency of a ligand between species. For example, previous research has shown that most compounds are significantly more potent at activating rat AhR than human AhR (Budinsky *et al.,* 2010; Silkworth *et al.,* 2005; Xu *et al.,* 2000), with the exception of a few atypical compounds (Bazzi *et al.,* 2009, Bucklund and Ingelman-Sundberg, 2004).

```
                                      Basic helix-loop-helix
Rat    M  SSGANITYASRKRRKPVQKTVKPVPAEGIKSNPSKRHRDRLNTEL
Mouse  M  SSGANITYASRKRRKPVQKTVKPIPAEGIKSNPSKRHRDRLNTEL
Human  MN SSANITYASRKRRKPVQKTVKPIPAEGIKSNPSKRHRDRLNTEL

DRLASLLPFPQDVINKLDKLSVLRLSVTYLRAKSFFDVALKSTPADRSRGQD
DRLASLLPFPQDVINKLDKLSVLRLSVSYLRAKSFFDVALKSTPADRNGGQD
DRLASLLPFPQDVINKLDKLSVLRLSVSYLRAKSFFDVALKSSPTERNGGQD

QCRAQV RDWQDLQEGEFLLQALNGFVLVVTADALVFYASSTIQDYLGFQQS
QCRAQI RDWQDLQEGEFLLQALNGFVLVVTADALVFYASSTIQDYLGFQQS
NCRAANFREGLNLQEGEFLLQALNGFVLVVTTDALVFYASSTIQDYLGFQQS

                              PAS A
DVIHQSVYELIHTEDRAEFQRQLHWALNPSQCTDSAQGVDETHGLPQPAVYY
DVIHQSVYELIHTEDRAEFQRQLHWALNP    DSAQGVDEAHGPPQAAVYY
DVIHQSVYELIHTEDRAEFQRQLHWALNPSQCTESGQGIEEATGLPQTVVCY

TPDQLPPENTAFMERCFRCRLRCLLDNSSGFLAMNFQGRLKYLHGQNKKGKD
TPDQLPPENASFMERCFRCRLRCLLDNSSGFLAMNFQGRLKYLHGQNKKGKD
NPDQIPPENSPLMERCFICRLRCLLDNSSGFLAMNFQGKLKYLHGQKKKGKD

GALLPPQLALFAIATPLQPPSILEIRTKNFIFRTKHKLDFTPIGCDAKGQLI
GALLPPQLALFAIATPLQPPSILEIRTKNFIFRTKHKLDFTPIGCDAKGQLI
GSILPPQLALFAIATPLQPPSILEIRTKNFIFRTKHKLDFTPIGCDAKGRIV

                              PAS B
LGYTEVELCNKGSGYQFIHAADMLHCAESHIRMIKTGESGMTVFRLLAKHSR
LGYTEVELCTRGSGYQFIHAADILHCAESHIRMIKTGESGMTVFRLLAKHSR
LGYTEAELCTRGSGYQFIHAADMLYCAESHIRMIKTGESGMIVFRLLTKNNR

WRWVQSNARLIYRNGRPDYIIATQRPLTDEEGREHLQKRSMTLPFMFATGEA
WRWVQSNARLIYRNGRPDYIIATQRPLTDEEGREHLQKRSTSLPFMFATGEA
WTWVQSNARLLYKNGRPDYIIVTQRPLTDEEGTEHLRKRNTKLPFMFTTGEA

VLYEISSPFSPIMDPLPIRTKSNTSRKDWAPQSTPSKDSFHPNSLMSALIQQ
VLYEISSPFSPIMDPLPIRTKSNTSRKDWAPQSTPSKDSFHPSSLMSALIQQ
VLYEATNPFPAIMDPLPLRTKNGTSGKDSATTSTLSKDSLNPSSLLAAMMQQ

DESIYLCPPSSP      APLDSHFLMDSMSECGSWQGSFAVASNEALLKHEEIR
DESIYLCPPSSP      ALLDSHFLMGSVSKCGSWQDSFAAAGSEAALKHEQIG
DESIYLPASSTSSTAPFENNFFNESMNECRNWQDNTAPMGNDTILKHEQID

HTQDVNLTLSGGPSELFPDNKNNDLYSIMRNLGIDFEDIRSMQNEEFFRTDS
HAQDVNLALSGGPSELFPDNKNNDLYSIMRNLGIDFEDIRSMQNEEFFRTDS
QPQDVNSFA GGHPGLFQDSKNSDLYSIMKNLGIDFEDIRHMQNEKFFRNDF

S   GEVDFKDIDITDEILTYVQDSLNNSTLLNSACQQQPVSQHL  SCMLQER
TAAGEVDFKDIDITDEILTYVQDSLNNSTLLNSACQQQPVTQHL  SCMLQER
S   GEVDFRDIDLTDEILTYVQDSLSKSPFIPSDYQQQQSLALNSSCMVQEH

LQLEQQQQLQQQHPTQTLEPQRQLCQVEVPQHELGQKTKHMQVNGMFVSWNP
LQLEQQQQLQQP PPQALEPQQQLCQMVCPQQDLGPK   HTQINGTFASWNP
LHLEQQQQHHQKQVVV  EPQQQLCQ        KMKHMQVNGMFENWNS

APPVSFSCPQQERKHICLLSGLQGTAQEFPYKSEVDSMPYTQNFAPCNQSLL
TPPVSFNCPQQELKHYQLFSSLQGTAQEFPYKPEVDSVPYTQNFAPCNQPLL
NQFVPFNCPQQDPQQYNVFTDLHGISQEFPYKSEMDSMPYTQNFISCNQPVL

PEHSKGTQLDFPGRDFERSLHPNVSNLEEFVSCLQVPENQRHGINSQSAMVS
PEHSKSVQLDFPGRDFEPSLHPTTSNL DFVSCLQVPENQSHGINSQSAMVS
PQHSKCTELDYPMGSFEPSPYPTTSSLEDFVTCLQLPENQKHGLNPQSAIIT

PQGYYAGAMSMYQCQAGPQDTPVDQMQYSPEIPGSQAFLSKFQSPSILNEAY
PQAYYAGAMSMYQCQGPGPQRTPVDQTQYSSEIPGSQAFLSKVQS
PQTCYAGAVSMYQCQPEPQHTHVGQMQYNPVLPGGQQAFLNKFQNGV LNETY

SADLSSIGHLQTAAHLPRLA      EAQPLPDITPSGFL

PAELNNINNTQTTTHLQPLHHPSEARPFPDLTSSGFL
```

Figure 1.3: Complete amino acid sequences of mouse, rat and human AhR– Sequences were taken from the National Centre for Biotechnology Information website on 22/9/2011. The average PAS domain was estimated to be around 100-200 aā from the start. The green highlighted area indicates the ligand binding domain (Burbach *et al.,* 1992; Coumailleau *et al.,* 1995; Crews *et al.,* 1988; Ema *et al.,* 1994; Fukunaga *et al.,* 1995; Hahn *et al.,* 1997).

The mechanism of action is thought to be the same in all mammalian species and the associated proteins such as Hsp90 and Arnt are thought to be very similar (Chen *et al.,* 2006; Hord and Perdew, 1994). The amino acid sequences of human and rat AhR share a high idenity with the ligand binding domain and the chaperone protein interacting domains being particularly similar (Table 4.6). What small differences are left may play a significant role in the differences in ligand potency observed between different species (Denison *et al.,* 2002; Hahn *et al.,* 1997). Figure 1.3 compares the amino acid sequences of mouse, rat and human showing that there is significant conservation between species. The bHLH domains are highly conserved with 100% between rat and mouse as well as 98% between rodent and human. Also highlighted are the LBDs (based on the mouse AhR LBD; Fukunaga *et al.,* 1995), which show that the two rodents share 97% conservation of amino acids, with both species sharing 85-87% idenity with the human LBD (Hahn *et al.,* 1997). The AhR protein can be found in other non-mammalian species such as the nematode *C. elegans* where it still shares up to 46% identity (Powell-Coffman *et al.,* 1998).

1.1.3 Mechanism of action

When AhR is not bound to a ligand, chaperone proteins keep the binding site of the receptor open and in the correct shape ready for activation. This AhR complex exists as a tetrameric complex consisting of a heat-shock protein 90 (Hsp90) dimer, immunophilin-like associated protein 2 (XAP2: X-associated protein 2 or AIP: Aryl hydrocarbon receptor interacting protein) and a 23KDa co-chaperone protein which appears to interact more with the Hsp90 called the Hsp90 accessory protein (p23; PTGES3: Prostaglandin E synthase 3; Bell and Poland, 2000; Carver *et al.,* 1994b; Carver and Bradfield, 1997; Kazlauskas *et al.,* 1999; Ma and Whitlock, 1997; Meyer *et al.,* 1998; Perdew, 1988; Petrulis and Perdew, 2002; Shetty *et al.,* 2003). Hsp90 is one of the most abundant proteins expressed in cells and shows significant conservation between species (Table 4.6; Chen *et al.,* 2006; Southworth and

Agard, 2008). The AhR complex resides in the cytoplasm of the cell until it is activated by an AhR ligand. Successful activation of the AhR leads to translocation of the AhR:ligand complex to the nucleus.
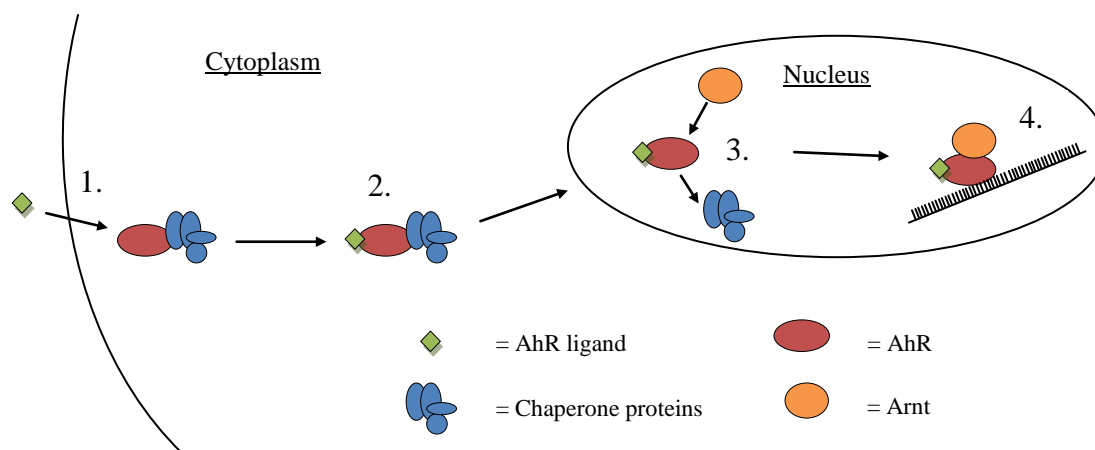
Figure 1.4: Mechanism of ligand-dependant activation of the AhR – 1. Ligand binds to the AhR complex in the cytoplasm. 2. AhR:ligand complex translocates to the nucleus. 3. Chaperone proteins dissociate from AhR, allowing it to bind to Arnt. 4. AhR:Arnt:ligand complex binds to DRE binding sites on DNA, transcribing several xenobiotic enzymes.

Once inside the nucleus, the chaperone proteins dissociate from the AhR:ligand complex and are replaced by the Arnt protein (Hankinson, 1994). This new AhR:Arnt:ligand complex then binds to specific locations on the DNA known as the dioxin responsive elements (DREs) or xenobiotic responsive elements (XREs). These are specific locations mainly upstream of the site of transcription and have the sequence of 5'-TNGCGTG-3' (Denison *et al.,* 1988). Successful binding at these sites leads to the transcription of a battery of xenobiotic metabolism genes including *CYP1A1*, *CYP1A2* and glutathione s-transferase (Denison and Whitlock, 1995; Hankinson, 1995; Nebert *et al.,* 1981, 2004; Whitlock, 1999). Figure 1.4 demonstrates a simplified mechanism of action of the AhR. The AhR is activated by a variety of endogenous and exogenous compounds with the most characterised being TCDD. There are no known endogenous ligands of significant potency (based on their concentration), but there are a number of naturally occurring compounds that interact with the receptor as well as exogenous environmental pollutants such as dibenzo-*p*-dioxins, dibenzofurans and biphenyls.

1.1.4 Cytochrome P4501A1 (CYP1A1)

Cytochrome P450 is a super-family of hemoproteins responsible for the metabolism of thousands of endogenous and exogenous compounds (Guengerich, 1991; Nebert and Gonzalez, 1987; Whitlock, 1999). Only activation of the AhR will induce the transcription of certain P450 enzymes such as *CYP1A1* (Behnisch *et al.*, 2001; Nebert *et al.*, 2000, 2004; Schmidt *et al.*, 1996; Vanden Heuvel *et al.*, 1994). The human and rat CYP1A1 genes are located on chromosome 15 (15q24.1) and chromosome 8 (8q24), respectively, which encodes the P450 enzyme *CYP1A1*. *CYP1A1* is found at low basal levels in most tissues in mammals (Benedict *et al.,* 1973). Induction of xenobiotic enzymes, in the presence of xenobiotics, is an adaptive process facilitating the detoxification of the xenobiotics. CYP1A1 induction does not necessarily imply a toxic response but is nevertheless a useful marker of AhR activation (Gonzalez *et al.,* 1996). Increased activation of the AhR would imply a more efficacious agonist so can therefore be used to estimate the toxic potency of AhR agonists. It can be assumed that increased activation of the AhR would lead to an increased induction of CYP1A1 which can be detected by a variety of methods. CYP1A1 induction is one of the most characterised endpoints of AhR activation and is a highly inducible marker allowing detection of either the CYP1A1 mRNA or protein (Whitlock, 1999; Whyte *et al.,* 2004). TCDD has been shown to increase induction of CYP1A1 mRNA by up to 500-fold above basal levels (Bazzi, 2008; Wall, 2008). CYP1A has been identified in a variety of species, including rat and human, although some significant interspecies differences in concentration have been noted (Ikeya *et al.,* 1989; Martignoni *et al.,* 2006). CYP1A1 binds to TCDD, with high affinity, although it does not metabolise it, which could be the reason that TCDD has a long half life in humans, in addition to its chemical stability (Inouye *et al.,* 2002).

1.1.5 Other xenobiotic metabolism genes (CYP1B1 and CYP1A2)

Activation of the AhR leads to the induction of a gene battery which includes CYP1B1 and CYP1A2 (Hankinson, 1995; Iwanari *et al.,* 2002; Walker *et al.,* 1999; Whitlock, 1999). In the same way as CYP1A1, CYP1B1 is regulated solely by the AhR and is induced upon successful AhR activation although it is not as highly induced as CYP1A1 (Santostefano *et al.,* 1997; Walker *et al.,* 1998, 1999). The gene and its connection with AhR activation was only identified relatively recently and encodes the protein *CYP1B1* which is involved in phase 1 drug metabolism (Bhattacharyya *et al.,* 1995; Lewis *et al.,* 1999; Sutter *et al.,* 1994; Walker *et al.,* 1995). CYP1B1 is normally expressed at high levels in the adrenal gland (Walker *et al.,* 1995) although CYP1B1 and CYP1A2 are expressed in various tissues at low basal levels (Drahushuk *et al.,* 1996; Edwards *et al.,* 1998; Iwanari *et al.,* 2002). CYP1A1 and CYP1A2 only share a 40% identity with CYP1B1 therefore the protein was assigned to a new CYP1 subfamily (Murray *et al.,* 2001; Nelson *et al.,* 1996). CYP1B1 is highly expressed in human tumours; thus, it may have important implications in the development of anti-cancer drugs (Liehr and Ricci, 1996; McFadyen *et al.,* 2001; Murray *et al.,* 2001). CYP1A2 is not exclusively induced by the AhR showing that it would be a non-specific biomarker of AhR activation. A wide variety of compounds have been shown to induce CYP1A2 but not CYP1A1 (or presumably activate the AhR). Caffeine was shown to induce CYP1A2, which in turn is responsible for metabolising caffeine as the presence of CYP1A2 increased the elimination of caffeine from the blood of wild-type mice, 7-fold above CYP1A2 knock-out mice (Buters *et al.,* 1996; Chen *et al.,* 1996). CYP1A2 mRNA has been found at significantly higher basal levels (2- to 30-fold) compared with CYP1A1 but is less inducible which reduces its sensitivity as a biomarker for AhR activation (Drahushuk *et al.,* 1996; Schweikl *et al.,* 1993). There is also a suggestion that TCDD binds to *CYP1A2* but the enzyme does not metabolise it (Olson *et al.,* 1994). The protein has been found at very high levels in the liver

compounding the reasons why TCDD is also found at high concentrations in the liver (Diliberto *et al.,* 1997). There is also suggestion that the levels of CYP1A2 are significantly different between rat and human, which binds TCDD thus reducing the availability of the compound to bind to the AhR possibly explaining some of the potency differences witnessed between these species (Ikeya *et al.,* 1989; Shinkyo *et al.,* 2003).

1.2 Toxicity and AhR-mediated response

1.2.1 Toxic effects

Activation of the AhR is required to instigate the toxic effects of AhR agonists. This is demonstrated in AhR-null mice, which are resistant to the acute toxicity of TCDD (Gonzalez and Fernandez-Salguero, 1998; Lin *et al.*, 2002; Stohs and Hassoun, 2011). TCDD-like AhR agonists all undergo the same mechanism of AhR activation and thus have similar toxic effects. TCDD induces the transcription of a diverse battery of xenobiotic enzymes including *CYP1A1* and *CYP1A2* as well as their dependant activities, glutathione s-transferase and NAD(P)H quinine oxidoreductase (Safe, 1986). Nevertheless, *CYP1A1* and *CYP1A2* have only minimal effect on TCDD metabolism (Olson *et al.,* 1994). Some of the most notable endpoints of TCDD toxicity include chloracne, which is an acne-like eruption of blackheads (Tindall *et al.,* 1985; Schulz, 1968), as well as carcinogenesis (NTP TR-521, 2006; Manz *et al.,* 1991; Huff, 1992). TCDD is described as a reproductive toxicant (Mann, 1997) in addition to causing hepatotoxicity, which is drug induced damage of the liver and thymic atrophy, which inhibits the development of the immune system in rat offspring (Gupta *et al.,* 1973; Vos *et al.,* 1974). Wasting syndrome, where the body weight is drastically reduced including muscle and fatty tissue mass, has been found as an effect of various concentrations of TCDD (Max and Silbergeld, 1987; Pohjanvirta and Tuomisto, 1994).

1.2.2 Structure-activity relationships

AhR agonists have been shown to increase the risk of cancer, cause long-term reproductive issues and liver damage (Pohjanvirta and Tuomisto, 1994). Although not necessarily as a direct result of AhR interaction, it has been shown that several different families of AhR agonists can cause these illnesses and that generally only successful activation of the AhR can lead to increased bioaccumulation and health problems (Brown *et al.,* 1994; Gonzalez and Fernandez-Salguero, 1998; Lin *et al.*, 2002; Stohs and Hassoun, 2011). The most characterised of these compounds is TCDD and it is generally accepted that compounds with a similar shape and polarity (at least where it binds to the receptor) will have similar TCDD-like effects. Research has shown that the most persistent and prevalent compounds such as PCDDs, polychlorinated dibenzofurans (PCDFs) and polychlorinated biphenyls (PCBs) can have very different affinity and efficacy depending on the number and location of the chlorine atoms.
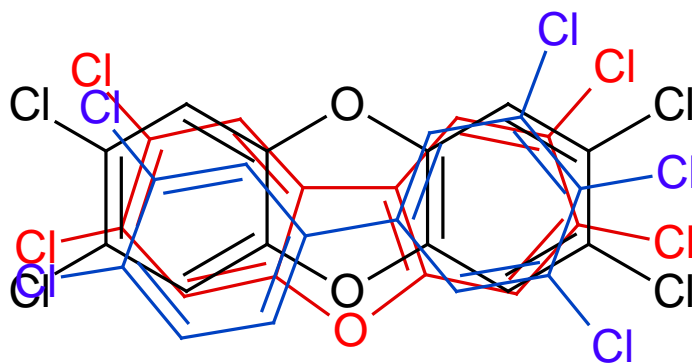
Figure 1.5: Overlay of TCDD, TCDF and PCB 126 – Demonstration of the similarities between the three most characterised families of AhR agonists, TCDD (black), 2,3,7,8-tetrachlorodibenzofuran (TCDF; red) and 3,3',4,4',5-pentachlorobiphenyl (PCB 126; blue).

Figure 1.5 shows the overlay of the three most potent compounds in their families; TCDD, 2,3,7,8-tetrachlorodibenzofuran (TCDF) and 3,3',4,4',5-pentachlorobiphenyl (PCB 126). TCDD and TCDF both have four chlorine atoms positioned equally on the compounds at positions 2, 3, 7 and 8. However TCDD is estimated to be about 10-fold more potent than

TCDF (Haws *et al.,* 2006), which is likely due to the reduced size of the dibenzofuran backbone as it only has one ether group (R-O-R). The most potent PCB congener is PCB 126 which has five chlorines positioned 3, 3', 4, 4' and 5. Despite the increase in chlorine substituents, the compound has the same potency as TCDF. This may be due to the reduced size of the biphenyl backbone structure due to the complete lack of oxygen between benzene rings and therefore an extra chlorine atom is required for the molecule to match the shape and size of TCDD.

1.2.3   Describing agonism and antagonism

The initial activation of the AhR depends on two important qualities of the ligand; affinity and intrinsic efficacy. The affinity is the property of attraction between a ligand and the receptor. Intrinsic efficacy is used to describe the property of agonism and relates receptor occupancy with receptor activation (Kenakin, 1997). A potent agonist is a compound which binds to the receptor and activates it meaning it has both a strong affinity and a high efficacy. A compound can have a good binding affinity for the receptor but a low efficacy resulting in no activation of the receptor. This type of compound is known as an antagonist and due to the relatively high affinity, can prevent an agonist from binding to the same receptor complex, reducing the agonist's ability to produce a response, known as its potency. Potency is the measure of the activity of the ligand required, in relation to concentration, to produce an observable effect (Jenkinson *et al.,* 1995). A partial agonist has both agonistic and antagonistic properties. This means that some of the molecules of the compound will bind to the receptor and activate it, whereas other molecules will bind but the receptor will remain dormant. One possible reason to account for this lack of activation is the orientation of the molecule as it binds to the receptor as activation requires a perfect fit which may not occur with a partial agonist/antagonist. The effective concentration that gives 50% of the maximal response (EC_{50}) can be used as a measure of the potency of a compound.

1.2.4 Measuring agonism and antagonism

The putative agonism and antagonism of various compounds can be tested using bioassays that measure a particular end-point to produce a concentration-response curve. Figure 1.6A shows a concentration-response curve of a potent agonist. The EC_{50} was calculated as the concentration of agonist giving 50% of the maximal induction and can be used as a method of comparing between compounds. In order to determine any putative antagonistic properties of the compound, a concentration which produces 20% of the maximum induction (Figure 1.6A) was treated simultaneously with various concentrations of pure agonist. Figure 1.6B shows the pure agonist in the presence and absence of a putative partial agonist. At lower concentrations of pure agonist, the partial agonist has agonistic properties which induce a 20% response (as shown in Figure 1.6A). At higher concentrations of pure agonist, the antagonistic properties of the partial agonist are easier to identify. The antagonist (partial agonist) forces the pure agonist concentration-response curve to the right, reducing the potency of the pure agonist to induce a response.
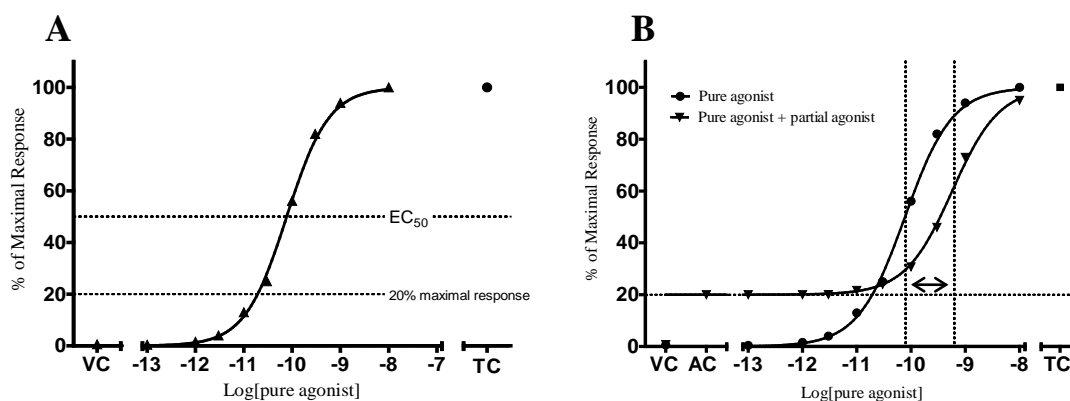
Figure 1.6: Calculating agonism and antagonism – Examples of A) agonism and B) partial agonism. VC: vehicle control, TC: maximal response of TCDD, AC: antagonist only (partial agonist) control (concentration that gives 20% response). Graphs are examples and therefore do not represent real data or give an accurate representation of the agonism by TCDD.

The exact method of calculating the EC_{50}s is discussed in more detail in the method (section 2.4.5) but is essentially the concentration of agonist that gives 50% of the maximal response. However in the presence of a partial agonist, this EC_{50} estimation is slightly different. The

EC_{50} is then calculated as the halfway point between the background induction (which in Figure 1.6B is 20%) and the maximal response (100%). All of the antagonism assays in this thesis are calculated in this way. This method will also be used to identify a pure antagonist, which is a compound that binds to the receptor but not activate it simultaneously preventing a pure agonist from binding and therefore reducing the overall potency of that pure agonist.

1.3 Ligands of the AhR

1.3.1 Dibenzo-*p*-dioxins

1.3.1.1 TCDD

TCDD (2,3,7,8-tetrachlorodibenzo-*p*-dioxin) is a potent agonist of the AhR belonging to a family of halogenated dibenzo-*p*-dioxin agonists, which are environmental pollutants and are colloquially known as dioxins. In the 1970s, TCDD was a by-product of plastic production and general industrial manufacture, although this unintentional production has now reduced due to regulations (Reviewed by Schecter, 1994). Today, the main source of TCDD is from incomplete burning of waste, which is more difficult to control. The environmental levels of TCDD have decreased over the last 20 years (Figure 1.7; Aylward and Hays, 2002; Lorber, 2002).
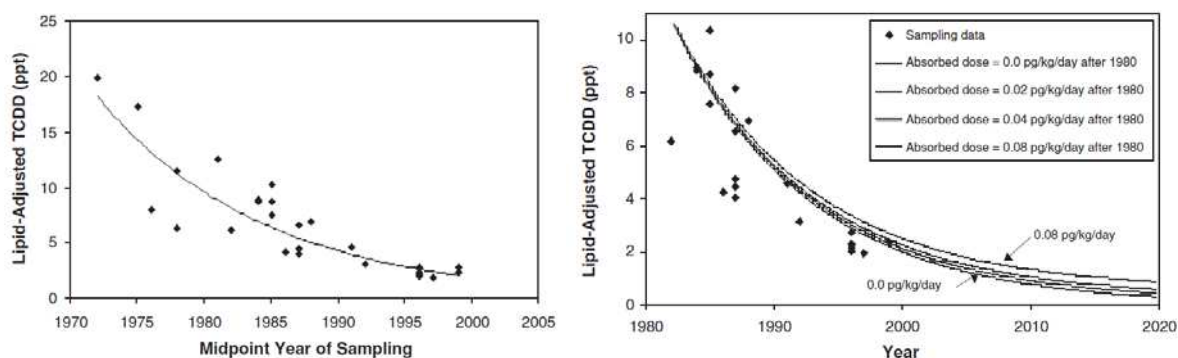
Figure 1.7: (A) Mean lipid-adjusted TCDD levels from the general population and (B) Predicted lipid-adjusted TCDD levels from 1980 onwards – Figures taken from Aylward and Hays (2002).

Nevertheless, due to its potency, tight controls of the levels found in food are still required. Low concentrations of TCDD are found in fat-containing food, and TCDD can accumulate in humans due to a half life of 6-7 years (Aylward and Hays, 2002; Päpke, 1998; Pirkle *et al.,* 1989; Poiger and Schlatter, 1986). TCDD is lipophilic and accumulates in adipose tissue hence the main concentration of TCDD is located in the fatty tissue. Diliberto *et al.* (1995) investigated the distribution of TCDD in rats over a time course of 35 days. The results showed that the majority of the TCDD was concentrated in the liver and the adipose tissue followed by minor quantities in the adrenal glands and the skin (Diliberto *et al.,* 1995). TCDD is the most characterised and amongst the most potent ligands of the AhR, thus making the compound ideal as a reference compound (Van den Berg *et al.,* 1998, 2006).

1.3.1.2   *Mixed halogenated dibenzo-p-dioxins* (*PXDDs)*

Development of Gas Chromatography/Mass Spectrometry (GC/MS) techniques for the identification of dibenzo-*p*-dioxins, dibenzofurans and biphenyls, has lead to the discovery of a variety of mixed halogenated compounds in various food samples (Fernandes *et al.,* 2011). Table 1.2 shows the concentration of several mixed halogenated compounds in several food items, taken from Fernandes *et al.* (2011), which were calculated using GC/MS. The table also gives the structure of dibenzo-*p*-dioxin and relative potencies (REPs; see section 1.4.2.1) calculated by other authors. Several mixed halogenated dibenzo-*p*-dioxins have been tested previously, producing a wide range of REPs for each compound (Behnisch *et al.,* 2003; Olsman *et al.,* 2007; Samara *et al.,* 2009). These REPs were calculated in rat H4IIE cells using ethoxyresorufin-O-deethylase (EROD) and Dioxin-Responsive-Chemical Activated LUciferase gene eXpression (DR-CALUX) techniques. The data suggest that several of the compounds, 2-B-3,7,8-TriCDD, 2,3-DiB-7,8-DiCDD and 2-B-1,3,7,8-TetraCDD, could have equal or increased potency compared with TCDD.

Concentration	Milk	Soft Cheese	Marine fish	River fish	Offal - Liver	Shellfish (oysters)	Composite vegetables
2-B-7,8-DiCDD	0.007	0.021	0.123	0.066	0.045	21.634	0.078
2-B-3,7,8-TriCDD	0.007	0.008	0.008	0.751	0.056	0.143	0.069
2,3-DiB-7,8-DiCDD	0.005	0.005	0.005	0.565	0.058	0.468	0.044
1-B-2,3,7,8-TetraCDD	0.006	0.005	0.007	0.225	0.022	0.031	0.066
2-B-1,3,7,8-TetraCDD	0.005	0.009	0.007	0.033	0.025	0.037	0.134
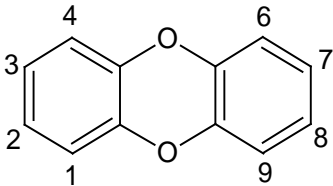
Structure	Potency	Behnisch *et al.,* 2003	Olsman *et al.,* 2007	Samara *et al.,* 2009
	2,3,7-TriBDD	0.033	0.081	0.0006
	2-B-7,8-DiCDD	-	0.061	-
dibenzo-*p*-dioxin (DD)	2,3,7,8-TetraCDD	1	1	1
	2-B-3,7,8-TriCDD	0.67	1.93	0.72
	2,3-DiB-7,8-DiCDD	0.86	1.00	0.43
	1-B-2,3,7,8-TetraCDD	0.28	-	-
	2-B-1,3,7,8-TetraCDD	0.37	1.52	-

Table 1.2: Examples of concentration and potency data for mixed halogenated dibenzo-*p*-dioxins –The table shows concentration data (in ng/kg fat) from food tested for mixed halogenated compounds (Fernandes *et al.,* 2011 supplementary data) and potency data shown as REPs (their potency in comparison to TCDD; see section 1.4.2.1; Behnisch *et al.,* 2003; Olsman *et al.,* 2007; Samara *et al.,* 2009) was gathered from the literature. Chemical names are organised as follows; 2-B-7,8-DiCDD = 2-bromo-7,8-dichlorodibenzo-*p*-dioxin: C = Chlorine (Cl), B = Bromine (Br).

1.3.2 Mixed halogenated dibenzofurans (PXDFs)

Previous work had characterised the agonistic properties of TCDF and 2,3,4,7,8-pentachlorodibenzofuran (PeCDF) in rat H4IIE cells (Bandiera *et al.,* 1984; Wall, 2008). The data showed they are strong-medium potency agonists of the AhR with EC_{50}s of 2.02 nM and 0.13 nM (Bandiera *et al.,* 1984), respectively and neither of the two compounds have any antagonistic properties (Wall, 2008). There is evidence of carcinogenic activity of PeCDF (NTP TR-525, 2006) especially in a mixture with TCDD (NTP TR-526, 2006) in rats. Human exposure to dibenzofurans has been identified in a variety of food samples (Huwe and Larsen, 2005; Theelen *et al.,* 1993) and even in human samples (Shen *et al.,* 2009). As of the 1st January 2012 (European Commission, 2011), the toxic equivalency factors (TEFs; see section 1.4.2.1) for TCDF and PeCDF are 0.1 and 0.3, respectively (Haws *et al.,* 2006; Van

den Berg *et al.,* 2006). This project looked at several mixed halogenated dibenzofurans (PXDFs), based on the structures of TCDF and PeCDF but with bromine substitutions. There is only limited potency data currently available in the literature for PXDFs. Concentration data from various food groups (Fernandes *et al.,* 2011) and REPs for several PXDFs, calculated using rat cell based bio-assays (Behnisch *et al.,* 2003; Olsman *et al.,* 2007; Samara *et al.,* 2009) are shown in Table 1.3.

Concentration	Milk	Soft Cheese	Marine fish	River fish	Offal - Liver	Shellfish (oysters)	Composite vegetables
2-B-7,8-DiCDF	0.005	0.012	0.018	0.045	0.024	0.878	0.579
3-B-2,7,8-TriCDF	0.005	0.007	0.023	0.346	0.068	0.173	0.077
2-B-6,7,8-TriCDF	0.005	0.009	0.03	1.031	0.016	0.605	0.075
2,3-DiB-7,8-DiCDF	0.007	0.009	0.011	0.08	0.147	0.558	0.056
1-B-2,3,7,8-TetraCDF	0.013	0.005	0.005	0.034	0.052	0.049	0.078
4-B-2,3,7,8-TetraCDF	0.014	0.012	0.022	0.044	2.454	2.585	0.072
1,3-DiB-2,7,8-TriCDF	0.007	0.011	0.006	0.023	0.045	0.043	0.004
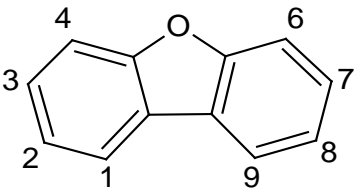
Structure	**Potency**	Behnisch *et al.,* 2003	Olsman *et al.,* 2007	Samara *et al.,* 2009
Dibenzofuran (DF)	2-B-7,8-DiCDF	-	0.000037	-
	2,3,7,8-TetraCDF	0.32	-	0.07
	3-B-2,7,8-TriCDF	0.74	-	0.38
	2-B-6,7,8-TriCDF	-	-	-
	2,3-DiB-7,8-DiCDF	-	-	-
	2,3,4,7,8-PentaCDF	0.5	-	0.46
	1-B-2,3,7,8-TetraCDF	-	-	-
	4-B-2,3,7,8-TetraCDF	-	-	-
	1,3-DiB-2,7,8-TriCDF	-	-	-

Table 1.3: Examples of concentration and potency data for mixed halogenated dibenzofurans –The table shows concentration data (in ng/kg fat) from food tested for PXDFs (Fernandes *et al.,* 2011 supplementary data) and potency data shown as REPs (their potency in comparison to TCDD; see section 1.4.2.1; Behnisch *et al.,* 2003; Olsman *et al.,* 2007; Samara *et al.,* 2009) was gathered from the literature. Chemical names are organised as follows; 2-B-7,8-DiCDF = 2-bromo-7,8-dichlorodibenzofuran: C = Chlorine (Cl), B = Bromine (Br).

1.3.3 Mixed halogenated biphenyls (PXBs)

1.3.3.1 Non-ortho-substituted PCBs and PXBs

Non-*ortho*-substituted PXBs (including PCBs), which can be described as biphenyls that do not have a halogenated atom on the *ortho*-substituted positions on the compound (i.e. 2,2',6,6'), have the same mechanism of action as dibenzo-*p*-dioxins. As with most PCBs, the non-*ortho*-substituted PCBs are associated with an increased risk of cancer (Hemming *et al.,* 1995). Many PCBs had widespread applications, used as coolants and additives, before they were banned in the 1970s once their toxicity and ability to bioaccumulate were identified. In this study PCB 126 will be tested as a comparison for the other, less studied PCBs. PCB 126 is the most potent and well characterised of the PCBs. Previous work has shown that this compound is a potent agonist of the AhR and has no antagonistic properties (Haws *et al.,* 2006; Wall, 2008). Based on the TEF guidelines produced on the potency of dioxin-like compounds, PCB 126 has a value of 0.1 (Haws *et al.,* 2006; Van den Berg *et al.,* 2006), suggesting it is approximately 10-fold less potent at inducing TCDD-like effects but is still a very potent AhR agonist (Peters *et al.,* 2004; Sanderson *et al.,* 1996; Silkworth *et al.,* 2005). Levels of PXB 126 compounds have been found in a variety of food samples which, depending on their potency, may have a significant effect on the TEQ in food (Fernandes *et al.,* 2011); for example, river fish had levels of 4'-B-3,3',4,5-TetraCB (PXB 126B; 1.681 ng/kg), 3',4'-DiB-3,4,5-TriCB (PXB 126H; 0.19 ng/kg) and 3',4',5-TriB-3,4-DiCB (PXB 126V; <0.076 ng/kg). The structure of biphenyl is shown in Table 1.4.

1.3.3.2 Mono-ortho-substituted PCBs and PXBs

Mono-*ortho*-substituted PXBs (including PCBs) can be described as biphenyls that contain at least on halogenated atom on the *ortho*-substituted positions on the compound (i.e. 2,2',6,6') and have been well studied in the past due to their abundance in the environment (Ahlborg, 1992; Fernandes *et al.,* 2008; Larebeke *et al.,* 2001; Kalantzi *et al.,* 2004; Polder *et al.,*

2008a, 2008b; Safe, 1990; Safe, 1994). Research has shown that several mono-*ortho*-substituted PCBs possess both agonistic and antagonistic properties (Chen and Bunce, 2004; Clemons *et al.,* 1998; Suh *et al.,* 2003). The compounds have been tested in rat H4IIE cells (Clemons *et al.,* 1998), trout RTL-W1 cells (Clemons *et al.,* 1998) and fish PLHC-1 cells (Hesterman *et al.,* 2000).

Composite sample	PCB 105	PCB 114	PCB 118	PCB 123	PCB 156	PCB 157	PCB 167	PCB 189	*Ortho*- PCBs TEQ (ng/kg)
Sprat	7.99	0.37	28.27	1.89	2.86	1.01	1.97	0.41	0.55
Sea Bass	13.03	0.60	51.17	2.15	6.24	1.92	4.32	0.81	0.76
Wild Turbot	12.95	0.65	50.97	2.26	5.92	2.02	4.39	0.73	0.28
Wild Dogfish	21.95	1.67	80.44	2.95	10.01	3.12	5.77	1.04	1.32
Wild Greenland Turbot	5.28	0.35	16.16	0.62	1.71	0.56	0.89	0.16	0.37
Wild halibut	6.49	0.49	22.79	0.68	2.57	0.73	1.45	0.30	0.22
Wild Whitebait	16.77	0.59	73.85	6.18	8.91	2.28	5.56	1.17	0.71
Wild Pilchard/ Sardines	10.68	0.32	44.77	2.61	5.09	1.69	3.71	0.76	1.20
Wild Hake	6.80	0.29	23.47	1.29	3.08	1.11	2.13	0.44	0.13
Fresh Crab	5.16	0.18	18.59	0.87	2.44	1.09	2.03	0.42	0.26
Farmed Turbot	14.96	0.69	56.62	2.89	6.36	2.10	4.62	0.55	0.18
Farmed Halibut	12.66	0.44	40.65	1.46	4.63	1.33	2.96	0.48	0.37

3,3',4,4',5-PentaCB (PCB 126)
4'-B-3,3',4,5-TetraCB (PXB 126B)
3',4'-DiB-3,4,5-TriCB (PXB 126H)
3',4',5-TriB-3,4-DiCB (PXB 126V)
3,3',4,4',5-PentaBB (PBB 126)
2,3,3',4,4'-PentaCB (PCB 105)
4'-B-2,3,3',4-TetraCB (PXB 105)
2,3',4,4',5-PentaCB (PCB 118)
4'-B-2,3',4,5-TetraCB (PXB 118)
2,3,3',4,4',5-HexaCB (PCB 156)
4'-B-2,3,3',4,5-PentaCB (PXB 156)
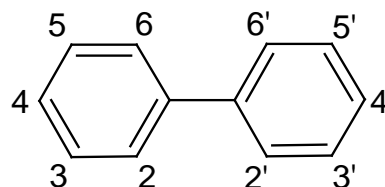
Table 1.4: GC/MS analysis of fish samples detecting mono-*ortho*-substituted PCBs – GC/MS was used to measure the concentrations of a variety of PCBs. Only the data for the most potent mono-*ortho*-substituted PCBs are included in this table. Amounts are in µg/kg fat. The TEQ values have been published previously (Fernandes *et al.,* 2008), individual PCB concentrations were taken from supplementary data. Chemical names are organised as follows; 4'-B-3,3',4,5-TetraCB = 4'-bromo-3,3',4,5-tetrachlorobiphenyl: C = Chlorine (Cl), B = Bromine (Br).

Risk assessment requires both potency and exposure data to fully understand the associated risk of the specific compound. A compound with a high potency can be harmless if there is

no environmental exposure of that compound so it was important to identify which of the more potent mono-*ortho*-substituted PCB congeners were abundant in the environment. As part of a project for the Food Standards Agency, the levels of AhR ligands including mono-*ortho*-substituted PCBs were measured in several species of fish from around the UK (Fernandes *et al.,* 2008). The analysis used GC/MS to measure the concentration of contaminants in the fish samples with the data presented as µg contaminant/kg fat (Table 1.4). A shortlist of samples, which gave the highest levels of PCB contamination, was selected (Fernandes *et al.,* 2008 supplementary data). The data shows that 2,3,3',4,4'-pentachlorobiphenyl (PCB 105), 2,3',4,4',5-pentachlorobiphenyl (PCB 118) and 2,3,3',4,4',5-hexachlorobiphenyl (PCB 156) are the most abundant of the PCBs measured suggesting they would have the biggest impact on the total toxic potency of a mixture (section 1.4.2.1). Table 1.4 also shows the structures of all of the biphenyls used in this project.
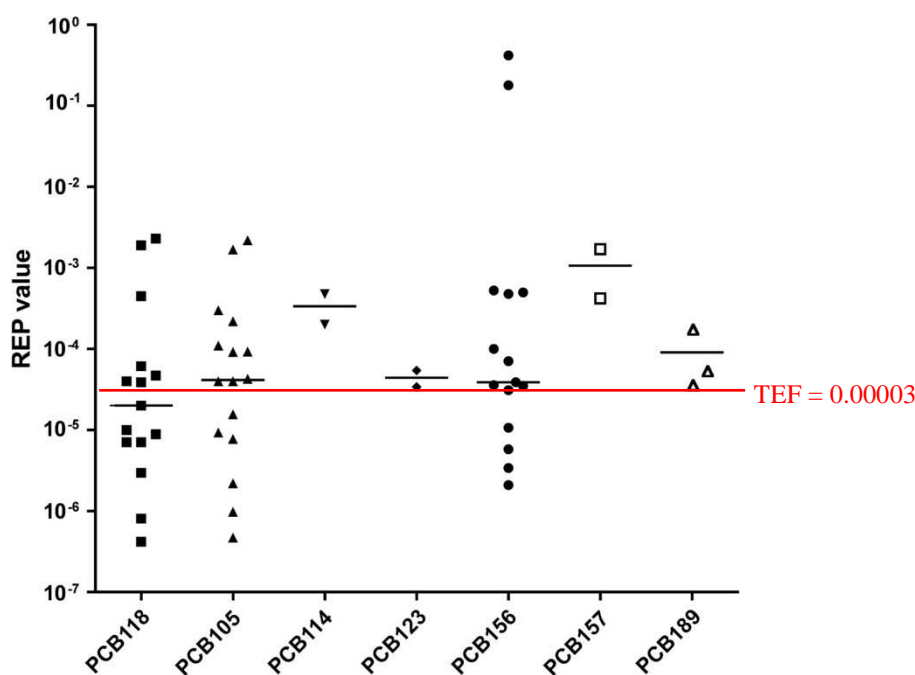
Figure 1.8: Distribution of REP values based on previous research – The REPs calculated from a variety of research was plotted as a meta-analysis to allow identification of the most appropriate TEF values. Figure was taken from the literature (Van den Berg *et al.,* 2006). The red line indicates the current TEF for all of the mono-*ortho*-substituted PCBs included in the TEQ system.

Figure 1.8 is taken from Van den Berg *et al.* (2006) and shows the range of REP values from the meta-analysis of the seven main mono-*ortho*-substituted PCBs spans several orders of magnitude. The mean REP from each compound was used to calculate the total mean of all of the compounds to produce a TEF of 0.00003 (van den Berg *et al.,* 2006). The figure shows that there is as much as a 100,000-fold difference in REP estimation depending on the reference data it was derived from (PCB 156). There are several explanations for this but the most likely explanation is that some of the samples were contaminated with more potent PXBs or dioxin-like compounds (Koistinen *et al.,* 1996) as even a trace amount would have an effect compared with the weaker PCB agonists. Koistinen *et al.* (1996) found that when conducting potency experiments to calculate the REP, some of the PCB congeners were contaminated with more potent compounds such as PCB 126 and TCDD. In order to confirm that only the PCB congener in question is inducing CYP1A1 and not any contamination, the composition of the compound solution used in this project will be tested using gas-chromatography with a mass spectrometer attached. This will identify any impurities in the compound solutions as even a 1% contamination can have an effect on the potency of these compounds (DeVito, 2003).

1.3.4 Other AhR ligands

1.3.4.1 CH223191
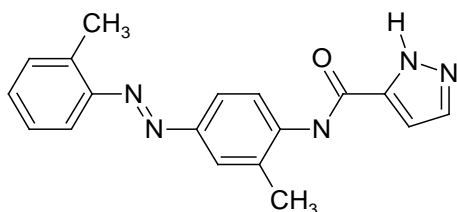
An example of a potent AhR antagonist is CH223191 or 2-methyl-2H-pyrazole-3-carboxylic acid (2-methyl-4-o-tolylazo-phenyl)-amide (Bazzi, 2008; Choi *et al.,* 2012; Kim *et al.,* 2006; Veldhoen *et al.,* 2008; Zhao *et al.,* 2010). CH223191 has previously been shown to have no agonistic activity up to a concentration of 10 µM and inhibited the induction of CYP1A1 by TCDD at

nanomolar concentrations in human hepatoma (HepG2) cells (Kim *et al.,* 2006). Zhao and

co-workers further investigated the antagonistic properties and showed that the compound is

actually a halogenated aromatic hydrocarbon (HAH) specific antagonist and did not have the

same properties in polycyclic aromatic hydrocarbon (PAH)-like compounds such as beta-

naphthoflavone (β-NF; Zhao *et al.,* 2010).

1.3.4.2 5F 203
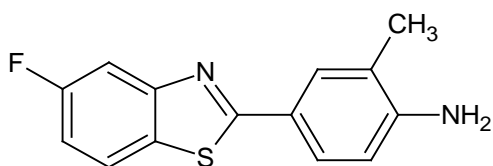
2-(4-Amino-3-methylphenyl)-5-fluorobenzothiazole
(5F 203) was part of a group of chemically similar
compounds that were synthesised as antitumor
agents (Hutchinson *et al.,* 2001). The compounds

were expected to interact with the AhR and inhibit cancer cell line (MCF-7) growth as

previously shown by 2-(3,4-dimethoxyphenyl)-5-fluorobenzothiazole (GW 610 or PMX

610). Amongst the fluorinated versions of these drugs, 5F 203 was shown to have very

positive results and is subsequently involved in phase 1 clinical trials (Aiello *et al.,* 2008,

Hutchinson *et al.,* 2002). The compound was shown to be a partial agonist in rat H4IIE cells

and a pure agonist in human MCF-7 cells (Bazzi *et al.,* 2009). One of the more interesting

characteristics of this compound was that it was found to be more potent in human cells than

rat. This compound was therefore identified as a useful compound when studying the species

differences in AhR activation.

1.3.5 Putative AhR ligands

1.3.5.1 AZFMHCs
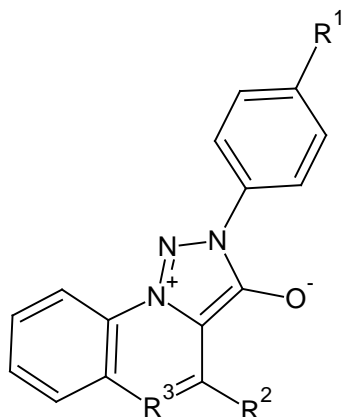
Several compounds received from AstraZeneca were thought to have a higher potency than TCDD when inducing CYP1A1 based on routine measurement of *CYP1A1* protein induction conducted on the compounds by AstraZeneca (Furber, Personal communication). At least one of the compounds was thought to have comparable potency to activate the AhR based on *CYP1A1* protein measurement (EROD; data not shown).

This family of fused mesoionic heterocycle compounds (AZFMHCs) was originally developed as part of a programme by AstraZeneca researching Th2 selective immune-suppressive agents (Abbott *et al.,* 2002) but are no longer in development as pharmaceuticals. Compounds with a similar structure to these have been shown to cause chloracne (Mackenzie and Brooks, 1998; Scerri *et al.*, 1995), which is a characteristic of dioxin-like toxicity (Tindall, 1985), which suggests they undergo the same mechanism of action.

1.3.5.2 2-Amino-isoflavones (*Chr*)
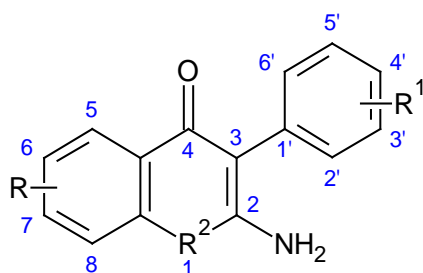
Several compounds, similar to isoflavones, but with an amino group on position 2, were shown in preliminary tests, using a luciferase based assay, to have some unusual agonistic and antagonist properties (Full structures are shown in Table 4.5; Wall *et al.,* 2012b).

The initial screening data was conducted using two recombinant AhR-responsive luciferase cell culture models, mouse H1L6.1c2 and human HG2L6.1c3 cells (Figure 4.2). The recombinant mouse (Hepa1c1c7) and human hepatoma (HepG2) cell lines (H1L6.1c2 and HG2L6.1c3, respectively) contain a stably transfected plasmid (pGudLuc6.1) which has the

firefly luciferase gene (*Photinus pyralis)* under AhR-responsive control of four DREs immediately upstream of the mouse mammary tumour virus (MMTV) viral promoter and luciferase gene (Aarts *et al.,* 1995; Garrison *et al.,* 1996; Han *et al.,* 2004). The screening data showed that Chr-15 was the most potent of the ligands tested and displayed a significant difference in induction between mouse and human however it was decided instead to focus on agonism/antagonism-related species differences rather than purely potency. 2-amino-3-(4-chlorophenyl)-7-methoxychromen-4-one (Chr-13) was shown in the preliminary work to be an agonist of AhR in mouse Hepa6.1.1 cells but an antagonist of AhR in human HepG26.1.1 cells (Wall *et al.,* 2012b). The other compound which was more intensely investigated was 6-chloro-3-(4'-methoxy)phenylcoumarin (Chr-19). The compound was a precursor in the production of a group of anticoagulants and was shown in the preliminary data to be an agonist of mouse AhR and a partial agonist of human AhR (Wall *et al.,* 2012b). Compounds from the coumarin family, which are similar in chemical structure, have considerable uses including anticoagulants such as warfarin (coumadin) and edema modifiers (coumarin) and can still be found in tobacco despite being a banned additive. This leads to the hypothesis that these compounds may also exhibit AhR activation ability.

1.4 Risk assessment

1.4.1 Food contamination

Accurately measuring the levels of dioxin-like HAH compounds (PCDDs, PCDFs and PCBs) is very important for the food industry and regulators, costing several millions of dollars to properly regulate (Vanden Heuvel and Lucier, 1993). Over the last decade many countries have monitored the levels of dioxin-like compounds in food on an *ad hoc* basis. The EU became the first body to set extensive and comprehensive limits for these compounds which first came into force in 2002 (Van den Berg *et al.*, 1998; European Commission, 2002b). There are three tiers of risk assessment levels in place: Maximum levels are set at 'a strict but

feasible level in food' in order that manufactures make continued effort to minimise the presence of dioxin-like compounds in food and feed. Action levels are used as an 'early warning' of potentially higher levels of dioxin-like compounds in food or feed allowing local authorities to identify potential contamination and eliminate it prior to the maximum level being reached. Target levels are in place to gradually reduce the levels of dioxin-like compounds in food and feed to more acceptable levels as recommended by scientific committees (European Commission, 2001, 2002a). There have been several cases where higher than normal levels have been detected causing the food to be recalled before sale to the general public. There have been several high profile exposures to dioxin-like HAHs such as the rice oil contamination in Yusho, Japan in 1968. Rice bran oil was found to be contaminated with PCBs and PCDFs affecting over 1000 people who had symptoms of chloracne (Kuratsune *et al.,* 1972; Schecter, 1994; Yoshimura, 2003). More recently in December 2008, routine sampling of pork and beef samples revealed levels up to 200-times higher than the legal limits of dibenzo-*p*-dioxins and PCBs (Casey *et al.,* 2010). The Irish pork industry is worth approximately £400 million a year exporting 50% abroad so the impact of these findings had a significant effect on the industry (Dixon, 2009; Kennedy *et al.,* 2010). Once the dibenzo-*p*-dioxin has been consumed by the animal, it accumulates in the fatty tissue until consumed by the general public or is removed from the animal's body as waste which may be used as fertiliser for crops.

1.4.2 Prediction of risk in humans

1.4.2.1 TEF estimation

The current internationally recognised method of calculating the TCDD-like toxicity of a mixture based on experimental data for individual compounds has been devised by the World Health Organisation (WHO; Van den Berg *et al.,* 2006) in 2005 and was officially initiated on the 1st January 2012 (European Commission, 2011). However, there have been various

versions of this method in the past that utilise a similar methodology to estimate risk, such as NATO I-TEFs (International toxicity equivalency factors; NATO/CCMS, 1988a, 1988b), WHO-ECEH TEF (WHO-European Centre for Environment and Health TEF; Ahlborg *et al.*, 1994) and the original WHO TEQ methodology devised in 1998 (Van den Berg *et al.*, 1998) which was revised to form the current WHO 2005 version. This data has been collected from various sources each using slightly different methodology (Haws *et al.,* 2006). The relative potency (REP) of a compound is a measure of its ability to bind and activate the AhR allowing direct comparison between compounds and different data sets. REPs are also calculated in relation to TCDD, which is set at 1, using the EC_{50}s gathered from concentration-response curves (Equation 1.1). The use of different experimental methods (i.e. *in vitro* and *in vivo*) as well as different data analysis, to calculate the REP makes it more difficult to compare between different data sets. The REP is calculated either *in vivo* or *in vitro* and is measured by a variety of methods such as PCR and EROD. This data was used to calculate toxic equivalency factors (TEFs), which are normalised REPs based on a meta-analysis of all of previous data from the literature producing an average of all of the (suitable) REPs found in the literature. TCDF, for example, has a TEF of 0.1 because it is 10-fold less potent at activating the AhR than TCDD (based on a variety of REPs found in the literature).

Compound	WHO 1998 TEF	WHO 2005 TEF
Chlorinated dibenzo-*p*-dioxins		
2,3,7,8-TCDD	1	1
1,2,3,7,8-PeCDD	1	1
1,2,3,4,7,8-HxCDD	0.1	0.1
1,2,3,6,7,8-HxCDD	0.1	0.1
1,2,3,7,8,9-HxCDD	0.1	0.1
1,2,3,4,6,7,8-HpCDD	0.01	0.01
OCDD	0.0001	**0.0003**
Chlorinated dibenzofurans		
2,3,7,8-TCDF	0.1	0.1
1,2,3,7,8-PeCDF	0.05	**0.03**
2,3,4,7,8-PeCDF	0.5	**0.3**
1,2,3,4,7,8-HxCDF	0.1	0.1
1,2,3,6,7,8-HxCDF	0.1	0.1
1,2,3,7,8,9-HxCDF	0.1	0.1
2,3,4,6,7,8-HxCDF	0.1	0.1
1,2,3,4,6,7,8-HpCDF	0.01	0.01
1,2,3,4,7,8,9-HpCDF	0.01	0.01
OCDF	0.0001	**0.0003**
Non-*ortho*-substituted PCBs		
3,3',4,4'-TCB (PCB 77)	0.0001	0.0001
3,4,4',5-TCB (PCB 81)	0.0001	**0.0003**
3,3',4,4',5-PeCB (PCB 126)	0.1	0.1
3,3',4,4',5,5'-HxCB (PCB 169)	0.01	**0.03**
Mono-*ortho*-substituted PCBs		
2,3,3',4,4'-PeCB (PCB 105)	0.0001	**0.00003**
2,3,4,4',5-PeCB (PCB 114)	0.0005	**0.00003**
2,3',4,4',5-PeCB (PCB 118)	0.0001	**0.00003**
2',3,4,4',5-PeCB (PCB 123)	0.0001	**0.00003**
2,3,3',4,4',5-HxCB (PCB 156)	0.0005	**0.00003**
2,3,3',4,4',5'-HxCB (PCB 157)	0.0005	**0.00003**
2,3',4,4',5,5'-HxCB (PCB 167)	0.00001	**0.00003**
2,3,3',4,4',5,5'-HpCB (PCB 189)	0.0001	**0.00003**

Table 1.5: List of WHO TEF values - Shows several examples of TEF values for a selection of chlorinated dibenzo-*p*-dioxins, dibenzofurans and PCBs. Values were calculated by the world health organisation (Haws *et al.,* 2006; Van den Berg *et al.,* 2006). The table was taken from Van den Berg *et al.* (2006). T: Tetra; Pe: Penta; Hx: Hexa; Hp: Hepta.

Table 1.5 demonstrates all of the current TEF values for dibenzo-*p*-dioxins, dibenzofurans and PCBs. The TEFs were recorded as half order of magnitude estimates demonstrating the high variability in TEF estimation (as shown in Figure 1.8). Environmentally, these dioxin-like compounds are found in complex mixtures therefore in order to predict the total toxicity, it is necessary to calculate the contribution of each compound in the mixture. The TEF-weighted concentration of each compound in the mixture is added together to calculate the

total toxic equivalency (TEQ; total TCDD-like toxicity) of the mixture (Equation 1.1). The estimate can then be compared between laboratories, although full analysis of the underlying data is usually required to understand the full impact of the TEQ.

$$\frac{[\text{TCDD}] \ \text{EC}_{50}}{[\text{Agonist}] \ \text{EC}_{50}} = \text{REP}$$

$$\frac{\text{REP}^2 + \text{REP}^2 + \ \cdots}{\text{REP}^\#} = \text{TEF}$$

$$(\text{TEF}^1 \ \text{x} \ \text{Conc.}^1) \ + \ (\text{TEF}^2 \ \text{x} \ \text{Conc.}^2) \ + \ \cdots \ = \ \text{TEQ of mixture}$$

Equation 1.1: TEQ equation for a mixture of HAHs – REP[n]: Relative potency for compound n; REP[#]: Total number of Relative potencies for compound; TEF[n]: Toxic equivalency factor for compound n; Conc[n]: Concentration of compound n in the mixture; TEQ: Total TCDD-like toxicity of the mixture. Equation is discussed further by the world health organisation (Haws *et al.,* 2006; Van den berg *et al.,* 2006).

Obviously in terms of risk assessment, it is better to overestimate the risk to human health rather than under estimate it; however, tight regulations and low environmental pollutant limits in food means an increase in the costs to regulate it. It is therefore crucial that these levels are correctly established.

1.4.2.2 Advantages of the TEQ method

The TEQ method employs an additivity approach that predicts the total TCDD-like toxicity of a mixture of TCDD-like compounds. The approach sums the potencies of all the compounds within the mixture in a dose dependent fashion and includes PCDDs, PCDFs and PCBs. This additivity approach assumes two important points, firstly, that TCDD-like toxicity is achieved by the same mechanism for each compound, and secondly that the toxicity of each compound can be added together and would therefore not affect the ability of another agonist from activating the receptor (Van den Berg *et al.,* 2006). Additivity between TCDD-like compounds has been shown by several authors performing their own mixture

experiments, confirming the total toxicity experimentally after prediction by the additivity method (Brown *et al.,* 1994; Fattore *et al.,* 2000; Hamm *et al.,* 2003; Walker *et al.,* 1996). Walker *et al.* (1996) tested a mixture of 14 TCDD-like and non TCDD-like compounds in rainbow trout. They showed that although the mixture was not completely additive, the method was more accurate than current toxicity predictions applied in ecology (Walker *et al.,* 1996).

The benefits of the TEQ system are that it is a simple method to calculate a potentially complicated subject. It incorporates potency data from a huge data set of *in vitro* and *in vivo* studies allowing confidence in the TEFs used. The TEQ method incorporates individual potency and prevalence data when calculating the TEQ allowing a more accurate estimate of toxicity. Having a universal table of TEF values allows for comparison between international regulatory bodies and makes it easier for governmental agencies to measure and compare risk from international sources.

1.4.2.3 *Disadvantages of the TEQ method*

There are several disadvantages with this method of prediction which could limit the accuracy of the method and reduce confidence in the estimation obtained. Firstly, the REP data used to derive the TEFs is, in some cases, highly variable (Figure 1.8), which reduces the confidence in the TEFs used for this assessment and highlights the uncertainty in estimating the TEQ. This uncertainty between laboratories is mostly like due to contamination of stock solutions with more potent AhR agonists such as TCDD, TCDF or PCB 126, which would give a higher response. Secondly, if an agonist with antagonistic properties (partial agonist; section 1.2.3) is in the presence of a pure agonist, the overall toxicity would decrease and the TEQ calculated by the additivity method would be higher than the actual risk (Howard *et al.,* 2010; Safe, 1994; Toyoshiba *et al.,* 2004; Walker *et al.,* 2005). Walker *et al.* (2005) followed work by Toyoshiba *et al.* (2004) and concluded that the

additivity method does not accurately predict potency despite considerable statistical power but instead requires a potency adjusted dose-additivity approach to be used, due to the lack of dose additivity and differences in the shape of dose-response curves (Toyoshiba *et al.,* 2004; Walker *et al.,* 2005). Compounds already included within the additivity scheme may be partial agonists (Clemons *et al.,* 1998). Certain PCBs have been found to possess both agonistic and antagonistic properties in the presence of TCDD which would ultimately reduce the overall TCDD-like toxicity of the mixture (Chu *et al.,* 2001; Clemons *et al.,* 1998). Clemons *et al.* (1998) showed that several PCB ligands had a less-than-additive interaction and concluded that the H4IIE bioassay could lead to lower TCDD-equivalent concentration than would be determined empirically (Clemons *et al.,* 1998). This problem could also extend to other exogenous AhR agonists found in the environment, which are not currently included within the TEQ method, such as polybrominated diphenylethers (PBDEs; Darnerud *et al.*, 2001) and mixed halogenated dioxin-like HAHs which, may further impact risk assessment of a mixture (Peters *et al.,* 2004).

The method does not consider the interaction between the exogenous mixture of environmental pollutants and naturally occurring AhR ligands found in the body and foods. Natural AhR ligands include; resveratrol (Casper *et al.,* 1999; Ciolino *et al.,* 1998, Ciolino and Yeh, 1999a), bilirubin (Phelan *et al.,* 1998), indirubin (Adachi *et al.,* 2001), indole-3-carbinol (Bjeldanes *et al.,* 1991) and flavones (Henry *et al.,* 1999). Suitable concentrations of these compounds may seriously affect the TCDD-like toxicity of further AhR agonists by acting as antagonists or partial agonists of the AhR. Furthermore, the presence of a natural antagonist may reduce the overall toxicity of an exogenous mixture. Additionally, even if natural agonists were taken into account, this assumes that the levels of natural AhR agonists will be the same between different people. If intra-species differences were high it would be very difficult to take these compounds into account when making a prediction.

1.5 Background of techniques used

1.5.1 Ligand binding assay

TCAOB
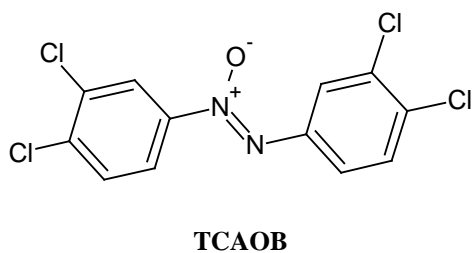
The ability of a compound to compete with tritiated TCDD ([^{3}H]-TCDD) for binding to the AhR was measured using a ligand binding assay (Bazzi *et al.,* 2009; Bradfield and Poland, 1988). The assay used [^{3}H]-TCDD which competes with the compound of interest for binding to the rat cytosolic protein containing cytosolic AhR. Two assays were conducted for each compound; (1) total binding of [^{3}H]-TCDD to all protein and (2) non-specific binding of [^{3}H]-TCDD to cytosolic proteins other than AhR. A high affinity AhR ligand, TCAOB (3,4,3',4'-tetrachloroazoxybenzene) was used as the competitor (Bazzi, 2008, Poland *et al.,* 1976). The [^{3}H]-TCDD is a low-energy beta emitter which was measured using liquid scintillation counter. The [^{3}H]-TCDD sample was suspended in scintillation fluid which, upon emission of beta radiation, emits light that can be measured by the scintillation counter.

1.5.2 Quantitative real-time PCR (qRT-PCR)

1.5.2.1 Overview

In order to measure the activation of the AhR, measurement of the induction of CYP1A1 was conducted in mRNA from rat liver cells (H4IIE) and human carcinoma cells (MCF-7) using quantitative real-time PCR (qRT-PCR). Measurement of the induction of CYP1A1 mRNA by a particular compound then allows the construction of a concentration-response curve. A method which can detect both the agonistic and antagonistic properties of a compound was formulated. A standard concentration-response curve will give the agonistic potency of the compounds. Antagonism was measured by treating cells with TCDD along with a set concentration of the antagonist.

1.5.2.2 Cell lines

The H4IIE cell line has several important advantages making it the most appropriate cell system to use for the measurement of CYP1A1 mRNA induction. One of the key features of H4IIE cells are their low basal AHH (CYP1A1) levels (Benedict *et al.,* 1973) and their high responsiveness to CYP1A1 mRNA induction by TCDD-like compounds. In addition, they have excellent growth characteristics allowing a high through-put (Whyte *et al.,* 2004). CYP1A1 induction was measured as it is a good indication of TCDD-like toxicity (Whitlock, 1999), however high CYP1A1 RNA induction does not imply high toxicity (Whyte *et al.*, 2004). Measurement of CYP1A1 RNA can be very robust with a high signal to noise ratio (Whitlock, 1999). There is a significantly large quantity of research of dioxin-like compounds in rat H4IIE cells with the majority of the data collected to calculate the TEFS derived from treatment of these cells allowing comparison with the literature (Haws *et al.,* 2006 supplementary data). MCF-7 cells have been widely used for the measurement of AhR activation (Bazzi *et al.,* 2009; Ciolino *et al.,* 1998; Coumoul *et al.,* 2001; Krishnan and Safe, 1993; Loaiza-Pérez *et al.,* 2002; Pang *et al.,* 1999; Peters *et al.,* 2004; Van Duursen *et al.,* 2003). Human MCF-7 cells were used in this project because they have been shown to be more sensitive at detecting AhR antagonism than other human cell lines (Zhang *et al.,* 2003). Iwanari *et al.* (2002) showed that several of the most characterised AhR ligands, such as TCDD and 3-methylchloranthrene (3-MC), showed a comparable pattern of induction of CYP1A1 mRNA in human HepG2 and human MCF-7 cells. The similar pattern of induction observed with a variety of flavonoids in both human HepG2 and human MCF-7 cells indicated that there were minimal inter-tissue differences in response (Zhang *et al.,* 2003). Human cells derived from human liver (to compare against rat liver H4IIE cells) were not used as human liver has been shown to have low levels of AhR (Dolwick *et al.,* 1993; Yamamoto *et al.,* 2004).

1.5.2.3 Taqman vs SYBR green

There are two methods of using qRT-PCR to measure gene expression, Taqman (uses a target specific probe) and SYBR green (binds non-specifically to all DNA) which are illustrated in Figure 1.9.

(A) TAQMAN

1. Polymerisation

Forward primer

R PROBE Q

Reverse primer

2. Strand

R Q

3. Cleavage

R Q

4. Polymerisation

R Q

(B) SYBR

1. Reaction setup

2. Denaturation

3. Polymerisation

4. Polymerisation
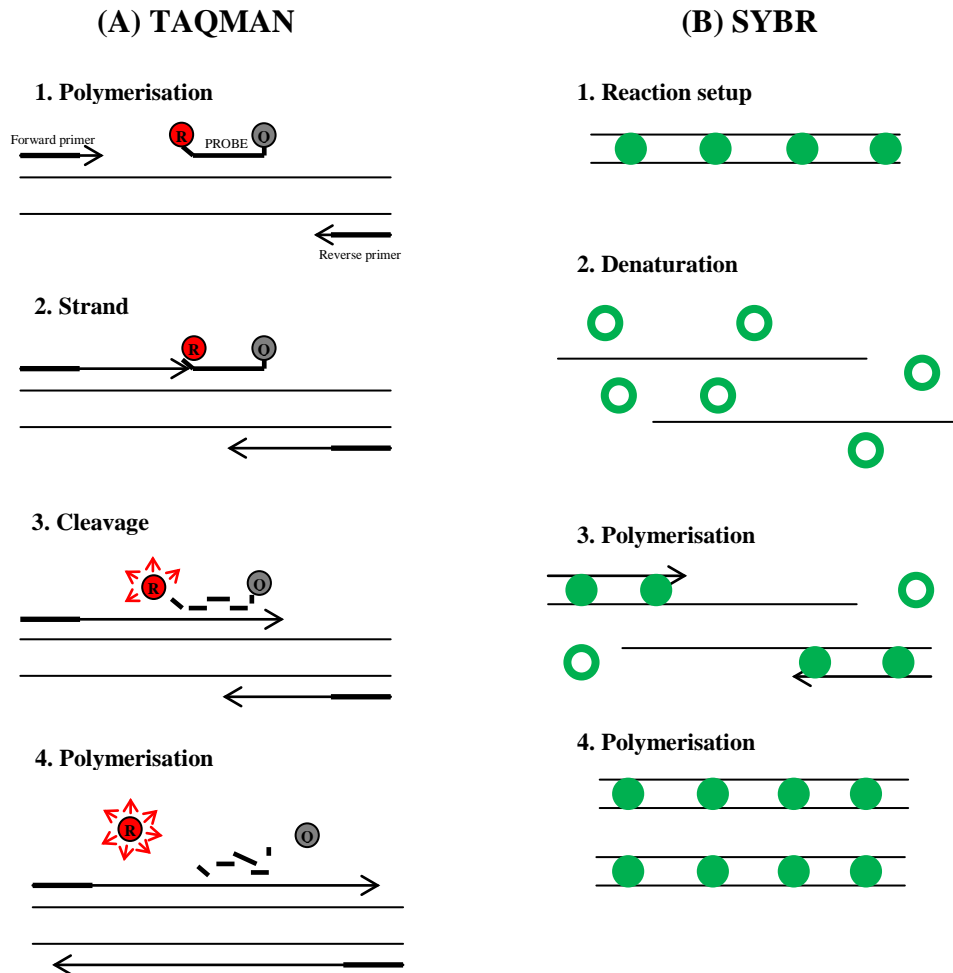
Figure 1.9: Comparison of Taqman and SYBR green methodologies – **(A) Taqman**: 1) A fluorescent reporter (R) dye and a quencher (Q) are attached to the 5' and 3' ends of a Taqman probe respectively. 2) When the probe is intact, the reporter dye emission is quenched. 3) During each extension cycle, the DNA polymerase cleaves the reporter dye from the probe. 4) Once separated from the quencher the reporter dye emits its characteristic fluorescence. **(B) SYBR green**: 1) The SYBR green II dye fluoresces when bound to double-stranded DNA. 2) When the DNA is denatured the SYBR green dye is released and the fluorescence is drastically reduced. 3) During extension, primers anneal and PCR product is generated. 4) When polymerisation is complete, SYBR green dye binds to the double-stranded product, resulting in a net increase in fluorescence detected by the machine. Figure from 'Absolute Quantitation using Standard Curve' (Applied Biosystems).

The Taqman method of qRT-PCR utilises a probe which is initially quenched to restrict fluorescence. Both the primers and probe bind to specific sites on the mRNA during the polymerisation step. As the polymerase is synthesising a copy of the mRNA, it breaks down the probe. The probe consists of a nucleotide sequence with a fluorescent reporter dye on one end and a light quencher on the other. In the probe's natural state, the fluorescent reporter is quenched so only a faint background level of fluorescence is detected. Once the probe is broken apart by the polymerase, the fluorescence reporter is released and in the absence of the quencher, is detectable by the qRT-PCR fluorescence readers. SYBR green dye binds non-specifically to double stranded DNA and therefore does not require a specific probe. The method is much cheaper than Taqman but is less specific. Only a single gene (primer pair) can be analysed in one reaction reducing the accuracy of the method over Taqman. A diagram showing the process of Taqman and SYBR green qRT-PCR is shown in Figure 1.9.

For both Taqman and SYBR green, the point at which the level of fluorescence is significantly different from the background (fluorescence threshold) is used to compare between samples. This point is called the cycle threshold (C_t) and is the point at which the signal passes the fluorescence threshold. The lower the C_t at which the sample can be identified above the background, the more mRNA is present and hence the more induced the gene is. For example, a sample treated with a high concentration of TCDD would have CYP1A1 mRNA levels at a higher level producing a lower C_t than a vehicle control. In this project, two reference genes will be run alongside CYP1A1 to allow normalisation between samples. Unlike CYP1A1, these genes are unaffected by the treatment of the AhR activating compounds so are expected to give approximately the same C_t in every experiment.

1.5.3 Viral infection

In this project a retroviral expression assay was used to allow creation of a target cell line expressing an exogenous gene. The gene of interest is isolated and cloned into a pRevTRE vector (via subcloning into pGEM-T). The vector is then transfected into a specialised packaging cell (PT67) which contains all of the genes required to synthesise a virus. The cell line is specifically designed for easy vector transfection and has all of the genes required to produce a virus (containing the vector DNA). The cell then produces a replication-defective virus which can be used to infect the target cell line. This virus can then infect other cells but does not contain the genes necessary to replicate itself and re-infect after the initial infection (Figure 1.10A). For successful transcription of the gene of interest, the assay requires dual vectors, one containing the gene of interest and the other containing the initiator sequence that would begin transcription from the first vector. Transcription of the gene of interest in the host cell requires both vectors. Initially a tTA (transactivator) regulatory element is encoded from the pRevTet-Off vector which binds to the Tet-response element (TRE) on the pRevTRE vector in the absence of tetracycline (Tc) or its derivative doxycycline (Dox). Binding of the tTA to this TRE site induces transcription of the gene of interest and is reduced in a dose dependent manner as Tc or Dox is added to the medium (Figure 1.10B).
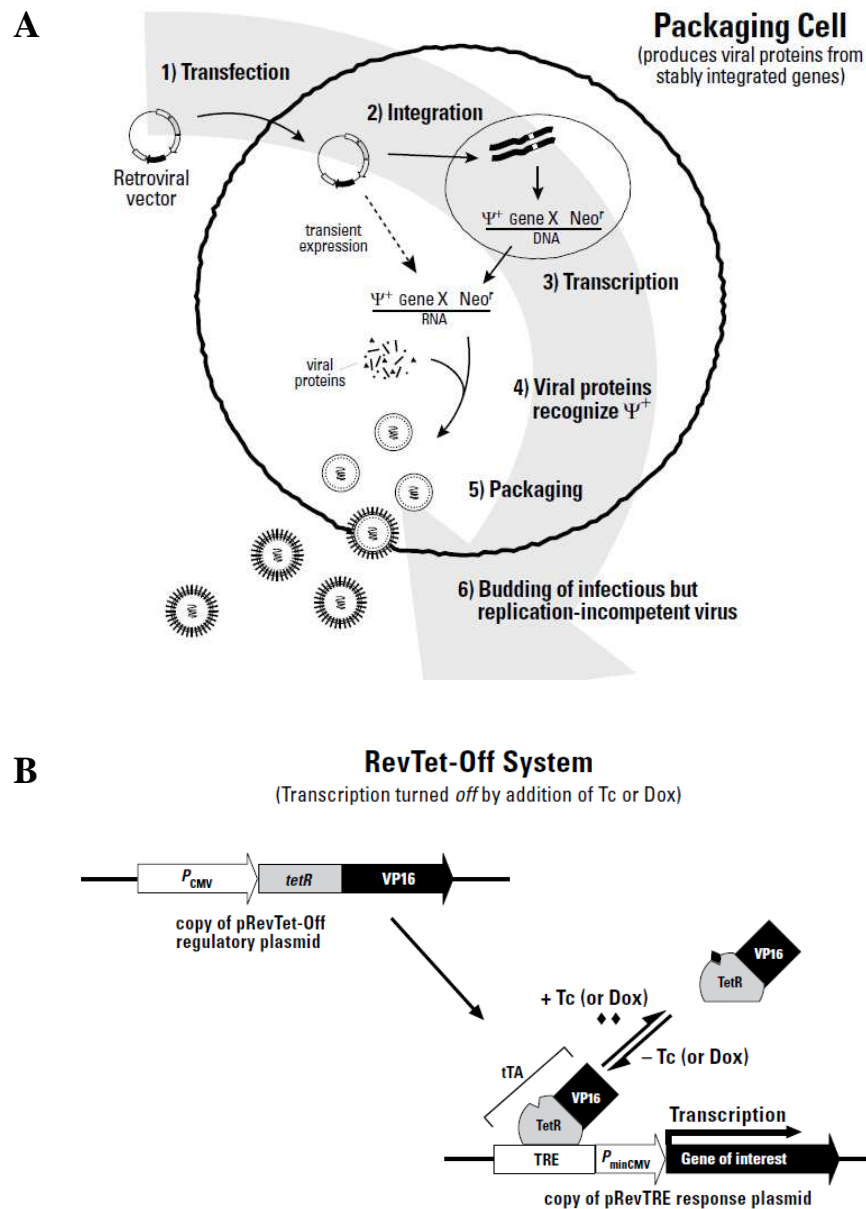
Figure 1.10: Summary of viral production and expression – **(A) Mechanism of packaging of infectious, replication incompetent, retroviral particles**. The vector is transfected into the cell[1], where it integrates into the DNA of the packaging cell[2], which contains the necessary genes required to produce a virus (pol: reverse transcriptase, integrase; gag: core structural proteins; env: coat glycoproteins) and transcription begins[3]. Viral proteins in the cell recognise the packaging signal (ψ) from the vector and begin viral particle formation[4]. This produces an infectious but replication incompetent virus which will be used to infect the target cell line[5]. **(B) Mechanism of pRevTet-Off gene expression.** Both vectors, pRevTet-Off and pRevTRE are required to be successfully integrated into the target cell line before transcription of the gene of interest can occur. The TRE is located upstream of the viral promoter which is silent when not activated by pRevTet-Off. The tTA (pRevTet-Off) binds the TRE and initiates transcription (in the absence of doxycycline). Both figures were taken from the RevTet System User Handbook.

1.5.4 Measurement of concentration

1.5.4.1 Gas Chromatography (GC)

The concentration of compounds can be measured using Gas chromatography (GC)/Mass spectrometry (MS). Sample (in nonane vehicle) introduction into the GC is carried out by injection into a PTV (programmed temperature volatilisation) injector which is initially held a little above ambient temperature (50°C) and programmed for constant helium flow. This combination of temperature and pressure forces the nonane to vaporise, leaving the compounds bound to the glass insert inside the injector. After removing the nonane (~3 min), the injector is heated to 330°C-350°C to volatilise the dioxin-like compounds. Under the pressurised flow of helium gas the compounds are transferred to the front of the GC column which is initially held at 60°C, a relatively cool temperature which allows focussing of the compounds for enhanced separation. When this process is completed, the temperature is increased in programmed stages in order to allow the compounds to traverse the length of the GC column. The rate at which the compounds move down the column depends on the interaction of each compound with the mobile phase of the GC column and on their individual boiling points. Even compounds of the same molecular weight will have a slightly different boiling point depending on their molecular arrangement therefore it is possible to separate the compounds for individual analysis by MS.

1.5.4.2 Mass spectrometry (MS)

Once leaving the GC, the compounds, separated by time, are sequentially introduced into the MS via a GC/MS interface which allows transfer into the ionisation source. The MS is in a vacuum so that the compounds can be detected without interference from molecules in the atmosphere. The compounds enter the ionisation chamber where they are bombarded by electrons produced by a special filament. The electrons produced are energised using an anion located on the opposite side of the chamber and collide with the compounds of interest

ionising them. Once an electron collides with a molecule of the compound, it breaks it, producing a range of different sized fragments of different polarities depending on the energy imparted to the electrons. In the current application, only positively charged ions are of interest and must therefore be selectively progressed through the mass analyser. In the initial stage this is done using a positively charged lens called a repeller which deflects positive ions away toward the next stage of the machine, attracting negative ions in the process (Figure 1.11).

Electro static filtration 1

Electromagnet

Electro static filtration 2

Magnifier and recorder

Electrons pulled through the sample, causing collisions which fractures the compounds

Anion which draws electrons towards it

From GC

Direction of sample from GC

Ionisation chamber

Deflector which pushes positively charged ions way from it

Filament that produces electrons

Figure 1.11: Mass spectrometer –Volatilised compound (positive ion) is bombarded by electrons then accelerated around the spectrometer, filtering out any fragments. The chamber of a mass spectrometer has been expanded**:** the sample enters the chamber, bombarded with electrons producing positive ions which are then deflected away towards the recorder.

After leaving the ionisation chamber the positive ions are directed through a series of focussing lenses and pass though a narrow slit into the mass analyser. Here, under the influence of electrostatic and magnetic fields, the ions accelerate through the analyser and separate based on their individual masses and mass to charge (m/z) ratios. The energies required to focus these ions are measured in order to allow computation of the accurate mass of each fragment. When the identity of the compound is known, as in the present case, a more

selective measurement process called selected ion recording is used. In this technique the MS is programmed to isolate and measure only the specified ions (which are derived from the compounds of interest). This results in a tremendous increase in measurement sensitivity. Selected ions collide with the recording unit, a photomultiplier, which magnifies the primary signals from the ion fragments before detection on a photosensitive plate. The response per retention time and molecular weight is recorded.

1.6 Aims

The main aim of this work is to improve our overall understanding of the mechanism of AhR activation by environmental pollutants and then apply this understanding to risk assessment. This includes further understanding of the structure-activity relationships of AhR ligands, species differences in the potency of AhR ligands and how risk assessment can be applied to other environmentally abundant AhR compounds**.**

Calibration of a qRT-PCR-based method to detect either agonism or antagonism - Measurement of the agonistic properties of a putative highly potent AhR ligand (AZ1) and characterisation of a known AhR antagonist (CH22319) will allow full calibration the measurement methods.

Measurement of the potency of newly identified dioxin-like compounds - Measure the potency and investigation of the structure-activity relationships of a range of mixed halogenated dibenzo-*p*-dioxins, dibenzofurans and biphenyls, in rat and human.

Accurate measurement of the agonistic and antagonistic properties of putative partial agonists - The agonistic and antagonist properties of three environmentally abundant mono-*ortho*-substituted PCBs will be determined as well as their effect on the TEQ.

Investigating structure activity relationships of AhR ligands between rat and human - The species-specific difference in the agonistic and antagonistic properties of novel 2-amino-isoflavones will be investigated.

Investigating species differences between rat and human with respect to agonism and antagonism - The AhR of rat and human will be isolated and transfected into an AhR deficient mouse cell line to directly compare between the two receptors. The new cell lines will then be treated with TCDD and 5F 203 to illustrate any differences from wild-type cells.

2. Method

2.1 Materials

2.1.1 Reagents and kits

- pGEM®-T Vector system (Promega; #A3600)

- RevTet-off™ System (Clontech; #631020)

- Absolutely RNA® Miniprep Kit (Stratagene #400800)

Lysis buffer-β-ME:	**RNase-Free DNase I:**
- 0.7 µl β-ME	- 50 µl of DNase Digestion Buffer
- 100 µl Lysis Buffer	- 5 µl of reconstituted RNase-Free DNase I

- High capacity RNA-to-cDNA kit (Applied Biosystems; #4387406)

- Extensor Hi-Fidelity PCR Master Mix (ABgene; AB-0792)
- Taqman® gene expression master mix (Applied Biosystems; #4369016)
- Brilliant SYBR Green QPCR master mix (Stratagene; #600548)

- Microamp fast optical 96-well plates (0.1 ml) with covers (Applied Biosystems #4346906 and #4360954)

- GeneJuice (Novagen; #70967-5)

- QIAquick gel extraction kit (Qiagen; #28704)

Buffer PE:	**Buffer PB:**
- 10 ml Buffer PE	- 30 ml Buffer PB
- 40 ml 100% Ethanol	- 120 µl pH indicator I

- QIAprep Spin Miniprep kit (DNA isolation; Qiagen; #27104)

Buffer P1:	**Buffer PE:**
- 20 ml Buffer P1	- 6 ml Buffer PE
- 200 µl RNase A	- 24 ml 100% Ethanol
- 20 µl LyseBlue reagent	

- SalI HF (Biolabs; #R3138S)
- HindIII (Biolabs; #R0104S)
- 10x T4 ligase (Biolabs; #M0202S)

- Quick-load®1 kbp DNA ladder (Biolabs; #N0468L)
- Quick-load®100 bp DNA ladder (Biolabs; #N0467L)

2.1.2 Solutions, buffers and medium

- JM109 E. coli bacterial cells (glycerol stock, Promega; #P9751)
- H4IIE rat liver cell line (ATCC; #CRL-1548)
- PT67 cell line (Clontech; #631510)
- Tao BpRc1 cell line (ATCC; #CRL-2218)

- Cell freezing medium-DMSO 1x (Sigma-Aldrich; #C6164)
- Dulbecco's phosphate buffered saline (Sigma #D8537)

- **Complete minimum essential medium (cMEM)**
  - 440 ml Minimum essential medium (Sigma #M2279)
  - 50 ml Fetal bovine serum (Sigma #F7524)
  - 5 ml 200 mM L-glutamine, 10,000 U/ml Pencillin and 10,000 µg/ml Streptomycin solution (Final conc. 2 mM, 100 U/ml and 100 µg/ml, respectively; Sigma #G1146)
  - 5 ml Non-essential amino acids (Sigma #M7145)

- **Complete Dulbecco's modified Eagle's medium (cDMEM)**
  - 435 ml Dulbecco's modified Eagle's medium (High glucose 4.5 g/L; Sigma #D5671)
  - 50 ml Tet system approved fetal bovine serum (Clontech #631101)
  - 5 ml 200 mM L-glutamine, 10,000 U/ml Penicillin and 10,000 µg/ml Streptomycin solution (Final conc. 2 mM, 100 U/ml and 100 µg/ml, respectively; Sigma #G1146)
  - 5 ml 200 mM L-glutamine (2 mM final concentration; Sigma #G7513)
  - 5 ml 100 mM Sodium pyruvate (1 mM final concentration; Sigma #S8636)

- **1x Trypsin-EDTA solution (trypsin)**
  - 1 ml 10X Trypsin-EDTA solution (Sigma #T4174)
  - 9 ml Dulbecco's phosphate buffered saline (Sigma #D8537)

- **De-proteinated water (DEPC treated water):**
  - 1 ml Diethyl Pyrocarbonate
  - 9 ml Ethanol
  - Distilled water to make up to 1 Litre (autoclaved after mixing to neutralise)

- **TfbI:**
  - 0.588 g Potassium acetate (30 mM)
  - 2.42 g Rubidium chloride (100 mM)
  - 0.294 g Calcium chloride (10 mM)
  - 2.0 g Manganese chloride (50 mM)
  - 30 ml Glycerol (15% v/v)
  - Distilled water up to 200 ml

  (pH 5.8 with dilute acetic acid)

- **TfbII:**
  - 0.21 g MOPS (10 mM)
  - 1.1 g Calcium chloride (75 mM)
  - 0.121 g Rubidium chloride (10 mM)
  - 15 ml Glycerol (15% v/v)
  - Distilled water to make volume up to 100 ml

  (pH 6.5 with dilute sodium hydroxide)

- **ALP Solution I:**
  - 50 mM Glucose
  - 25 mM Tris. Cl (pH 8)
  - 10 mM EDTA (pH 8)

  - Kept at 4°C

- **ALP Solution II:**
  - 0.2 M NaOH
  - 1% SDS

- **TNES buffer (DNA extraction)**
  - 18.1 mg Tris, pH 7.5 (10mM)
  - 350.6 mg NaCl (400mM)
  - 3 ml 0.5 M EDTA (100mM)
  - 900 µl 10% SDS (0.6%)
  - Distilled water up to 15 ml

- **10 mg/ml G418 antibiotic**
  - 0.5 g G418 powder (Clontech #80561)
  - 35 ml DMEM (Sigma #D5671 – without supplements)

  (Note: The effective weight is 0.7 g per 1 g of powder (Clontech Revtet manual); Filter sterilised, 0.2 µM filter)

- **50 mg/ml Doxycycline hyclate**
  - 0.5 g Doxycycline hyclate powder (Sigma #D9891)
  - 10 ml distilled water
  (Filter sterilised, 0.2 µM filter)

- **MN stock buffer**
  - 25 mM MOPS
  - 0.02 % Sodium Azide.
  (pH 7.5 at 4°C)

- **ALP Solution III:**
  - 60 ml Potassium acetate
  - 11.5 ml Glacial acetic acid
  - 28.5 ml dH$_2$O
    (5 M acetate, 3 M potassium)

- **Orange G 10x**
  - 30 ml glycerol
  - 1 ml 1 M Tris pH 7.6
  - 0.05 ml 1 M EDTA
  - 200 mg Orange G

- **50 mg/ml Hygromycin B antibiotic**
  - 0.5 g Hygromycin B powder (Sigma #H3274)
  - 10 ml DMEM (sigma #D5671 – without supplements)

  (Filter sterilised, 0.2 µM filter)

- **1 mg/ml Hexadimethrine bromide (Polybrene®)**
  - 20 mg Hexadimethrine bromide powder (Sigma #H9268)
  - 18 mg NaCl
  - 20 ml distilled water

  Autoclaved

- **MEN stock buffer**
  - MN buffer
  - 1 mM EDTA.
  (pH 7.5 at 4°C)

- **1x Agarose gel**
  - 0.3 g Agarose
  - 0.3 ml 10% SDS
  - 30 ml 1x TBE buffer

- **MDENG stock buffer (pH 7.5, 4°C)**
  - MEN buffer
  - 10 % (w/v) glycerol
  - 1 mM dithiothreitol (DTT).
  (DTT is freshly supplemented to the buffer before the protein preparation).

- **5x Bradford dye concentrate**
  - 100 mg Coomassie brilliant blue G-250
  - 50 ml 95% Ethanol
  - 100 ml Phosphoric acid
  - Distilled water up to 200 ml

- **10x TBE buffer**
  - 108 g Tris
  - 55 g Boric Acid
  - 40 ml 0.5 M EDTA pH 8
  - Distilled water to make up to 1 L
  (Working concentration was 1x dilution)

- **LB plates with ampicillin**
  - 1 L LB medium
  - 15 g agar
  - 100 µg/ml (final) Ampicillin

  Cool below 50°C before addition of Amp.

- **LB medium**
  - 10 g Bacto-tryptone
  - 5 g Bacto-yeast extract
  - 5 g NaCl
  - 1 L distilled water

  pH adjusted to 7.0 with NaOH

- **SOC medium**
  - 2 g Bacto-tryptone
  - 0.5 g Bacto-yeast extract
  - 1 ml 1M NaCl
  - 0.25 ml 1M KCl
  - 1 ml 2M Mg^{2+} stock, filter sterilised
  - 1 ml 2M glucose, filter sterilised
  - 97 ml distilled water

2.1.3 Compounds

2,3,7,8-Tetrachlorodibenzo-*p*-dioxin **(TCDD;** purity 99%) was purchased from Cerilliant Cambridge Isotope Laboratories (Middlesex, UK). A 155 µM top stock of TCDD was made with dimethyl sulfoxide (DMSO) which was kept at room temperature and protected from light. Further dilution of TCDD was done in DMSO to 10 µM which was aliquoted into eppendorf tubes and stored at -20°C. All further dilutions of TCDD were made using conditioned medium (See section 2.4.1), giving a final DMSO concentration of <0.02%. 2,3,3',4,4'-pentachlorobiphenyl **(PCB 105;** purity 98%), 2,3',4,4',5-pentachlorobiphenyl **(PCB 118;** purity 98%), 2,3,3',4,4',5-hexachlorobiphenyl **(PCB 156;** purity 98%) was purchased from Cambridge Isotope Laboratories (Massachusetts, USA). A 10 mM top stock was made by dissolving the PCB in DMSO. The solution was then stored at -20°C.

The mixed halogenated compounds were a kind gift from Dr Alwyn Fernandes and Dr. Martin Rose (The Food and Environment Research Agency, UK). They were previously obtained either from Wellington Laboratories Inc. (Ontario, Canada) or from Cambridge Isotope Labs (Massachusetts, USA). Where required the standards were solvent exchanged to DMSO and the concentrations verified. The chemical names for the 3,3',4,4',5-substituted-mixed halogenated biphenyls have been published previously (Falandysz *et al.*, 2012). The compounds were dissolved in DMSO up to a concentration of 100 µM or 1 mM.

2-methyl-2H-pyrazole-3-carboxylic acid (2-methyl-4-o-tolylazo-phenyl)-amide (**CH223191**; purity 95.71%) was purchased from Calbiochem (Nottingham, UK). A 10 mM top stock was made by dilution into DMSO. The solution was stored at -20°C and protected from light.

The AZFMHCs were a kind gift from Dr. Mark Furber (AstraZeneca Mölndal, Sweden). The full synthesis of the compounds has been published previously (Abbott *et al.*, 2002). AZ1 was dissolved in DMSO to make a concentration of 1 µM. AZ2, 3 and 4 were dissolved in purified water at concentrations of 3 µM – 10 µM.

- 3-Hydroxy-2-[4-(trifluoromethyl)phenyl]-[1,2,3]-triazolo[1,5-*a*]quinolinium hydroxide (**AZ1**)
- 4-Methyl-3-hydroxy-2-[4-(trifluoromethyl)phenyl]-[1,2,3]triazolo[1,5-*a*]quinoxalinium hydroxide (**AZ2**)
- 4-Methyl-3-hydroxy-2-[4-(methyl)phenyl]-[1,2,3]-triazolo[1,5-*a*]quinolinium hydroxide (**AZ3**)
- 4-Amine-3-hydroxy-2-[4-(trifluoromethyl)phenyl]-[1,2,3]triazolo[1,5-*a*]quinoxalinium hydroxide (**AZ4**)

2-(4-Amino-3-methylphenyl)-5-fluorobenzothiazole (**5F 203**) was synthesised at the Cancer Research Laboratories, University of Nottingham with the full synthesis published previously (Hutchinson *et al.*, 2001). 5F 203 was dissolved in DMSO to a concentration of 10 mM.

2-Amino-3-(4-chlorophenyl)-7-methoxychromen-4-one (**Chr-13**) and 6-chloro-3-(4' methoxy)phenylcoumarin (**Chr-19**) were a kind gift from Prof. Gianfranco Balboni (University of Cagliari, Italy). Chr-13 can be purchased from Life Chemicals (Braunschweig,

Germany) and Chr-19 was synthesised as reported by Quezada *et al.* (2010). Chr-13 and Chr-19 were prepared as 100 mM and 30 mM solutions, respectively, in DMSO.

The radio-ligand [^{3}H]-2,3,7,8-tetrachlorodibenzo-*p*-dioxin (**[^{3}H]-TCDD)** was purchased from ChemSyn Laboratories (Kansas, USA) and had a specific activity of 29.7 Ci/mmol. 3,4,3',4'-Tetrachloroazoxybenzene (**TCAOB**) was purchased from AccuStandard, USA and dissolved to 3 mM in MDENG buffer. It may be important to note that the [^{3}H]-TCDD is approximately 70% of the original specific activity as the compound was purchased at least 5 years ago. Therefore the compound now has a specific activity of ~20.79 Ci/mmol.

2.1.4 Gas Chromatography/Mass Spectrometry (GC/MS) analysis

Research from other authors regarding the agonistic and antagonist properties of the three PCBs has given widely different estimates of potency (Van den Berg *et al.,* 1998, 2006). One possible reason for this discrepancy is that the compounds were actually contaminated by other, more potent AhR agonists. Therefore the stock aliquots of the three PCBs used were tested to confirm that they contained no contamination. Gas chromatography/mass spectrometry (GC/MS) was conducted at FERA (Sand Hutton, York). Samples were transferred from DMSO into Acetone then diluted again in Nonane. An aliquot was taken from this for analysis along with the addition of ^{13}C containing dibenzo-*p*-dioxins, dibenzofurans and PCBs to allow identification and quantitation. 10 µl of the samples (with ^{13}C compounds) was added into the injector by an automated dispensing robot. The gas chromatograph (HRGC, Agilent) was fitted with a 60m x 0.25mm i.d. DB5-MS column which was temperature programmed from 60°C to 330°C in 3 stages and the compounds were separated (see section 1.5.4.1 for more details). Compounds were then transferred to the high resolution mass spectrometer (HRMS; Autospec Premier Series, Micromass, UK) which characterises molecules based on their exact molecular weight and structure (see section

1.5.4.2). The HRMS used electron ionisation (EI) mode with selected ion monitoring (SIM). An internal control of perfluorokerosene (PFK; Fluka), which splits into known fragments, was used to calibrate the mass axis of the instrument. The raw data from the HRMS was analysed with MassLynx software to allow more accurate identification and quantitation of the contaminants as well as the compound itself. Toluene and nonane were run through after the samples to remove any residual material and ensure that the GC/MS system was free of any carryover between injections. The actual work was carried out by staff at FERA (Sand Hutton, UK) in the presence of the author.
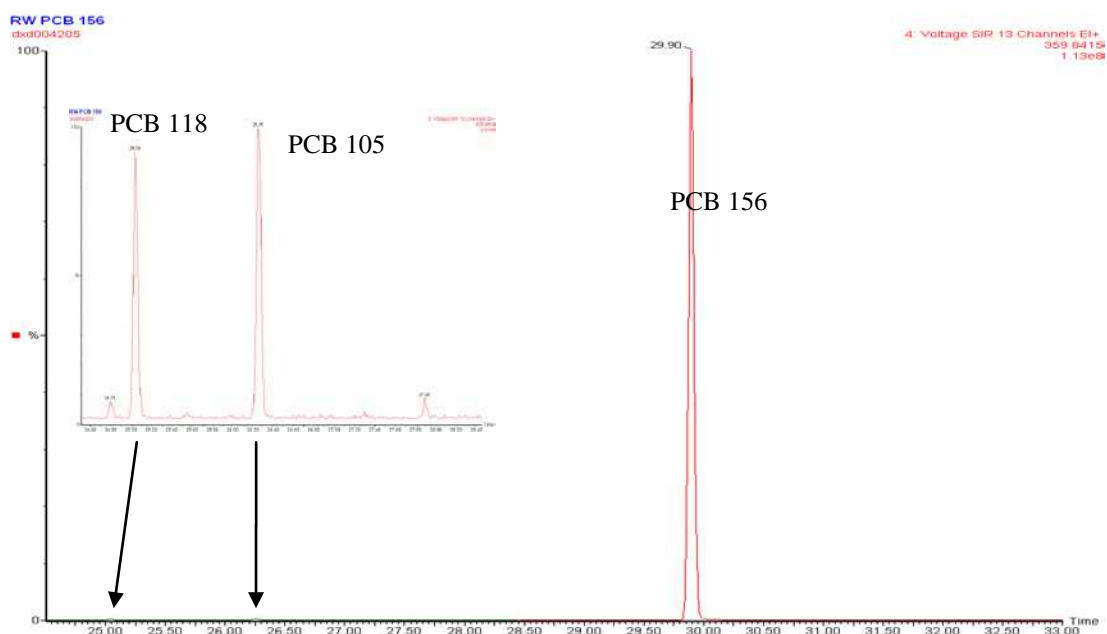
Figure 2.1: Graphical representation of the ratio of compounds in the PCB 156 stock – The data was collected using a gas chromatograph with attached mass spectrometer. The graph shows a magnified view of the levels of PCB 105 and PCB 118 compared against PCB 156.

The graph in Figure 2.1 shows the comparison of the amount of PCB 156 against the levels of contaminants: PCB 105 and PCB 118. It shows that although there is contamination present, the levels are insignificant in comparison to PCB 156. The results of this analysis can be seen in Table 2.1 with an example of the graphical representation of the data peaks shown in Figure 2.1.

Contaminant (pg/µl)	PCB 105	PCB 118	PCB 156
PCB 77	<0.05	0.69	<0.05
PCB 81	-	-	-
PCB 126	-	-	<0.05
PCB 169	<0.05	<0.05	-
PCB 123	<0.05	-	-
PCB 118	0.57	121.42	0.26
PCB 114	<0.05	0.10	<0.05
PCB 105	116.93	<0.05	0.34
PCB 167	<0.05	<0.05	<0.05
PCB 156	0.10	0.24	188.84
PCB 157	0.14	<0.05	-
PCB 189	-	<0.05	<0.05

Table 2.1: GC/MS analysis of the three PCB stock aliquots – Analysis was conducted using gas chromatography with mass spectrometry. The table shows the concentration of the most common PCBs including confirmation of the concentration of the actual PCB. Concentrations are shown in pg/µl. In most cases no compound could be found or only a small trace.

The main source of contamination that was found in the samples was actually PCB 105, PCB 118 and PCB 156. Further to this, the PCB 156 stock was found to contain trace levels of PCB 126 (<3777-fold less than PCB 126) which, according to the WHO TEF values, is more than 3000-fold more potent than PCB 156 (Van den Berg *et al.,* 2006). This could therefore have a small impact on the potency of PCB 156, inducing CYP1A1 mRNA above the normal levels achievable by this compound. The other two compounds were found to be clean of highly potent AhR agonists however the trace amounts of PCB 77, PCB 156 and PCB 157 could still have an agonist effect at the higher concentrations if they exhibit an additive response. No detectable trace of any of the most potent compounds such as TCDD, or any of the other potent PCDD/PCDF congeners was observed during this analysis.

The two 2-amino-isoflavone compounds, Chr-13 and Chr-19, were also tested. The same protocol was used but with the addition of a clean-up step before conducting the GC. The

dibenzo-*p*-dioxin and PCB ^{13}C standards were added to the two samples. The solutes were then passed through mini-columns consisting of silanised glass wool, sodium sulphate, acid modified silica gel topped with another thin layer of sodium sulphate. Samples were rinsed through the column using hexane. Concentrated samples were then run through the GC. The purpose of this step was to remove any reactants from the mixture which may bind and damage the GC coil. Chr-19 was found to be free of contamination (or at least traces of contamination were below the level of detection). However, a small trace of PCB 118 contamination (120 ng/ml; 0.3 nM) was found at the highest concentration of Chr-13 (100 µM). Based on the data collected on this compound (Figure 3.19) it was concluded that <0.3 nM PCB 118 would have no effect on the potency of Chr-13 to agonise or antagonise.

2.1.5   Gene identification

The GenBank mRNA numbers for the genes used in this study are shown in Table 2.2.

	Rat	**Mouse**	**Human**
AhR	NM_013149.2	NM_013464.4	NM_001621.4
Arnt	NM_012780.1	NM_001037737.2	NM_001668.3
β-actin	NM_031144	NM_007393	NM_001101
CYP1A1	NM_012540	NM_009992	NM_000499
CYP1A2	NM_012541	-	-
CYP1B1	NM_012940	-	-
Hsp90	NM_175761.2	NM_010480.5[a]	NM_005348.3
p23	NM_001130989.1	NM_019766.4	NM_006601.5
XAP2	NM_172327.2	NM_016666.2	NM_003977.2

Table 2.2: GenBank reference numbers of all the genes discussed in this project – Reference numbers were last accessed on the 27/5/12. [a]Mouse Hsp90 alpha was used for comparison.

2.1.6   Cell Culture

2.1.6.1 Cell culture maintenance

Cells (described below) were passaged every 2-3 days into a new 25 cm^2 flask with fresh cMEM or cDMEM. To passage the cells, the old medium was removed and the cells were

washed with 2.5 ml PBS. The PBS was then removed and 1.5 ml 1x trypsin-EDTA was then added to the cells and incubated for 2 min at 37°C, 5% CO_2 to separate the cells from the base of the flask. After the allotted time, 3.5 ml fresh complete medium was added to the trypsin/cell mixture to neutralise the trypsin. A 1 ml aliquot of this was transferred to 9 ml of fresh complete medium in a new flask. Cells were incubated at 37°C, 5% CO_2 in an incubator (Sanyo). All work was done in a class II Microbiological safety cabinet (Walker, Derbyshire), using sterile equipment with work surfaces cleaned with 1% Trigene to prevent contamination of the cells.

2.1.6.2 Freezing cells for storage

Cells were processed as discussed in section 2.1.6.1, however, instead of being transferred to a new flask after neutralisation of the trypsin, the cell mixture was added to a 15 ml centrifuge tube and centrifuged for 5 min at room temperature (RT; 20 - 25°C) and maximum speed (Max; 14,000 rpm) in an eppendorf 5417R centrifuge (used in all experiments unless otherwise stated), to form a cell pellet. The medium was removed and the cells were re-suspended in 1 ml 1x cell freezing medium-DMSO. This cell mixture was added to a cryotube, frozen in a Nalgene Cryo 1°C freezing container at -80°C (-1°C/min rate of freezing; to prevent cell damage) and then stored at -196°C until required.

2.1.6.3 H4IIE Rat liver cells

Cells reached complete confluence within 6 days with a concentration of ~2 x 10^5 cells/well from a starting concentration of 1 x 10^2 cells/well (Wall, 2008). Cells were grown in cMEM and incubated at 37°C, 5% CO_2. The cells were passaged every 3 days as described in section 2.1.6.1.

2.1.6.4 MCF7 Human breast carcinoma cells

The MCF7 human breast carcinoma cells were a kind gift from Dr Tracey Bradshaw (Centre for Biomolecular Science, University of Nottingham). Cells have been previously show to reach confluence after 7 days starting from a concentration of 2.5 x 10^3 cells/well with total confluence providing 1 x 10^5 cells/well (Bazzi, 2008). Cells were grown in cMEM and incubated at 37^oC, 5% CO_2. The cells were passaged every 3 days as described in section 2.1.6.1.

2.1.6.5 RetroPack PT67 packaging cell line

The packaging cell line, PT67, was derived from the NIH/3T3 cell line. It contains three viral genes from the Moloney murine leukaemia virus (MoMuLV); *pol, gag and env*, integrated into its genome which are necessary for virus replication and packaging. A virus packaged by these cells can enter the host cell in two different ways, either through the RAM1 or GALV receptors. The cells were purchased from Clontech Laboratories Inc, USA and upon receipt, were grown (section 2.1.6.1), separated into aliquots and stored in liquid nitrogen (-196^oC) for future use as previously discussed in section 2.1.6.2. Cells were passaged as described previously in section 2.1.6.1. The cell line does not normally demonstrate any significant hygromycin or G418 antibiotic resistance. The cells were grown in cDMEM and kept in a 5% CO_2 atmosphere at 37^oC.

2.1.6.6 Taoc1BP^{r}c1 AhR-defective cell line

The AhR-defective Taoc1BP^{r}c1 cell line (BpRc1; AhR-defective clone, AhR-D) was created in the lab of Whitlock and co-workers (Miller *et al.,* 1983). The clones were created using Hepa1c1c7 mouse cells which in turn were derived from the Hepa-1 cell line (Hankinson, 1979). TCDD treated hepa1c1c7 cells were shown to be induced by 127-fold over vehicle control. The BpRc1 cells have a basal CYP1A1 level of 10-fold less than wild-type

Hepa1c1c7 cells and an induced level of CYP1A1 (by TCDD) which is 20-fold less than wild-type cells (Miller *et al.,* 1983). The cell line was purchased from ATCC (LGC standards). The cells were grown in cDMEM (section 2.1.6.1) and kept in a 5% CO_2 atmosphere at $37^{o}C$. Before experimentation, several aliquots of cells were frozen in liquid nitrogen ($-196^{o}C$) in cell freezing medium-DMSO (1x). Pilot experiments using the two antibiotics used for selection of vector-integrated cells, G418 and hygromycin, were conducted on the cell line before exposure to the viruses to establish the optimal concentrations (See section 2.5.6.2).

2.1.6.7 NIH/3T3 mouse embryonic fibroblast cell line

The cells were first isolated from desegregated NIH Swiss mouse embryo fibroblast cell line. The cells were a kind gift from Dr Andrew Johnson (School of Biology, University of Nottingham). The cells were grown in cDMEM. It was recommended by the Johnson lab that the cells should be grown in medium containing 1% non-essential amino acids and β-ME. Research into the cell line showed that these additional additives were not required (ATCC cell lines). To confirm this, cells were grown in cDMEM with the addition and absence of non-essential amino acids and β-mercaptoethanol (β-ME) over a period of 9 days (3 passages). Visual inspection showed no difference in cell growth or health. It was therefore concluded that the additional additives were not required. ATCC encourage the use of calf bovine serum (CBS; serum taken from <20 day old calves) as opposed to fetal bovine serum (FBS; serum taken from unborn fetus) (ATCC cell lines), however the Johnson lab recommended FBS. Therefore the cells could be grown in exactly the same medium as the BpRc1 cells and the PT67 packaging cells. The cells were used to estimate the titer of the viruses produced by the stable PT67 virus producing cell lines reducing variables between the three cell lines.

2.1.6.8 JM109 E.coli cells

In order to identify successful AhR containing plasmids, JM109 *Escherichia coli* (*E. coli*) chemically competent cells were transformed with the vector:insert. Lysogeny broth (LB medium) is a nutritionally rich media used for the growth of the bacteria (Bertani, 1951). The medium contains vitamins and minerals necessary for successful bacteria growth and is made by adding 25 g LB to 1 L of purified water followed by autoclaving. The JM109 cells do not normally demonstrate ampicillin resistance. Chemically competent cells were created using the method shown in section 2.1.6.9.

2.1.6.9 Producing chemically competent JM109 bacterial cells

A single bacteria colony (grown from stock, Promega; #P9751) was grown in 1 ml LB medium at 37^oC overnight with aeration. This was then added to 100 ml of fresh LB medium and incubated until the optical density (O.D.) at 595 nm was ~0.6 which took about 2-3 hours. All the reagents were kept on ice and the procedure was done a quickly as possible. The cells were centrifuged (4000 g, 5 min, 4^oC) to obtain a pellet of the bacterial cells. The cells were re-suspended in 40 ml of ice cold TBF1 solution and incubated for 5 min on ice. The cells were then centrifuged a second time (4000 g, 5 min, 4^oC). The resulting pellet was re-suspended in 4 ml of TBF2 solution then incubated on ice for 1 hour. Aliquots of 150 μl were flash frozen in liquid nitrogen and stored at -80^oC for future use.

2.2 General molecular biology techniques

2.2.1 Gel electrophoresis

End-point PCR was conducted using a PCR thermocycler with the specific conditions and primer sequences of each reaction discussed in each section or figure legend (section 2.2.8). The 1x agarose gel was made as described in the materials (section 2.1.2). Generally a single gel would be run however two gels were run simultaneously for extraction work, one for gel

extraction and one for taking a photo. This was to avoid DNA damage to the PCR fragments caused by the UV from the camera. The RNA was loaded on the gel with 1x Orange G loading dye and compared against a 100 bp or 1 kbp DNA ladder (BioLabs, USA). The gels were run for 70 min at 90 V. After electrophoresis, the gel was briefly washed then stained with 5 µl ethidium bromide for 20 min then washed again for 30 min in distilled water. A photo of the gel was taken using BioRad chemdoc UV camera.

2.2.2 Purification of DNA from mammalian cells

The cell DNA was isolated using the following DNA extraction method which uses a high salt buffer and proteinase K. The cells were pelleted by removing the conditioned medium after treatment and washing the cells with 60 μl PBS. Cells were then treated with 60 μl 1x trypsin-EDTA and left to incubate for 1 min at $37^{o}C$, 5% CO_2. 120 μl of conditioned medium was then added immediately to each well to dilute and neutralise the trypsin. The contents of each individual well was transferred to an eppendorf tube and centrifuged (5 min; RT, 6000 rpm), forming a cell pellet (remove supernatant). 300 µl TNES buffer and 17.5 µl proteinase K (10 mg/ml) were added to the cell pellet which was then left to incubate overnight at $55^{o}C$. The following day, 100 µl 5M NaCl was added and the mixture was vortexed for 15 sec. The cell mixture was centrifuged (5 min, RT, Max). The supernatant was transferred to a new eppendorf tube with 420 µl 95% ethanol. This was then centrifuged (10 min, $4^{o}C$, Max). The supernatant was removed and the remaining pellet (DNA) was washed with 100 µl 70% ethanol, centrifuged (1 min, RT, Max), then re-suspended in 50 µl of filtered UHP water.

2.2.3 RNAse treatment

The isolated DNA was incubated at $37^{o}C$ for 30 min with 2 µl of 10 µg/ml RNAse A. After incubation 4 µl of 3 M sodium acetate and 80 µl of 95% ethanol were added. This solution was incubated on ice for 10 min then centrifuged (5 min, RT, Max). The supernatant was

removed and the remaining pellet was washed with 70% ethanol. This was then centrifuged again (1 min, RT, Max) and the remaining DNA pellet was re-suspended in DEPC-treated water. The samples were frozen at -20°C.

2.2.4 Gel extraction

The product was run on a 1x agarose gel (section 2.2.1) then the band of interest was identified using a UV transilluminator UVP, extracted and purified using a QIAquick gel extraction kit (Qiagen). Briefly, the gel fragment was dissolved in buffer QG. Once bound to the filter membrane, the DNA was washed with 0.75 ml of buffer PE and centrifuged (1 min, RT, Max) before being eluted into an eppendorf tube. Finally 40 µl of elution buffer was added directly to the filter, left for 1 min then centrifuged (1 min, RT, Max).

2.2.5 Ethanol precipitation of DNA

The volume of the DNA sample was measured. A volume of half the original sample volume of 10 M NH$_3$Acetone was added to give a final concentration of 3.3 M. Then two times the sample original volume of 100% ethanol was added and vortexed thoroughly. This was then left at -20°C overnight. The following day, the sample was centrifuged (10 min, 4°C, Max) to form a pellet and the liquid was aspirated. 175 µl of 70% ethanol was then added and the samples were centrifuged again at (1 min, 4°C, Max). The liquid was then aspirated again and the sample was centrifuged (1 min, 4°C, Max) and any remaining ethanol was removed. The samples were left to air dry for 5 min then re-suspended in dH$_2$O and frozen at -20°C for further use.

2.2.6 DNA isolation (alkaline lysis protocol) from bacteria

Successful colonies were picked from the plate with a pipette tip and grown in 10 ml LB medium overnight in an aeration incubator (37°C). In order to perform the alkaline lysis protocol (ALP), an aliquot of 1.5 ml this bacteria was centrifuged (4 min, RT, 9000 rpm).

The supernatant was aspirated and the cell pellet was re-suspended in 100 µl of ALP solution I. Then 200 µl of ALP solution II was added and the sample was mixed by inverting the eppendorf tube 5 times. 150 µl of ALP solution III was added to the sample. The formulation of the three ALP solutions is shown in section 2.1.2. The tubes were then instantly inverted to mix the sample leaving a white curdled precipitate of protein and cellular membrane. This mixture was centrifuged (5 min, RT, Max) and the supernatant was decanted into a new eppendorf tube. 350 µl isopropanol was added to the supernatant and mixed. This was centrifuged (5 min, RT, Max) forming a white DNA pellet. The supernatant was removed and the pellet was washed with 175 µl of 70% ethanol then centrifuged again (1 min, RT, Max). The supernatant was removed and the remaining pellet was left to dry for 5 min. Finally the pellet was re-dissolved in 40 µl of DEPC treated water and frozen at -20°C. This method was taken from Sambrook *et al.* (1989).

2.2.7   DNA isolation (Qiagen) from bacteria

Once a positive colony (containing the vector) was identified using the ALP method, a method that provides a more purified sample of DNA was used, so that sequencing could be conducted on the DNA. The vector needed to be sequenced to confirm that the vector contains the correct insert. The QIAprep kit was used for a better quality of isolation of DNA. Firstly, 1.5 ml of the bacterial overnight culture (see section 2.2.6) was centrifuged (4 min, RT, 9000 rpm) then the supernatant was removed and the pellet was re-suspended in 100 µl P1 buffer. Following this 250 µl of buffer P2 was added to the sample and mixed by inverting the tube 5 times. 350 µl of buffer N3 was then added and again the sample was mixed by inverting the tube. A white precipitate was formed after this step. The sample was centrifuged (10 min, RT, Max) forming a white pellet at the bottom of the tube. The supernatant was carefully decanted from the eppendorf tube into a spin column and centrifuged (1 min, RT, Max). 0.5 ml of buffer PB was then added to clean the sample of

nuclease activity. A further wash was conducted by adding 0.75 ml of buffer PE. The sample was then centrifuged (1 min, RT, Max) and the supernatant removed. Finally 40 µl of buffer EB was added directly to the filter and left for 1 min before centrifugation (1 min, RT, Max). The isolated samples were then frozen at -20°C ready for sequencing.

2.2.8 End-point PCR

PCR was conducted using an Eppendorf thermocycler (Germany). Specific primers are shown in each section. The method used is the same as for the qRT-PCR discussed in section 2.4.4.3. Briefly, a master mix containing: 21 µl of 2x Taqman master mix, 1 µl of each of the primers (10 µM), 150-200 µg cDNA, all made up to 42 µl (20 µl per well; allowing for error). The protocol used was 1 cycle (2 min at 50°C; 10 min at 95°C) followed by 40 cycles (20 sec at 95°C; 90 sec at 59°C) unless otherwise stated in the section text.

2.3 Ligand binding assay

2.3.1 Overview

The method of ligand-binding was adapted from Bradfield and Poland (1988) but used 3,4,3',4'-tetrachloroazoxybenzene (TCAOB; section 2.1.3) as a competitor because it binds with high affinity to the AhR (Poland *et al.,* 1976). The method has been fully validated previously (Bazzi *et al.,* 2009, Fan *et al.,* 2009, Fried *et al.*, 2007; Jiang *et al.,* 2009). Bazzi (2008) validated many of the key elements of the experiment so the method used here applied the same controls and calculations. All of the experiments were conducted at 4°C. Once the [^{3}H]-TCDD and compound were added to the rat liver cytosol, they were incubated at 4°C for 16 hrs. All the experimental parameters were obtained from Bazzi (2008). The methods are explained in more detail in section 2.3.2 and 2.3.3.

2.3.2 Protein separation and calculation of dissociation constant

2.3.2.1 AhR protein preparation

The AhR protein was prepared from a rat liver of a recently culled female Charles River Wistar rat. The liver was a kind gift from Tim Smith (IBIOS Laboratory, University of Nottingham, UK). Every care was taken to ensure the liver was kept at 4^oC to avoid degradation by proteases. The liver was weighed, shredded using scissors then homogenised in MDENG buffer at 4^oC using a Potter-elvehjem glass homogeniser fitted with a Teflon pestle. The homogenate was centrifuged (20 min, 4^oC, 12,000x g) using a Beckman J21-21 centrifuge. The supernatant was then carefully removed and centrifuged (25 min, 4^oC, 440,000x g) in an Optima Max ultracentrifuge. Care was taken not to disturb the lipid layers on the top of the supernatant before removal. Aliquots of the supernatant were frozen down at -80^oC until required.

2.3.2.2 Determination of total protein concentration

A Bradford assay was performed to measure the concentration of protein in the rat liver cytosol. A Bradford assay is a colorimetric protein assay based on absorbance shift of a dye. Initially protein standards were prepared from 0 to 100 µg of bovine serum albumin (BSA) in 20 µl from a 10 mg/ml stock. The hepatic cytosol prepared in section 2.3.2.1 was diluted several times, to give several 10-fold dilutions. The 5x Bradford dye was diluted to 1x with distilled water and filtered with a 0.45 µm syringe. 1 ml of the 1x Bradford dye was added to each 20 µl sample and allowed to develop for 5 min. The absorbance at 595 nm was measured. The concentration of the BSA versus absorbance at 595 nm was plotted and the protein concentration of the hepatic cytosol was extrapolated.

2.3.2.3 [³H]-TCDD binding standard

The equilibrium dissociation constant (K_d) was required for [³H]-TCDD to allow the calculation of the inhibition constants for the competitors. This was done slightly differently to the normal binding assay as instead of a fixed concentration of [³H]-TCDD, various concentrations were used. This was done in the presence and absence of 200 nM TCAOB to calculate the total binding and the non-specific binding. The protein samples were incubated at 4°C for 16 hours upon which the reaction was terminated by the addition of 30 µl of 10 mg/ml dextran-coated charcoal. After centrifugation (10 min; 4°C; Max), the supernatant was transferred into scintillation vials. The radiation produced by this supernatant was measured using liquid scintillation spectroscopy. The data was converted from dpm into nM [³H]-TCDD binding (Bazzi, 2008) then plotted with Graphpad Prism 5 using the 'One site – Total and nonspecific binding' option. This option then calculated the K_d and the maximum concentration of specific binding (B_{max}).

2.3.3 Competitive [³H]-TCDD binding assay

2.3.3.1 Total binding

The total binding was calculated by adding 1 µl 1 nM [³H]-TCDD to 200 µl of cytosolic protein along with various concentrations of the compound to be tested. The assay was done in triplicate then the average total binding of [³H]-TCDD was plotted against log concentration. A positive control of 1 nM [³H]-TCDD and 200 µl rat liver cytosol was used to show full binding of TCDD to the AhR protein. The samples were incubated at 4°C for 16 hours upon which the reaction was terminated by the addition of 30 µl of 10 mg/ml dextran-coated charcoal. After centrifugation (10 min; 4°C; Max), the supernatant was transferred into scintillation vials. The radiation produced by this supernatant was measured using liquid scintillation spectroscopy.

- Control: Total binding = cytosol + 1 nM [^{3}H]-TCDD

- Assay: Total binding = cytosol + 1 nM [^{3}H]-TCDD + various concentrations of compound

2.3.3.2 Non-specific binding

Non-specific binding was determined in a similar way to the total [^{3}H]-TCDD binding. 1 µl 1 nM [^{3}H]-TCDD was added to 200 µl of cytosol in the presence of various concentrations of the compound to be tested. In addition to this 200 nM TCAOB was added which is 200-fold more than the [^{3}H]-TCDD so competitively binds to the AhR completely displacing [^{3}H]-TCDD. The non-specific binding assay was performed in triplicate. A positive control consisting of cytosol, 1 nM [^{3}H]-TCDD and 200 nM TCAOB was used to show complete displacement of [^{3}H]-TCDD. The samples were incubated at 4°C for 16 hours upon which the reaction was terminated by the addition of 30 µl of 10 mg/ml dextran-coated charcoal. After centrifugation (10 min; 4°C; Max), the supernatant was transferred into scintillation vials. The radiation produced by this supernatant was measured using liquid scintillation spectroscopy.

- Control: Non specific binding = cytosol + 1 nM [^{3}H]-TCDD + 200 nM TCAOB

- Assay: Non specific binding = cytosol + 1 nM [^{3}H]-TCDD + 200 nM TCAOB + various concentrations of compound

2.3.3.3 Specific binding and analysis of binding data

The specific binding was calculated as total binding of [^{3}H]-TCDD minus the non-specific binding of [^{3}H]-TCDD. This was plotted against log concentration of test compound. A positive control of [^{3}H]-TCDD without test compound was included as a positive control and to indicate maximum binding.

- Control: Specific binding = Total – Non specific

- Assay: Specific binding = Total – Non specific

The total binding data obtained from each concentration of compound was averaged and the non-specific binding was taken away from this average to give the specific binding for each concentration. This data was plotted with Graphpad Prism 5. The IC_{50} (half maximal inhibitory concentration) was calculated by plotting the $[^3H]$-TCDD specific binding (% of maximal response of vehicle control) vs. the concentration of the competitor (nM), then using the 'log(inhibitor) vs, response' option. The equilibrium inhibition constant (K_i) was calculated using the 'one site – fit K_i' option where the concentration of $[^3H]$-TCDD was 1 nM, and the K_d of the $[^3H]$-TCDD was calculated as 1.24 nM (95% CI = 0.58 nM – 1.90 nM; calculated in Figure 3.28).

2.4 *Measurement of mRNA using quantitative real time-PCR*

2.4.1 Cell Treatment

The investigation utilised two different types of assay which measure two different properties of the compounds tested. Firstly, an agonist assay was performed on each compound to confirm that it is an agonist of the AhR and that it induces CYP1A1. Secondly, the antagonistic property of the compound was tested by treating cells with a combination of the putative partial agonist/antagonist and TCDD. The induction of CYP1A1 was used as a measure of AhR activation by treating cells with various compounds for 4 hours. The compounds were diluted in medium to minimise the concentration of DMSO/solvent. Two flasks were prepared for each curve. The first was used purely to seed the 96-well plate and the second was for conditioning the medium. The cells were prepared several days in advance to allow approximately 90% confluence to occur. Research has shown that the fetal bovine serum contains known agonists including indirubin which has been shown to affect

the background levels of CYP1A1 mRNA (Adachi *et al.,* 2001; Bazzi, 2008). It was therefore necessary to condition the medium to remove any pre-existing AhR agonists from the medium. The cells were transferred in a volume of 150 µl medium per well. The 96-well plate and flask containing the conditioned medium were left for 24 hours to allow for ~90% confluence. Agonist curves used 9 different concentrations of agonist with three biological replicates for each concentration. Antagonist curves also used 9 concentrations as well as an 'antagonist only' control. The controls consisted of a vehicle control which was always included, as well as an antagonist only control (antagonism assay only) and a 10 nM TCDD control. After 4 hours of treatment, the conditioned medium (with compound) was removed and the cells were pelleted exactly as described in section 2.2.2. Briefly, the contents of each individual well was transferred to an eppendorf tube (using 1x trypsin-EDTA) and centrifuged (5 min; RT, 6000 rpm), forming a cell pellet. The supernatant was removed and the cell pellet was frozen at -20°C for further processing.

Several of the compounds were originally dissolved in different solvents before being transferred into DMSO. The final concentrations of these compounds was <0.1% after dilution in conditioned medium. Behnisch *et al.* (2003) transferred mixed halogenated compounds from their original solvents (including nonane and toluene) to DMSO and found no loss of test compound or effects from the original solvents. Iso-octane has been previously shown not to interact with the AhR or affect the growth of the cells during treatment (~0.02%; Villeneuve *et al.,* 1998). In this study, DMSO was used up to a maximum concentration of <0.02% whereas it has been previously used up to concentrations of >0.04% with no effect on the induction of the AhR or cell growth (Behnisch *et al.,* 2003; Wahl *et al.,* 2008; Zeiger *et al.,* 2001).

2.4.2 RNA purification

RNA purification was carried out using an 'Absolutely RNA® Miniprep Kit' (Stratagene, The

Netherlands) but due to the small sample size several changes were made to the method to

reduce material loss. Initially, 100.7 μl of the lysis buffer-β-ME was added to each sample,

mixed thoroughly then 100 μl 70% Ethanol was added with further mixing using the pipette.

This mixture was then added to a white spin cup and centrifuged (1 min, RT, Max). The

'Appendix I: Protocol Modifications for small sample' was followed which omitted the pre-

filtration step. The filtrate was discarded and 300 μl low salt wash buffer was then added and

centrifuged (2 min, RT, Max) until the filter was dry. The filtrate was once again discarded

then 55 μl RNase-free DNase I was added and incubated at $37^{o}C$, 5% CO_2 for 15 min. The

RNA was centrifuged (1 min, RT, Max) with 300 μl high salt wash buffer followed by 300 μl

then 150 μl low salt wash buffer to remove the DNase I. Once the filter was dry, 30 μl elution

buffer was added and left to incubate for 2 min before the sample was centrifuged in a fresh

eppendorf tube. The sample was then immediately frozen at $-20^{o}C$ ready for cDNA synthesis.

Quantitative analysis of the average amount of RNA purified in each sample was conducted

using a NanoDrop 1000 spectrophotometer (Thermo Scientific, USA). A concentration of 20

ng/μl mRNA was recorded although this analysis was not conducted on every sample. A 1x

agarose gel was run to confirm the quality of the extracted RNA. The protocol for running a

gel is discussed in section 2.2.1. RNA is refered to mRNA in later sections for simplicity.

2.4.3 cDNA synthesis

cDNA was then synthesised using a 'High capacity RNA-to-cDNA Kit' (Applied

Biosystems, USA) by adding 9 μl RNA to 11 μl of RNA-to-cDNA master mix (including 1

μl RT enzyme mix). Samples were then incubated for 60 min at $37^{o}C$ followed by 5 min at

$95^{o}C$ using an Eppendorf thermocycler (Germany). A 'no RevT' containing no reverse-

transcriptase and a 'no RNA' control were also conducted to measure for contamination in

the reagents. cDNA samples were then immediately frozen at -20°C ready for PCR analysis (section 2.4.4).

2.4.4 Quantitative Real Time-PCR

2.4.4.1 Overview

The quantitative real-time polymerase chain reaction (qRT-PCR) was conducted using an ABI 7500fast RT-PCR machine. The method was adapted from previous work which used a Stratagene MX4000 RT-PCR machine using reagents from Stratagene (Wall, 2008). This new machine required the same level of calibration as the original machine to confirm PCR efficiency and accurate measurement of mRNA levels. CYP1A1 mRNA was measured and normalised against two reference genes, β-actin and AhR. This method meant that even if there was a slight variation in RNA concentration or reagent quantities, the CYP1A1 mRNA could still be normalised against other samples as the mRNA levels of β-actin and AhR would always remain the same in every sample. An internal normalisation dye, 5(6)-carboxy-X-rhodamine (ROX) dye, was used, so the dye on the β-actin probe was changed to CY5 from previous work (Bell *et al.,* 2007; Bazzi, 2008; Wall, 2008). The probe and primer sequences for rat and human (Table 2.3) for CYP1A1, β-actin and AhR were designed previously (Bell *et al.,* 2007) with the exception of the CY-5 dye used for the two β-actin probes. The primers and probes for the mouse genes, rat CYP1A2 and CYP1B1 were designed using the NCBI database (http://www.ncbi.nlm.nih.gov) and Primer3 software.

2.4.4.2 Primers and probes

Bell *et al.,* (2007) found that the three pairs (CYP1A1, AhR and β-actin) of primers for rat or human could be run in the single multiplex reaction. To measure the efficiency of the primers and probes used, stand curves were conducted. Standard curves were constructed for all of the primer pairs to confirm that they worked at ~100% efficiency.

Gene		Sequence	Dye
Rat CYP1A1	Primer (f)	CCACAGCACCATAAGAGATACAAG	
	Primer (r)	CCGGAACTAGTTTGGATCAC	
	Probe	ATAGTTCCTGGTCATGGTTAACCTGCCAC	FAM-BH1
Rat AhR	Primer (f)	GCAGCTTATTCTGGGCTACA	
	Primer (r)	CATGCCACTTTCTCCAGTCTTA	
	Probe	TATCAGTTTATCCACGCCGCTGACATG	HEX-BH1
Rat β-Actin	Primer (f)	CTGACAGGATGCAGAAGGAG	
	Primer (r)	GATAGAGCCACCATCCACA	
	Probe	CAAGATCATTGCTCCTCCTGAGCG	CY-5-BH2
Rat CYP1A2	Primer (f)	CTCAACCTCGTGAAGAGCAG	
	Primer (r)	CTCCTGAGGGATGAGACCAC	
Rat CYP1B1	Primer (f)	AGGATGTGCCTGCCACTATT	
	Primer (r)	TGACGTATGGTAAGTTGGGTTG	
Human CYP1A1	Primer (f)	GTTGTGTCTTTGTAAACCAGTG	
	Primer (r)	CTCACTTAACACCTTGTCGATA	
	Probe	CAACCATGACCAGAAGCTATGGGT	FAM-BH1
Human AhR	Primer (f)	ATACAGAGTTGGACCGTTTG	
	Primer (r)	CTTTCAGTAGGGGAGGATTT	
	Probe	TCAGCGTCAGTTACCTGAGAGCCA	HEX-BH1
Human β-Actin	Primer (f)	GACATGGAGAAAATCTGGC	
	Primer (r)	AGGTCTCAAACATGATCTGG	
	Probe	ACACCTTCTACAATGAGCTGCGTGT	CY-5-BH2
Mouse CYP1A1	Primer (f)	TCACCATCCCCCACAGCACCA	
	Primer (r)	CGCTTGTCCAGAGTGCCGCT	
	Probe	CCATGACCGGGAACTGTGGGG	FAM-BH1
Mouse AhR	Primer (f)	GGATTTGCAAGAAGGAGAGTTC	
	Primer (r)	TTGTGCAGAGTCTGGGTTTAGA	
	Probe	GCTGGTTGTCACAGCAGATG	HEX-BH1
Mouse β-Actin	Primer (f)	AGATGACCCAGATCATGTTTGA	
	Primer (r)	CGTGAGGGAGAGCATAGCC	
	Probe	GTCGTACCACAGGCATTGTG	CY-5-BH2

Table 2.3: Sequences of rat, human and mouse primers and probes – Forward (f) and Reverse (r) primers and probes are indicated. Sequences are shown from 5' to 3'. FAM: iscarboxy fluorescein, HEX: hexachlorofluorescein and CY-5: 3'-deoxy-5-(cyanine dye 3)uridine 5'-trisphosphate. The reporter dye is located at the 5' end of the probe, and the quencher dye, Black Hole-1 or -2 (BH1 or BH2), is found at the 3' end. The nucleotide sequences for rat and human: CYP1A1, AhR and β-actin were obtained from Bell *et al.,* 2007 (with the exception of the CY-5 dye used for β -actin). Primers and probes for the mouse genes and for rat CYP1A2 and CYP1B1 were designed using the NCBI database (http://www.ncbi.nlm.nih.gov) and Primer3 software

The efficiency of all of the primers and associated probe (for each species) to bind and transcribe the target gene was calculated for each primer set. RNA and cDNA were produced from untreated cells as described earlier. Five dilutions were then determined (1, 0.5, 0.25, 0.125, 0.062) then measured using qRT-PCR. Each dilution should shift the PCR curve a set distance to the right, indicating that there is one cycle worth of RNA less than the previous dilution.

$$Efficiency = 10^{\left(\frac{-1}{slope}\right)} - 1$$

Equation 2.1: Calculation of the PCR efficiency

The PCR efficiency was calculated using Equation 2.1 and are presented in the results (Figure 3.3). The slope was calculated using Graphpad Prism 5. The rat CYP1A1 primers produced a product of 124 bp, the AhR primers produced a product of 133 bp and the β-actin primers produced a product of 107 bp. The PCR product size of the CYP1B1 and CYP1A2 primers was 192 bp and 264 bp, respectively. The human CYP1A1 primers produce a PCR product of 122 bp, the AhR primers produced a product of 151 bp and the β-actin primers produce a product of 139 bp. The PCR product size for mouse was: CYP1A1 was 175 bp, for β-actin it was 168 bp and for AhR it was 233 bp. The primer and probe sequences for mouse CYP1A1, AhR and β-actin genes are shown in Table 2.3.

2.4.4.3 Measurement of mRNA induction with Taqman probes

qRT-PCR was conducted using an ABI 7000fast PCR machine. A previously calibrated method (Wall, 2008) was adapted for use with this machine. The Taqman® master mix used in this new method requires the activation of Uracil-DNA Glycosylase (UDG) and AmpliTaq Gold® DNA polymerase; Ultra Pure (UP) enzyme activation before cycling and real-time measurement takes place. UDG prevents the re-amplification of previously synthesised PCR products by removing any uracil incorporated in the amplicons (Taqman master-mix

protocol, 2007). The master mix also contains a ROX™ passive reference dye (ROX) which is used to normalise between cycles. A complete master mix was prepared containing; 21 µl 2x Taqman master mix, set concentrations of primers and probes as indicated in Table 2.4, 150-200 µg cDNA, all made up to 42 µl (20 µl per well; allowing for error). Each sample was first mixed in an eppendorf tube before being transferred to the qRT-PCR plate.

		Rat	Human	Mouse
CYP1A1	Primers	100 nM	200 nM	200 nM
	Probe	50 nM	100 nM	100 nM
Actin	Primers	200 nM	100 nM	100 nM
	Probe	100 nM	50 nM	50 nM
AhR	Primers	300 nM	300 nM	300 nM
	Probe	150 nM	150 nM	150 nM

Table 2.4: Primer and probe concentrations for qRT-PCR – The required concentrations of all the probes and primers in order to create the complete master mix. The initial concentration of the probes and primers was 5 μM and 10 μM respectively and are shown in Table 2.3.

Taqman		Time	Temperature
1 cycle	UDG activation	2 min	50^oC
	AmpliTaq gold, UP enzyme activation	10 min	95^oC
40 cycles	Denature	20 sec	95^oC
	Anneal/Extension	90 sec	X^1

SYBR green		Time	Temperature
1 cycle	Denature	10 min	95^oC
40 cycles	Denature	30 sec	95^oC
	Anneal	1 min	58^oC
	Extension	1 min	72^oC

Table 2.5: Thermal cycling conditions for qRT-PCR – Shows the times and temperatures for each step of the qRT-PCR protocol for the 7500fast RT-PCR machine when using Taqman gene expression master mix. X^1: 58^oC for rat, 59^oC for human, 60^oC for mouse and 63^oC for rat AhR (section 3.2.7).

For UDG activation, 2 min at 50°C is required followed by 10 min at 95°C for AmpliTaq gold UP enzyme activation. These two stages are critical for accurate PCR results. The full cycling conditions are described in Table 2.5. Addition conditions for other primer pairs will be described when stating the primer nucleotide sequences.

2.4.4.4 *Measurement of mRNA induction with SYBR green dye*

SYBR green dye allows the quantition of a single gene without requiring a probe. The dye binds non specifically to double stranded DNA which is the reason only a single gene can be measured per reaction. CYP1B1 and CYP1A2 were run separately using: 20 µl Brilliant SYBR Green QPCR master mix, CYP1B1 or CYP1A2 primers (10 µM) and 150 ng cDNA, made up to 40 µl with DEPC treated water (providing 2 x 20 µl reactions). The genes were then normalised against AhR and β-actin which were run separately as a multiplex. A 20 µl of each sample was added to each well of a 96-well qRT-PCR plate. The PCR analysis was conducted using an Applied Biosystems 7500fast RT-PCR machine and used the protocol shown in Table 2.5.

2.4.5 Data Analysis and controls

The EC_{50} was used to compare between compounds and was calculated as 50% of the maximal induction with the error used being the 95% confidence interval (95% CI). As well as the cDNA synthesis controls (No RevT and No RNA), each run conducted contained several important inter-run controls for normalising the data against other curves. Firstly, a known positive control from cells treated with a 10 nM TCDD only and a vehicle control cDNA was used in every experiment. These are from pre-existing batches of cDNA so should be the same for each experiment by removing the inter-experiment error. These two samples will be used to normalise between curves. The next control used was 10 nM TCDD only control which was treated the same time as the other samples in the experiment. This

control is used to normalise the data within a particular run so that the normalised data can be graphically depicted with 10 nM TCDD as 100% of the maximal response. Finally, a no template control (NTC) was performed to confirm that the complete master mix was free of cDNA contamination.

The software associated with the ABI 7500fast collected all of the raw fluorescence data from each run and provided the C_t at which the level of RNA crossed the fluorescence threshold. As discussed previously, the master mix contains ROX fluorescent dye which is used to normalise between wells in a plate and removes some of the error associated with sample volume. The next stage of the data analysis uses qBasePlus (Hellemans *et al.,* 2007; Vandesompele *et al.,* 2002) which normalises the CYP1A1 RNA levels against the two reference genes (normalisation genes), β-actin and AhR. β-actin mRNA was chosen because it is in high abundance in the genome and AhR mRNA was chosen to confirm that it was present. Furthermore, both genes were unaffected by the treatments (Head and Kennedy, 2007; Laupeze *et al.*, 2002; Walker *et al.*, 1999; Wu *et al.*, 2002). An excel worksheet was used to sort the data in to the correct format for qBasePlus by removing errors and correcting the certain jargon words and columns titles. The data was then normalised in qBasePlus, which assumes that the PCR efficiency for all three genes is always 100%. The normalised data is transferred to another excel worksheet where it is initially normalised against the two reference cDNA samples; 10 nM TCDD control and vehicle control. The same cDNA is used on each curve reducing the error of inter-experiment differences. This allows normalisation between curves in the same experiment. Finally, each curve has a 10 nM TCDD only control which is automatically assigned as 100% of the maximal response for each curve. This data is then plotted on to an XY graph using GraphPad Prism 5 as % maximum response against log[agonist]. The % maximal response data was plotted using the standard deviation of the data derived from the three replicates after qBasePlus analysis. GraphPad Prism allows the

estimation of the EC_{50} of each of the curves as well as providing the 95% confidence interval of this estimation. The EC_{50} can then be used to calculate the TEF by dividing the EC_{50} of the agonist by the EC_{50} for TCDD alone. Curves were generated using the settings: 'log[agonist] vs. normalised response'(Equation 2.2).

$$Y = Bottom + \frac{Top - Bottom}{1 + 10^{(Log EC_{50} - X)}}$$

Equation 2.2: Concentration-response curve equation – The following equation was used to calculate the EC_{50} for all of the compounds tested using GraphPad Prism 5 (log[agonist] vs. normalised response). Bottom: lower plateau; Top: upper plateau; X: concentration of agonist; Y: response. Equation assumes hill slope = 1.0.

Some of the figures show the raw qRT-PCR data which was shown as ΔR_n against C_t. The R_n (normalised reporter) is the ratio of the fluorescence emission intensity of the reporter dye verses the fluorescence emission intensity of the internal ROX reference dye. ΔR_n is the normalisation of R_n by subtracting the baseline fluorescence.

2.4.6 Schild regression

Schild regression is a measure of an antagonist's potency and is used to calculate the K_d for the antagonist-complex (Equation 2.3; Kenakin, 1997).

$$Dose\ Ratio = \frac{B^{EC_{50}}}{A^{EC_{50}}}$$

$$Dose\ Ratio = \frac{[B]}{K_B} + 1$$

$$Log(Dose\ Ratio - 1) = Log([Antagonist]) - Log(K_B)$$

Equation 2.3: Schild equation – $A^{EC_{50}}$: EC_{50} of TCDD alone, $B^{EC_{50}}$: EC_{50} of TCDD in the presence of antagonist, [B]: Concentration of antagonist, K_B: equilibrium dissociation constant of the antagonist.

The dose-ratio is calculated which is a measure of the increase in agonist concentration required to achieve the same response as the antagonist concentration is increased. It can be calculated by dividing the EC_{50} of the agonist in the presence of an antagonist by the EC_{50} of

the agonist in the absence of an antagonist. Increasing the concentration of antagonist will move the curve further to the right. Several different concentration-response curves in the presence of various concentrations of antagonist are required for K_d (K_B) calculation. The log(Dose ratio-1) is plotted against log[Antagonist] for each concentration-response curve. For competitive antagonism a straight line is expected, with the point at which the line intersects the x-axis equalling the K_d for that antagonist. In order to improve accuracy it is necessary to perform several different concentrations of antagonist to accurately predict the position of the trend line.

2.5   Retroviral expression of AhR in a mouse cell line

2.5.1   Overview

This study and previous work have shown that there are significant species differences in AhR activation between rat and human by dioxin-like compounds. It is not currently understood what confers these differences; whether it is a difference in the mechanism of activation or purely as a result of the ligand binding potential of the AhR. This section of the project aimed to discover if the AhR is, at least in part, responsible for these differences by directly comparing the activation of rat and human AhR in a common background. This involved isolating the AhRs from rat and human then transfecting them into a cell line with low levels of AhR. A recombinant Hepa1 mouse cell line with reduced levels of AhR was used allowing direct comparison of the two AhRs. Previously the AhR cDNAs were cloned into pFastBac1 vectors (Fan *et al.,* 2009). pGEM-T was used to subclone the AhR fragments out of pFastBac1 and into pRevTRE retroviral vector. Retroviral expression was used to create a stable cell line as previous research had shown direct transfection did not stably re-introduce the AhR (Ma, personal communication). The new cell lines were then treated with TCDD and 5F 203 to see if there was a difference in compound potency and associated

CYP1A1 induction compared with wild-type cells. The mRNA levels of CYP1A1 were measured using qRT-PCR as described earlier (section 2.4).

2.5.2 Preparing AhR for subcloning

2.5.2.1 Rat AhR vector

The rat AhR cDNA was isolated previously and cloned into pFastBac1 as described by Fan *et al.* (2009). Briefly liver mRNA from a Charles River Wistar rat was extracted and PCR was used to clone the AhR. The AhR PCR fragment was then inserted into a pFastBac1 plasmid between the SalI and HindIII sites to make the completed AhR vector as shown in Figure 2.2 (Fan *et al.,* 2009).
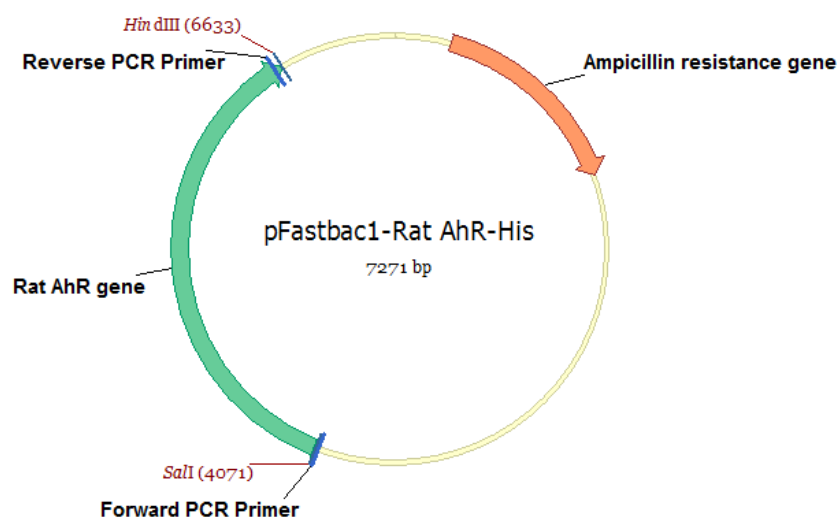
Figure 2.2: Vector map of rat AhR in pFastBac1 – The vector map shows the structure of the pFastBac1 plasmid and the location of the most important restriction sites. The vector is 7271bp in size including the AhR which is 2556bp (excluding restriction sites). The vector was cloned previously by Fan *et al.* (2009). The diagram shows the location of primer sites for PCR of gene of interest. The vector is ampicillin resistant.

The AhR construct cloned by Fan *et al.* (2009) contained a polyhistidine-tag (Hexa histidine-tag; His-tag), containing 6 histamine amino acids, directly at the end of the AhR gene before the stop codon and HindIII restriction site. This tag was removed for this experiment to avoid

the possibility of interference with the expression of the protein and its capacity to bind AhR ligands. This was done using PCR and is described in Figure 2.4.

2.5.2.2 Human AhR vector

The human AhR cDNA (pSporthAhR2) was a kind gift from Susan Moran (McArdle Laboratory for Cancer Research, University of Wisconsin-Madison Medical School) and was initially cloned in a pSV-Sport1 vector (Dolwick *et al.,* 1993) from human HepG2 hepatoma cells. This was then subcloned into pFastBac1 by Fan *et al.* (2009) between the SalI and HindIII binding sites (Figure 2.3).
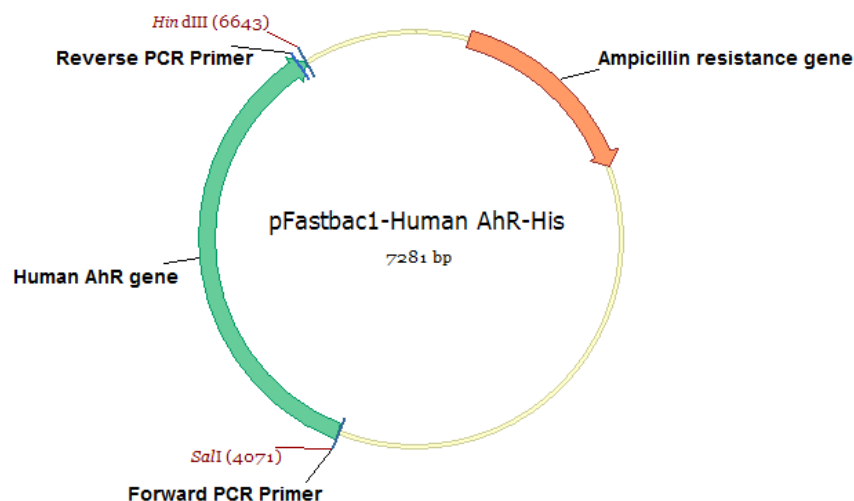
Figure 2.3: Vector map of human AhR in pFastBac1 – The vector map shows the structure of the pFastBac1 plasmid and the location of the most important restriction sites. The vector is 7281bp in size including the AhR which is 2566bp (excluding the restriction sites). The vector was subcloned previously by Fan *et al.,* 2009. The diagram shows the location of primer sites for PCR of gene of interest. The vector has ampicillin resistance.

A His-tag was also added directly after the AhR sequence by Fan *et al.* (2009) to allow purification of the AhR protein however for this experiment it was removed in case it interfered with the expression and capability to bind AhR ligands.

2.5.2.3 Removal of AhR from pFastBac1

In order to make sure both of the AhR proteins expressed properly in the mouse cell line, it was necessary to remove the His-tags. Two primers were designed to PCR the AhR gene out of the pFastBac1 plasmid (rat or human). The reverse primer had a secondary role as it contained an overhang forcing a stop codon and a HindIII restriction site directly after the AhR gene, bypassing the His-Tag completely. This is shown more clearly in Figure 2.4.

```
 Pro   Ser   Gly   Phe   Leu   His   His   His   His   His   His   ***
C C C A G C G G A T T C C T G C A T C A C C A T C A C C A T C A C T A G
| | | | | | | | | | | | | | | | | | | | | | | | | | | | | | | | | | |
G G G T C G C C T A A G G A C G T A G T G G T A G T G G T A


G G G T C G C C T A A G G A C A T C T T C G A A          (Reverse Primer)


 Pro   Ser   Gly   Phe   Leu   ***      HindIII
C C C A G C G G A T T C C T G T A G A A G C T T
| | | | | | | | | | | | | | | | | | | | | | | |
G G G T C G C C T A A G G A C A T C T T C G A A
```
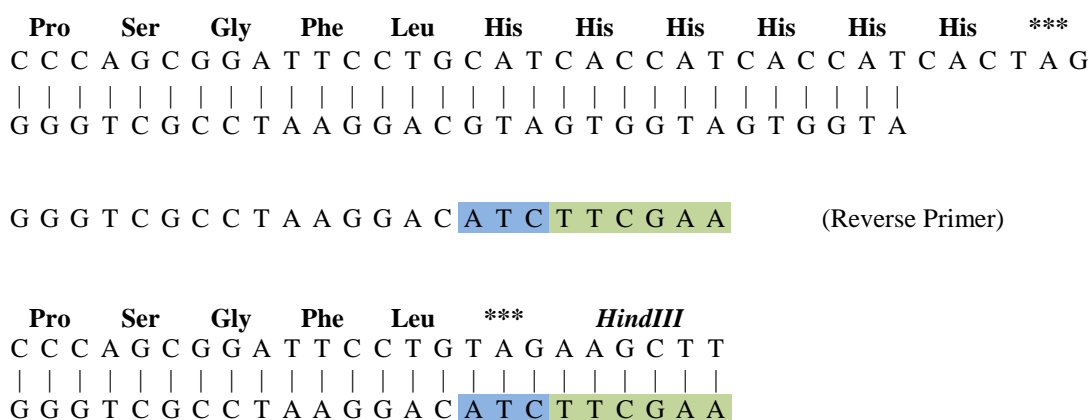
Figure 2.4: Primer design with restriction site and stop codon overhang for rat– The figure shows the nucleotide and amino acid sequences for rat before and after the use of the reverse primer which forced in a new HindIII restriction site and stop codon (***). Reverse primer is shown with the overhang highlighted; Blue: stop codon, Green: HindIII restriction site. Amino acid sequence is in bold. The primer is shown from 3' to 5' and the AhR sequences are both shown from 5' to 3'. Note: this principle also applies to the human reverse primer as well as rat.

PCR was conducted using Extensor Hi-Fidelity PCR Master Mix (ABgene, UK) as it has a low copy error rate. Each reaction consisted of 12.5 µl of extensor master mix (Buffer 1), 2.5 µl of 2 µM forward and reverse primers (final concentration of 200 nM), DNA to a final concentration of 50 ng and RNA/DNA free water. See Table 2.6 for primer sequences.

Gene	Sequence
Human AhR vector	
Primer (f)	GTCGACATGAACAGCAGCA
Primer (r)	**AAGCTTCTA**CAGGAATCCACTGGATGTC
Rat AhR vector	
Primer (f)	GCGGAATTCAAAGGCCTAC
Primer (r)	**AAGCTTCTA**CAGGAATCCGCTGGGTGT

Table 2.6: PCR primers for rat and human AhR removal from pFastBac1 – Primer sequences for rat and human AhR removal and adjustment of restriction site locations. Sequences are from 5' to 3'. Nucleotides in bold are the overhang; blue: stop codon, green: HindIII restriction site. Sequences were designed with assistance from VectorNTI and Primer 3 software.

The Extensor master mix was used as per manufactures instructions. A PCR thermocycler was used with the protocol shown in Table 2.7.

Step	Temperature	Time	Number of Cycles
Initial denaturation	94°C	2 min	1 cycle
Denaturation	94°C	10 sec	
Annealing	58°C	30 sec	25 cycles
Extension	68°C	2 min	
Final Extention	68°C	7 min	1 cycle

Table 2.7: Times and temperatures for Extensor Hi-Fidelity PCR to isolate AhR from pFastBac1- PCR was carried out using a thermocycler. Information was taken from the Extensor Hi-Fidelity PCR master mix manual (ABgene, UK).

PCRs product of 2569 bp and 2578 bp was obtained for rat AhR and human AhR, respectively. These products were then purified using a gel to remove any vector debris (section 2.3.2.4) then inserted into pGEM-T vectors for further processing (section 2.3.3).

2.5.2.4 Purifying the PCR fragment

The product of the PCR reaction discussed in section 2.5.2.3 was run on a 1x agarose gel (section 2.2.1) to remove any pFastbac1 vector debris or unwanted fragments. A small background band may also be expected at ~7 kbp bp due to pFastBac1 vector as well as various primer dimers. A quick load 1 kbp DNA ladder (Biolabs) was run alongside the samples for fragment size measurement.

The band of interest was excised from the gel manually using a UV transilluminator UVP and purified using a QIAquick gel extraction kit (Qiagen) to remove sample from the agarose gel (section 2.2.4). The concentration of the PCR product was then measured using a Nano-drop spectrophotometer and kept at -20°C ready for subcloning into pGEM-T.

2.5.3 Subcloning into a pGEM-T plasmid

2.5.3.1 Ligation of PCR product with pGEM-T vector

The PCR product formed by the Extensor PCR was inserted into pGEM-T by forcing in 3' terminal T-overhangs on to the PCR fragment which greatly improves the efficiency of the ligation as described in the pGEM-T manual (pGEM-T Vector Systems - Technical Manual, 2009). The vector contains specific binding sites and promoters for T7 and SP6 polymerase for low error rate transcription, located either side of the multiple cloning site (containing the 3' T-overhangs and a wide range of restriction sites). The vector also contains a pUC site which allows high-copy replication in *E. coli* and a phage F1 region to allow rescue of single-stranded DNA (pGEM-T Vector Systems - Technical Manual, 2009).
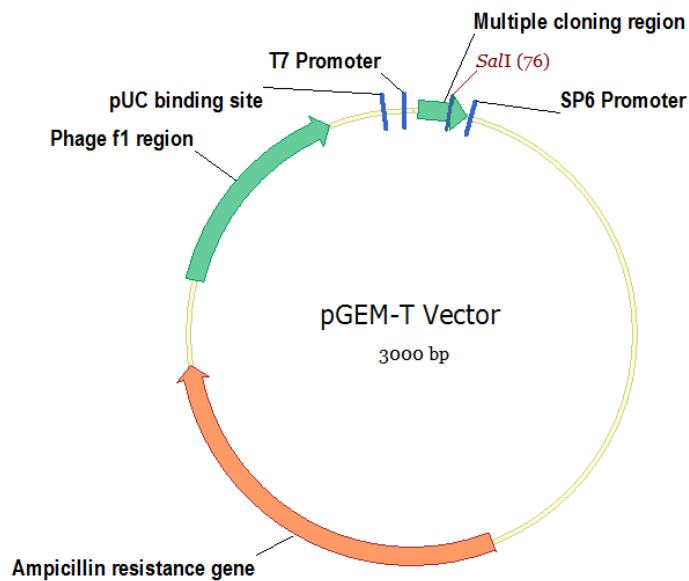
Figure 2.5: Vector map of pGEM-T without AhR insert – pGEM-T was used to subclone the AhR fragments out of pFastBac1 and into pRevTRE retroviral vector. Two new restriction sites were added, SalI and HindIII, when inserting the AhR PCR fragments. The AhR, either rat or human, was inserted in the multiple cloning region (3' T-overhangs). Note: Although the vector is shown to be circular in the above diagram, before insertion of the gene with 3' T overhangs, it is always linear. The vector has ampicillin resistance.

The reactions were set up as described in Table 2.8 using the protocol described in the pGEM-T manual (pGEM-T Vector Systems - Technical Manual, 2009). The mixtures were incubated overnight at 4°C to obtain the maximum number of transformants. Freeze-thaw cycles were avoided to reduce the chance of degradation of the T4 ligase buffer.

Reaction Component	Standard Reaction	Positive Control	Background Control
2X Rapid Ligation Buffer, T4 DNA Ligase	5 µl	5 µl	5 µl
pGEM-T vector (50ng)	1 µl	1 µl	1 µl
PCR Product	X µl*	-	-
Control Insert DNA	-	2 µl	-
T4 DNA Ligase (3 Weiss units/µl)	1 µl	1 µl	1 µl
Nuclease-free water to a final volume of	**10 µl**	**10 µl**	**10 µl**

Table 2.8: Ligation reaction volumes for pGEM-T reaction – Shows volumes required for ligation of PCR product to p-GEM-T vector. Values taken from the p-GEM-T manual (pGEM-T Vector Systems - Technical Manual, Promega, 2009). *PCR product mass calculated using Equation 2.2 (Rat/human = 250 ng/µl).

A simple calculation (Equation 2.3) was used to calculate the amount of PCR product (AhR genes; section 2.5.2.4) required for successful ligation. A molar ratio of 5:1 (insert:vector) was used. The pGEM-T vector was 3000 bp in size at a mass of 50 ng.

$$\frac{\text{ng of vector } \times \text{kbp size of insert}}{\text{kbp size of vector}} \times \text{insert: vector molar ratio} = \text{ng of insert}$$

Equation 2.4: Calculation of the concentration of insert required for ligation - Initial concentration of insert was measured using a Nano-drop spectrophotometer.

The rat and human inserts were 2569 bp and 2578 bp (including a small section of upstream region due primer binding), respectively, with a concentration of 250 ng/µl therefore 15 ng of insert was added to the standard reaction (Table 2.8). Once the reactions were completed it was necessary to use competent bacteria cells to grow successful clones.

2.5.3.2 Transformation of pGEM-T

The plasmids produced, when the insert was ligated into the cloning vector, were transformed into the chemically competent JM109 cells to allow selection of the successfully ligated plasmids. 10 µl of rat or human vector formed from the ligation reaction described in section

2.5.3.1 was added to 30 µl chemically competent JM109 cells and left on ice for 20 min. This was then incubated at $42^{o}C$ for 1 min before being incubated on the ice again for a further 2 min. 200 µl LB medium (warmed to $37^{o}C$) was added to the cells and incubated at $37^{o}C$ for 20 min. After incubation, the mixture was spread over an LB agar plate, with ampillicin antibiotics and incubated overnight at $37^{o}C$. Two controls were also run simultaneously with the ligation products; a positive control which consisted of an uncut vector (pRevTRE) and a negative control of just JM109 cells with no vector, and hence, no ampicillin resistance. After this, 4-5 colonies were selected from each plate and grown in an aeration incubator overnight at $37^{o}C$ in 10 ml LB broth.

The bacteria were processed by one of two methods depending on the intended use of the vector after isolation. A simple alkaline lysis protocol (ALP) was used (section 2.2.6) when the purity of the DNA was not important and allows quick and efficient isolation of unknown colonies ready for testing by double digestion. A Qiagen miniprep DNA isolation kit was used (section 2.2.7) when the purity of the sample is important such as sequencing but is significantly more expensive to conduct.

2.5.3.3 Double digestion to confirm successful cloning

The concentration of DNA obtained from the transformation was measured with a Nanodrop spectrophotometer. Gel electrophoresis was then used to confirm the presence of the positive clone with ligated AhR gene. The plasmid was double digested with SalI and HindIII restriction enzymes using the volumes described in Table 2.9. The reaction was incubated at $37^{o}C$ for 2 hours before being returned to ice.

Component	Volume
DNA	3 µl (~100 ng)
SalI enzyme	1 µl
HindIII enzyme	1 µl
NEBuffer 2	1 µl
dH$_2$O	14 µl

Table 2.9: Volumes required for double digestion of vector (with AhR insert) – The components were kept on ice until required. The mixture was incubated at 37°C for 2 hours. The products formed were then run on a 1x agarose gel for conformation.

The digestion products were run on a 1x agarose gel as described in section 2.2.1. Double digestion of a successful clone should give fragments of 2544 bp and 2553 bp for rat AhR and human AhR (including removal of upstream region), respectively, as well as 3000 bp for the pGEM-T vector. Additional single digestions with SalI and HindIII were conducted on the clones for confirmation of successful insertion of the AhR gene. The putative successful clones were then sequenced to confirm that the new restriction site and stop codon had been successfully forced into the sequence. The sequencing was done at Source Bioscience LifeSciences (Oxford, UK) and used the stock primers; T7F: TAATACGACTCACTATAGGG and SP6: ATTTAGGTGACACTATAG. Comparison of the known AhR sequence and the sequence of the clones was done using AlignX software (VectorNTI). A further double digest was then conducted, run on a 1x agarose gel and extracted ready for ligation into pRevTRE (section 2.5.4).

2.5.4 Cloning into pRevTRE

2.5.4.1 Ligation of insert to pRevTRE

The gene of interest was removed from the pGEM-T vector by double digestion with SalI and HindIII restriction enzymes as described in section 2.5.3.3. This was then run on a 1x agarose gel to separate the gene from the vector (section 2.2.1). A quick gel extraction kit

was used to remove the digested insert as described in section 2.5.2.4. The concentration of the insert was measured using a Nanodrop spectrophotometer.
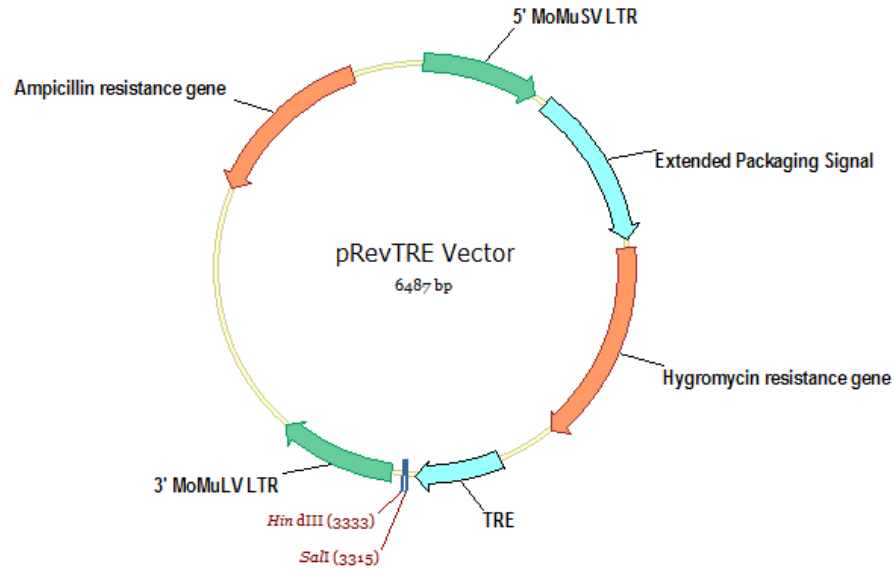
Figure 2.6: Vector map of pRevTRE without AhR insert – The vector used to produce retrovirus (although specific packaging cells are also required). Both rat and human AhRs used SalI and HindIII restriction sites. The vector requires the presence of the pRevTet-Off vector (without tetracycline/doxycyline) in order for transcription of the gene in the host cells.

At the same time the new vector, pRevTRE (Figure 2.6), was also double digested with the same enzymes (HindIII and SalI; section 2.5.3.3). The mixture was then run on a 1x agarose gel to remove the unwanted part of the vector (section 2.2.1). A gel extraction kit was used to excise the double digested vector using the method described in section 2.5.2.4. The concentration of the vector was measured using a Nanodrop spectrophotometer. The double digested insert and vector DNA obtained from the gel extraction were concentrated using an ethanol based assay (section 2.2.5).

Component	Volume
Plasmid	1 µl
Insert	7 µl
Ligation buffer	1 µl
Ligase enzyme	1 µl

Table 2.10: Volumes of the components required for ligation of the AhR insert with pRevTRE – The enzyme was kept on ice at all times. The highest concentration possible of insert was used. The reaction was left overnight at 16°C.

The double digested gene and vector were then ligated together using T4 ligase overnight at 16°C. Table 2.10 shows the volumes of ligation components required for the reaction. The enzyme was kept on ice however the buffer was warmed to room temperature to allow it to be mixed properly before use. The ligation products were then transformed into chemically competent JM109 cells.

2.5.4.2 *Transformation of pRevTRE:insert*

The pRevTRE:insert vectors were transformed into JM109 cells as discussed previously in section 2.5.3.2. Briefly, the JM109 cells with vector were transformed overnight until colonies had formed. From these plates, 4 colonies were selected and grown overnight in 10 ml LB broth. The samples were then centrifuged to produce a bacterial pellet allowing purification using the ALP method as previously discussed in section 2.5.3.2. The concentration of the resulting purified vector was measured using a Nanodrop spectrophotometer.

2.5.4.3 *Confirmation of successful cloning*

The clones were double digested with SalI and HindIII (described in section 2.5.3.3) and run on a 1x agarose gel (section 2.2.1) to confirm that the ligation was successful. Bands would be expected at 2544 bp and 2553bp for the rat and human AhR inserts, respectively, and at 6487 bp for the pRevTRE vector. Successful clones were purified from the bacterial cells

again using the Qiagen miniprep kit (section 2.2.7). Sequencing was conducted on the successful clones using the following primers; pRevTREfor: TCCACGCTGTTTTGACCTCC and pRevTRErev: CCCCCTTTTTCTGGAGAC. It was necessary to concentrate the DNA in order to fulfil the requirements of the sequencing protocols. This was conducted using ethanol precipitation (section 2.2.5). Sequencing showed that the pRevTRE vectors contained the relevant AhR gene.

2.5.5   Creation of stable virus producing cell lines

2.5.5.1   Safety of RevTet system

Although the Moloney murine leukemia virus (MoMuLV) retrovirus is not normally capable of infecting human cells, the Revtet system produces a virus which *is* capable of infecting human cells (pRevTet System Handbook). Therefore all of the experiments were conducted using Biosafety Level 2 practices and safety equipment. This involves using a designated class II laminar flow hood, protective lab attire and decontamination of potentially infectious waste in Trigene disinfectant prior to disposal. The AhR genes which were to be infected into the BpRc1 cells do not pose a risk to human health.

2.5.5.2   RevTet system overview

The retroviral expression was conducted using the RevTet system (Clontech, USA) which utilises the MoMuLV retrovirus to infect target cells with the gene of interest. The retrovirus system utilises a packaging cell line to synthesise the virus before infecting the host cells. In order to start this synthesis, two vectors are required, pRevTet-Off and pRevTRE. The gene of interest, AhR, is inserted into the pRevTRE vector with its transcription regulated by the pRevTet-Off vector (Figure 2.7). Both vectors are initially treated separately using the packaging cells creating two viruses. Both vectors, pRevTet-Off and pRevTRE, contain the viral packaging signal (ψ+) as well as transcription and processing elements. When the vector

is introduced to the packaging cell, a high titer, replication incompetent infectious virus is created which can be used to infect the host cells, mouse BpRc1 cells (RevTet System Handbook). The pRevTet system (Tet-Off) requires two vectors for gene expression of the AhR. pRevTet-Off was added to initiate the transcription of the gene contained in pRevTRE. If the pRevTet-Off vector is deactivated by Dox or not present at all, the AhR gene will not be transcribed.
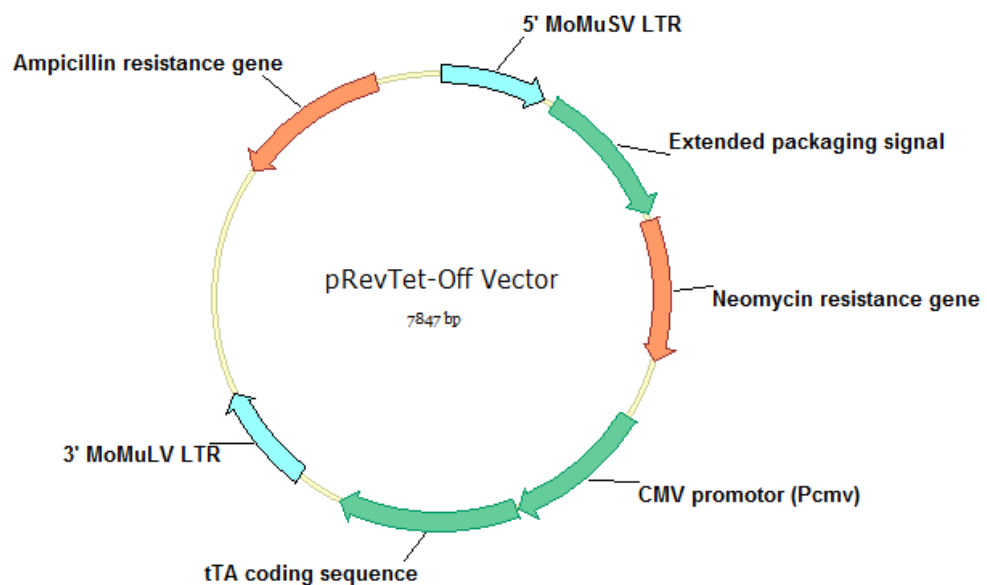
Figure 2.7: Vector map of pRevTet-Off vector

Firstly the host cells, mouse BpRc1 cells, are infected with the pRevTet-Off containing virus. The pRevTet-Off vector (inside the virus) contains the Neomycin gene for antibiotic selection. Once the virus has been introduced to the host cell, a neomycin antibiotic, G418, is added to the medium to select only successfully infected cells. The cells are then infected again with the pRevTRE virus (which contains the gene of interest). The pRevTRE contains a hygromycin gene for antibiotic selection. Successfully infected cells are selected in the same way as before but this time by adding hygromycin B antibiotic to the medium. The cell lines which will be created in this section are shown in Table 2.11.

Cell line	Main attribute	Section
PT67 off	Packaging cell line PT67 which contains pRevTet-Off vector only	PT67 cell lines; section 2.5.5.3
PT67 hAhR	Packaging cell line PT67 which contains pRevTRE human vector only	
PT67 rAhR	Packaging cell line PT67 which contains pRevTRE rat vector only	
BpRc1 off	AhR deficient mouse cell line containing the pRevTet-Off genetic material only	BpRc1 cell lines; section 2.5.6.4
BpRc1 hAhR	AhR deficient mouse cell line containing the pRevTet-Off and the pRevTRE human genetic material (Human AhR)	
BpRc1 rAhR	AhR deficient mouse cell line containing the pRevTet-Off and the pRevTRE rat genetic material (Rat AhR)	

Table 2.11: Summary of cell lines to be produced in this section

2.5.5.3   Creation of stable virus-producing PT67 cell line

The virus was produced by transfecting PT67 packaging cells with either the pRevTet-Off vector or the pRevTRE:rAhR/pRevTRE:hAhR vector. Initially the PT67 cells were incubated and passaged as discussed in section 2.1.6.1. The cells were then transfected with the vector using a chemical transfection reagent called GeneJuice (Novagen). PT67 cells were plated on a 35 mm dish overnight with a concentration of 2×10^4 cells/cm^2. Before treatment the cells were approximately 60% confluent. 3 µl GeneJuice was added to 100 µl of serum-free DMEM and mixed thoroughly using a vortex. This mixture was then incubated at room temperature for 5 min. 1 µg DNA was then added to the GeneJuice mixture and mixed gently using a pipette before being further incubated for 10 min at room temperature. This allows formation of the GeneJuice:DNA complex without the presence of fetal bovine serum. This mixture was then added to the PT67 cells which were in cDMEM.

In order to generate a virus-producing cell line, the packaging cells were plated in selective medium for 6-7 days. The selection process started approximately 3 days after transfection

and utilised either 500 µg/ml G418 (pRevTet-Off) or 300 µg/ml hygromycin (pRevTRE). No selection of individual colonies was conducted. The cells were allowed to reach confluence. Three different PT67 packaging cell variants were created; PT67 off, PT67 hAhR and PT67 rAhR. To confirm the presence of the vector in the packaging cell line, end-point PCR was carried out using the primers shown Table 2.12.

Primer name	Sequence
TREFW	GCCTCGATCCTCCCTTTATC
TRERV	TATCCACGCCCTCCTACATC
OFFTETFW	TGAATGAACTGCAGGACGAG
OFFTETRV	ATACTTTCTCGGCAGGAGCA

Table 2.12: Primers used to confirm the presence of either pRevTet-Off and pRevTRE in PT67 and BpRc1 cell lines

End-point PCR was conducted as discussed in section 2.2.8. The resultant mRNA fragments were then run on a 1x agarose gel as described previously in section 2.2.1. Once it was confirmed that they possessed the required vector, the cells were stored in liquid nitrogen until required or passaged as normal. The viral titre was then calculated to confirm that the virus is viable and to help estimate the multiplicity of infection (MOI).

2.5.6 Creation of BpRc1 cell lines

2.5.6.1 Determination of the viral titer

The viral titer was estimated using NIH/3T3 cells (plated 24 hours prior to the experiment) and virus-containing medium collected from the three packaging cell lines. Polybrene was added to the medium to give a final concentration of 4 µg/ml and filtered through a 0.45 µm filter. Six 10-fold dilutions were prepared using fresh medium. Cells were infected with the dilutions then, after 48 hours, were subjected to antibiotic selection (pRevTet-Off: 0.5 mg/ml G418, pRevTRE: 0.3 mg/ml hygromycin). The virus titer related to the number of colonies present at the highest dilution, which actually contains colonies, multiplied by the dilution

factor. This gave a viral titer of 6×10^4 recombinant virus particles per ml for PT67 off, 7×10^4 for PT67 rAhR and 5×10^3 for PT67 hAhR.

2.5.6.2 Estimation of optimum concentrations of antibiotics

The optimum concentration of the two selective antibiotics, G418 and hygromycin, were calculated by dosing the BpRc1 cells with various concentrations of the antibiotics then identifying the lowest concentration required to kill all of the cells within 1 week. A 6-well plate was seeded with approximately 1×10^5 cells in 5 ml fresh cDMEM and left overnight to settle. The medium was then aspirated and replaced with 5 ml of new cDMEM containing 0, 50, 100, 200, 400 or 800 µg/ml of either G418 or hygromycin. The selective medium was changed every 4 days and the cell density was checked every two days. The optimum concentration would be as low as possible but still kill all of the cells within 7 days. The experiments showed that the optimum concentrations for G418 and hygromycin were 400 µg/m and 600 µg/ml, respectively.

2.5.6.3 Creation of double-stable cell line

The BpRc1 cells were first infected with virus-containing medium from the PT67 off cell line. The wild-type BpRc1 cells were plated in a 100 mm plate overnight at a concentration that would give approximately 50% confluence at the time of infection. Virus-containing medium was collected from the PT67 off cell line once confluence had occurred and used at the highest virus concentration possible (no dilution). Polybrene was added to the medium to give a final concentration of 4 µg/ml then it was filtered with a cellulose acetate 0.45 µM filter. The cDMEM from BpRc1 cells was then removed and replaced with the PT67 off virus-containing medium. The cells were then incubated for 24 hours at 37°C in a 5% CO_2 incubator. After 24 hours the virus-containing medium was replaced by fresh complete DMEM medium. Three days after infection, the cells were sub-cultured and subjected to 400

µg/ml G418 antibiotic selection for 7 days. Once visible and healthy colonies of cells were found, they were isolated using cloning cylinders.
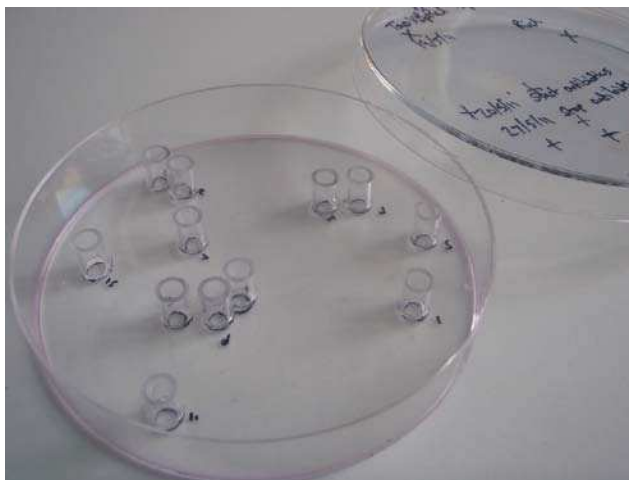
Figure 2.8: Photograph of cloning cylinders used for cell isolation

To isolate the colonies, the medium was first removed. The cloning cylinders were gently placed into Vaseline then positioned around the cell colony (See Figure 2.8). The Vaseline was required to produce a watertight seal around the colony. The cloning cylinders, the Vaseline and the forceps were autoclaved before use and kept sterile throughout the experiment. Once the cylinder was secured, 20 µl 1x trypsin-EDTA was added and incubated at $37^{o}C$ for 2 min. Once the cells were detached from the plate, 60 µl medium was added and the cells were transferred to a 25 cm^{2} flask (containing 10 ml of cDMEM) and grown to confluence. Aliquots were then frozen down in liquid nitrogen for future use (section 2.1.6.2). This produced a stable new cell line called BpRc1: pRevTet-Off (BpRc1 off) and will be required to make the two AhR cell line variants.

In order to produce the BpRc1 cell lines with rat and human AhR, it was necessary to infect the BpRc1 off cells with either the virus created from the PT67 rAhR cells or from the PT67 hAhR cells. The virus from the PT67 rat cells would produce a double-stable cell line called Tao BpRc1 rat AhR (BpRc1 rAhR) whereas the virus from the PT67 hAhR cells would

produce a double-stable cell line called Tao BpRc1 human AhR (BpRc1 hAhR). Infection and selection was done based on the same principle as for the BpRc1 off cell line. The BpRc1 off cells were plated giving a 50% confluence at the time of infection. Virus-containing medium (at maximum viral concentration) was taken either for the PT67 rAhR or the PT67 hAhR cells and filtered through a 0.45 µM syringe filter. Polybrene was added to the medium giving a final concentration of 4 µg/ml and the medium was added to the BpRc1 off cells. Cells were infected for 24 hours whereupon the medium was replaced with fresh DMEM. The cells were then sub-cultured in antibiotic containing medium after 3 days using 600 µg/ml hygromycin for 7 days. Healthy colonies were isolated with the cloning cylinders as described previously. The chosen cells were then grown in 6-well plates, then in 25 cm^2 flasks to reach confluence before being frozen down in liquid nitrogen for future use. Confirmation of the presence of the genes was conducted using qRT-PCR (section 2.5.7).

2.5.6.4 Creation of transient expression cell line

The creation of a double stable cell line was unsuccessful after several attempts so the BpRc1 cells were infected to allow transient expression of the AhR proteins instead of stable expression. Infection of the BpRc1 cell lines with the virus from the PT67 off cell line was conducted simultaneously with either the virus from the PT67 rat or human cell lines to create either BpRc1 rAhR or BpRc1 hAhR. Virus-containing medium (at maximum viral concentration) was taken from PT67 off and either the PT67 rAhR or the PT67 hAhR cells and filtered through a 0.45 µM syringe filter. Polybrene was added to the medium giving a final concentration of 4 µg/ml. The medium was added to BpRc1 cells (at 80% confluence) and after 24 hours of infection the cells were transferred to a 96-well plate and left to grow for a further 24 hours. Cell treatment with compounds was conducted 48 hours after cell infection with the pRevTREs (AhR) and pRevTet-Off vectors (see section 2.4.1). Cells were treated with the test compounds (TCDD and 5F 203) prior to confirmation that the infection

was successful. Once successful infection was confirmed, the concentration-response curves were processed as discussed in section 2.5.8.

2.5.7 Confirmation of successful infection

2.5.7.1 Presence of cell infection of pRevTet-Off and pRevTRE

Once BPRc1 cells were infected by the PT67 viruses, it was necessary to confirm the presence of the vectors; pRevTet-Off and either pRevTRE:rAhR or pRevTRE:hAhR in the new cell lines. Confirmation of the presence of the vectors was done in the same way as it was for the PT67 packaging cells (section 2.5.5.3) by using end-point PCR with primers that detect either the pRevTet-Off vector or the pRevTRE vector (Table 2.12; section 2.2.8).

2.5.7.2 Confirmation of the presence of AhR DNA

It was important; not only to confirm the presence of the required vectors, but also to confirm only one of the AhR vectors was present in each cell line. Therefore a second experiment was conducted using primers for the rat and human AhR (Table 2.3). The level of AhR DNA located in the cell was required to assess the relative concentrations of the AhRs. BpRc1 wild-type, BpRc1 rAhR and BpRc1 hAhR cell lines were tested for rat AhR, human AhR and mouse AhR (genomic) which were normalised against mouse β-actin (genomic). The primers for mouse genomic AhR and β-actin are shown in Table 2.13. A separate experiment showed that the RNA had been successfully removed from all of the DNA samples (β-actin primers for mRNA gave negative results).

Primer name	Sequence
AhRFWgen	CGGGCTTCCGCCAGGTGATG
AhRRVgen	AGCTGCTGTGCTGTGTTTGTTCT
ActinFWgen	ATGGAGGGGCCGGACTCATCG
ActinRVgen	AGGGGAATCCCAGCACCCAGA

Table 2.13: Primers to measure mouse genomic AhR and β-actin.

2.5.7.3 *Absence of PT67 cell contamination*

It was also required to confirm that the infected BpRc1 cell lines were not contaminated with PT67 cells. As only a small number of BpRc1 cells were isolated after antibiotic resistance, of which the PT67 cells should be resistant too, there would be time for a small number of PT67 cells to grow to confluence. Primers were designed to identify PT67 cells by binding to the env region (gp70 SU) of the integrated Moloney murine leukemia virus genomic structure. The primers should make a 100 bp product and should not be present in the BpRc1 cells as they do not possess the viral genes. The primer sequences were; PT67FW: TTTTCTTCTCCCCCGGGGCCC and PT67RV: TGCACCGAGGGGTGAGGGAG. Due to the failure of the stable infected cell lines, this step was no longer required as contamination by a limited number of PT67 cells would have no effect on the measurement of induction from the BpRc1 cells.

2.5.8 Species specific investigation measuring CYP1A1 expression

2.5.8.1 *Expression of AhR mRNA*

The ability of AhR mRNA to be transcribed from the pRevTRE vectors was measured using qRT-PCR. The three BpRc1 cell lines (wild-type, rAhR and hAhR) were measured for rat AhR, human AhR, mouse AhR and mouse β-actin mRNA after 4 hours treatment with the vehicle (0.1% DMSO). The rat AhR primers were run at $63^{\circ}C$ to increase their specificity as they were binding non-specifically to the mouse AhR as well. The mRNA levels for the three AhR genes were normalised against β-actin by normalising the C_t threshold value for all three AhR genes. The same conditions were used for each of the three genes (excluding the anneal/extension temperature) and assumed that all three genes worked at 100% efficiency. The protocol for mRNA preparation and qRT-PCR was discussed previously (section 2.4).

2.5.8.2   *Treatment with TCDD and 5F 203*

The method of qRT-PCR previously discussed in section 2.4 was utilised to measure the induction of CYP1A1 mRNA in the genetically engineered BpRc1 cells upon treatment with various AhR agonists. After confirmation of successful infection the cells, which were treated either with TCDD or 5F 203 were processed as previously discussed in section 2.4. Briefly, the cells (plated in a 96-well plate) were treated with various concentrations of either TCDD or 5F 203 for 4 hours. Treatment used conditioned medium as discussed in section 2.4.1. The RNA was purified from the cells and stabilised into cDNA. qRT-PCR was then used to measure the levels of mouse CYP1A1 and mouse β-actin. The sequences of the mouse primers and probes are shown in section 2.4.4.2. A 10 nM TCDD only control and a vehicle only control were also conducted. Concentration-response curves of TCDD and 5F 203 were also conducted in BpRc1 wild-type cells as a comparison.

3. Results

3.1 *PCR measurement of CYP1A1 mRNA induction as a measure of AhR agonism and antagonism*

3.1.1 Overview

In order to measure activation of the AhR, measurement of the induction of CYP1A1 was conducted using mRNA isolated from rat liver cells (H4IIE), human breast carcinoma cells (MCF-7), mouse fibroblast cells (NIH/3T3) and mouse AhR-deficient cells (BpRc1) using qRT-PCR. The levels of CYP1A1 mRNA were normalised against two reference genes, AhR and β-actin, which were unaffected by the treatments (Head and Kennedy, 2007; Laupeze *et al.*, 2002; Walker *et al.*, 1999; Wu *et al.*, 2002).

3.1.2 Method optimisation

3.1.2.1 *The use of conditioned medium*

Bazzi (2008) showed that the fetal bovine serum (added to the cMEM/cDMEM medium) used to treat the cells also contained AhR ligands such as indirubin (Adachi *et al.,* 2001).
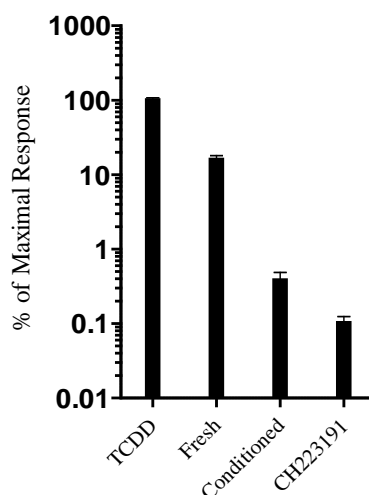
Figure 3.1: Effect of conditioned vs. fresh medium – Rat H4IIE cells were treated with either 10 nM TCDD in 0.1% DMSO, fresh cMEM, conditioned (24 hrs) cMEM or 1 µM CH223191 in 0.1% DMSO for 4 hours. Cell treatment, RNA isolation and qRT-PCR analysis was as described in method. The normalised response (% of maximal CYP1A1 mRNA induction by 10 nM TCDD) is shown on a log scale, and each bar represents the mean of 3 biological replicates ± S.D.

The effect of the cMEM medium on the induction of CYP1A1 was confirmed in rat H4IIE cells (Figure 3.1). A positive control of 10 nM TCDD and a known antagonist of the AhR (negative control), CH223191, were used to compare against values derived from the medium samples. The fresh medium induced CYP1A1 mRNA by 15% of the maximum induction by 10 nM TCDD (100% or maximal induction). Conditioned medium and CH223191 (in 0.1% DMSO) gave mRNA levels of 0.4% and 0.1%, respectively, of the maximal response by 10 nM TCDD. There is a 30-fold difference between fresh and conditioned medium. Furthermore fresh medium gives a maximum signal to noise ratio of only 7-fold whereas conditioned medium gives a ratio of 250-fold. Based on this evidence, conditioned medium was always used when treating cells for concentration-response curves.

3.1.2.2 Isolated RNA quality

In order to confirm the quality of RNA purified from the rat H4IIE, human MCF7 and mouse NIH/3T3 cells, RNA samples were run on a 1x agarose gel. Initially the RNA was isolated and purified from cells using 'Absolutely RNA® Miniprep Kit' (Stratagene, Netherlands). The RNA samples were then run on a 1x agarose gel for 60 min at 100 V. Figure 3.2 shows the gel with the three species; rat (H4IIE), human (MCF-7) and mouse (BpRc1).
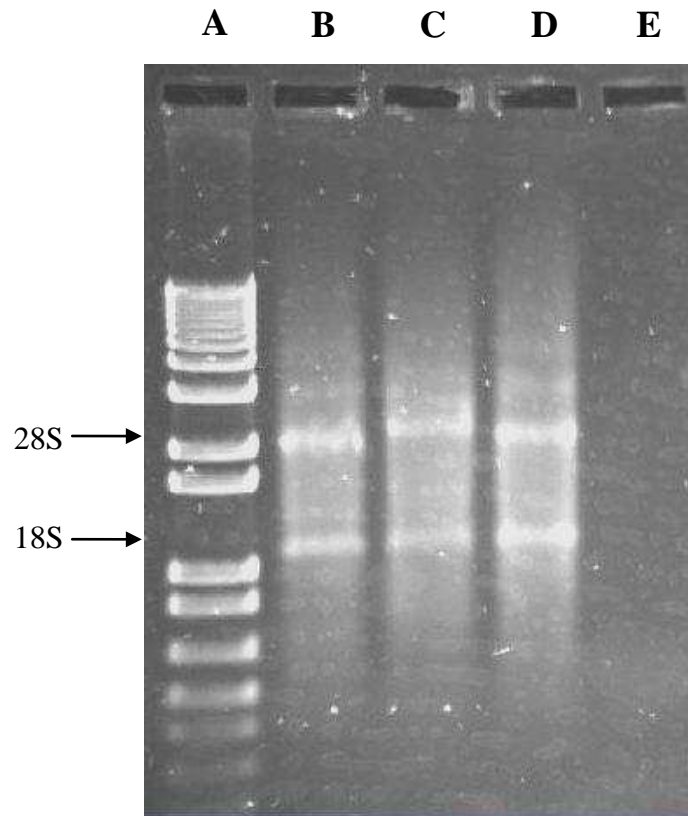
Figure 3.2: Agarose gel of RNA quality – RNA samples of rat H4IIE-C3, human MCF-7 and mouse BpRc1 cells were run on a 1x agarose gel. The 1x gel was made as described in section 2.2.1 and run for 60 min at 100 V. The gel was stained with ethidium bromide for 20 min before being photographed with a BioRad chemdoc UV camera. (A) 1 kbp Plus DNA ladder (Invitrogen), (B) rat H4IIE-C3, (C) human MCF-7, (D) mouse BpRc1 cells and (E) Negative control. The bands 18S and 26S are labelled.

Figure 3.2 shows that the purified RNA is of good quality with two distinct bands seen at 28S and 18S. This also indicates that the RNA has negligible genomic contamination or RNA degradation.

3.1.2.3 Standard curves

In order to validate the primer set and probe, the PCR efficiency was measured. A known amount of cDNA was diluted in master mix with the relevant probe and primers for the particular gene of interest. The efficiency curves were produced by diluting a known concentration of cDNA followed by measurement using qRT-PCR.
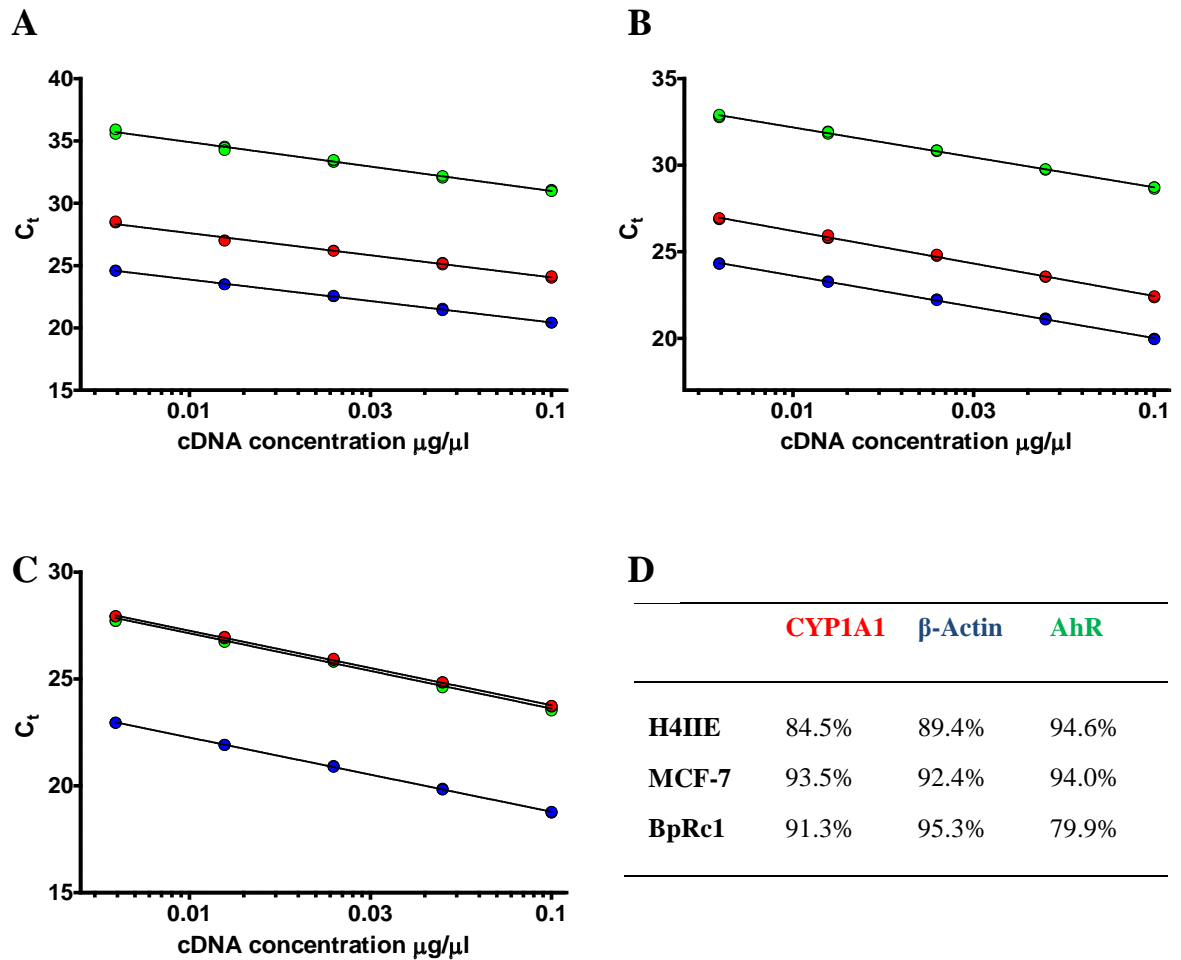
Figure 3.3: PCR efficiency for CYP1A1, β-actin and AhR measured in (A) rat H4IIE cells, (B) human MCF-7 cells and (C) mouse BpRc1 cells - A 5 point dilution series of cDNA was used to produce a concentration gradient. cDNA quantity is plotted against the C_t where the fluorescence threshold is crossed. Red: CYP1A1; green: AhR; blue: β-actin. The initial quantity of input cDNA is shown on the x-axis as a relative amount, and the C_t for each dilution is shown on the Y-axis, graph shows all 3 replicates separately. The fit of the data to the line was determined by r^2 analysis, and the efficiency of PCR was determined from the slope of the line. (D) The table shows the calculated efficiencies as percentage. Final probe and primer concentrations were 50-300 nM.

Figure 3.3 shows the PCR efficiencies of all three genes in (A) rat, (B) human and (C) mouse cells. The β-actin, CYP1A1 and AhR PCR efficiencies are shown in Figure 3.3D. There was no interference between the three dyes used (FAM, HEX and CY-5) validating the use of CY-5 for the probe dye. This also confirms both the ability of the assay to detect all three genes and that they all have the desired efficiency. The r^2 values for β-actin, CYP1A1 and AhR in all species were >0.99 demonstrating the precision of the dilutions

used. The PCR reactions were run in the same well in a multiplex for all of the genes hence these efficiencies demonstrate the PCR efficiency in multiplex.

3.1.2.4 *Normalisation genes are unaffected by the treatment*

An important aspect of the qRT-PCR strategy of normalising CYP1A1 against two reference genes, β-actin and AhR, is that the two genes are unaffected by the treatment. In order to test this, rat or human cells were treated with TCDD for 4 hours as a model agonist, and qRT-PCR performed for the two reference genes, β-actin and AhR. This data was normalised as fold difference of vehicle control (Figure 3.4).
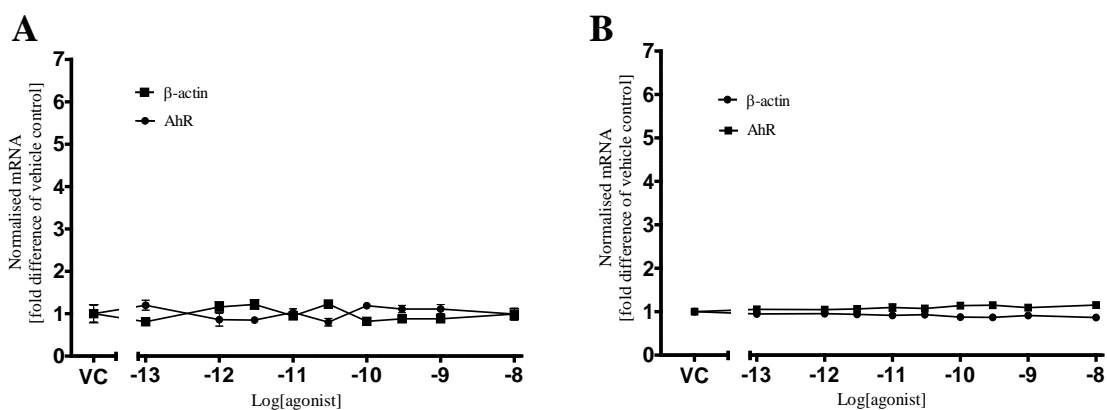
Figure 3.4: Effect of TCDD on the normalisation genes, β-actin and AhR measured in (A) rat H4IIE cells and (B) human MCF-7 cells – Cells were treated with various concentration of TCDD. qRT-PCR was conducted to measure AhR and β-actin mRNA levels. The graph shows the normalised fold-difference mRNA levels against vehicle control. The graphs show that β-actin and AhR are not affected by the treatment compounds. Each point is the mean of three biological replicates ± S.D.

Both graphs show that the normalisation genes are not affected by the TCDD treatment and are therefore suitable to normalise CYP1A1 mRNA. Mouse AhR and β-actin were also unaffected by the treatment (data not shown).

3.1.3 Validating the method of mRNA measurement

3.1.3.1 *Agonism - TCDD*

The method of measuring agonism was developed previously (Bazzi, 2008; Bell *et al.,* 2009; Wall, 2008). Additional improvements were made during this project so the method was

validated again. Furthermore, in order to confirm the repeatability of the assay between experiments and to confirm that each experiment will give the same EC_{50}, several TCDD concentration-response curves, which were conducted over the period of the study, were compared (Figure 3.5). Rat H4IIE and human MCF-7 cells were treated with various concentrations of TCDD which were then plotted against normalised CYP1A1 mRNA and compared against a vehicle control (VC).
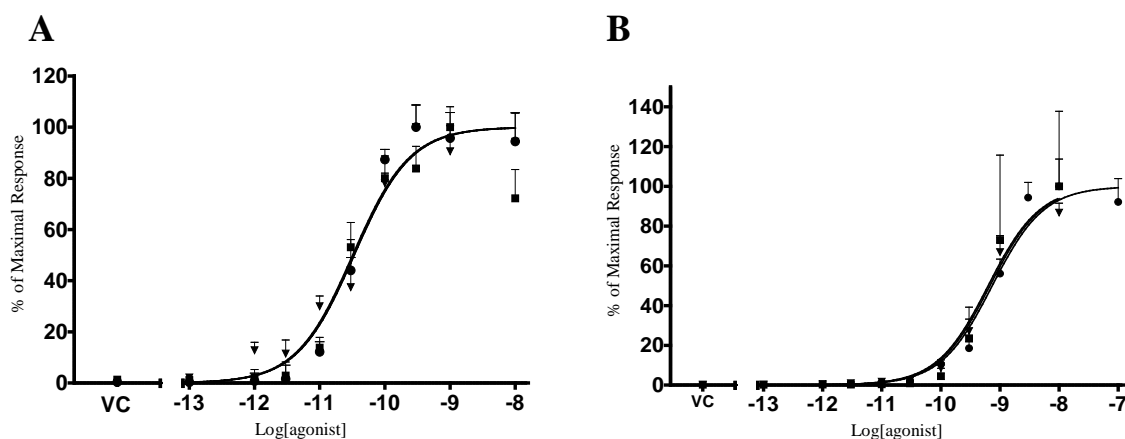
Figure 3.5: Comparison of three TCDD concentration-response curves in A) rat H4IIE cells and B) human MCF-7 cells - H4IIE cells or MCF-7 cells were treated with the indicated concentrations of TCDD for 4 hours. The graph shows four curves taken from various experiments and calibrations over a period of the study. Concentration-response curves were created by plotting the % of maximal CYP1A1 mRNA induction by 10 nM TCDD against concentration of agonist. qRT-PCR was used to measure the level of induction of CYP1A1 and compared against control genes, β-actin and AhR. QbasePlus was used to normalise the data, which was plotted using 10 nM TCDD only control as 100% of the maximal response. Each point is the mean of three biological replicates ± S.D.VC: Vehicle control.

The graph shows that a concentration of more than 1 nM, in rat, and 10 nM, in human, is required to reach the maximal response. Furthermore the vehicle control provides less than 0.5% of the maximal response in both cell lines. The EC_{50} of the three rat cell curves were 33.7 pM, 33.9 pM and 32.0 pM (Mean = 33 pM, S.D. = 1 pM) and the three human cell curves were 675 pM, 633 pM and 740 pM (Mean = 683 pM, S.D. = 50 pM). This shows that the method provides reproducible results and can therefore be used for accurate comparison between other experiments.

3.1.3.2 Antagonism - CH223191

CH223191 has been shown to have antagonistic activity for the AhR in mouse and human cells, but the antagonistic activity has not been quantified (Kim *et al.,* 2006). Initially, an experiment was conducted to confirm that CH223191 has no agonistic activity in rat cells. Cells were treated with various concentrations of CH223191 up to a concentration of 1 μM.
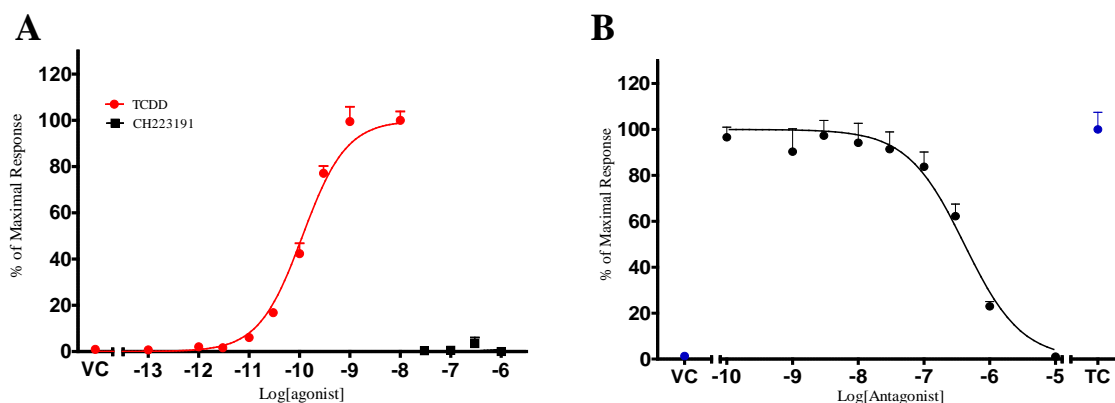
Figure 3.6: CH223191 has no agonistic properties and is an antagonist of TCDD induction of CYP1A1 – (A) CH223191 has no agonistic properties (compared with a TCDD only curve). (B) Concentration-response curve for CH223191 antagonism of CYP1A1 induction by 1 nM TCDD. For both experiments rat H4IIE cells were treated with test compounds for 4 hours. Concentration-response curves were created by plotting the % of maximal CYP1A1 mRNA induction by 10 nM TCDD against concentration of agonist. qRT-PCR was used to measure the level of induction of CYP1A1 and compared against control genes, β-actin and AhR. QbasePlus was used to normalise the data which was plotted using 10 nM (A) or 0.1 nM (B) TCDD only control as 100% of the maximal response. Results were compared with a vehicle control (VC) and a 10 nM TCDD only (TC). Each point is the mean of three biological replicates ± S.D.

Figure 3.6A shows CH223191 compared with a TCDD only concentration-response curve. The graph demonstrates that compared with TCDD, CH223191 has no agonistic properties in this experiment. A concentration-inhibition curve was constructed using a set concentration of 1 nM TCDD which gave approximately 90-100% of the maximal induction of CYP1A1 in the presence of various concentrations of CH233191 (Figure 3.6B). The inhibition of 1 nM TCDD induction of CYP1A1 in the presence of increasing concentrations of CH223191 was compared against a vehicle control (VC) and a 10 nM TCDD only control (TC). The IC_{50} was 411 nM (95% CI = 300 nM – 562 nM). In order to perform a Schild

analysis, several concentration-response curves are required to get a reliable estimate for the K_d. Using the concentration-inhibition curve in Figure 3.6B, it was possible to find the window of measurable response where the CH223191 affected the induction of CYP1A1 by TCDD. Another limiting factor was the maximum concentration of TCDD that could be used which is 10 nM. Previous work had shown that a higher concentration would not stay in solution and could therefore provide inaccurate information. Therefore, TCDD concentration response curves in the range of 1 pM to 10 nM were performed in the presence of four concentrations of CH223191; 30 nM, 100 nM, 300 nM and 1 µM (Figure 3.7A).
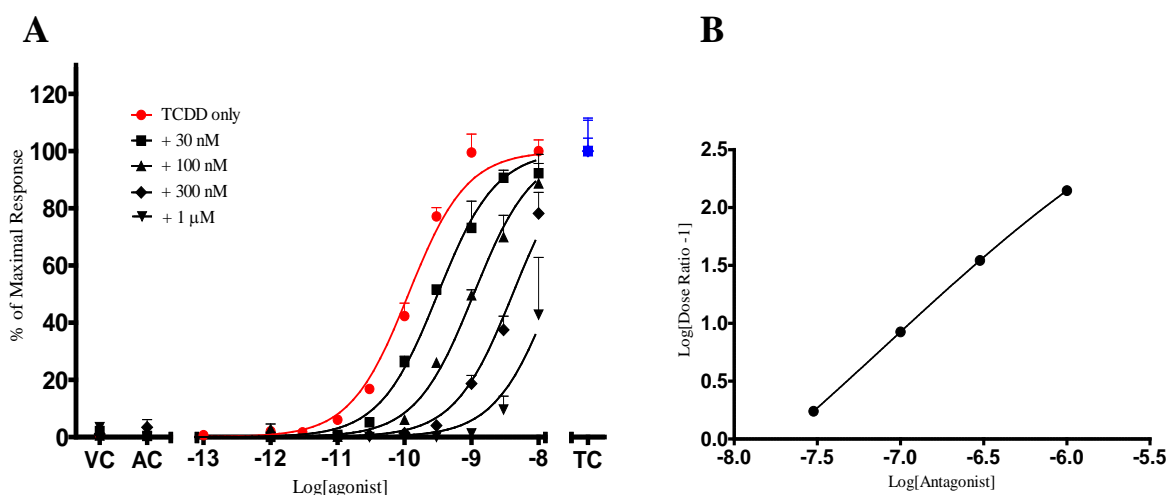
Figure 3.7: Schild analysis of CH223191 – (A) TCDD concentration-response curves in the absence and presence of 30 nM, 100 nM, 300 nM and 1 µM CH223191, (B) Schild plot of CH223191. Cells were treated with various concentrations of TCDD in the presence or absence of either: 30 nM, 100 nM, 300 nM or 1 µM CH223191 for 4 hours in rat H4IIE cells. Concentration-response curves were created by plotting the % of maximal CYP1A1 mRNA induction by 10 nM TCDD against concentration of agonist. qRT-PCR was used to measure the level of induction of CYP1A1 and compared with control genes, β-actin and AhR. QbasePlus was used to normalise the data which was plotted using 10 nM TCDD only control as 100% of the maximal response. Results were compared with an antagonist only control (AC), a vehicle control (VC) and a 10 nM TCDD only control (TC). Schild plot was plotted as the Log[Dose Ratio –1] against Log[Antagonist]. Schild shift was calculated by GraphPad Prism 5. Each point (A) is the mean of three biological replicates ± S.D.

Cells were treated for the particular combination of compounds for 4 hours. An antagonist only control (AC), vehicle control (VC) and a 10 nM TCDD only control (TC) were included. The TCDD only control (TC) was included for comparison as well as accurate

measure of the 100% maximal induction. A TCDD only curve was included as comparison which included a vehicle control (VC). The graph shows that as the concentration of antagonist is increased, the further to the right the curve is in comparison to the TCDD only curve. The EC_{50} for TCDD alone was 115 pM (95% CI = 89 pM – 147 pM), +30 nM: EC_{50} was 313 pM (95% CI = 266 pM -368 pM), +100 nM: EC_{50} was 1.08 nM (95% CI = 933 pM - 1.24 nM), +300 nM: EC_{50} was 4.11 nM (95% CI = 3.34 nM - 5.04 nM) and +1 µM: EC_{50} was 16.2 nM (95% CI = 12.4 nM - 21.0 nM). This shift to the right can be used to calculate the K_d of CH223191 by measuring the EC_{50}'s of each curve and compare them with the TCDD only curve. This analysis was done automatically by GraphPad Prism 5 software. The Log[Dose ratio -1] was plotted against Log[Antagonist Dose] as shown in Figure 3.7B. The K_d was calculated to be 18.2 nM (95% CI = 14.1 nM to 23.6 nM). The slope of the line was 1.26 ± 0.03 with an r^2 value of 0.99 showing that the line fits well to the data.

3.1.4   Mixed halogenated dibenzo-*p*-dioxins

3.1.4.1   Summary of substituted-dibenzo-p-dioxins in rat H4IIE cells

Concentration data in food, combined with previous potency research, has shown that these compounds may have a significant impact on TEQ based risk assessment (Table 1.2). Therefore calculating the potency of these compounds will allow a better estimation for risk assessment. Rat H4IIE cells were treated with various chlorinated, brominated or mixed halogenated dibenzo-*p*-dioxins for 4 hours to calculate their potency based on the induction of CYP1A1 mRNA. The structures, EC_{50}s and REP values calculated in this work are summarised in Table 3.1 to allow comparison.
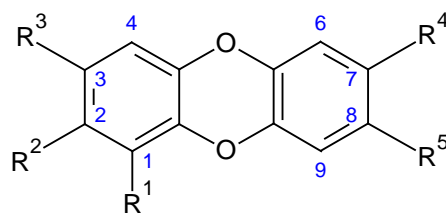
Structure	EC_{50} (95% CI)	REP
2-B-7,8-DiCDD $R^1=H; R^2=Br; R^3=H; R^4=Cl; R^5=Cl$	904 pM (710 pM – 1.15 nM)	0.05
2,3,7-TriBDD $R^1=H; R^2=Cl; R^3=Cl; R^4=Br; R^5=H$	1160 pM (813 pM – 1640 pM)	0.04
TCDD $R^1=H; R^2=Cl; R^3=Cl; R^4=Cl; R^5=Cl$	47.6 pM (36.4 pM – 62.2 pM)	1[a]
2-B-3,7,8-TriCDD $R^1=H; R^2=Br; R^3=Cl; R^4=Cl; R^5=Cl$	23.7 pM (15.4 pM – 36.6 pM)	2.01
2,3-DiB-7,8-DiCDD $R^1=H; R^2=Br; R^3=Br; R^4=Cl; R^5=Cl$	168 pM (138 pM – 206 pM)	0.28
1-B-2,3,7,8-TetraCDD $R^1=Br; R^2=Cl; R^3=Cl; R^4=Cl; R^5=Cl$	398 pM (264 pM - 599 pM)	0.12
2-B-1,3,7,8-TetraCDD $R^1=Cl; R^2=Br; R^3=Cl; R^4=Cl; R^5=Cl$	86.4 pM (65.3 pM – 114 pM)	0.55

Table 3.1: A summary of the potency of substituted-dibenzo-*p*-dioxins as AhR agonists in rat H4IIE cells - EC_{50} values are shown with their 95% confidence intervals. 1[a]: The REP is a comparison with the EC_{50} of TCDD within this experimental group.

The results show that all of the compounds are within 25-fold less potent than TCDD with the exception of 2-B-3,7,8-TriCDD which is shown to be 2-fold more potent than TCDD. The full concentration response curves are also shown below (Figure 3.8 to Figure 3.11). Some of the compounds were also tested in human MCF-7 cells (Figure 3.9).

3.1.4.2 Tri-substituted-dibenzo-p-dioxins

The potency of two tri-substituted dibenzo-*p*-dioxins, 2-B-7,8-DiCDD and 2,3,7-TriBDD, was measured in rat H4IIE cells. The compounds are structurally similar to 2,3,7-TriCDD which is a known low potency AhR ligand (REP = 0.0015; Behnisch *et al.,* 2003) but was not considered in the WHO TEF 2005 risk assessment (Van den Berg *et al.,* 2006). The increase in the levels of CYP1A1 mRNA was used as a measure for AhR activation. Figure 3.8 shows the potency of the two compounds compared against TCDD in rat H4IIE cells.
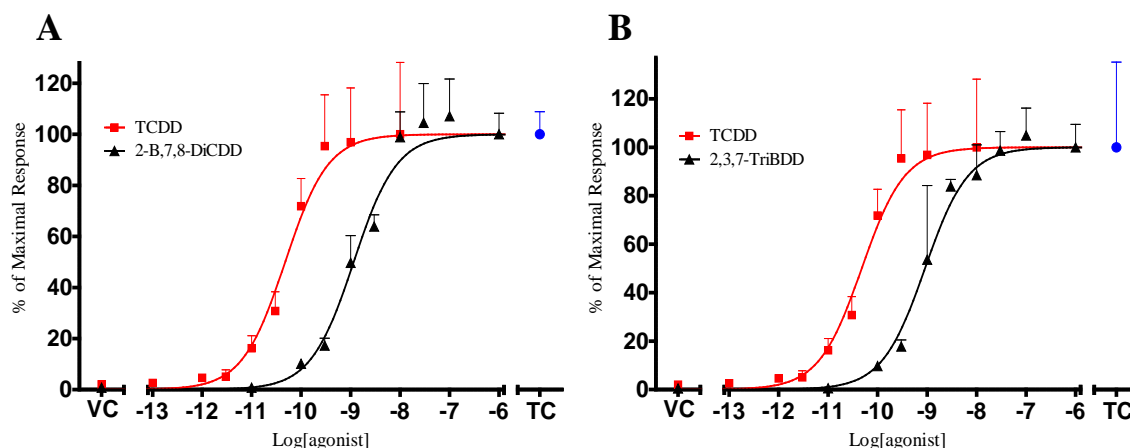
Figure 3.8: Potency of 2-B-7,8-DiCDD and 2,3,7-TriBDD as AhR agonists – Rat H4IIE cells were treated with various concentrations of either: 2-B-7,8-DiCDD, 2,3,7-TriBDD or TCDD. Concentration-response curves were created by plotting the % of maximal CYP1A1 mRNA induction by 10 nM TCDD against concentration of agonist. qRT-PCR was used to measure the level of induction of CYP1A1 and compared against control genes, β-actin and AhR. QbasePlus was used to normalise the data which was plotted using 10 nM TCDD only control as 100% of the maximal response. Results were compared with a vehicle control (VC) and a 10 nM TCDD only control (TC). Each point is the mean of three biological replicates ± S.D.

The potencies of 2-B-7,8-DiCDD (Figure 3.8A) and 2,3,7-TriBDD (Figure 3.8B) were estimated to be 1.16 nM (95% CI is shown in Table 3.1) and 904 pM, respectively. This produced REPs of 0.04 and 0.05 for 2-B-7,8-DiCDD and 2,3,7-TriBDD, respectively. The EC$_{50}$ of TCDD was calculated to be 47.6 pM (36.4 pM – 62.2 pM) and was used throughout sections 3.1.4 and 3.1.5.

3.1.4.3 Tetra-substituted-dibenzo-p-dioxins

TCDD is one of the most potent chlorinated congeners and is the most characterised of the AhR ligands. Two mixed halogenated dibenzo-*p*-dioxins with the same backbone structure as TCDD, 2-B-3,7,8-TriCDD and 2,3-DiB-7,8-DiCDD, were tested to investigate the effect of substituting chlorine for bromine. All of the compounds were tested in rat H4IIE cells. Additionally TCDD and 2-B-3,7,8-TriCDD were tested in human MCF-7 cells to allow species comparison. Figure 3.9 shows the comparison of these two compounds in rat and human.
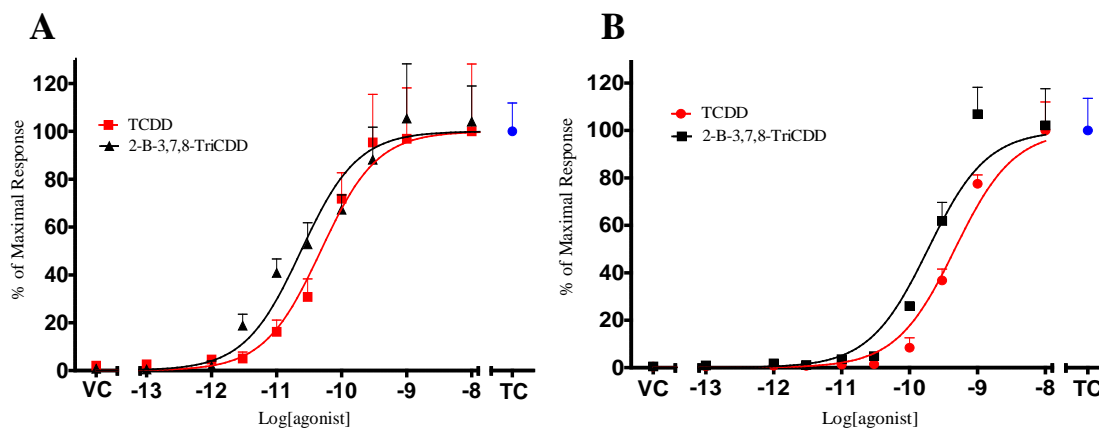
Figure 3.9: Comparison of 2-B-3,7,8-TriCDD and TCDD agonism of AhR in different species – (A) Rat H4IIE and (B) human MCF-7 cells treated with 2-B-3,7,8-TriCDD or TCDD for 4 hours. Concentration-response curves were created by plotting the % of maximal CYP1A1 mRNA induction by 10 nM TCDD against concentration of agonist. qRT-PCR was used to measure the level of induction of CYP1A1 and compared with control genes, β-actin and AhR. QbasePlus was used to normalise the data which was plotted using 10 nM TCDD only control as 100% of the maximal response. Results were compared with a vehicle control (VC) and a 10 nM TCDD only control (TC). Each point is the mean of three biological replicates ± S.D.

The EC_{50}s of TCDD and 2-B-3,7,8-TriCDD in rat (Figure 3.9A) were 47.6 pM and 23.7 pM, respectively. The data shows that 2-B-3,7,8-TriCDD is 2-fold more potent than TCDD at inducing CYP1A1 mRNA ($p<0.0001$). The two compounds were then tested in human MCF-7 cells under the same experimental conditions (Figure 3.9B). The EC_{50}s in human were 465 pM (95% CI = 341 pM – 633 pM) for TCDD and 187 pM (95% CI = 111 pM – 319 pM) for 2-B-3,7,8-TriCDD. Analysis showed that 2-B-3,7,8-TriCDD was ~2.5-fold more potent at inducing CYP1A1 mRNA than TCDD ($p<0.005$). 2-B-3,7,8-TriCDD gave a REP of 2.01 and 2.49 in rat H4IIE and human MCF-7 cells, respectively.
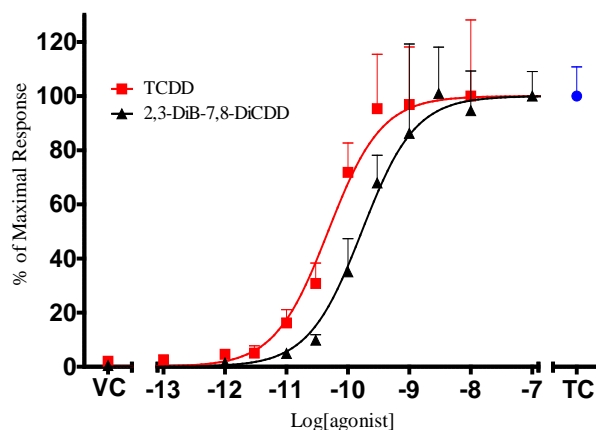
Figure 3.10: Potency of 2,3-DiB-7,8-DiCDD as an AhR agonist- Rat H4IIE cells were treated with 2,3-DiB-7,8-DiCDD or TCDD for 4 hours. Concentration-response curves were created by plotting the % of maximal CYP1A1 mRNA induction by 10 nM TCDD against concentration of agonist. qRT-PCR was used to measure the level of induction of CYP1A1 and compared against control genes, β-actin and AhR. QbasePlus was used to normalise the data which was plotted using 10 nM TCDD only control as 100% of the maximal response. Results were compared with a vehicle control (VC) and a 10 nM TCDD only control (TC). Each point is the mean of three biological replicates ± S.D.

Investigation of the potency of 2,3-DiB-7,8-DiCDD found an EC_{50} of 168 pM (Figure 3.10) which produced a REP of 0.28. This shows that the compound is still a potent agonist which is ~3-fold less potent than TCDD.

3.1.4.4 *Penta-substituted-dibenzo-p-dioxins*

A selection of penta-substituted halogenated dibenzo-*p*-dioxins, 1-B-2,3,7,8-TetraCDD and 2-B-1,3,7,8-TetraCDD, were tested in rat H4IIE cells and compared against TCDD. 1,2,3,7,8-PentaCDD is a potent AhR ligand in the same magnitude as TCDD with a TEF of 1 (Van den Berg *et al.,* 2006).
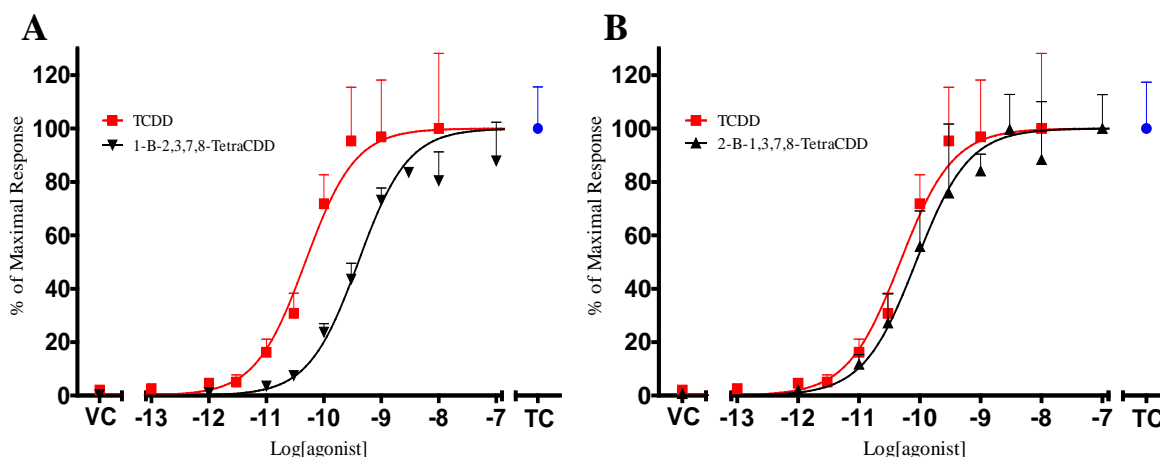
Figure 3.11: Potency of 1-B-2,3,7,8-TetraCDD and 2-B-1,3,7,8-TetraCDD as AhR agonists – Rat H4IIE cells were treated with 1-B-2,3,7,8-TetraCDD and 2-B-1,3,7,8-TetraCDD for 4 hours. TCDD was also plotted for comparison. Concentration-response curves were created by plotting the % of maximal CYP1A1 mRNA induction by 10 nM TCDD against concentration of agonist. qRT-PCR was used to measure the level of induction of CYP1A1 and compared against control genes, β-actin and AhR. QbasePlus was used to normalise the data which was plotted using 10 nM TCDD only control as 100% of the maximal response. Results were compared with a vehicle control (VC) and a 10 nM TCDD only control (TC). Each point is the mean of three biological replicates ± S.D.

According to the results in Figure 3.11A, the EC_{50} for 1-B-2,3,7,8-TetraCDD was 398 pM (whereas the EC_{50} for TCDD was 47.6 pM). This means that the compound is 10-fold less potent than TCDD with a REP of 0.12. Figure 3.11B shows rat H4IIE cells treated with 2-B-1,3,7,8-TetraCDD which gives an EC_{50} of 86.4 pM (95% CI = 65.3 pM – 114 pM). This means that the compound is only approximately 2-fold less potent than TCDD producing a REP of 0.55.

3.1.5   Mixed halogenated dibenzofurans

3.1.5.1   Summary of substituted-dibenzofurans in rat H4IIE cells

Concentration data in food, combined with previous potency research, has shown that these compounds may have a significant impact on TEQ based risk assessment (Table 1.3). Rat H4IIE cells were treated with various chlorinated, brominated or mixed halogenated dibenzofurans for 4 hours to calculate their potency based on the induction of CYP1A1

mRNA. The structures, EC_{50}s and REP values calculated in this work are summarised in Table 3.1 to allow comparison.
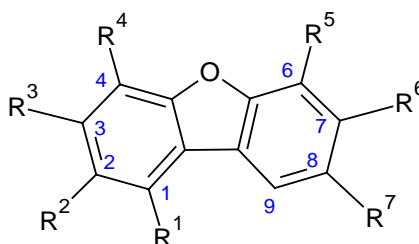
Structure	EC_{50} (95% CI)	REP
2,7,8-TriBDF $R^1=H; R^2=Br; R^3=H; R^4=H; R^5=H; R^6=Br; R^7=Br$	2020 pM (1100 pM – 3710 pM)	0.02
2-B-7,8-DiCDF $R^1=H; R^2=Br; R^3=H; R^4=H; R^5=H; R^6=Cl; R^7=Cl$	129 nM (90.1 nM – 184 nM)	0.0004
TCDF $R^1=H; R^2=Cl; R^3=Cl; R^4=H; R^5=H; R^6=Cl; R^7=Cl$	413 pM (196 pM - 869 pM)	0.12
3-B-2,7,8-TriCDF $R^1=H; R^2=Cl; R^3=Br; R^4=H; R^5=H; R^6=Cl; R^7=Cl$	151 pM (106 pM - 214 pM)	0.32
2,3-DiB-7,8-DiCDF $R^1=H; R^2=Br; R^3=Br; R^4=H; R^5=H; R^6=Cl; R^7=Cl$	80.3 pM (65.0 pM – 99.1 pM)	0.59
2-B-6,7,8-TriCDF $R^1=H; R^2=Br; R^3=H; R^4=H; R^5=Cl; R^6=Cl; R^7=Cl$	305 pM (214 pM – 434 pM)	0.16
PeCDF $R^1=H; R^2=Cl; R^3=Cl; R^4=Cl; R^5=H; R^6=Cl; R^7=Cl$	278 pM (179 pM - 433 pM)	0.17
4-B-2,3,7,8-TetraCDF $R^1=H; R^2=Cl; R^3=Cl; R^4=Br; R^5=H; R^6=Cl; R^7=Cl$	150 pM (86.9 pM - 260 pM)	0.32
1-B-2,3,7,8-TetraCDF $R^1=Br; R^2=Cl; R^3=Cl; R^4=H; R^5=H; R^6=Cl; R^7=Cl$	351 pM (275 pM – 449 pM)	0.14
1,3-DiB-2,7,8-TriCDF $R^1=Br; R^2=Cl; R^3=Br; R^4=H; R^5=H; R^6=Cl; R^7=Cl$	214 pM (119 pM – 386 pM)	0.22

Table 3.2: A summary of the potency of substituted-dibenzofurans as AhR agonists in rat H4IIE cells - EC_{50} values are shown with their 95% confidence intervals. The REP is comparison with the EC_{50} of TCDD within this experimental group (See Table 3.1).

The results show that all of the compounds are within 43-fold less potent than TCDD with the exception of 2-B-7,8-DiCDF which is shown to be ~2700-fold less potent than TCDD. The full concentration response curves are also shown below (Figure 3.12 to Figure 3.14).

3.1.5.2 Tri-substituted-dibenzofurans

The potency of 2-B-7,8-DiCDF was tested in rat H4IIE cells and compared against TCDD. The compound has the same backbone structure as 2,7,8-TriCDF although one of the

chlorine atoms is substituted with bromine. 2,7,8-TriCDF has been previously tested with a REP of 0.0015 (Behnisch *et al.,* 2003), however the compound is not included in the WHO TEF estimations.
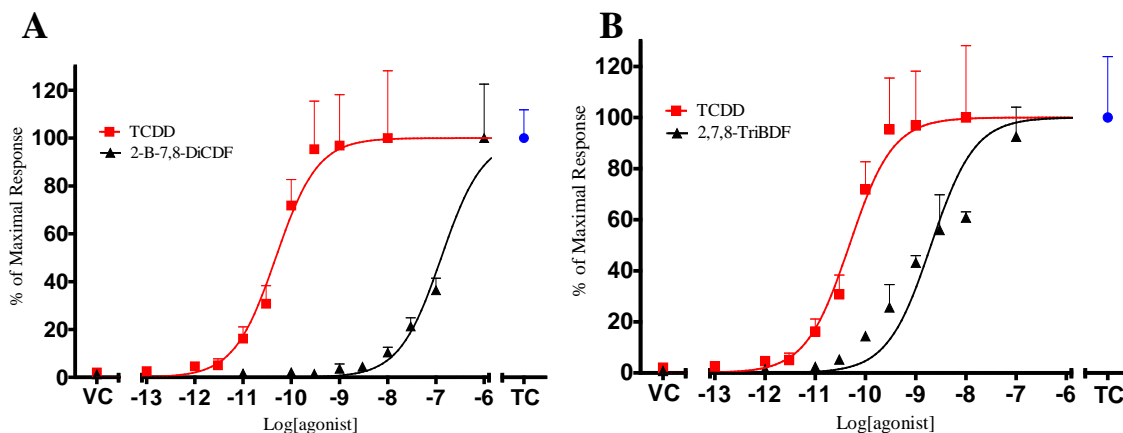
Figure 3.12: Potency of 2-B-7,8-DiCDF and 2,7,8-TriBDF as AhR agonists – Rat H4IIE cells were treated with 2-B-7,8-DiCDF or 2,7,8-TriBDF for 4 hours. TCDD was also plotted for comparison. Concentration-response curves were created by plotting the % of maximal CYP1A1 mRNA induction by 10 nM TCDD against concentration of agonist. qRT-PCR was used to measure the level of induction of CYP1A1 and compared against control genes, β-actin and AhR. QbasePlus was used to normalise the data which was plotted using 10 nM TCDD only control as 100% of the maximal response. Results were compared with a vehicle control (VC) and a 10 nM TCDD only control (TC). Each point is the mean of three biological replicates ± S.D.

Figure 3.12A shows the potency of 2-B-7,8-DiCDF which was calculated as 129 nM (95% CI is shown in Table 3.2). This was 10,000-fold less potent than TCDD and gave a REP of 0.00037. This was compared with 2,7,8-TriBDF, which provided an EC_{50} of 2.02 nM (Figure 3.12B) and was calculated to be approximately 50-fold less potent than TCDD with a REP of 0.024.

3.1.5.3 Tetra-substituted-dibenzofurans

TCDF is one of the most potent members of the dibenzofuran family (TEF = 0.1; Van den Berg *et al.,* 2006). Two mixed halogenated versions of the compound, 3-B-2,7,8-TriCDF and 2,3-DiB-7,8-DiCDF, were tested and compared alongside TCDD. The compounds were tested in rat H4IIE cells for 4 hours to measure the induction of CYP1A1 mRNA.
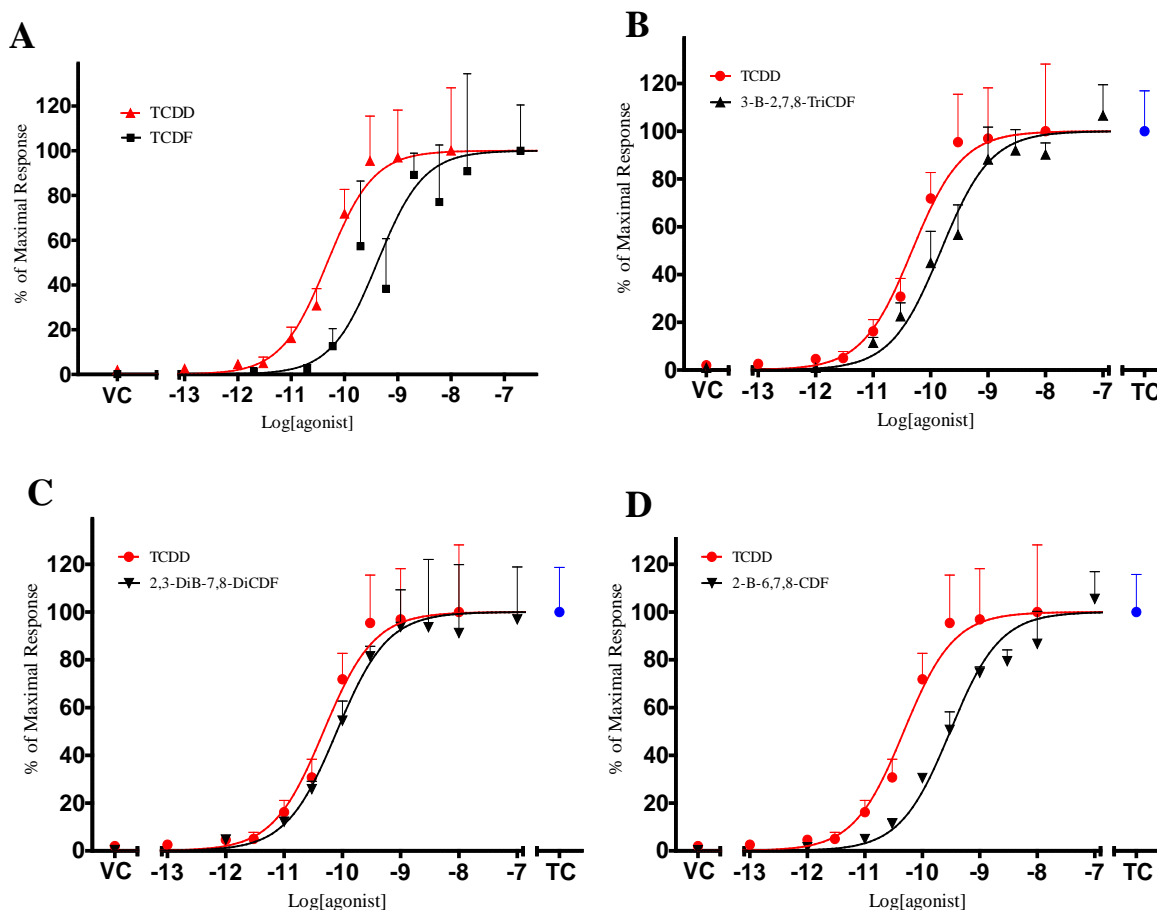
Figure 3.13: Potency of TCDF, 3-B-2,7,8-TriCDF, 2,3-DiB-7,8-DiCDF and 2-B-6,7,8-TriCDF as AhR agonists - Rat H4IIE cells were treated with (A) TCDF, (B) 3-B-2,7,8-TriCDF, (C) 2,3-DiB-7,8-DiCDF, (D) 2-B-6,7,8-TriCDF or TCDD for 4 hours Concentration-response curves were created by plotting the % of maximal CYP1A1 mRNA induction by 10 nM TCDD against concentration of agonist. qRT-PCR was used to measure the level of induction of CYP1A1 and compared against control genes, β-actin and AhR. QbasePlus was used to normalise the data which was plotted using 10 nM TCDD only control as 100% of the maximal response. Results were compared with a vehicle control (VC) and a 10 nM TCDD only control (TC). Each point is the mean of three biological replicates ± S.D.

Previous work by this author (which was newly calibrated based on GC/MS data) calculated the EC_{50} of TCDF (A) as 413 pM (95% CI = 196 pM – 869 pM; Wall, 2008). Figure 3.13 shows the potency of (B) 3-B-2,7,8-TriCDF, (C) 2,3-DiB-7,8-DiCDF and (D) 2-B-6,7,8-TriCDF compared with TCDD. The EC_{50} for 3-B-2,7,8-TriCDF was 151 pM, the EC_{50} for 2,3-DiB-7,8-DiCDF was 80.3 pM and the EC_{50} for 2-B-6,7,8-TriCDF was 305 pM. The results show that the three mixed halogenated dibenzofurans are between 2 and 10-fold less

potent than TCDD (p<0.0001 for all three compounds) and the three mixed halogenated dibenzofurans are also statistically different from one another using a T-test (p<0.005). The REP for 3-B-2,7,8-TriCDF, 2,3-DiB-7,8-DiCDF and 2-B-6,7,8-TriCDF was calculated to be 0.32, 0.59 and 0.16, respectively.

3.1.5.4 Penta-substituted-dibenzofurans

Based on the WHO TEQ summary, PeCDF is a high potency ligand approximately 3-fold less potent than TCDD (REP = 0.3; Van den Berg *et al.*, 2005).
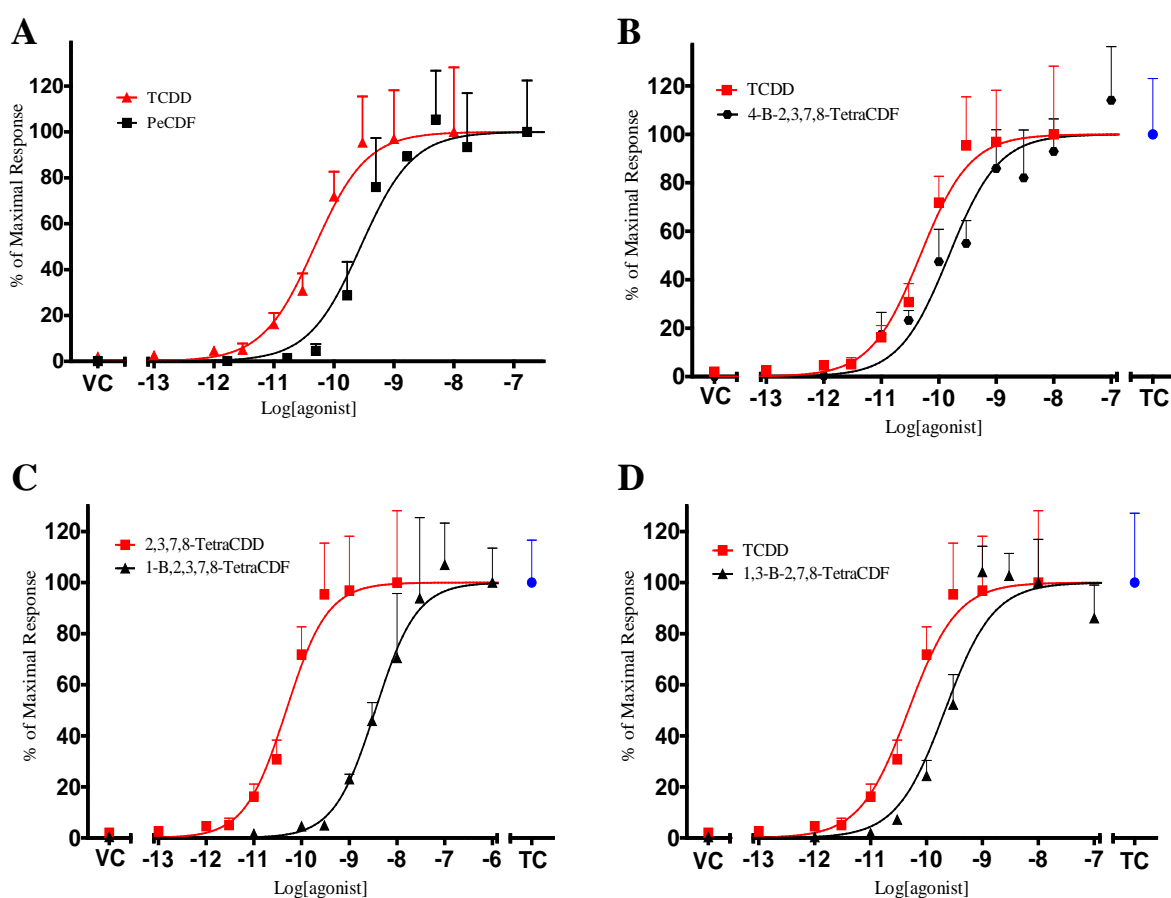
Figure 3.14: Potency of PeCDF, 4-B-2,3,7,8-TetraCDF, 1-B-2,3,7,8-TetraCDF and 1,3-DiB-2,7,8-TriCDF as AhR agonists - Rat H4IIE cells were treated with (A) PeCDF, (B) 4-B-2,3,7,8-TetraCDF, (C) 1-B-2,3,7,8-TetraCDF and (D) 1,3-DiB-2,7,8-TriCDF for 4 hours. Concentration-response curves were created by plotting the % of maximal CYP1A1 mRNA induction by 10 nM TCDD against concentration of agonist. qRT-PCR was used to measure the level of induction of CYP1A1 and compared against control genes, β-actin and AhR. QbasePlus was used to normalise the data which was plotted using 10 nM TCDD only control as 100% of the maximal response. Results were compared with a vehicle control (VC) and a 10 nM TCDD only control (TC). Each point is the mean of three biological replicates ± S.D.

Four penta-substituted dibenzofurans were tested including PeCDF (2,3,4,7,8-PeCDF) and 4-B-2,3,7,8-TetraCDF which have the same structure. 1-B-2,3,7,8-TetraCDF and 1,3-DiB-2,7,8-TriCDF are based on the structure 1,2,3,7,8-PeCDF (TEF = 0.03, Van den Berg *et al.,* 2006) which is 50-fold less potent than TCDD. The four compounds were tested in rat H4IIE cells for 4 hours and compared against a concentration-response curve of TCDD.

The EC_{50} for PeCDF shown in Figure 3.14A was calculated previously by this author (newly calibrated) as 278 pM (95% CI = 179 pM – 433 pM; Wall, 2008), which was shown to be 5-fold less potent than TCDD. Figure 3.14B shows the potency of 4-B-2,3,7,8-TetraCDF compared against TCDD in rat H4IIE cells which was 150 pM which gave a REP of 0.32. The EC_{50} for 1-B-2,3,7,8-TetraCDF was calculated to be 351 pM producing a REP of 0.14. Finally the EC_{50} for 1,3-DiB-2,7,8-TriCDF was calculated to be 214 pM giving a REP of 0.22.

3.1.6 Mixed halogenated biphenyls

3.1.6.1 Summary of substituted-biphenyls in rat H4IIE cells

Concentration data in food, combined with previous potency research, has shown that these compounds may have a significant impact on TEQ based risk assessment (section 1.3.3). Rat H4IIE cells were treated with various chlorinated, brominated or mixed halogenated biphenyls for 4 hours to calculate their potency based on the induction of CYP1A1 mRNA. The structures, EC_{50}s and REP values calculated in this work are summarised in Table 3.3 to allow comparison.

R⁴ positions labeled, biphenyl structure with substituents R^1–R^6 at positions 1–6 and 2'–6'.
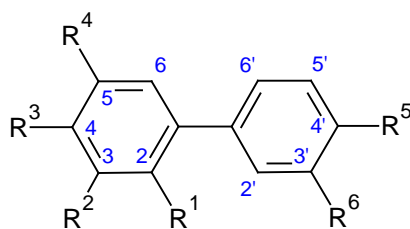
Structure	EC$_{50}$ (95% CI)	REP
TCDD $R^1=H; R^2=Cl; R^3=Cl; R^4=Cl; R^5=Cl$	28.9 pM (19.9 pM – 41.9 pM)	1[b]
3,3',4,4',5-PentaCB (PCB 126) $R^1=H; R^2=Cl; R^3=Cl; R^4=Cl; R^5=Cl; R^6=Cl$	281 pM (225 pM – 352 pM)	0.10
4'-B-3,3',4,5-TetraCB (PXB 126B) $R^1=H; R^2=Cl; R^3=Cl; R^4=Cl; R^5=Br; R^6=Cl$	130 pM (92.2 pM – 183 pM)	0.22
3',4'-DiB-3,4,5-TriCB (PXB 126H) $R^1=H; R^2=Cl; R^3=Cl; R^4=Cl; R^5=Br; R^6=Br$	200 pM (78.2 pM – 513 pM)	0.14
3',4',5-TriB-3,4-DiCB (PXB 126V) $R^1=H; R^2=Br; R^3=Cl; R^4=Br; R^5=Br; R^6=Br$	72.2 pM (48.4 pM – 108 pM)	0.40
3,3',4,4',5-PentaBB (PBB 126) $R^1=H; R^2=Br; R^3=Br; R^4=Br; R^5=Br; R^6=Br$	622 pM (487 pM – 796 pM)	0.05
2,3',4,4'-PentaCB (PCB 105) $R^1=Cl; R^2=H; R^3=Cl; R^4=Cl; R^5=Cl; R^6=Cl$	1.60 µM (1.56 µM – 1.63 µM)	0.000002
4'-B-2,3,3',4-TetraCB (PXB 105) $R^1=Cl; R^2=H; R^3=Cl; R^4=Cl; R^5=Br; R^6=Cl$	2.46 µM (2.10 µM – 2.90 µM)	0.00001
2,3',4,4',5-PentaCB (PCB 118) $R^1=Cl; R^2=Cl; R^3=Cl; R^4=H; R^5=Cl; R^6=Cl$	11.8 µM (10.5 µM – 13.2 µM)	0.000003
4'-B-2,3',4,5-TetraCB (PXB 118) $R^1=Cl; R^2=Cl; R^3=Cl; R^4=H; R^5=Br; R^6=Cl$	775 nM (655 nM – 917 nM)	0.0001
2,3,3',4,4',5-HexaCB (PCB 156) $R^1=Cl; R^2=Cl; R^3=Cl; R^4=Cl; R^5=Cl; R^6=Cl$	122 nM (104 nM – 144 nM)	0.0002
4'-B-2,3,3',4,5-PentaCB (PXB 156) $R^1=Cl; R^2=Cl; R^3=Cl; R^4=Cl; R^5=Br; R^6=Cl$	139 nM (95.5 nM – 203 nM)	0.0002

Table 3.3: A summary of the potency of substituted-biphenyls as AhR agonists in rat H4IIE cells - EC$_{50}$ values are shown with their 95% confidence intervals. 1[b]: The REP is comparison with the EC$_{50}$ of TCDD within this experimental group.

The results show that all of the non-*ortho*-substituted biphenyls are within 10-fold less potent than TCDD. The mono-*ortho*-substituted biphenyls were shown to be at least 5000-fold less potent than TCDD (PCB 156 and PXB 156) and up to 500,000-fold less potent than TCDD (PCB 105). The full concentration-response curves are also shown below (Figure 3.15 to Figure 3.22). Three compounds, PCB 105, 118 and 156, were selected for further analysis based on their high environmental abundance. These congeners may have a less-

than-additive effect on the total TCDD-like toxicity of a mixture and could therefore be useful when studying the theory of additivity. The use of qRT-PCR will be applied to measure CYP1A1 mRNA induction of the compounds in the presence of TCDD to determine if the compounds have any antagonistic properties.

3.1.6.2 *3,3',4,4',5-substituted biphenyls* (*PXB 126*)

PCB 126 is the most characterised and one of the most potent of the polychlorinated biphenyls. Several congeners with the same backbone structure but with different substitutions were tested to see if they had equally potent properties. Several PCB 126 congeners, PXB 126B, PXB 126H, PXB 126V and 3,3',4,4',5-PentaBB (PBB 126), were tested to see if the addition of bromine had a positive impact on the ability of the compound to elicit a AhR-mediated response. These compounds were all tested in rat H4IIE cells. The induction of CYP1A1 mRNA by PCB 126 and PXB 126B were also tested in human MCF-7 cells to gauge the species-specific response of the compounds.
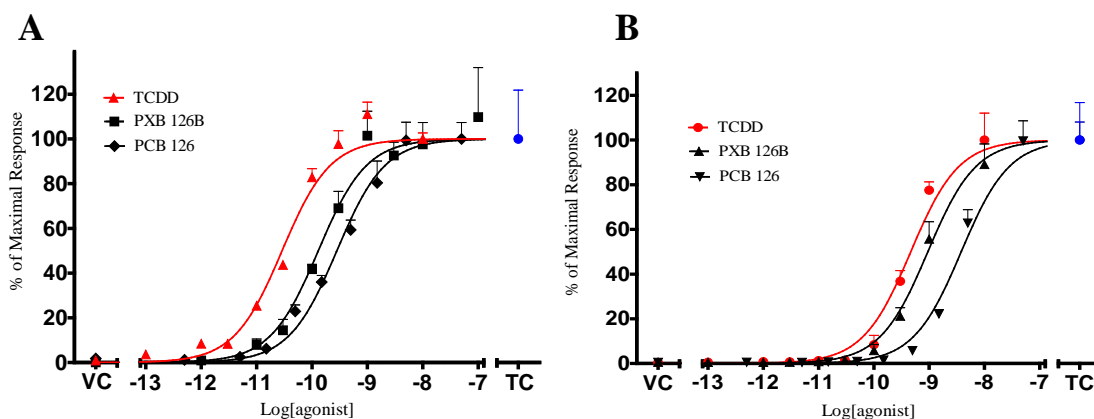
Figure 3.15: Potency and species comparison of PXB 126B and PCB 126 as AhR agonists – (A) Rat H4IIE and (B) human MCF7 cells were treated with various concentrations of PXB 126B or PCB 126. Concentration-response curves were created by plotting the % of maximal CYP1A1 mRNA induction by 10 nM TCDD against concentration of agonist. qRT-PCR was used to measure the level of induction of CYP1A1 mRNA and compared against control genes, β-actin and AhR. QbasePlus was used to normalise the data which was plotted using 10 nM TCDD only control as 100% of the maximal response. Results were compared with a vehicle control (VC) and a 10 nM TCDD only control (TC). Each point is the mean of three biological replicates ± S.D.

The agonistic properties of TCDD, PCB 126 and PXB 126B were tested in rat H4IIE (Figure 3.15A) and human MCF-7 cells (Figure 3.15B). In rat, the EC_{50} for TCDD was 28.9 pM (95% CIs are shown in Table 3.3), PCB 126 was 281 pM and PXB 126B was 130 pM. PCB 126 was 10-fold less potent than TCDD with a REP of 0.10. This corresponds well with the WHO TEF value of 0.1 (Van den Berg *et al.,* 2006). PXB 126B was 5-fold less potent than TCDD and, in turn, 2-fold more potent than PCB 126. A REP of 0.22 was calculated for this compound. The EC_{50}s for PCB 126 and PXB 126B were significantly different (p = 0.0006). In human MCF-7 cells, the EC_{50} for TCDD was 464 pM (95% CI = 341 pM – 633 pM), PCB 126 was 3.81 nM (95% CI = 2.89 nM – 5.02 nM) and PXB 126B was 947 pM (95% CI = 807 pM – 1.11 nM). The REP calculated for PCB 126 was 0.12 which is supported by the REP calculated in rat H4IIE cells and WHO TEF (0.1; Van den Berg *et al.,* 2006). PXB 126B is 2-fold less potent than TCDD giving a REP of 0.49 and is 5-fold more potent than PCB 126 in human MCF-7 cells. TCDD and PCB 126 were shown to be 15-fold more potent in rat than in human cells. PXB 126B was shown to be 7-fold more potent in rat than human cells. Two other PXB 126 substituted compounds and PBB 126 were tested in rat H4IIE to measure their potencies.
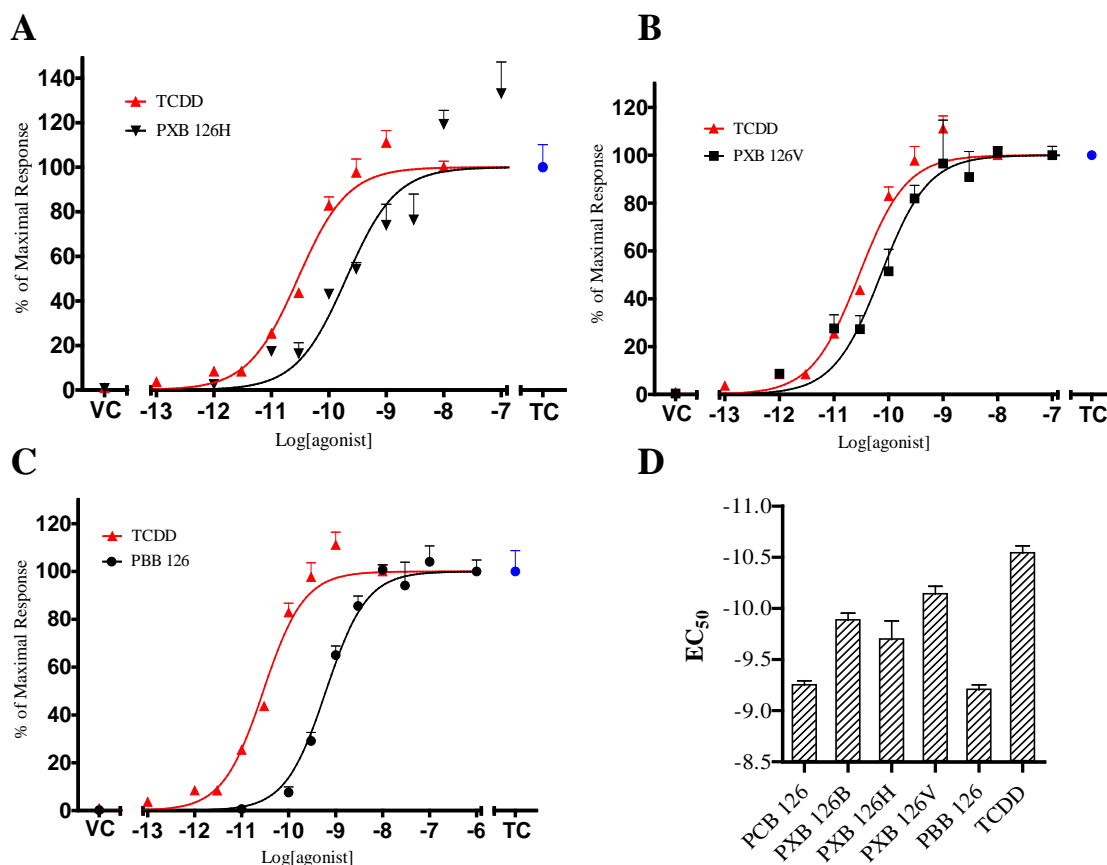
Figure 3.16: Potency of PXB 126H, PXB 126V and PBB 126 as AhR agonists – Rat H4IIE were treated with various concentrations of (A) 3',4'-DiB-3,4,5-TriCB (PXB 126H), (B) 3',4',5-TriB-3,4-DiCB (PXB 126V) or (C) 3,3',4,4',5-PentaBB (PBB 126). TCDD was also plotted for comparison. (D) Comparison of REPs and EC_{50}s for non-*ortho*-substituted biphenyls (PXB 126). Concentration-response curves were created by plotting the % of maximal CYP1A1 mRNA induction by 10 nM TCDD against concentration of agonist. qRT-PCR was used to measure the level of induction of CYP1A1 and compared against control genes, β-actin and AhR. QbasePlus was used to normalise the data which was plotted using 10 nM TCDD only control as 100% of the maximal response. Results were compared with a vehicle control (VC) and a 10 nM TCDD only control (TC). Each point is the mean of three biological replicates ± S.D.

The potency of PXB 126H, PXB 126V and PBB 126 are shown in Figure 3.16. The EC_{50}s were 200 pM for PXB 126H, 72.2 pM for PXB 126V and 622 pM for PBB 126. The EC_{50} of TCDD was shown in Figure 3.15A. This gave REPs of 0.15, 0.40 and 0.05 for PXB 126H, PXB 126V and PBB 126, respectively. All three compounds were within 2- to 20-fold less potent than TCDD in rat H4IIE cells.

3.1.6.3 2,3,3',4,4'-substituted biphenyls (*PXB 105*)

PCB 105 was identified as an environmentally abundant AhR ligand. Furthermore previous research has suggested in may also have antagonist properties. Therefore to investigate what impact these properties could have on risk assessment, the agonistic and antagonistic properties of the compound were investigated. The activation of the AhR was measured by the subsequent induction of CYP1A1. Figure 3.17 shows the potency of PCB 105 and TCDD in rat H4IIE and human MCF-7 cells.
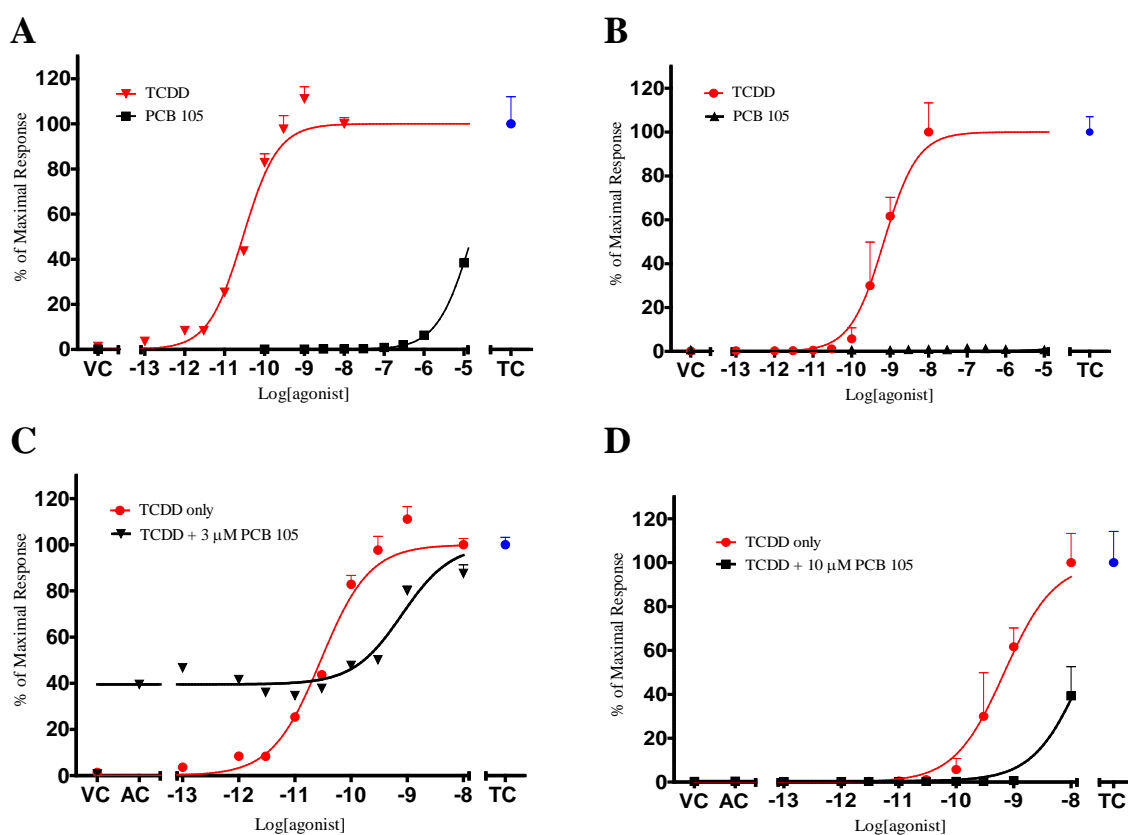
Figure 3.17: PCB 105 is a partial agonist of rat AhR but an antagonist of human AhR – (A) Rat H4IIE or (B) human MCF7 cells were treated with various concentrations of PCB 105. (C) Rat H4IIE or (D) human MCF-7 cells were treated with various concentrations of TCDD in the absence or presence of 3 µM and 10 µM PCB 105, respectively. Concentration-response curves were created by plotting the % of maximal CYP1A1 mRNA induction by 10 nM TCDD against concentration of agonist. qRT-PCR was used to measure the level of induction of CYP1A1 and compared against control genes, β-actin and AhR. QbasePlus was used to normalise the data which was plotted using 10 nM TCDD only control as 100% of the maximal response. Results were compared with a vehicle control (VC), putative antagonist only (AC) and a 10 nM TCDD only control (TC). Each point is the mean of three biological replicates ± S.D.

Figure 3.17 shows that PCB 105 was shown to be a relatively weak agonist with EC_{50}s of 16.0 µM (95% CI = 15.6 µM – 16.3 µM) in rat H4IIE cells (Figure 3.17A) and no measurable response up to 10 µM PCB 105 in human MCF-7 cells (Figure 3.17B). TCDD gave an EC_{50} of 28.9 pM (95% CI = 19.9 pM – 41.9 pM) in rat H4IIE cells and 241 pM (95% CI = 161 pM – 362 pM) in human MCF-7 cells. The data shows that PCB 105 is 55,000-fold less potent at inducing CYP1A1 mRNA than TCDD in rat cells. A REP value of 0.0000018 was calculated from the data in rat H4IIE cells which is 15-fold less than the TEF value of 0.00003 derived by the 2005 WHO consortium (Van den Berg *et al.,* 2006). The antagonistic property of the compound was assessed by treating cells with various concentrations of TCDD but in the presence of a set concentration of PCB 105. Figure 3.17 also shows TCDD concentration-response curves in rat H4IIE cells (C) or human MCF-7 cells (D) in the presence or absence of PCB 105. The concentration of PCB 105 added was the concentration required to produce 20% of the maximal response which was 3 µM in rat cells based on the data in Figure 3.17A. As no response was detected in human cells, the highest possible concentration (10 µM) was used instead. The antagonist effects were assessed by the ability of PCB 105 to compete with TCDD. The EC_{50} for TCDD in the presence of PCB 105 was increased to 806 pM (95% CI = 191 pM – 3.39 nM) from 28.9 pM in its absence. These results clearly indicate that PCB 105 has a statically significant (p<0.0001) effect on the ability of TCDD induce CYP1A1 mRNA (activate the AhR). These results, in combination with Figure 3.17A, show that PCB 105 is a partial agonist (agonist and antagonist properties) in rat cells. Figure 3.17D shows human MCF-7 cells treated in the same way. The data show that there is a significant antagonistic effect on the potency of TCDD when in the presence of 10 µM PCB 105: the EC_{50} for TCDD was significantly (p<0.0001) increased to 16.6 nM (95% CI = 13.9 nM – 19.7 nM) from 28.9 pM. This compound is therefore a partial agonist in rat and an antagonist in human.

The effect of substituting a chlorine atom with a bromine atom was investigated by treating rat H4IIE cells with PXB 105 for 4 hours.

Figure 3.18: PXB 105 is a partial agonist of rat AhR – (A) Agonist properties, rat H4IIE cells were treated with various concentrations of PXB 105 for 4 hours. (B) Antagonistic properties, rat H4IIE cells were treated with various concentrations of TCDD in the presence or absence of 1 µM PXB 105. Concentration-response curves were created by plotting the % of maximal CYP1A1 mRNA induction by 10 nM TCDD against concentration of agonist. qRT-PCR was used to measure the level of induction of CYP1A1 and compared against control genes, β-actin and AhR. Results were compared with an antagonist only control (AC), a vehicle control (VC) and a 10 nM TCDD only control (TC) which is normalised as 100% of the maximal response. Each point is the mean of three biological replicates ± S.D.

Figure 3.18A shows the potency of PXB 105 in comparison with TCDD. The EC_{50} was estimated to be 2.46 µM (95% CI = 2.10 µM – 2.90 µM) based on the assumption that the curve would reach 100% response. The data shows that PXB 105 is about 100,000-fold less potent at inducing CYP1A1 mRNA than TCDD with a REP of 0.00001. The compound is also shown to be 5-fold more potent than the chlorinated substituent, PCB 105. The antagonistic properties were measured by treating rat H4IIE cells with various concentrations of TCDD in the presence of 1 µM PXB 105, which was shown to produce ~25% of the maximal response (Figure 3.18B). The EC_{50} for TCDD in the presence of PXB 105 was 5.56 nM (95% CI = 1.60 nM – 19.3 nM) which is statistically different from TCDD alone, EC_{50} = 28.9 pM (p <0.0001). This was a decrease of 200-fold in the ability of TCDD to induce CYP1A1 mRNA and clearly shows that PXB 105 is a partial agonist.

3.1.6.4 2,3',4,4',5-substituted biphenyls (*PXB 118*)

The next compound to be analysed was PCB 118. This was shown to be the most environmentally prevalent PCB based on previous literature. Figure 3.19 shows rat and human cells treated with PCB 118 or TCDD for 4 hours. CYP1A1 mRNA was measured using qRT-PCR and normalised against 10 nM TCDD only (defined as 100% response).
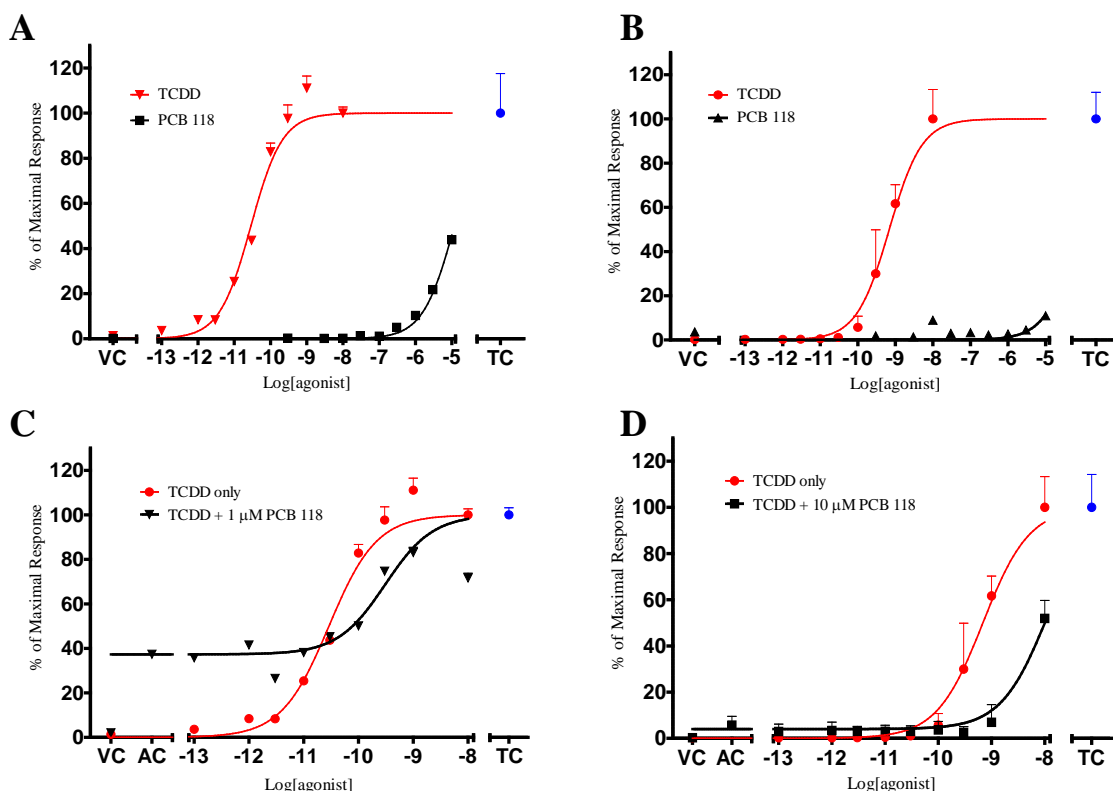
Figure 3.19: PCB 118 is a partial agonist of AhR of rat and human AhR – (A) Rat H4IIE or (B) human MCF7 cells were treated with various concentrations of PCB 118. (C) Rat H4IIE cells and (D) human MCF-7 cells were treated with various concentrations of TCDD in the presence or absence of 1 µM or 10 µM PCB 118, respectively. All of the graphs show a TCDD concentration-response curve for comparison. Concentration-response curves were created by plotting the % of maximal CYP1A1 mRNA induction by 10 nM TCDD against concentration of agonist. qRT-PCR was used to measure the level of induction of CYP1A1 and compared against control genes, β-actin and AhR. QbasePlus was used to normalise the data which was plotted using 10 nM TCDD only control as 100% of the maximal response. Results were compared with an antagonist only control (AC), a vehicle control (VC) and a 10 nM TCDD only control (TC). Each point is the mean of three biological replicates ± S.D.

The agonistic potency of PCB 118 was measured in rat H4IIE (Figure 3.19A) and human MCF-7 cells (Figure 3.19B). The EC$_{50}$ for PCB 118 in rat cells was 11.8 µM (95% CI = 10.5

μM – 13.2 μM) but no accurate EC_{50} could be derived from the human data. This was compared to rat and human cells treated with TCDD. The data shows that PCB 118 is ~400,000-fold less potent than TCDD in rat. No REP could be calculated from the data derived from the human cells but for rat the REP is 0.000003 which is 10-fold lower than the TEF calculated by the 2005 WHO consortium (0.00003; Van den Berg *et al.,* 2006). In order to calculate the antagonistic properties of the compounds, the concentration that produced 20% of the maximal response was extrapolated from the data in Figure 3.19. The value for PCB 118 in rat was 3 μM but as there was no significant response detected in human, the highest concentration available was used which was 10 μM. The concentration of PCB 118 was treated simultaneously with various concentrations of TCDD to detect if the compound has any effect on the potency of TCDD. Figure 3.19C shows TCDD in the presence and absence of 3 μM PCB 118 in rat H4IIE cells. The EC_{50} for TCDD in the presence of PCB 118 was increased from 28.9 pM (p<0.001) to 306 pM (95% CI = 75.2 pM – 1.25 nM). The graph also shows TCDD without the addition of PCB 118. The two EC_{50}s are statistically different based on the 95% confidence intervals, with the graph showing a distinctive shift of the TCDD curve to the right suggesting it has a reduced ability to induce CYP1A1. The compound was next tested in human MCF-7 cells, shown in Figure 3.19D. The EC_{50} for TCDD in the presence of 10 μM PCB 118 gives an EC_{50} of 10.9 nM (95% CI = 8.6 nM – 13.8 nM) compared to 28.9 pM (TCDD alone) which is a statistically significant shift of the TCDD curve to the right (p <0.0001). The two EC_{50}s are also significantly different from one another based on their 95% confidence intervals. A concentration of 10 μM had very little agonistic effect but produced a measurable antagonist effect. From this combined data it is possible to conclude that PCB 118 is a partial agonist in rat H4IIE and human MCF-7 cells. A mixed halogenated PXB 118 was tested, which has a chlorine atom (position 4';

Table 3.3) substituted with a bromine atom. The compound was tested in rat H4IIE cells to measure any putative agonist and antagonist properties.
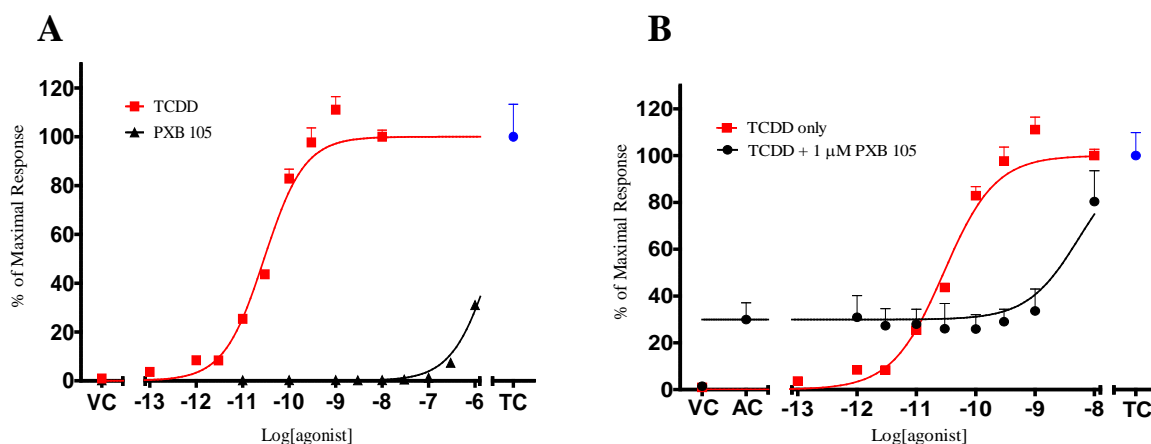

Figure 3.20: PXB 118 is a partial agonist of AhR in rat – (A) Agonist properties, rat H4IIE cells were treated with various concentrations of PXB 118 for 4 hours. (B) Antagonistic properties, rat H4IIE cells were treated with various concentrations of TCDD in the presence or absence of 300 nM PXB 118. Concentration-response curves were created by plotting the % of maximal CYP1A1 mRNA induction by 10 nM TCDD against concentration of agonist. qRT-PCR was used to measure the level of induction of CYP1A1 and compared against control genes, β-actin and AhR. Results were compared with an antagonist only control (AC), a vehicle control (VC) and a 10 nM TCDD only control (TC) which is normalised as 100% of the maximal response. Each point is the mean of three biological replicates ± S.D.

Figure 3.20A shows the EC_{50} of PXB 118 in rat H4IIE cells to be 775 nM (95% CI = 655 nM – 917 nM) which is 25,000-fold less potent than TCDD and is 10-fold more potent than PCB 118 at inducing CYP1A1 mRNA under the same conditions. The antagonist properties were measured by treating cells with various concentrations of TCDD in the presence of 300 nM PXB 118 (Figure 3.20B) which gave an EC_{50} of 96.2 pM (95% CI = 45.5 pM – 203 pM) compared with TCDD alone (EC_{50} = 28.9 pM). The two EC_{50}s were shown to be significantly different (p <0.005) with PXB 118 reducing the potency of TCDD by 3-fold. This data shows that PXB 118 is a partial agonist, nearly 10-fold more potent than the structurally similar but fully chlorinated congener, PCB 118. A REP of 0.00003 was calculated for PXB 118.

3.1.6.5 2,3,3',4,4',5-substituted biphenyls (*PXB 156*)

The final compound to be tested with qRT-PCR was PCB 156. Previous research has suggested this is the most potent of the mono-*ortho*-substituted PCBs at inducing CYP1A1 mRNA (Van den Berg *et al.,* 1998) although also the less environmentally prevalent of the three compounds tested. Figure 3.21 shows the potency of PCB 156 in comparison to TCDD in rat H4IIE and human MCF-7 cells.
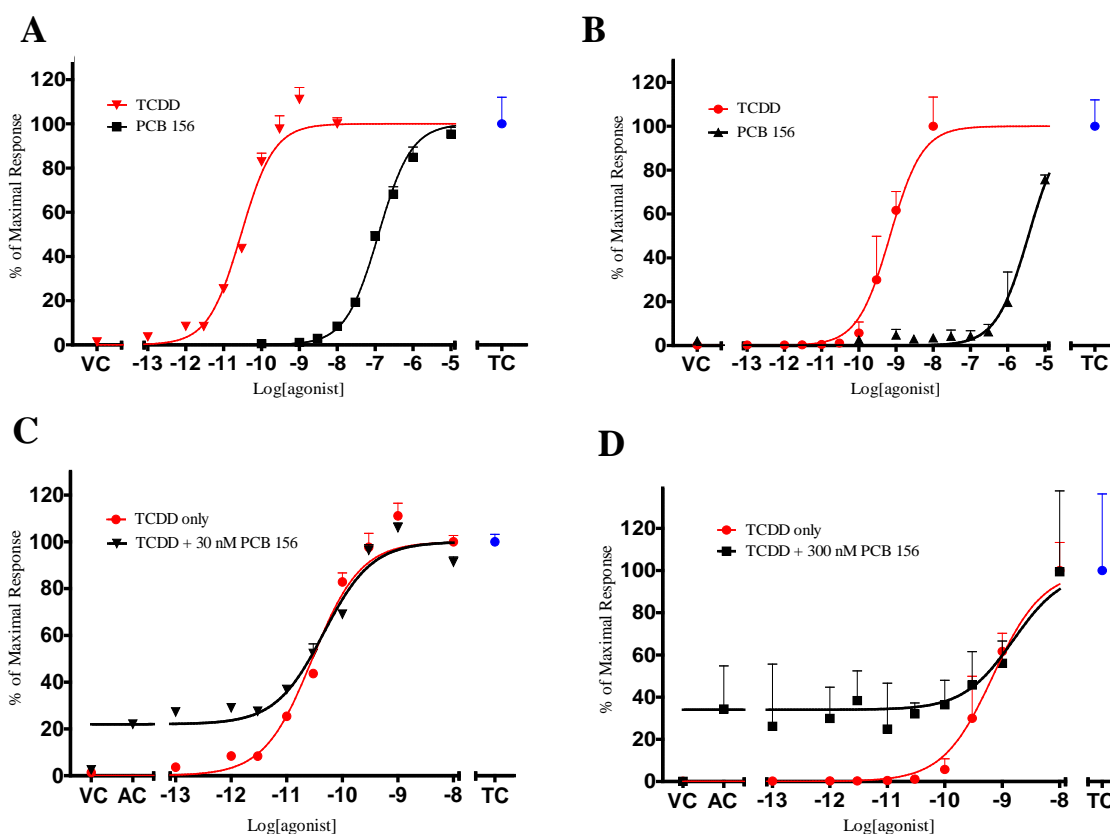
Figure 3.21: PCB 156 is a pure agonist of rat and human AhR – (A) Rat H4IIE or (B) human MCF7 cells were treated with various concentrations of PCB 156. The graphs also show a TCDD concentration-response curves for comparison. (C) Rat H4IIE cells or (D) human MCF-7 cells were treated with various concentrations of TCDD in the presence or absence of 30 nM or 300 nM PCB 156, respectively. Concentration-response curves were created by plotting the % of maximal CYP1A1 mRNA induction by 10 nM TCDD against concentration of agonist. qRT-PCR was used to measure the level of induction of CYP1A1 and compared against control genes, β-actin and AhR. Results were compared with an antagonist only control (AC), a vehicle control (VC) and a 10 nM TCDD only control (TC) which is normalised as 100% of the maximal response. Each point is the mean of three biological replicates ± S.D.

According to the data, PCB 156 is the most potent AhR agonist of the three fully chlorinated mono-*ortho*-substituted PCBs with an EC_{50} of 122 nM (95% CI = 104 nM – 144 nM) in rat (Figure 3.21A) and EC_{50} of 3.59 µM (95% CI = 2.81 µM – 4.59 µM) in human (Figure 3.21B). This clearly indicates that PCB 156 is an agonist in rat and human cell lines. The 2005 WHO TEF for PCB 156 is 0.00003 (Van den Berg *et al.,* 2006) however this data gives a REP value of ~0.0003 in rat and human. This is a 10-fold increase in the REP/TEF estimation but is supported by the original 1998 WHO TEF value (0.0005; Van den Berg *et al.,* 1998). The data clearly shows that there is a 30-fold difference in the potency of PCB 156 between rat and human AhR compared with a 10-fold difference with TCDD. The antagonistic effects were measured by treating cells with TCDD in the presence of 1 µM and 10 µM, respectively. In rat H4IIE cells (Figure 3.21C), the EC_{50} for TCDD with PCB 156 was 46.3 pM (95% CI = 24.8 pM – 86.2 pM). The 95% confidence overlap between the two EC_{50}s shows that they are not statistically different leading to the conclusion that PCB 156 is not an antagonist of rat AhR ($p = 0.175$). Figure 3.21D shows the same experiment in human MCF-7 cells. The EC_{50} for TCDD in the presence of 300 nM PCB 156 in human cells was 1.55 nM (95% CI = 411 pM – 5.88 nM). This shows that there is a statistically significant difference between the EC_{50} of TCDD alone and that of TCDD with PCB 156 ($p < 0.005$) which signifies that this compound is a partial agonist of AhR in human MCF-7 cells in these conditions.

Another structurally similar compound, PXB 156, was tested on rat H4IIE cells to see if it shared similar AhR activation characteristics with PCB 156.
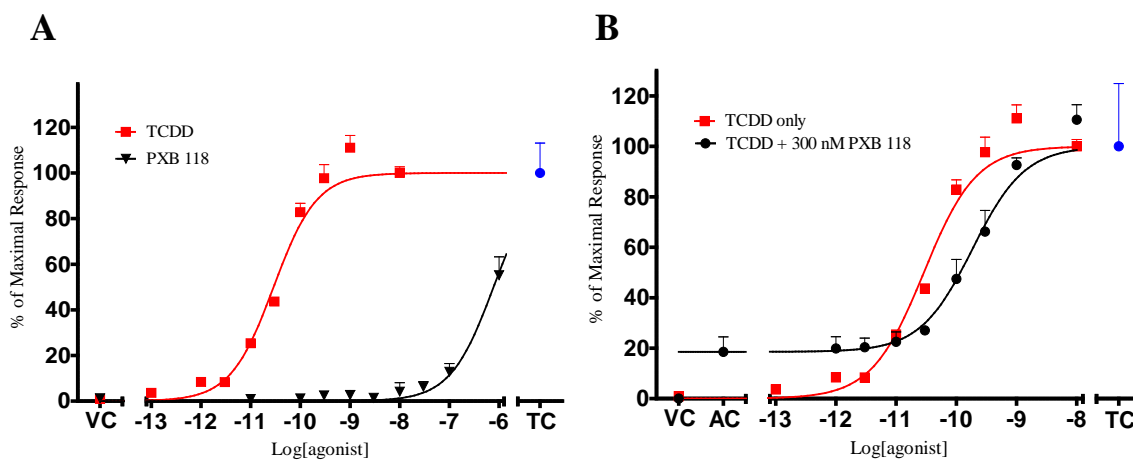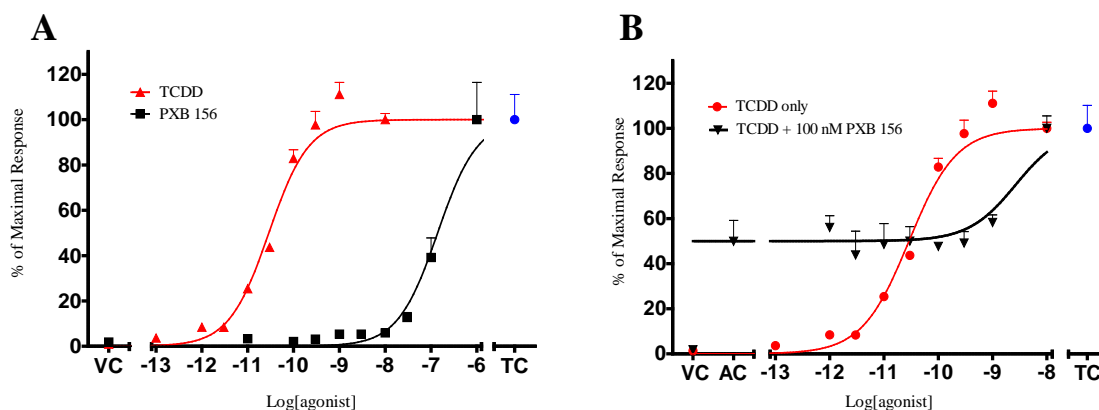
Figure 3.22: PXB 156 is a partial agonist of AhR in rat – (A) Agonist properties, rat H4IIE cells were treated with various concentrations of PXB 156 for 4 hours. (B) Antagonistic properties, rat H4IIE cells were treated with various concentrations of TCDD in the presence or absence of 100 nM PXB 156. Concentration-response curves were created by plotting the % of maximal CYP1A1 mRNA induction by 10 nM TCDD against concentration of agonist. qRT-PCR was used to measure the level of induction of CYP1A1 and compared against control genes, β-actin and AhR. Results were compared with an antagonist only control (AC), a vehicle control (VC) and a 10 nM TCDD only control (TC) which is normalised as 100% of the maximal response. Each point is the mean of three biological replicates ± S.D.

Figure 3.22A shows that PXB 156 is an agonist of the AhR with an EC_{50} of 139 nM (95% CI = 95.5 nM – 203 nM). This was 5,000-fold less potent than TCDD and of equal potency to PCB 156 based on 95% confidence intervals but statistically different based on a t-test analysis (p-value <0.05). A REP of 0.0002 was calculated for PXB 156 which demonstrates that the compound has equal potency to PCB 156 (p=0.48). The antagonistic effects were measured using cell treated with TCDD in the presence of 100 nM PXB 156 (Figure 3.22B). The TCDD EC_{50} was estimated to be 2.68 nM (95% CI = 166 pM – 43.0 nM) compared with 28.9 pM for TCDD alone and was shown to be significantly different (p=0.0021). This data shows that PXB 156 is partial agonist in rat H4IIE cells.

3.1.7 2-Amino-isoflavones

3.1.7.1 Chr-13 is a partial agonist in rat and an antagonist in human
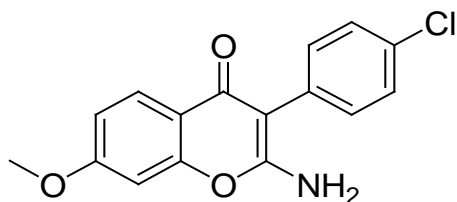
The initial screening of a library of 2-amino-isoflavones with respect to their ability to agonise or antagonise mouse or human AhR was conducted by Dr. Michael Denison and Dr. Guochun He (University of California, USA). Based on the results from this screening, two compounds, which showed unusual species differences, were selected for further analysis with qRT-PCR in rat H4IIE and human MCF-7 cells (Wall *et al., 2012b*). Due to the high similarities in the ligand binding domains of the mouse and rat AhRs (Hahn *et al., 1997*), it was expected that the compounds would elicit a similar response. Measurement of CYP1A1 mRNA by qRT-PCR was utilised as it is a more accurate method of detecting AhR activation than luciferase-based reporter assays. Therefore, 2-amino-3-(4-chlorophenyl)-7-methoxychromen-4-one (Chr-13) and 6-chloro-3-(4-methoxyphenyl)chromen-2-one (Chr-19) were chosen for further analysis. Figure 3.23 shows rat H4IIE cells and human MCF-7 cells treated with either Chr-13 or TCDD. EC_{50}s of 113 pM (95% CI = 83.0 pM – 152 pM) and 661 pM (95% CI = 515 pM – 847 pM) for rat and human AhR, respectively, were estimated for cells treated with TCDD, showing that the potency of TCDD was 6-fold lower in the human MCF-7 cell line compared with rat H4IIE cells (p<0.0001). Furthermore, it is clear that Chr-13 was significantly less potent than TCDD at activating the AhR. Assuming that Chr-13 can achieve a maximal response, the EC_{50} for rat H4IIE cells treated with Chr-13 was 41.5 µM (95% CI = 35.2 µM – 49.0 µM), which is comparable to the data obtained in mouse H1L6.1c2 cells where a 10 µM concentration of Chr-13 gave a 50% response (See section 4.4.2.1). In human MCF-7 cells, no agonism was detected even at the highest concentration of 100 µM. These results indicate that the compound is an agonist in rat but not in human (at

the concentrations used), and is similar to the initial screening results which showed Chr-13 to be agonist in mouse but not human cells (See section 4.4.2.1). This result is not surprising given the high sequence identity of the mouse and rat AhR ligand binding domain (Pandini *et al.,* 2009).

Figure 3.23: Chr-13 is a pure agonist of rat AhR and a pure antagonist of human AhR – (A) Rat H4IIE or (B) human MCF-7 cells were treated with various concentrations of Chr-13 for 4 hours to measure its agonist properties. (C) rat H4IIE or (D) human MCF-7 cells were treated with various concentrations of TCDD in the presence of 10 µM (rat) or 100 µM (human) Chr-13 for 4 hours. Concentration-response curves were created by plotting the % of maximal CYP1A1 mRNA induction by 10 nM TCDD against concentration of agonist. qRT-PCR was used to measure the level of induction of CYP1A1 and compared against control genes, β-actin and AhR. QbasePlus was used to normalise the data which was plotted using 10 nM TCDD only control as 100% of the maximal response. Vehicle control (VC), an antagonist only control (AC) and a 10 nM TCDD only control (TC). Each point is the mean of three biological replicates ± S.D.

Investigation of the antagonistic effects of Chr-13 was performed by treating rat or human cells with various concentrations of TCDD but in the presence of a set concentration of Chr-13 which induces ~20% of the maximal agonistic response of 10 nM TCDD. This was

estimated to be 10 µM for the rat cells, but as no response was detected in human cells, at concentrations up to 100 µM Chr-13. The antagonistic effect of Chr-13 in rat H4IIE cells is shown in Figure 3.23C. Although the screening data showed that Chr-13 was not antagonistic in the mouse H1L6.1c2 cell line (section 4.4.2.1) it was still important to confirm its effect in the rat H4IIE cell line. The addition of 10 µM Chr-13 to the TCDD concentration-response curve resulted in a background induction of ~25% of the maximal induction which corresponds well with the data shown in Figure 3.23A. The EC_{50} for TCDD in the presence of 10 µM Chr-13 was 237 pM (95% CI = 24.9 pM – 2.25 nM) in rat H4IIE cells which was not significantly different (p>0.05) from the EC_{50} for TCDD alone. The results confirm that Chr-13 has no antagonistic effects. Figure 3.23D shows human MCF-7 cells treated with TCDD in the presence and absence of 100 µM Chr-13. A concentration of 100 µM was shown in Figure 3.23B to have no AhR agonistic activity consequently there is no background of induction when treated simultaneously with TCDD. However, the data did show a shift of the TCDD concentration-response curve to the right, reducing the potency of TCDD by 5-fold compared to TCDD in the absence of Chr-13. The EC_{50} for TCDD in the presence of 100 µM Chr-13 was 3.02 nM (95% CI = 2.55 nM – 3.55 nM) which was significantly higher (p<0.0001) than the EC_{50} of TCDD alone. Consequently, these data show that Chr-13 is a weak antagonist in human MCF-7 and an agonist in rat H4IIE cells.

3.1.7.2   Chr-19 is an agonist in rat and a partial agonist in human
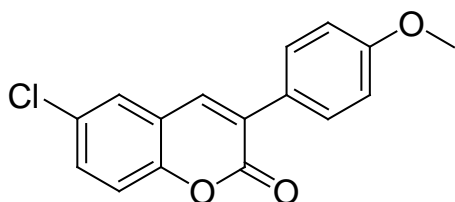
Figure 3.24 shows the concentration-response curves of Chr-19 and TCDD agonism of AhR in rat H4IIE and human MCF-7 cells, as measured by qRT-PCR of CYP1A1 induction. Rat H4IIE (Figure 3.24A) and human MCF-7 cells (Figure 3.24B) were treated with either Chr-19 or TCDD. Chr-19 was agonistic in both rat H4IIE and human MCF-7 cells, with the compound being

approximately 20-fold more potent in rat cells (p<0.0001). Assuming that the compound will attain maximal response, the EC_{50} for Chr-19 in rat H4IIE cells was 7.70 µM (95% CI = 5.22 µM – 11.3 µM), and in human MCF-7 cells, the EC_{50} was estimated to be 140 µM (95% CI = 65.4 µM – 317 µM). The data shows that Chr-19 is significantly less potent at activating the AhR and inducing CYP1A1 than TCDD.
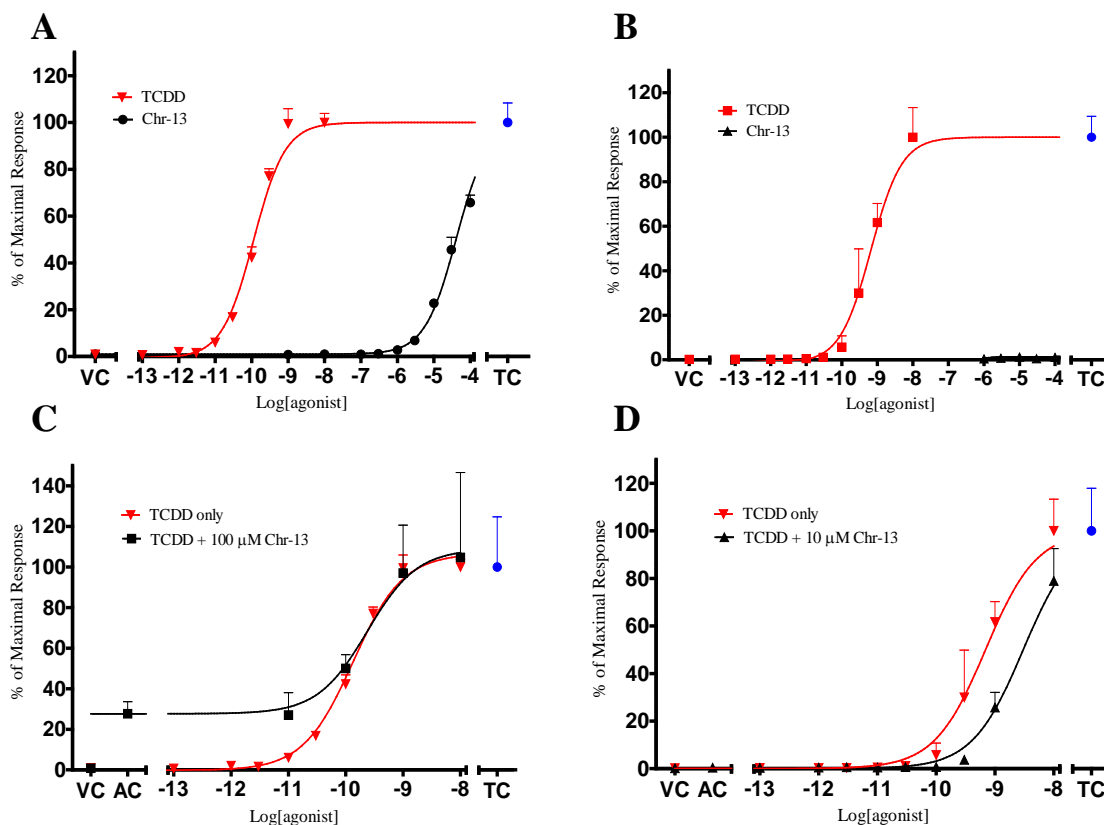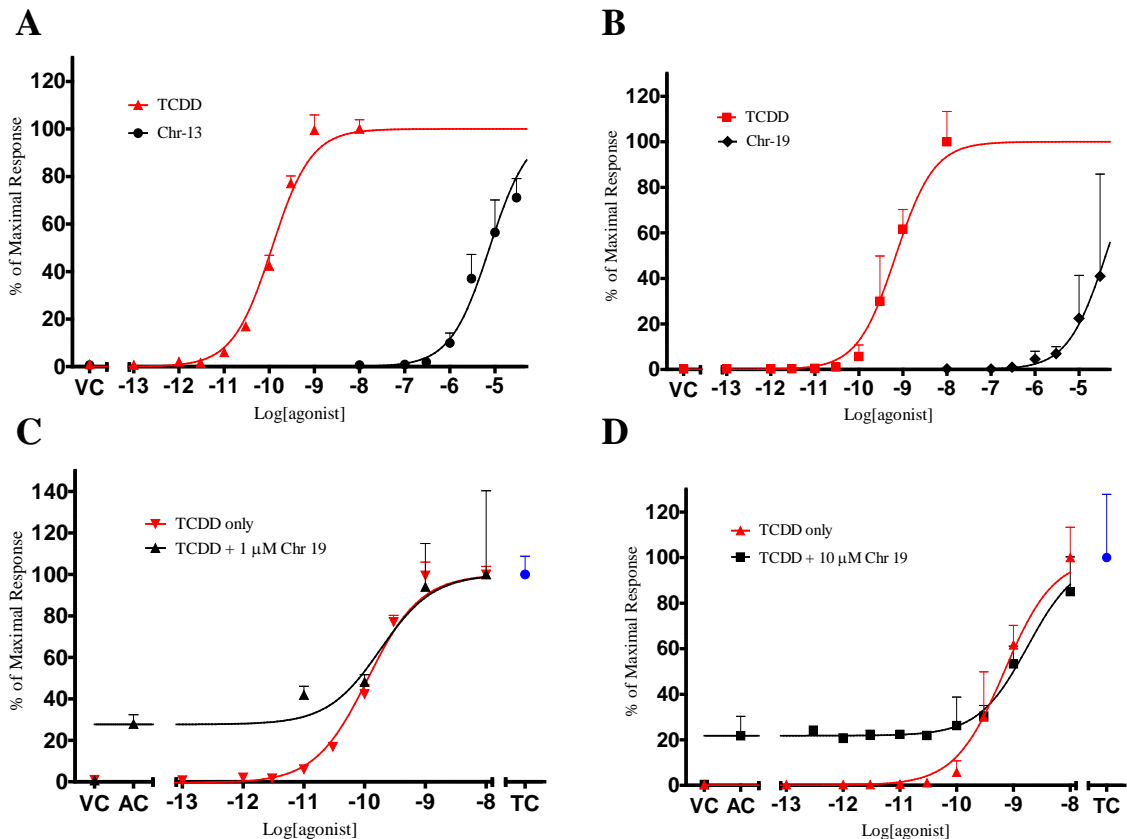

Figure 3.24: Chr-19 is a pure agonist of rat AhR and a partial agonist of human AhR – (A) Rat H4IIE and (B) human MCF-7 cells were treated with various concentrations of Chr-19 for 4 hours. (C) Rat H4IIE and (D) human MCF-7 cells were treated with various concentrations of TCDD in the presence of 3 µM (rat) or 30 µM (human) Chr-19 for 4 hours. Concentration-response curves were created by plotting the % of maximal CYP1A1 mRNA induction by 10 nM TCDD against concentration of agonist. qRT-PCR was used to measure the level of induction of CYP1A1 and compared against control genes, β-actin and AhR. QbasePlus was used to normalise the data which was plotted using 10 nM TCDD only control as 100% of the maximal response separately for rat and human. Results were compared with a vehicle control (VC) and a 10 nM TCDD only control (TC). Each point is the mean of three biological replicates ± S.D.

The antagonistic effects of Chr-19 were examined by treating cells with TCDD in the presence or absence of a set concentration of Chr-19 (i.e. that produces ~20% of maximal

induction response). This value was found to be 1 µM and 10 µM for rat and human, respectively. Figure 3.24 shows the analysis of antagonistic activity of Chr-19 in C) rat H4IIE cells and D) human MCF-7 cells. It can be seen in Figure 3.24C that there was no shift of the TCDD curve to the right. The EC_{50} for TCDD in the presence of 1 µM Chr-19 was 182 pM (95% CI = 31.0 pM – 1.07 nM) which was not significantly different (p>0.05) from the EC_{50} obtained from cells treated with TCDD only. Figure 3.24D shows human MCF-7 cells treated with TCDD in the presence and absence of Chr-19. An EC_{50} of 1.76 nM (95% CI = 897 pM – 3.47 nM) for TCDD with 10 µM Chr-19 was calculated which was statistically significantly higher than that obtained with TCDD alone (p<0.05). This indicates that Chr-19, at 10 µM, reduces the potency of TCDD activation of AhR by 3-fold and is hence a weak antagonist of the AhR. Combined with the data from Figure 3.24B, which showed Chr-19 was an agonist of human AhR, it can be concluded that this compound is a partial agonist in human MCF-7.

3.1.8 AZFMHCs

3.1.8.1 Overview
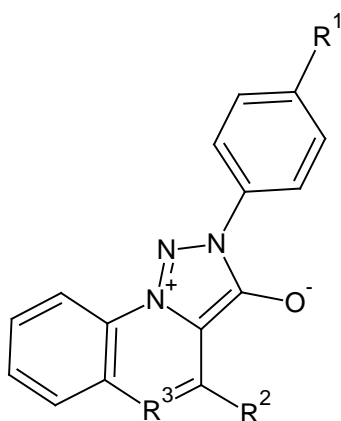
AZ1: R^1=CF$_3$, R^2=H, R^3=C
AZ2: R^1=CF$_3$, R^2=CH$_3$, R^3=N
AZ3: R^1=CH$_3$, R^2=CH$_3$, R^3=C
AZ4: R^1=CF$_3$, R^2=NH$_2$, R^3=N

Several compounds received from AstraZeneca were thought to have a higher potency than TCDD when activating the AhR based on medicinal research conducted on the compounds so were deemed suitable to test with the validated method of measuring AhR activation. A full characterisation of the family was conducted, measuring the potency of the compounds to activate the AhR based on the induction of CYP1A1, CYP1B1 and CYP1A2 and measuring the affinity using a competitive ligand binding assay.

3.1.8.2 Measurement of AhR activation by mRNA induction

The fused mesoionic heterocycle compounds (AZFMHCs) were tested to measure their agonistic and antagonistic properties in rat H4IIE cells (Figure 3.25).
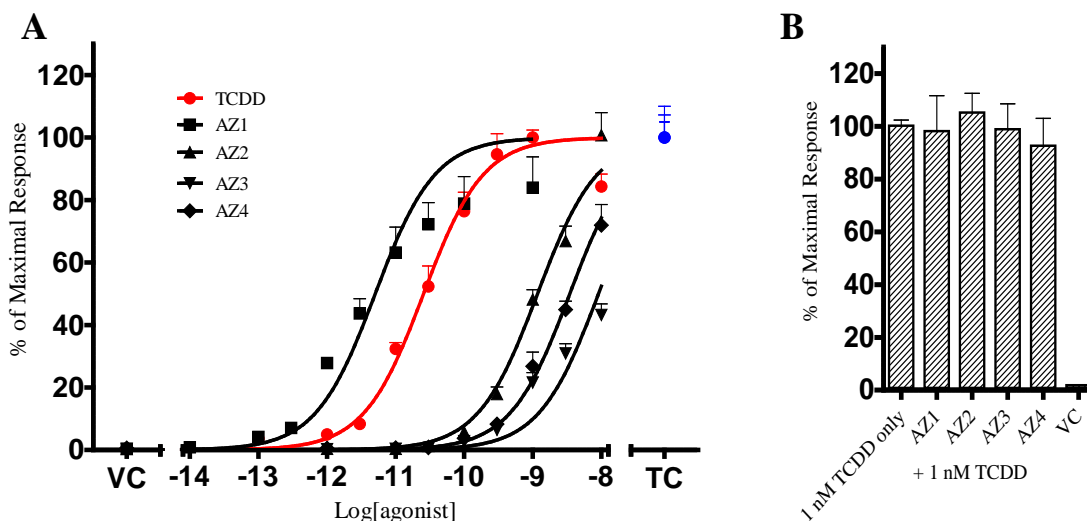
Figure 3.25: Agonistic and antagonistic properties of the AZFMHCs in comparison to TCDD – (A) Agonistic properties were measured by treating rat H4IIE cells with various concentrations of the compounds for 4 hours. Concentration-response curves were created by plotting the % of maximal CYP1A1 mRNA induction by 10 nM TCDD against concentration of agonist. Results were compared with a vehicle control (VC) and a 10 nM TCDD only control (TC). (B) The antagonistic properties were measured by treating H4IIE cells with a concentration that gives approximately 20% of the maximal induction by 10 nM TCDD for that compound in the presence of 1 nM TCDD. qRT-PCR was used to measure the level of induction of CYP1A1 in both experiments and was compared against control genes, β-actin and AhR. QbasePlus was used to normalise the data which was plotted using the TCDD only control as 100% of the maximal response. In both cases, each point is the mean of three biological replicates ± S.D.

Figure 3.25A shows the agonistic potencies of the four AZFMHCs. The EC_{50} and 95% confidence intervals (95% CI) for TCDD and the four AZFMHCs were as follows; TCDD was 25.5 pM (95% CI = 18.2 pM – 36.0 pM), AZ1 was 5.05 pM (95% CI = 2.81 pM – 9.09 pM), AZ2 was 1.17 nM (95% CI = 888 pM – 1.55 nM), AZ3 was 9.08 nM (95% CI 6.01 nM – 13.7 nM) and AZ4 was 3.46 nM (95% CI = 3.07 nM – 3.90 nM). The EC_{50}s for AZ2, 3 and 4 are estimates based on the predicted maximal induction equal to 10 nM TCDD. AZ1

was shown to be the only compound which was significantly more potent that TCDD (p<0.0001) by 5-fold and was investigated further.

Figure 3.25B shows each of the four compounds in the presence of 1 nM TCDD. The data showed that none of the compounds elicit an antagonist effect on TCDD induction of CYP1A1 under these test conditions. To confirm that AZ1 induces other genes associated with AhR activation, the induction of CYP1B1 and CYP1A2 mRNA was also measured (Figure 3.26) in rat H4IIE.
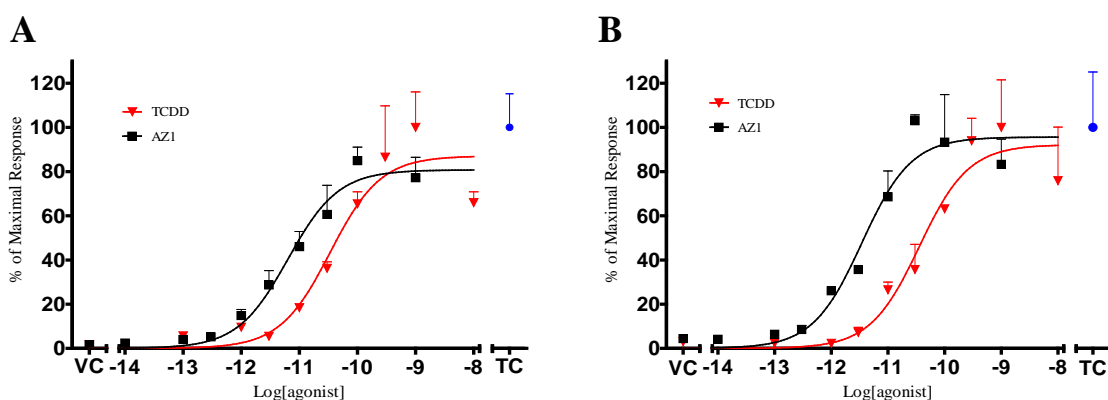
Figure 3.26: Induction of AhR-mediated genes – (A) CYP1B1, (B) CYP1A2. Rat H4IIE were treated with various concentrations of TCDD for 4 hours. CYP1B1 and CYP1A2 were measured separately from the normalisation genes using SYBR green qRT-PCR master mix. Concentration-response curves were created by plotting the % of maximal CYP1B1 or CYP1A2 mRNA induction by 10 nM TCDD against concentration of agonist. qRT-PCR was used to measure the level of induction of CYP1A1 and compared against control genes, β-actin and AhR. QbasePlus was used to normalise the data which was plotted using 10 nM TCDD only control as 100% of the maximal response. Results were compared with a vehicle control (VC) and a 10 nM TCDD only (TC). Each point is the mean of three biological replicates ± S.D.

Figure 3.26A shows the levels of CYP1B1 mRNA induction in rat cells treated with either TCDD or AZ1. The EC_{50} for TCDD was 34.0pM (95% CI = 13.9pM – 82.9pM) and AZ1 was 6.3pM (95% CI = 4.0pM – 10.0pM). The data shows that AZ1 is 5-fold more potent at inducing CYP1B1 than TCDD in rat H4IIE cells (p<0.0001) with no overlap in the 95% confidence intervals. The mRNA levels of CYP1A2 are shown in Figure 3.26B. The EC_{50} of TCDD was 35.7pM (95% CI = 17.3pM – 73.6pM) and AZ1 was 3.4pM (95% CI = 1.7pM –

6.8pM). This shows that AZ1 is 10-fold more potent than TCDD (p<0.0001) with no overlap of 95% confidence intervals. TCDD and AZ1 were then tested in human MCF-7 cells to determine if the compound has the same high potency across species.
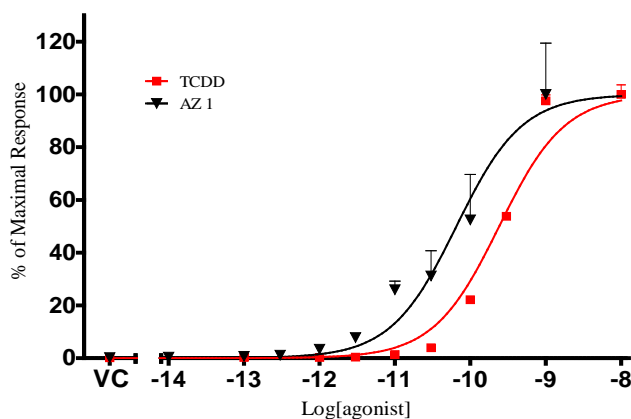
Figure 3.27: Concentration-response curve for AZ1 induction of CYP1A1 in human MCF7 cells – Human MCF7 cells were treated with various concentrations of TCDD for 4 hours. Concentration-response curves were created by plotting the % of maximal CYP1A1 mRNA induction by 10 nM TCDD against concentration of agonist. qRT-PCR was used to measure the level of induction by CYP1A1 and was compared against control genes, β-actin and AhR. QbasePlus was used to normalise the data which was plotted using 10 nM TCDD only control as 100% of the maximal response. Results were compared with a vehicle control (VC). Each point is the mean of three biological replicates ± S.D.

It can be seen from Figure 3.27 that AZ1 is 4-fold more potent than TCDD in human MCF-7 cells as well as rat H4IIE-C3 cells. The EC_{50} for AZ1 was 65.4pM (95% CI = 45.6pM – 93.7pM) and the EC_{50} for TCDD was 241 pM (95% CI = 161 pM – 362 pM) which are significantly different (p<0.0001). This shows that AZ1 is a significantly more potent agonist than TCDD in both rat H4IIE and human MCF-7 cells.

3.1.8.3 Saturation binding ([³H]-TCDD) and competitive binding (TCDD and AZ1)

As part of an investigation into the potency of AZ1, the ligand binding was measured to confirm that the compound underwent the same mechanism of action as TCDD to induce CYP1A1. Unlabelled TCDD was also measured and used for comparison. The method of ligand-binding was adapted from Bradfield and Poland (1988) and Bazzi *et al.* (2009). A rat

liver from a female Charles River Wistar rat was homogenised and repeatedly centrifuged to separate the cytosolic protein from the rest of the tissue. A Bradford assay using different concentrations of BSA was used to calculate the protein concentration of the rat cytosol. This was diluted to 5 mg/ml for subsequent experiments. The K_d and B_{max} were calculated using 5 mg/ml rat cytosol treated with various concentrations of [^{3}H]-TCDD in the presence and absence of TCAOB (section 1.5.1). Figure 3.28 shows total and non-specific binding which were measured experimentally and the specific binding which was calculated.
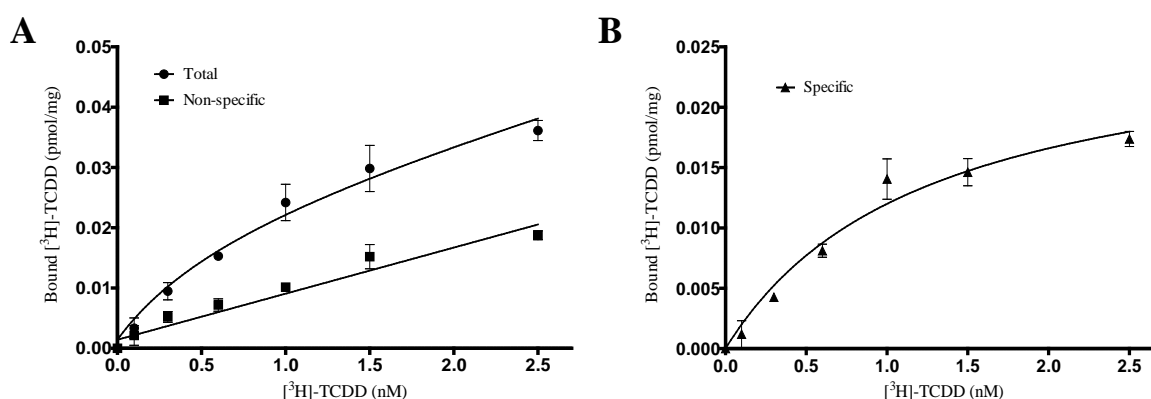
Figure 3.28: (A) Total and non-specific binding of [^{3}H]-TCDD, (B) Specific binding of [^{3}H]-TCDD – (A) 200 µl of 5 mg/ml rat liver cytosol was treated with various concentration of [^{3}H]-TCDD (0 nM – 2.5 nM) in the absence (total binding) and presence (non-specific binding) of 200 nM TCAOB. Samples were incubated for 16 h at 4°C. Incubation was terminated with the addition of 10 mg/ml dextran-coated charcoal. The counts per minute (cpm) were measured using a scintillation counter then converted into bound [^{3}H]-TCDD in pmol/mg. Data points are mean ± S.D (n = 4). (B) The specific binding was calculated from total binding minus non-specific binding and plotted as mean ± S.D. The K_d and B_{max} were calculated from this data using a quadratic curve equation (GraphPad Prism 5).

Figure 3.28 shows the binding of [^{3}H]-TCDD to the rat liver cytosol. The K_d was estimated, using the GraphPad Prism 5 software, to be 1.24 nM (95% CI = 0.58 nM – 1.90 nM). The B_{max} was estimated to be 26.9 fmol/mg (95% CI = 20.0 fmol/mg – 33.7 fmol/mg) or 0.13 nM (95% CI = 0.10 nM – 0.16 nM) when incorporating the 0.2 ml volume of the reaction.

The K_i of unlabelled (non-radiolabelled) TCDD was calculated by competitive binding analysis. A 200 µl aliquot of 5 mg/ml rat liver cytosol was incubated with 1 nM [^{3}H]-TCDD,

various concentrations of unlabelled TCDD and 200 nM TCAOB (non-specific binding only). The mixture was then incubated for 16 h at $4^{\circ}C$. The incubation was terminated with 10 mg/ml dextran-coated charcoal. The counts per minute (cpm) were measured using a scintillation counter and converted into bound [^{3}H]-TCDD (nM). The % of maximally bound [^{3}H]-TCDD (nM) was plotted against the concentration of unlabelled TCDD (Figure 3.29A). The IC_{50} (concentration that inhibits/displaces 50% of [^{3}H]-TCDD) was extrapolated from the graph, then the K_i was calculated using data obtained from Figure 3.28 (1 nM [^{3}H]-TCDD with a K_d of 1.24 nM).
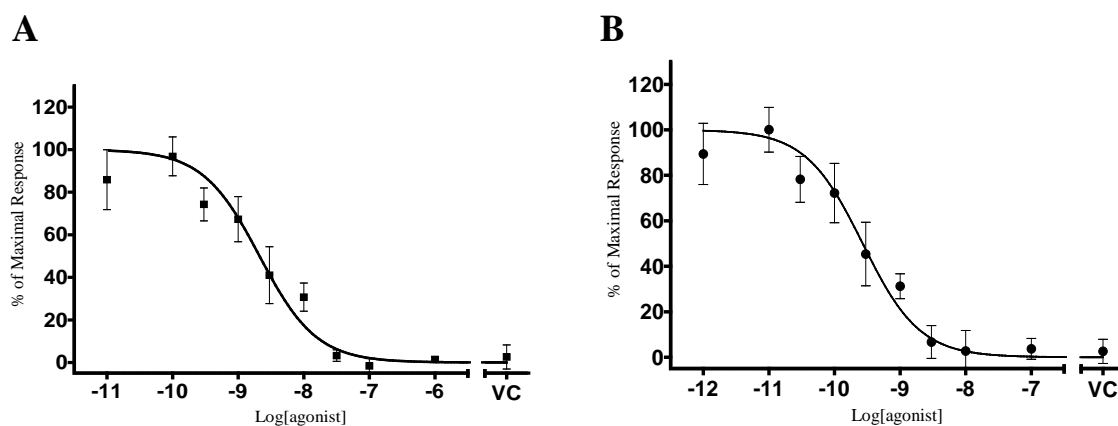
Figure 3.29: Competitive binding of (A) unlabelled TCDD and (B) AZ1 – Rat liver cytosol was treated with various concentrations of TCDD in the presence of 1 nM [^{3}H]-TCDD ± 200 nM TCAOB. Total (without TCAOB) and non-specific (with TCAOB) binding was measured to allow the calculation of specific binding of (A) TCDD or (B) AZ1 to the AhR. Rat liver cytosol was incubated with TCDD or AZ1 and 1 nM [^{3}H]-TCDD (with and without TCAOB) for 16 h at $4^{\circ}C$. The specific binding was plotted against concentration of TCDD. This allowed measurement of the IC_{50} and K_i. Data points are mean ± S.D. (n = 3; total binding only).

The IC_{50} for unlabelled TCDD was calculated to be 2.11 nM (95% CI = 1.32 nM – 3.40 nM). The K_i was calculated to be 1.17 nM (95% CI = 729 pM – 1.88 nM). The binding properties of AZ1 were investigated as part of its comparison with TCDD (Wall *et al.,* 2012a). The IC_{50} was estimated as for unlabelled TCDD and the K_d was calculated using parameters calculated from section 3.1.8.3. Figure 3.29B shows the specific binding of [^{3}H]-TCDD plotted against the concentration of the competitor, AZ1. The IC_{50} of AZ1 was

calculated to be 269 pM (95% CI= 182 pM – 396 pM) and the K_i was calculated to be 149 pM (95% CI = 101 pM – 219 pM). Thus AZ1 has a statistically significantly higher affinity (~8-fold) than TCDD (p < 0.0001).

3.2 Investigation of AhR species differences

3.2.1 Overview

The AhR cDNA from rat and human were isolated and cloned into pFastbac1 vectors as discussed previously in section 2.5.2 (Fan *et al.,* 2009). The AhR cDNA were cloned into the pRevTRE vector which was then subsequently used to infect AhR deficient mouse BpRc1 cells. All the transfection and infection procedures were conducted in exactly the same way for rat and human AhR genes. Briefly, high fidelity PCR was used to copy the cDNA out of the pFastbac1 vector. At the same time the His-tag was removed and a new HindIII restriction site was added directly after the stop codon of the AhR gene. This PCR product was ligated and subcloned into pGEM-T before being double digested out with SalI and HindIII and re-ligated into pRevTRE. The pRevTRE vectors (rat and human) were transfected into PT67 packaging cells to produce a virus along with pRevTet-Off. The replication-defective viruses were then used to infect the mouse BpRc1 cells to produce BpRc1 rAhR and BpRc1 hAhR.

3.2.2 Preparing the pGEM-T:insert vectors

The AhR cDNA were copied from the pFastBac1 vector using high-fidelity PCR. The concentrations were measured using a Nanodrop spectrophotometer and diluted to 250 ng/µl. The PCR products were run on a 1x agarose gel to confirm the size of the products and to allow extraction of the AhRs from background debris. The size of the fragments for human and rat AhR were calculated to be 2569 bp (rat) and 2578 bp (human) in size using

VectorNTI Advance 11™ (Invitrogen). Figure 3.30 shows that there was no contamination or other PCR products.
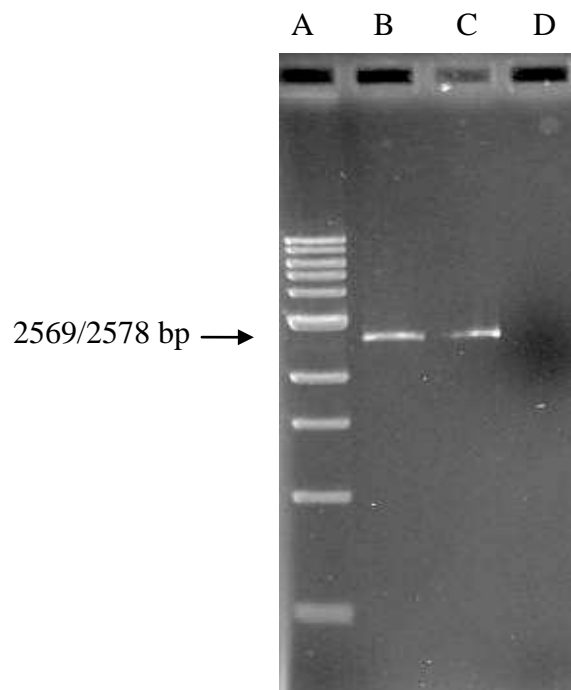
Figure 3.30: Gel of AhR PCR products – The products of the PCR reaction which copied the AhR gene from the pFastbac1 vector were run on a 1x gel. (A) 1 kbp DNA ladder (Biolabs), (B) rat AhR (C) human AhR. (D) Negative control, which consisted of the loading dye and distilled water, was also clear of contamination. The gel was made as described in section 2.2.1 and run for 70 min at 100 V. The gel was stained with ethidium bromide for 20 min (and washed for 30 min) before being photographed with a BioRad chemdoc UV camera.

After extraction and purification, the PCR fragments were ligated into pGEM-T. Successful colonies were picked and grown overnight. After further purification, potential clones were selected and double digested with SalI and HindIII. Once a successful clone was identified, a more detailed investigation was conducted which included single digestions as well as a double digestion.
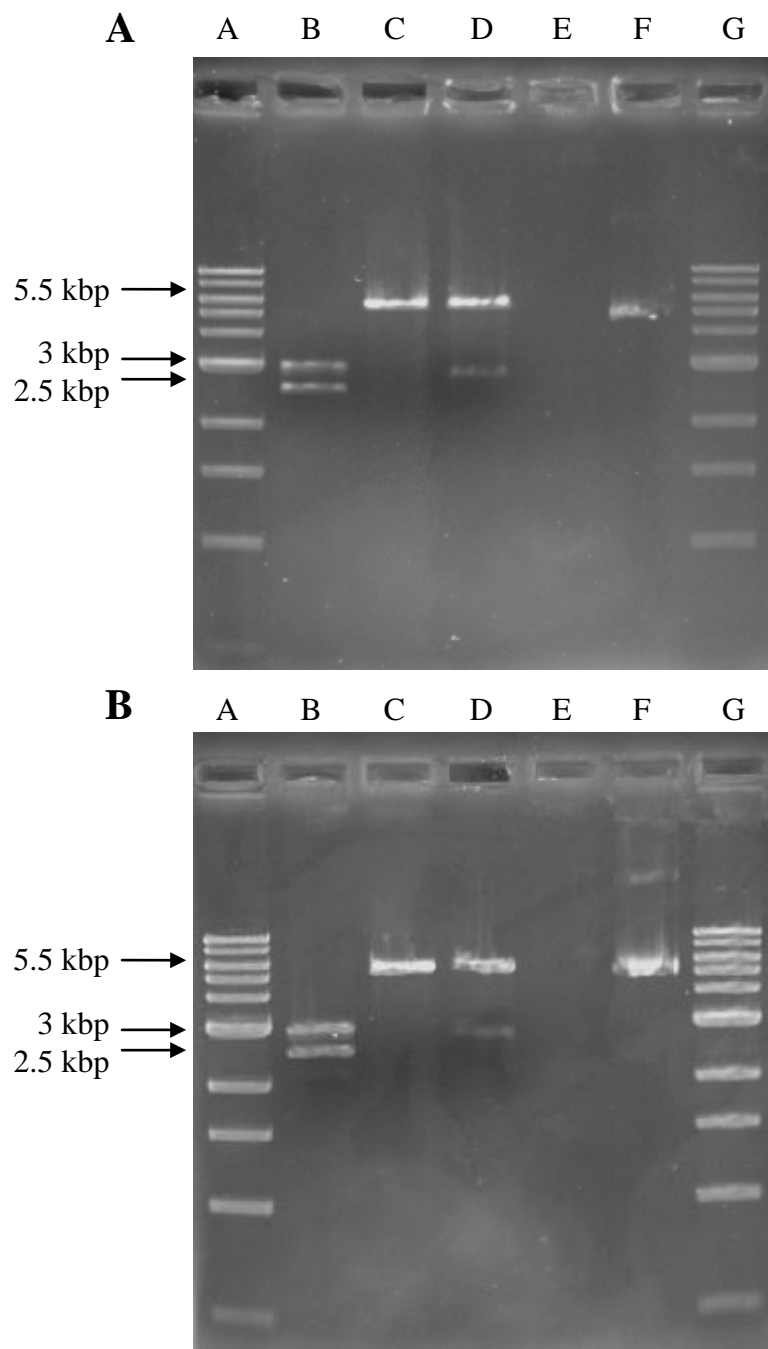
Figure 3.31: Gel of digestion products of pGEM-T with ligated the A) rat AhR insert or B) human AhR insert – All the digests were compared against a 1 kbp DNA ladder (Biolabs; A and G). (B) Double digest was conducted on the pGEM-T with insert using SalI and HindIII. Single digests with (C) SalI only and (D) HindIII only were also conducted. A negative control (E) was run to confirm the loading dye and distilled water used was free of contamination. The pGEM-T with insert was also run on the gel uncut (F). The gel was made as described in the legend of Figure 3.30 (70 min; 90 V).

Figure 3.31 shows pGEM-T with insert digested with either SalI, HindIII, both or neither. The total size of the linear vector was 5.5 kbp (rat was 5569 bp and human was 5578 bp). This consisted of the 3 kbp pGEM-T vector and the 2.5 kbp AhR insert (2544 bp for rat and 2553 bp for human). The pGEM-T vector does have a SalI digestion site already so SalI should cut twice. The two gels show that the gene was ligated in the 5' direction, based on the bands from SalI digestion sites, which shows that only one visible digestion has occurred (Figure 3.31). A single digestion with HindIII cut the vector as expected but also appeared to have experienced star activity and randomly cut in a different location to produce a low concentration 3 kbp product. This is a common problem with HindIII but in this instance has no effect on the confirmation of successful ligation. Sequencing was conducted at Source Bioscience (Life Science, Nottingham) on both pGEM-T vectors to confirm the presence of the AhR and successful removal of the His-tag. The sequencing data was analysed using Align X software (VectorNTI Advance 11™, Invitrogen) by comparing against the predicted sequence of the pGEM-T and vector insert (data not shown).

3.2.3   Subcloning to pRevTRE vectors

The AhR cDNA were then cloned out of pGEM-T and into the viral vector, pRevTRE. The gene was double digested out of pGEM-T using SalI and HindIII. The same confirmation checks were also carried out on the pRevTRE: insert vectors. The digested vectors were run on a 1x agarose gel so that the pRevTRE: insert fragments could be cut out and purified. The gene was then ligated into the new vector. Figure 3.32 shows the ligation product digested with either SalI, HindIII, both or neither. The gels also show the pRevTRE vector (digested once with SalI; lane F), the AhR gene only (E) and a negative digestion sample (G).
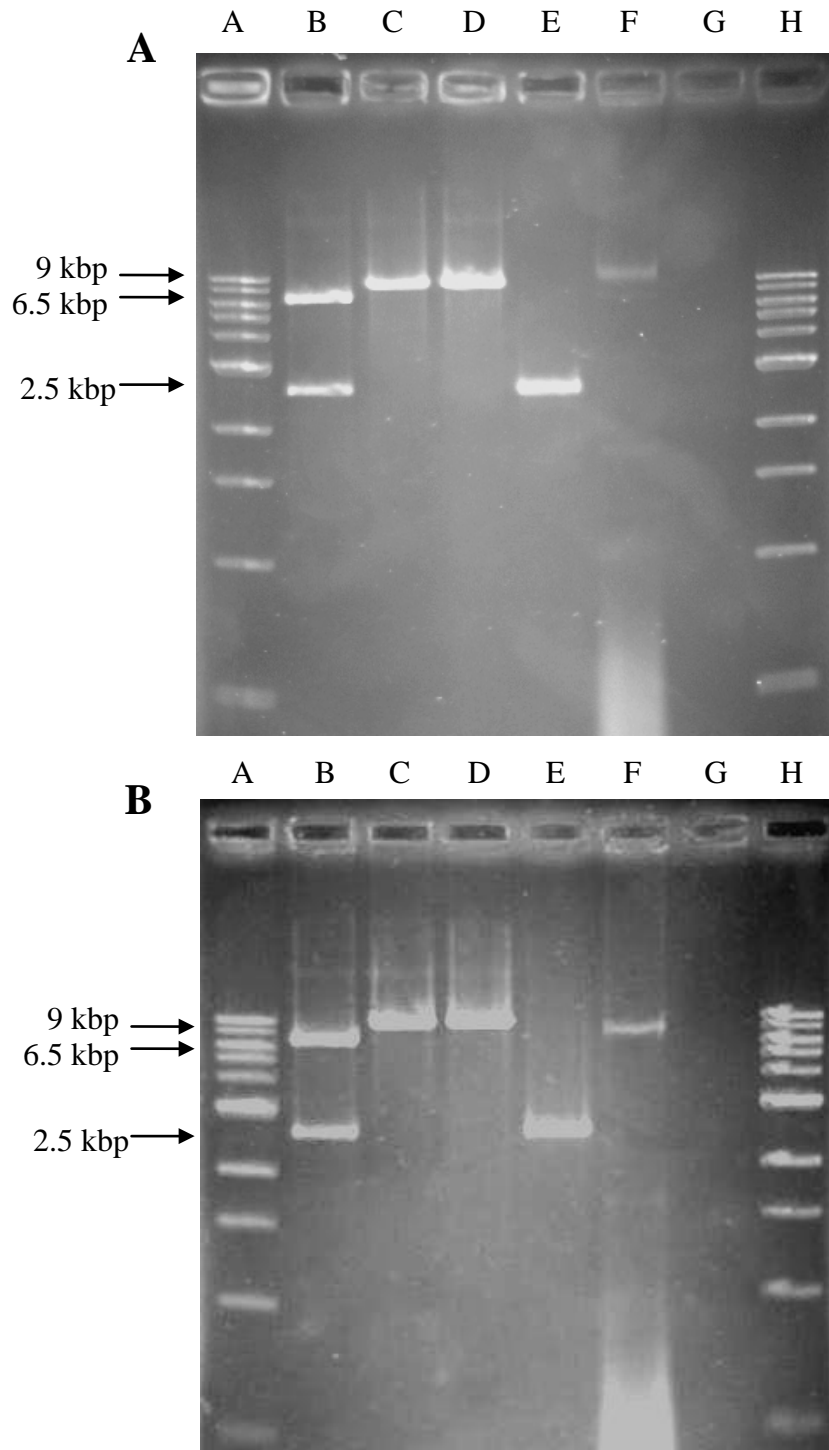
Figure 3.32: Gel of digestion products of pRevTRE ligated with (A) rat AhR insert or (B) human AhR insert – All the digests were compared against a 1 kbp DNA ladder (Biolabs; A and H). A double digest (B) was conducted on the pRevTRE with insert using SalI and HindIII. A single digest with SalI only (C) and HindIII only (D) was also conducted. Controls of AhR only and pRevTRE were run to compare against (E and F). A negative control (G) was run to confirm the loading dye and distilled water used was free of contamination. The 1x gel was made as described in the legend of Figure 3.30 (70 min; 90 V).

The two gels in Figure 3.32 show that the AhR was successfully subcloned from pGEM-T into pRevTRE. Single digestion (C and D) produced bands of ~9 kbp whereas double digestion produced bands of ~6.5 kbp (pRevTRE vector) and 2.5 kbp (AhR gene). There was no detectable contamination in the experiment (G). Sequencing was then conducted on the purified pRevTRE: insert vectors to confirm the cDNA was present in the vector. The data (not shown) was analysed using Align X software (VectorNTI Advance 11™, Invitrogen). Alignment showed only the 3' end of the AhR gene (HindIII; stop codon) and clearly shows that the His-tags were successfully removed during the high-fidelity PCR (whilst still retaining the stop codon and HindIII digestion site).

3.2.4   Producing stable virus producing PT67 cell lines

PT67 packaging cell lines were individually transfected with one of the three vectors to produce three stable-virus producing cell lines. The cell lines were called PT67 off, PT67 hAhR and PT67 rAhR, which are explained further in section 2.5.5.3. To confirm that the vectors were stably integrated into the genomic DNA, endpoint PCR was used to confirm either the presence or absence of the vectors. Briefly, genomic DNA was isolated from the cells and RNAse treated. PCR was then conducted to identify the pRevTet-Off or pRevTRE vectors. Figure 3.33 shows two 2x agarose gels of the PCR products formed by the pRevTet-Off or pRevTRE primers from the three virus producing cell lines. A band should form at 171 bp to indicate the presence of the pRevTet-Off vector and a band at 232 bp should indicate the pRevTRE vector.
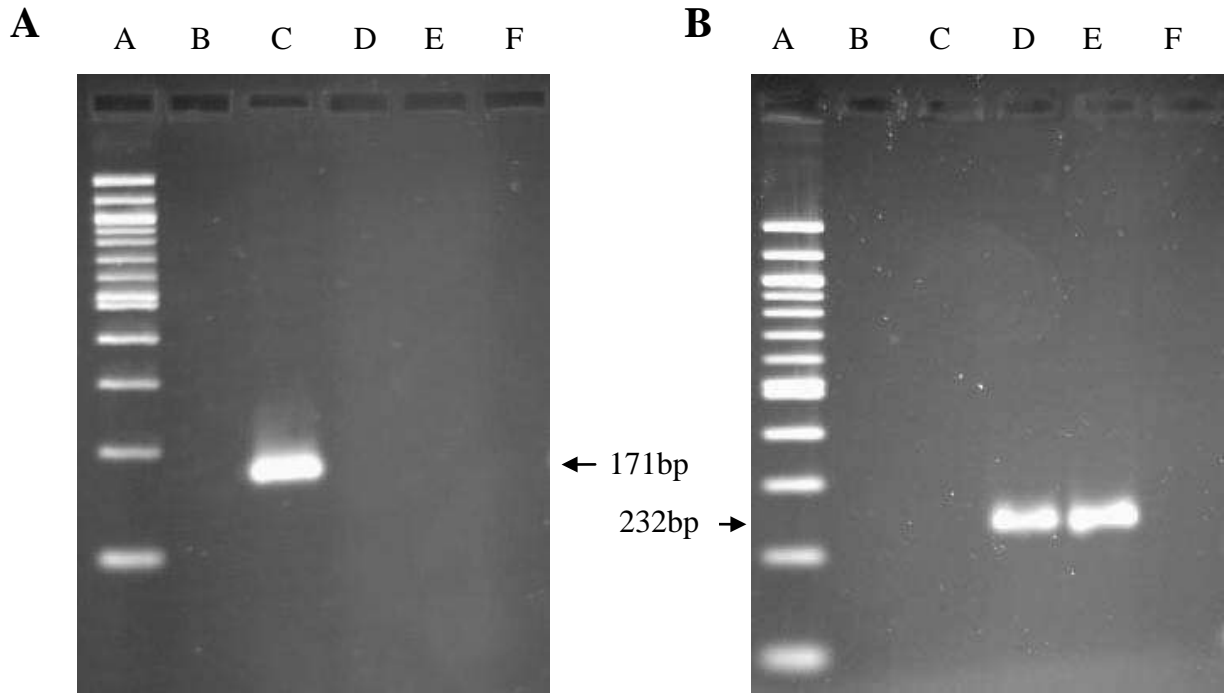
Figure 3.33: Agarose gel confirming the presence of A) pRevTet-Off vector and B) pRevTRE vector – Genomic DNA was isolated as described in the method. End-point PCR was conducted. A: The primers were designed to detect only the pRevTet-Off vector and not the pRevTRE vector. The resultant mRNA fragments were run on a 2x agarose gel (60 min; 90 V). B: The primers were designed to detect only the pRevTRE vector (human or rat) and not the pRevTet-Off vector. The resultant mRNA fragments were run on a 2x agarose gel (70 min; 90 V). (A) ladder, (B) PT67 wild-type, (C) PT67 off, (D) PT67 hAhR, (E) PT67 rAhR and (F) negative control.

Figure 3.33A shows that only the PT67 off cell line contains the pRevTet-Off vector. Figure 3.33B shows the PCR products formed by the pRevTRE primers, confirming that only PT67 rAhR and PT67 hAhR contain the pRevTRE vector with a band at 232 bp.

3.2.5   Stable expression of AhR in BpRc1

The antibiotic concentrations for selection were experimentally calculated for the BpRc1 cells. BpRc1 cells were treated with six different concentrations of antibiotic for 7 days. The lowest concentration that killed all of the cells was then recorded. The concentrations were found to be 400 µg/ml for G418 and 600 µg/ml for hygromycin. BpRc1 cells were then infected with the PT67 viruses as discussed in the method. The related antibiotic was then

added to kill any cells that did not contain the resistance to the antibiotic (located within the vector). The cells were left to grow to confluence over a period of approximately 1 month at which time the cells were harvested. After selection and growth, the BpRc1 cells were tested to confirm the presence of the required vectors. Each cell line should have pRevTet-Off with either pRevTRE:rAhR or pRevTRE:hAhR. End-point PCR was conducted using genomic DNA isolated from the cells. The PCR was designed to locate either the vector or the AhR insert however the experiments produced negative results and did not produce a double stable cell line with rat and human AhR expressed. Therefore a cell line that transiently expresses AhR was produced by simultaneously infecting the BpRc1 cells with the two vectors then immediately (~48 hours) testing for AhR activation. If stable cells had been created, a control would have been conducted to show that the BpRc1 cell lines were not contaminated with any PT67 cells which already have the vectors transfected in. Primers designed to detect the env gene in the PT67 cells would be used to identify the cell line.

3.2.6 Transient expression of AhR in BpRc1

Transiently infected BpRc1 cell lines were created to allow comparison between rat and human AhR without double stable cell lines. They were infected for 72 hours with the viruses then treated with either TCDD or 5F 203 for 4 hours. As briefly discussed in section 3.2.5, three important conformational assays were performed to: (1) confirm the presence of the two vectors, (2) confirm the presence of the relevant AhR DNA and (3) confirm absence of any PT67 cells or viral genes. Firstly, vector specific primers were used to confirm the presence of the two vectors in both of the cell lines. The system requires both vectors to be present in order to successfully transcribe the gene of interest (AhR). Primers have already been shown to be specific to the vector only (Figure 3.33).
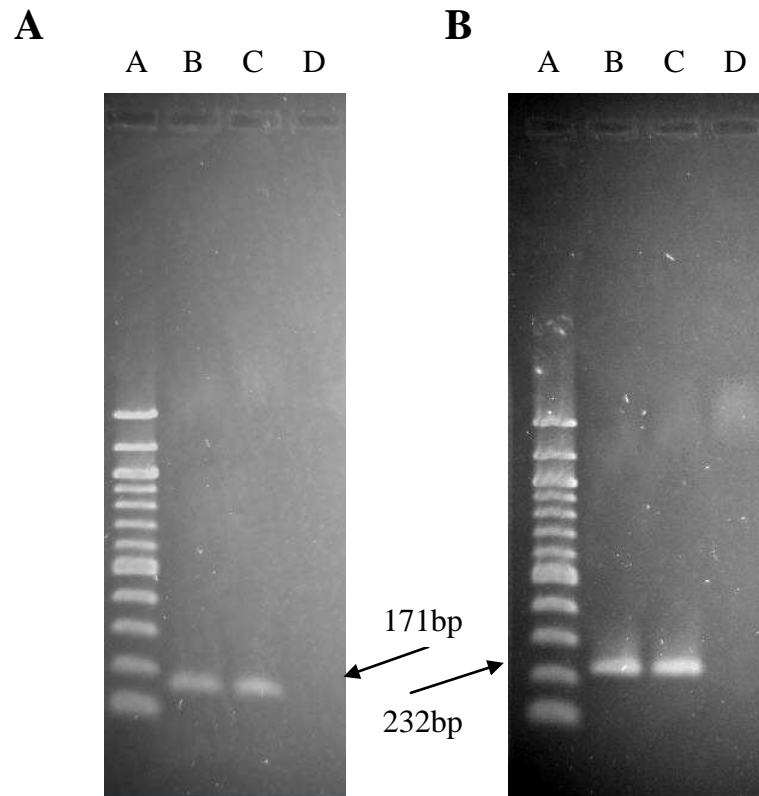
Figure 3.34: Confirmation of the presence of (A) pRevTet-Off and (B) pRevTRE vectors in BpRc1 – Cells were grown as previously described. Genomic DNA was isolated and end-point PCR was conducted as described is sections 2.2.2 and 2.2.8. The resultant PCR products were run on a 1x agarose gel (70 min; 100 V). Two primer pairs were used which were designed to locate pRevTet-Off and pRevTRE. (A) 100bp Ladder, (B) BpRc1 rAhR, (C) BpRc1 hAhR and (D) BpRc1 wild-type.

The two gels in Figure 3.34 show the two vectors, pRevTet-Off and pRevTRE, in the BpRc1 rAhR and BpRc1 hAhR cell lines. Figure 3.34A shows that there are distinctive bands at 171 bp for the rat and human clones showing the presence of pRevTet-Off vectors. Figure 3.34B confirms the presence of the pRevTRE vectors with bands at 232 bp in the rat and human clones. Confirmation of the correct AhR was conducted on genomic DNA using qRT-PCR as the primers are more specific with the probe included. The human AhR primers were run as a multiplex with mouse β-actin mRNA primers (negative control) at $59^{o}C$. The rat AhR primers were run separately at $63^{o}C$ to make binding more specific to the rat AhR only. Mouse β-actin was also run separately with the rat samples as a negative control.
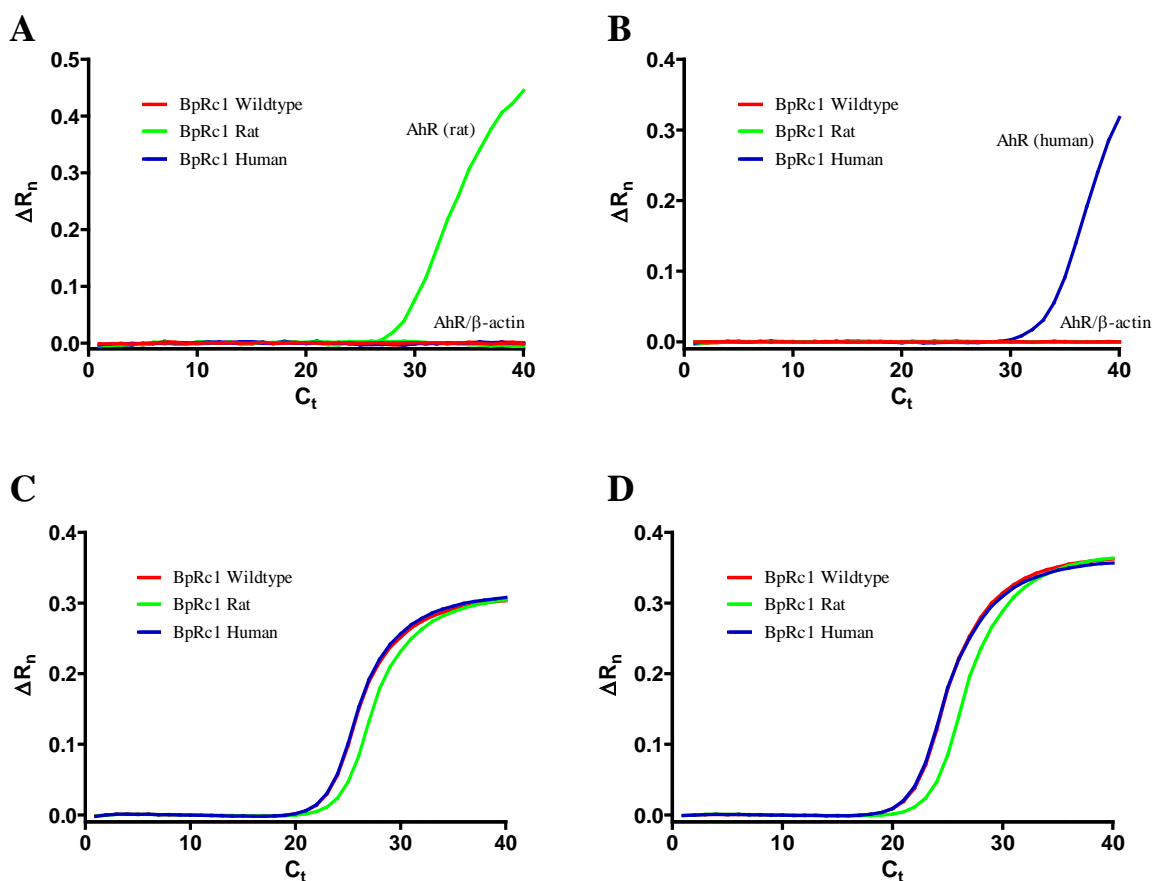
Figure 3.35: Confirmation of the presence of either rat or human AhR DNA in BpRc1– (A) Rat AhR and (B) human AhR. Genomic DNA was obtained from BpRc1 wild-type, BpRc1 rAhR and BpRc1 hAhR cell lines. Rat and human AhR primers were used in a multiplex with mouse β-actin primers (negative control). (C) Mouse β-actin and (D) mouse AhR. Genomic DNA was obtained by BpRc1 cell line variants using either β-actin or AhR with SYBR green dye. Cells were grown as previously described. Genomic DNA was isolated as described in the method. The experiment was repeated to confirm the results. ΔR_n is the normalisation of R_n (normalised reporter) by subtracting the baseline fluorescence. C_t (cycle threshold) is the point at which the signal passes the fluorescence threshold.

Figure 3.35 shows the genomic DNA levels of rat, human and mouse AhR (with mouse genomic β-actin as a reference gene). Figure 3.35A clearly shows that rat AhR primers amplify the target only in BpRc1 rAhR cells and Figure 3.35B shows that the human AhR primers only detected a target in BpRc1 hAhR cells. No cross contamination of AhR genes was identified. Furthermore mouse β-actin mRNA primers/probe was run with the genomic DNA as a negative control to show that there was no mRNA contamination in the DNA samples (not shown). Figure 3.35C and D show mouse β-actin and AhR, respectively, were

induced equally in all three cell lines. Along with the evidence from Figure 3.34, this shows that the AhR genes have been successfully introduced into the AhR deficient BpRc1 mouse cell line and are at a concentration that can be measured using qRT-PCR. The next step was to confirm if the genes are being transcribed by the pRevTet-Off vector. Similar to the DNA experiment, the mRNA was isolated from the cells and qRT-PCR was used to detect the levels of rat, human and/or mouse mRNA levels which were compared against β-actin mRNA levels. Confirmation of PT67 cells was not conducted as an effect from accidental contamination would have no noticeable effects on the activation of the infected AhRs in the time frame between infection and CYP1A1 mRNA measurement.

3.2.7 Confirmation of rat/human AhR mRNA transcription

Although both the pRevTet-Off and pRevTRE vectors were successfully identified, confirmation of the presence of AhR mRNA transcription still needed to be confirmed. In the process of confirming the AhR, it was also possible to quantitate the mRNA produced from transcription. Figure 3.36 show the qRT-PCR analysis of mRNA isolated from BpRc1 wild-type, BpRc1 rAhR and BpRc1 hAhR. qRT-PCR was used to improve the selectivity of the primers by utilising a probe. Primers were used to identify AhR mRNA (rat, human and mouse), and a mouse β-actin mRNA primer/probe set which was used to normalise the data. AhR and β-actin were run as a duplex with the C_t threshold normalised so that all three AhR genes could be directly compared for quantitation purposes. Figure 3.36 shows the AhR levels in the three cell lines. Mouse AhR mRNA was further measured in NIH/3T3 cells (positive control) and H4IIE/MCF-7 cells (negative control). qRT-PCR was conducted as it provided more accuracy than end-point PCR due to the addition of a species specific probe. The rat AhR primers were run at $63^{o}C$ to stop the primers from binding to the mouse AhR which shares high homology to the rat AhR.

A

B

C

D

E

Primer sets	BpRc1 wild-type	BpRc1 rat	BpRc1 human
Mouse AhR (mRNA)	100	71.6	73.2
Rat AhR (mRNA/genomic)	N/D	26.7	N/D
Human AhR (mRNA/genomic)	N/D	N/D	1.2
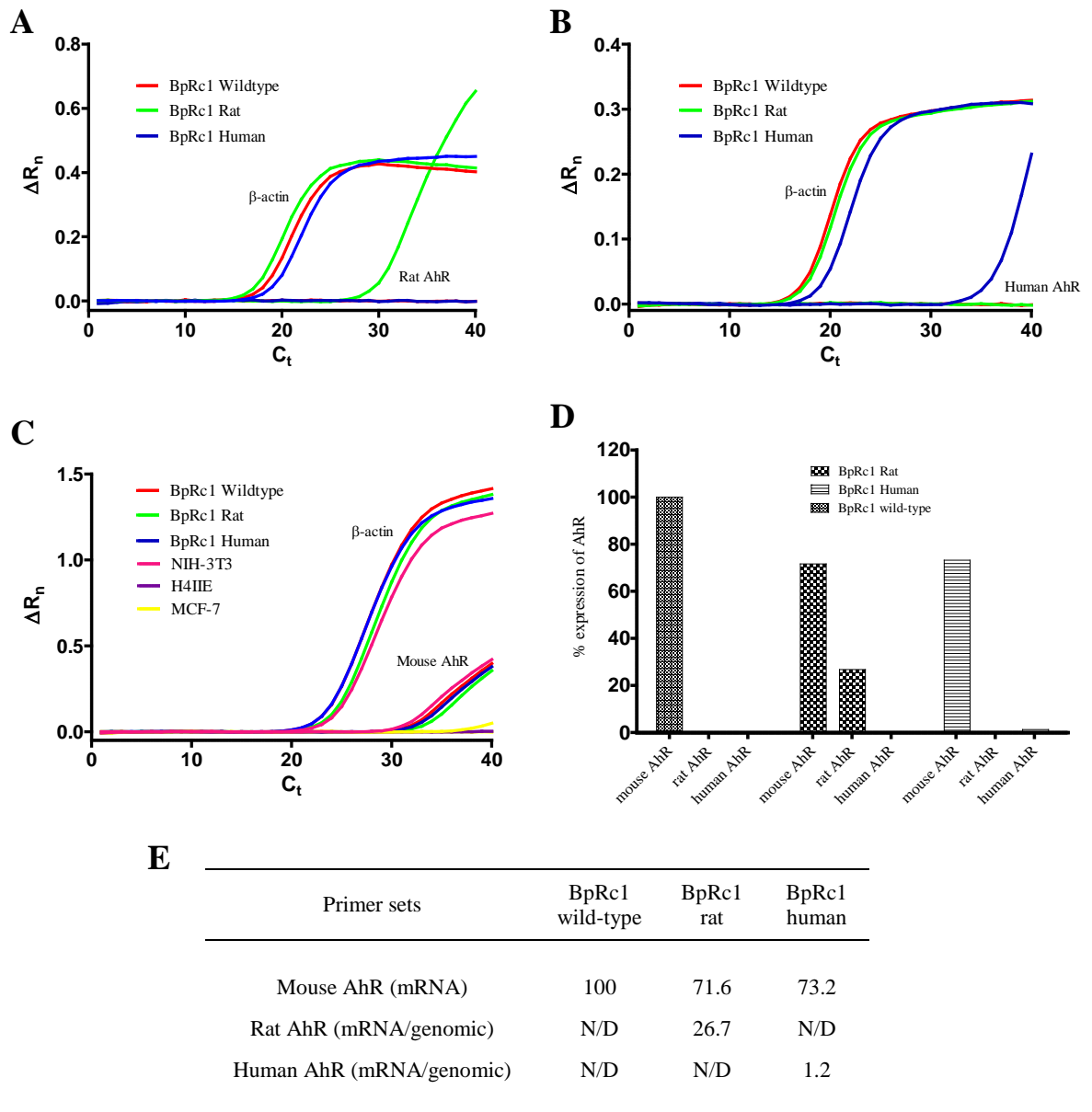
Figure 3.36: Confirmation of the presence of either rat or human AhR mRNA in the BpRc1 cell lines – Cells were created as previously described and genomic DNA was isolated (section 2.5). Primers that amplify mouse β-actin mRNA and either, (A) rat AhR or (B) human AhR, where used to detect the appropriate AhR vector (as a multiplex reaction). (C) Mouse AhR and β-actin were measured in the three BpRc1 cell lines (as a multiplex reaction), a positive control (NIH/3T3 cells) and two negative controls (H4IIE and MCF-7) cells. (D and E) AhR mRNA levels were normalised against mouse β-actin mRNA and compared. ΔR_n is the normalisation of R_n (normalised reporter) by subtracting the baseline fluorescence. C_t (cycle threshold) is the point at which the signal passes the fluorescence threshold.

Figure 3.36 confirms that the two AhR genes are being transcribed by the pRevTet-Off vector to produce AhR mRNA. Figure 3.36A shows that only BpRc1 rAhR contains rat AhR mRNA which shows the pRevTRE: rAhR vector is been successfully transcribed. Figure

3.36B shows that only BpRc1 hAhR has transcribed human AhR mRNA demonstrating that this cell line has undergone successful transcription of the pRevTRE: hAhR vector. The levels of mouse AhR mRNA was measured in the three BpRc1 cell lines as well as in the three controls (Figure 3.36C). The BpRc1 cell lines have equal quantities of AhR mRNA as expected. The BpRc1 cell line only has deficient levels of AhR so the PCR should still detect significant levels. Another mouse cell line, NIH/3T3, was used as a positive control producing similar quantities of mouse AhR mRNA as BpRc1 cell lines. Rat H4IIE and human MCF-7 were used as negative controls and the figure shows that the mouse AhR primers did not amplify any part of the rat or human mRNA. All of the mRNA levels were normalised against β-actin and tabulated to compare between cell lines (Figure 3.36D and E). The levels of mouse AhR mRNA were approximately similar for all three of the BpRc1 cell lines and NIH/3T3 which does not confirm that the BpRc1 cell line has a reduced AhR concentration. However, as the BpRc1 and NIH/3T3 come from different tissue direct comparisons of the levels of AhR, using β-actin as a normalisation gene was limited.

3.2.8 Species/tissue specific differences

Evidence from previous authors (Bazzi, 2008; Budinsky *et al.,* 2010; Silkworth *et al.,* 2006; Xu *et al.,* 2000) and this research has shown that many persistent organic pollutants are significantly more potent at inducing rat AhR than human AhR. BpRc1 cells were derived from the Hepa1c1c7 cell line which according to the literature has an EC_{50} of 88.5 pM when treated with TCDD (Hepa1c1c7; Dere *et al.,* 2006). To demonstrate this, both rat and human cells were treated with various concentrations of TCDD for 4 hours.
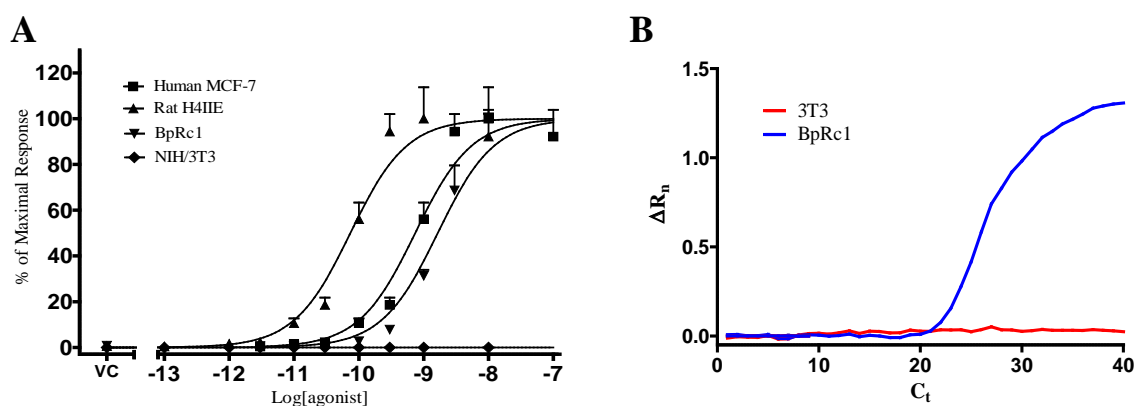
Figure 3.37: TCDD concentration-response curve in rat H4IIE, human MCF-7, mouse NIH/3T3 and mouse BpRc1 –
(A) Rat (H4IIE), human (MCF-7), mouse (NIH/3T3) and mouse (BpRc1) cells were treated with various concentrations of TCDD for 4 hours, after which, RNA was purified and cDNA was synthesised. Concentration-response curves were created by plotting the % of maximal CYP1A1 mRNA induction against concentration of agonist. qRT-PCR was used to measure the induction of the gene of interest, CYP1A1 and the two normalisation genes, AhR and β-actin. VC: Vehicle control, TC: 10 nM TCDD only control (in H4IIE cells). Each point is the mean of three biological replicates ± S.D. (B) Raw qRT-PCR data showing CYP1A1 mRNA levels in mouse NIH/3T3 and BpRc1 cells. ΔR_n is the normalisation of R_n (normalised reporter) by subtracting the baseline fluorescence. C_t (cycle threshold) is the point at which the signal passes the fluorescence threshold.

Figure 3.37A shows the induction of CYP1A1 mRNA in rat (H4IIE), human (MCF-7) and mouse (BpRc1 and NIH 3T3) cells treated with TCDD for 4 hours. The EC_{50} for TCDD induction of CYP1A1 in BpRc1 cells was1.65 nM (95% CI = 1.12 nM – 2.44 nM) compared with 74 pM (95% CI = 4.9 pM - 110 pM) in H4IIE cells and 675 pM (95% CI = 524 pM – 869 pM) in MCF-7 cells. This reiterates the previous finding that the potency of TCDD is approximately 10-fold higher in rat cells than in human. The same maximal response was reached in the BpRc1 rAhR, BpRc1 hAhR and BpRc1 wild-type cell lines but not for the mouse (NIH/3T3) cells. CYP1A1 mRNA was not detected in NIH/3T3 cells although the ability of the primers to amplify mouse CYP1A1 mRNA was confirmed in BpRc1 cells. Primers will detect either variant of the mouse CYP1A1 mRNA. This is confirmed in Figure 3.37B which shows that NIH/3T3 does not express CYP1A1 mRNA compared with BpRc1 which did express CYP1A1 mRNA.

3.2.9 Comparison of wild-type vs. Infected BpRc1 cells

Previous research has shown that 5F 203 is more potent at inducing CYP1A1 mRNA in human cells than in rat cells (Bazzi, 2008) making it a useful compound for comparison between the two species. Based on this rat and human cells were treated with various concentrations of 5F 203 and compared with cells treated with TCDD. 5F 203 concentration-response curves were conducted in the presence of a 10 nM TCDD only control to allow normalisation of the relative mRNA levels against the TCDD only curve. All of the curves also contained a vehicle control to show the background levels of CYP1A1 mRNA. Figure 3.38 shows wild-type BpRc1 cells treated with TCDD or 5F 203 for 4 hours.
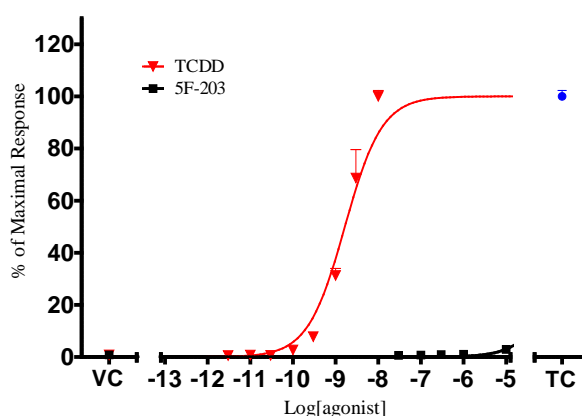
Figure 3.38: Comparison of 5F 203 and TCDD as AhR agonists in mouse BpRc1 wild-type cells – Mouse BpRc1 wild-type cells were treated with various concentrations of 5F 203. Concentration-response curves were created by plotting the % of maximal CYP1A1 mRNA induction by 10 nM TCDD against concentration of agonist. qRT-PCR was used to measure the level of induction of mouse CYP1A1 and compared against control gene, mouse β-actin. QbasePlus was used to normalise the data which was plotted using 10 nM TCDD only control as 100% of the maximal response. Results were compared with a vehicle control (VC) and a 10 nM TCDD only control (TC). Each point is the mean of three biological replicates ± S.D.

Figure 3.38 shows that the EC_{50} for wild-type BpRc1 cells treated with TCDD was 1.65 nM (95% CI = 1.12 nM – 2.44 nM) however 5F 203 did not give a recordable EC_{50} value. Figure 3.39 and Figure 3.40 shows rat (H4IIE and BpRc1 rAhR) and human (MCF-7 and hAhR) cells, respectively, treated with 5F 203 or TCDD for 4 hours.
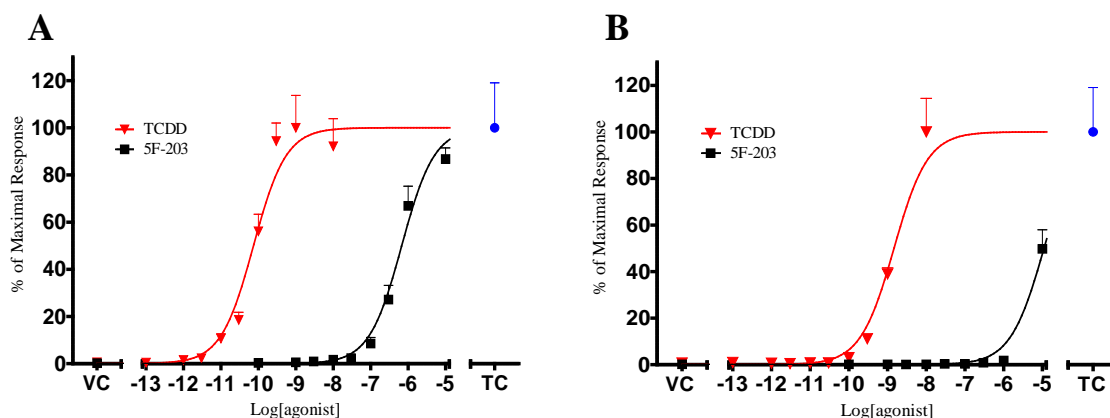
Figure 3.39: Comparison of 5F 203 with TCDD as AhR agonists in rat H4IIE cells and BpRc1 rAhR cells – (A) Rat H4IIE or (B) BpRc1 rAhR cells were treated with various concentrations of 5F 203. Concentration-response curves were created by plotting the % of maximal CYP1A1 mRNA induction by 10 nM TCDD against concentration of agonist. qRT-PCR was used to measure the level of induction of mouse CYP1A1 and compared against control gene, mouse β-actin. QbasePlus was used to normalise the data which was plotted using 10 nM TCDD only control as 100% of the maximal response. Results were compared with a vehicle control (VC) and a 10 nM TCDD only control (TC). Each point is the mean of three biological replicates ± S.D.

Figure 3.39A shows concentration-response curves of CYP1A1 mRNA induction by 5F 203 and TCDD in rat H4IIE cells. The EC_{50} of 5F 203 was 675 nM (95% CI = 524 nM – 869 nM) and TCDD was 74 pM (95% CI = 49 pM – 111 pM). From this analysis it is possible to conclude that 5F 203 is a weak AhR agonist in rat cells. The same experiment was conducted in the BpRc1 rAhR cell line using the same concentrations of TCDD and 5F 203 (Figure 3.39B). The EC_{50} for TCDD was 1.46 nM (95% CI = 1.02 nM – 2.10 nM) and for 5F 203 was 11.0 μM (95% CI = 8.98 μM – 13.5 μM). TCDD was shown to be approximately 1000-fold more potent than 5F 203 at inducing CYP1A1 mRNA in the BpRc1 rAhR cells. However both TCDD and 5F 203 were 20-fold more potent in the wild-type H4IIE cell line than the BpRc1 rAhR cell line. Further to this, the results from BpRc1 rAhR were compared against those obtained from BpRc1 wild-type when treated with TCDD. Comparison shows that the two EC_{50}s (BpRc1 wild-type vs. BpRc1 rAhR) are not significantly different (p = 0.6133). The same experiment was then carried out in human MCF-7 and BpRc1 hAhR cells.
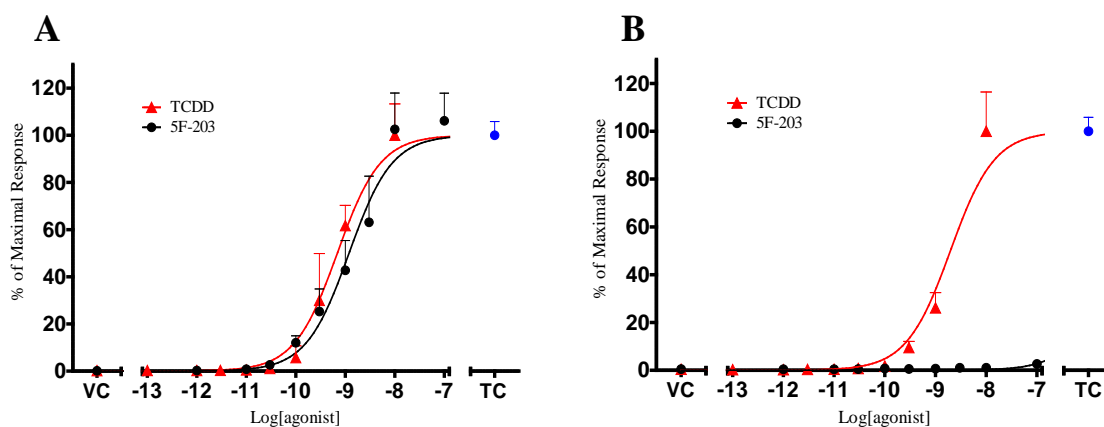
Figure 3.40: Comparison of 5F 203 with TCDD as AhR agonists in human MCF-7 cells and BpRc1 hAhR cells – (A) Human MCF7 or (B) BpRc1 hAhR cells were treated with various concentrations of 5F 203. Concentration-response curves were created by plotting the % of maximal CYP1A1 mRNA induction by 10 nM TCDD against concentration of agonist. qRT-PCR was used to measure the level of induction of mouse CYP1A1 and compared against control gene, mouse β-actin. QbasePlus was used to normalise the data which was plotted using 10 nM TCDD only control as 100% of the maximal response. Results were compared with a vehicle control (VC) and a 10 nM TCDD only control (TC). Each point is the mean of three biological replicates ± S.D.

Figure 3.40A shows that the EC_{50} for 5F 203 induction of CYP1A1 was 1.18 nM (95% CI = 818 pM – 1.72 nM) and for TCDD the EC_{50} was 689 pM (95% CI = 550 pM – 861 pM). This data shows that 5F 203 is a potent agonist of human AhR and is only approximately 5-fold less potent than TCDD at inducing CYP1A1 mRNA in human cells. The two compounds were tested in BpRc1 hAhR cells (Figure 3.40B). TCDD gave an EC_{50} of 1.97 nM (95% CI = 1.21 nM – 3.20 nM) however 5F 203 did not produce a measurable response. The response of TCDD in BpRc1 hAhR was shown not to be statistically significantly different to BpRc1 wild-type (p=0.54). Furthermore TCDD was found to be 3-fold more potent at inducing CYP1A1 mRNA in human MCF-7 cell line than in the BpRc1 hAhR cell line (p=0.0004). The induction of CYP1A1 mRNA of TCDD in BpRc1 hAhR was compared against the response in BpRc1 rAhR cells and the two EC_{50}s were also found not to be statistically significantly (p=0.27).

4. Discussion

4.1 Alternative methods

4.1.1 mRNA measurement

Recent research by Hu *et al.* (2007) showed that CYP1A1 induction is a non-specific biomarker of AhR activation and supports the hypothesis that CYP1A1 may not necessarily be related to dioxin-like toxicity. However their work was conducted *in vivo* which is a much more complex model to investigate compared with *in vitro*, using potentially complex atypical compounds which may not bind in the same binding site as the more conventional dioxin-like AhR agonists. There is also a significant volume of research that shows CYP1A1 is a specific biomarker for AhR activation by dioxin-like compounds (Behnisch *et al.*, 2001; Nebert *et al.*, 2000, 2004; Schmidt *et al.*, 1996; Vanden Heuvel *et al.*, 1994). Another method of mRNA quantitation is northern blotting which has high specificity but low sensitivity. The chemicals used are toxic and there is a risk of RNAse contamination. Microarray analysis measures the expression of large numbers of genes but has low resolving power. The method is also too expensive and this project is only interested in the expression of CYP1A1 (as a measure of AhR activation). In both northern blot and microarray assays, large sample sizes are required which is why qRT-PCR was chosen. Finally, the use of luciferase based assays containing AhR (DRE) binding sites, has become a common method of measurement of AhR activation as it is both quick to use and cheap to operate allowing large numbers of samples to be analysed on a budget (Burke and Mayer, 1974; Sanderson *et al.*, 1996). Covered briefly in section 1.3.5.2, the luciferase cells were created by transfecting the firefly (*Photinus pyralis*) luciferase gene into the cell genome along with DRE binding sites and promoter regions upstream. The activated AhR binds to these DRE sites allowing transcription, and ultimately translation, of the exogenous luciferase protein which can then be measured using a luminometer. However measurement of CYP1A1 mRNA by qRT-PCR was utilised for

these studies over luciferase based assays because it not only allows detection and a more exacting quantitation of AhR-dependent expression of an endogenous gene (CYP1A1), but it would confirm that the responses examined were not due to selective effects on expression from the integrated luciferase reporter plasmid that might not be seen on other AhR-responsive genes. qRT-PCR has a large advantage over other methods of CYP1A1 mRNA measurement in that it allows the analysis of several genes in a single experiment which can be used as reference genes.

4.1.2 Protein measurement

Quantitative analysis of the activation of AhR, through measurements of CYP1A1 mRNA, is critically dependent on the methodology for mRNA measurement. CYP1A1 (EROD and AHH) are induced by TCDD-like compounds (Kennedy, 1993). EROD activity has historically been used as a measure of AhR activation (Clemons *et al.,* 1997, 1998; Hilscherova *et al.,* 2001; Peters *et al.,* 2004; Sanderson *et al.,* 1996; Schmitz *et al.,* 1995; Silkworth *et al.,* 2005). EROD activity measures the rate of CYP1A1-mediated deethylation of 7-ethoxyresorufin (7-ER) leading to the production of highly-fluorescent resorufin, measured using a plate reader. The method replaced AHH activity in the mid 1980's due to the increased safety and economy of EROD, compared with AHH measurement. The system also has a greater efficiency and is much more cost effective (Whyte *et al.,* 2004). The advantage of EROD, which measures the rate of deethylation of 7-ethoxyresorufin, is that it measures the whole mechanism of AhR activation and CYP1A1 translation unlike PCR. PCR technology has allowed the measurement of CYP1A1 mRNA which provides a more sensitive measurement of AhR activation compared with EROD (Vanden Heuvel *et al.,* 1994). Research has shown that certain compounds (e.g. PCBs) inhibit the EROD enzyme-substrate reaction at high concentrations making mixture experiments impossible to measure accurately, and illustrating the generic pitfall that enzyme activity measurement can be a

flawed measure of AhR activation (Garrison *et al.,* 1996; Kennedy *et al.,* 1993; Petrulis *et al.,* 1999; Sawyer *et al.,* 1984). CYP1A1 mRNA induction is one of the most potent effects of AhR activation so would be expected to give both the most accurate and most sensitive results. Measurement of resorufin requires that the cells are treated for longer periods of time to allow translation of the enzymes. Longer periods of treatment can lead to the metabolism of some compounds, including 3-MC (Riddick *et al.,* 1994) and TCDF (Clemons *et al.,* 1997). In this thesis, a method of measuring the induction of CYP1A1 was calibrated using qRT-PCR. Several variables that affect accurate measurement of CYP1A1 mRNA were identified and optimised, yielding a methodology with considerable statistical power for the determination of the potency of an agonist for inducing CYP1A1 mRNA. Statistical power is a prerequisite for detecting small differences in potency. Such quantitative measurement of induction potency enables the application of a variety of pharmacological tools to investigate the nature of agonism.

4.2 qRT-PCR method optimisation

4.2.1 Calibration of PCR method

This study required a robust method of measuring the agonistic and antagonistic properties of a variety of AhR-related compounds. The measurement of CYP1A1 mRNA induction was decided to be the most accurate way to measure ligand induced AhR activation and was therefore chosen as the marker for AhR activation. Measurement of CYP1A1 mRNA was conducted using qRT-PCR which required optimisation before RNA quantitation. The PCR efficiency was measured using a dilution curve of known cDNA which found the efficiency of CYP1A1, β-actin and AhR to be approximately 100% for all of the species tested (Figure 3.3). The use of conditioned medium significantly reduced the effect of AhR ligands contained within the cell culture medium increasing the background to noise ratio (Figure 3.1). This demonstrates that the concentrations of the probes and primers are satisfactory and

that the assay is robust. An overlay of several separate TCDD concentration-response curves in rat and human cells, show that the results are reproducible and therefore comparison between curves is possible (Figure 3.5). qRT-PCR has been shown to be a reliable tool for measuring the differences in CYP1A1 mRNA between samples providing a high discriminatory power for statistically significant differences between concentration-response curves. TCDD concentration-response curves from rat H4IIE and human MCF-7 cells were compared to demonstrate the reproducibility of the qRT-PCR method of CYP1A1 mRNA measurement (Figure 3.5).

4.2.2 CH223191 is a potent antagonist

The ability of the qRT-PCR method to detect antagonism was demonstrated using a known antagonist, CH223191. The initial experiment confirmed that CH223191 was a pure antagonist and showed no significant increase in CYP1A1 induction compared with TCDD which was confirmed by previous research (Kim *et al.,* 2006). Further experimentation effectively demonstrated the antagonistic properties of CH223191 with the chosen assay. The IC_{50} for antagonism of 1 nM TCDD induced CYP1A1 mRNA (411 nM) compared favourably to that obtained by Kim *et al.* (2006) despite the different cell line and protocols used. Based on the IC_{50}, four concentrations of the antagonist were selected to perform Schild analysis on the TCDD concentration-response curve (Figure 3.7). Cells were treated with TCDD in the presence of each of the four concentrations of CH223191 to extrapolate the K_d of the antagonist which was calculated to be 18.2 nM. Choi *et al.* (2012) investigated a range of compounds based on the structure of CH223191. They found that CH223191 was a potent antagonist and gave an IC_{50} of 10 nM -100 nM. The other compounds tested were shown to be a range of high to low potency antagonists showing that substitutions on the pyrazole group were important for antagonistic potency. Figure 3.7 successfully demonstrated the shift of the concentration-response curve to the right as the concentration of antagonist was

increased. It was also noted during experimentation that the antagonist reduced the induction potency of various AhR agonists present in the unconditioned cell culture medium used hence the use of conditioned medium with significantly reduced AhR agonist levels. Furthermore, the experiment has characterised the potency of the antagonist using five significantly different EC_{50}s derived from the TCDD concentration-response curves shown in Figure 3.7A. More importantly this experiment has successfully shown that this method of antagonist detection can actually detect antagonistic properties of a compound and furthermore these properties can be quantitated.

4.3 Reliability of the results obtained

4.3.1 TCDD

TCDD is a well characterised standard when calculating the potency of dioxin-like HAHs and REPs of AhR agonists. The EC_{50}s calculated in this work were compared with the literature (derived from various techniques) to determine the reliability of the data obtained in this project (Table 4.1)

Method	TCDD EC_{50}	Study
qRT-PCR[a]	**33 pM (± 1 pM)**	**Current study**
EROD[c]	9.0 pM (± 2.1 pM)	Clemons *et al.,* 1998
CALUX[b]	10 pM	Murk *et al.,* 1996
EROD[d]	10 pM	Peters *et al.,* 2004
EROD[b]	11.8 pM (± 3.9 pM)	Clemons *et al.,* 1997
EROD[c]	14 pM (± 4 pM)	Chen *et al.,* 2001
EROD[d]	19.6 pM (± 5.6 pM)	Sanderson *et al.,* 1996
EROD[d]	34.5 pM (± 1.96 pM)	Hilscherova *et al.,* 2001
qRT-PCR[a]	40 pM (± 13 pM)	Bazzi, 2008
EROD[c]	41 pM (23 pM – 74 pM)	Silkworth *et al.,* 2005
EROD[c]	50 pM (± 13 pM)	Schmitz *et al.,* 1995
EROD[c]	50 pM (37 pM – 65 pM)	Zeiger *et al.,* 2001

Table 4.1: Comparison of TCDD EC_{50} values taken from the literature - All data was derived from H4IIE cells. Values in parentheses are 95% confidence intervals or ± Standard Deviation/Standard Error. Cells were treated for: [a]4 hours, [b]24 hours, [c]48 hours, [d]72 hours. qRT-PCR: Quantitative Real-time Polymerise Chain Reaction, EROD: Ethoxyresorufin-O-deethylation. CALUX: Chemical Activated LUciferase gene eXpression.

The EC_{50} calculated in this work corresponds well with the values found in the literature. The majority of the values calculated previously use EROD analysis to calculate the EC_{50}; however, it was deemed suitable to compare directly with the values calculated in this work (Chaty *et al.,* 2008).

4.3.2   TCDF, PeCDF and PCB 126

REPs are based on a mixture of data derived from biochemical, receptor binding, toxicity and carcinogenicity studies (Haws *et al.,* 2006; Van den Berg *et al.,* 2006).

Compound	Method	REP	Study
TCDF	**qRT-PCR**[a]	**0.115**	**Current study**
	EROD[b]	0.03	Bols *et al.,* 1997
	EROD[c]	0.092	Bandiera *et al.,* 1984
	AHH[d]	0.12	Wiebel *et al.,* 1996
	EROD[c]	0.15	Li *et al.,* 1999
PeCDF	**qRT-PCR**[a]	**0.171**	**Current study**
	AHH[c]	0.28	Bandiera *et al.,* 1984
	EROD[c]	0.28	Sanderson *et al.,* 1996
	EROD[b]	0.4	Bols *et al.,* 1997
	EROD[d]	0.41	Behnisch *et al.,* 2002
	Luciferase[d]	0.69	Sanderson *et al.,* 1996
	DR-CALUX[d]	0.84	Behnisch *et al.,* 2002
PCB 126	**qRT-PCR**[a]	**0.103**	**Current study**
	Luciferase[d]	0.017	Sanderson *et al.,* 1996
	EROD[c]	0.02	Tillitt *et al.,* 1991
	EROD[c]	0.047	Sanderson *et al.,* 1996
	EROD[c]	0.05	Koistinen *et al.,* 1996
	EROD[b]	0.1	Bols *et al.,* 1997
	EROD[d]	0.1	Hanberg *et al.,* 1990
	EROD[b]	0.18	Schmitz *et al.,* 1995
	EROD[c]	0.323	Sawyer and Safe, 1982

Table 4.2: Comparison of REP values taken from the literature – Potency data shown as REPs (their potency in comparison to TCDD; see section 1.4.2.1). All REPs were calculated from assays on H4IIE cells. Cells were treated for: [a]4 hours, [b]48 hours, [c]72 hours, [d]24 hours. qRT-PCR: Quantitative Real-time Polymerise Chain Reaction, EROD: Ethoxyresorufin-O-deethylation. Luciferase: Luciferase cells. AHH: Aryl hydrocarbon hydroxylase.

TCDF, PeCDF and PCB 126 were tested in rat (H4IIE or primary cultures) in previous work by this author but the concentrations were re-adjusted after they were confirmed using GC/MS. The new EC_{50}s calculated from this adjustment were compared with the literature (Table 4.2). The WHO gave TCDF a TEF of 0.1 based on previous REPs calculated *in vivo* (DeVito and Birnbaum, 1995; Takagi *et al.,* 2003; Weber *et al.,* 1984) and *in vitro* models in rat H4IIE cells (Table 4.2; Haws *et al.,* 2006). In this study, the REP for TCDF was calculated to be 0.115 which compares well with the TEF of 0.1. The REP also compares well with values from the literature (REPs: 0.03 – 0.15). A TEF of 0.3 was estimated for PeCDF from *in vivo* (Fattore *et al.,* 2000; Johnson *et al.,* 2000; NTP TR-525, 2006; Pluess *et al.,* 1998; Wærn *et al.,* 1995; Walker *et al.,* 2005) and *in vitro* data (Table 4.2; Haws *et al.,* 2006 supplementary data). PeCDF gave a REP of 0.171 in this work which is slightly lower than the TEF of 0.3. It is also slightly lower than the values calculated in the literature (REPs: 0.28 - 0.84). The reason for this difference may be due to the preparation of the compound prior to treatment of the cells or the contamination of the stock. The original 1998 TEF for this compound was 0.5 (Van den Berg *et al.,* 1998) which appears to match the literature data more closely. Finally a TEF of 0.1 was calculated for PCB 126 from *in vivo* (Hemming *et al.,* 1995; NTP TR-520, 2006; Van Birgelen *et al.,* 1994) and *in vitro* data (Table 4.2; Haws *et al.,* 2006 supplementary data). A REP of 0.103 was calculated for PCB 126 in this work which corresponds well with the TEF of 0.1. The literature also supports the use of a TEF of 0.1 (REPs: 0.017 - 0.323). This comparison shows that the REPs calculated in this project match with the predicted values from the WHO consortium (Van den Berg *et al.,* 2006) and REPs calculated in previous literature. The antagonistic properties of the three compounds have been investigated previously and found that none of the three compounds are partial agonists in rat H4IIE cells (Wall, 2008).

4.3.3 Mixed halogenated dioxin-like HAHs

One of the main aims of this project was to characterise the agonist properties of several mixed halogenated dioxin-like AhR ligands based on their ability to induce CYP1A1 mRNA. REPs were calculated, based on the EC_{50} of TCDD, for all of the compounds tested (PXDDs: Table 3.1; PXDFs: Table 3.2; PXBs: Table 3.3). Several of the compounds tested were well known AhR agonists which already have allocated TEFs calculated through meta-analysis of REP data which corresponds well with the REPs in this project (section 4.3.2).

Compound	WHO 2005 TEF	Estimated REP from this study*	Difference
2,3,7,8-TetraCDD	**1**	1	=
2-B-3,7,8-TriCDD		3	+ 3-fold
2,3-DiB-7,8-DiCDD		0.3	- 3-fold
1,2,3,7,8-PentaCDD	**1**		
1-B-2,3,7,8-TetraCDD		0.1	- 10-fold
2-B-1,3,7,8-TetraCDD		0.3	- 3-fold
2,3,7,8-TetraCDF	**0.1**	0.1	=
3-B-2,7,8-TriCDF		0.1	=
2,3-DiB-7,8-DiCDF		0.3	+ 3-fold
2,3,4,7,8-PentaCDF	**0.3**	0.3	=
4-B-2,3,7,8-TetraCDF		0.3	=
1,2,3,7,8-PentaCDF	**0.03**		
1-B-2,3,7,8-TetraCDF		0.1	+ 3-fold
1,3-DiB-2,7,8-TriCDF		0.3	+ 10-fold
3,3',4,4',5-PentaCB	**0.1**	0.1	=
4'-B-3,3',4,5-TetraCB		0.3	+ 3-fold
3',4'-DiB-3,4,5-TriCB		0.1	=
3',4',5-TriB-3,4-DiCB		0.3	+ 3-fold
3,3',4,4',5-PentaBB		0.03	- 3-fold
2,3,3',4,4'-PentaCB	**0.00003**	0.000003	- 10-fold
4'-B-2,3,3',4-TetraCB		0.00001	- 3-fold
2,3',4,4',5-PentaCB	**0.00003**	0.000003	- 10-fold
4'-B-2,3',4,5-TetraCB		0.00003	=
2,3,3',4,4',5-HexCB	**0.00003**	0.0003	+ 10-fold
4'-B-2,3,3',4,5-PentaCB		0.0003	+ 10-fold

Table 4.3: Estimated REPs compared with TEFs – TEFs were taken from Van den Berg *et al.,* 2006. *REP values from this study were rounded to the nearest half log to allow more simplistic comparison with the TEFs.

These compounds were used as controls to show reproducibility of the data and allow comparison with REPs found in the literature (Table 1.2, Table 1.3; Behnisch *et al.,* 2003; Olsman *et al.,* 2007; Samara *et al.,* 2009). There was general agreement between this work and literature for all of the compounds with a few exceptions. 2-B-7,8-DiCDF was found to be 10-fold more potent in this project than in the literature (0.000037; Olsman *et al.,* 2007), 2,7,8-TriBDF was found to be 50-fold more potent in this study compared with the literature (0.00049; Olsman *et al.,* 2007) and finally 2-B-6,7,8-TriCDF was ~250-fold more potent in this study then compared with the literature (0.00066; Olsman *et al.,* 2007). Previous literature has used the TEFs of only chlorinated compounds (Table 1.5) for the equivalent brominated and mixed halogenated congeners in order to calculate their TEQs (Ohta *et al.,* 2004; Food Standards Agency, 2006a, 2006b, 2006c; Colles *et al.,* 2008; Fernandes *et al.,* 2008). Table 4.3 compares the REPs calculated in this paper with the TEF of the equivalent chlorinated congener. A few compounds of notable potency were identified including 2-B-3,7,8-TriCDD which was found to be 3-fold more potent than TCDD in both rat and human cell lines and which has been confirmed in the literature (Olsman *et al.,* 2007). Only a few other compounds have been found to be more potent than TCDD so this is a remarkable finding. Also identified as very potent AhR agonists were 2-B-1,3,7,8-TetraCDD and 2,3-DiB-7,8-DiCDF, which gave REPs of 0.3 corresponding well with values found in the literature (Behnisch *et al.,* 2003; Olsman *et al.,* 2007). 2,3-DiB-7,8-DiCDD was found to be slightly less potent in this paper compared with other authors (Behnisch *et al.,* 2003; Olsman *et al.,* 2007; Samara *et al.,* 2009).

4.3.4 PCBs

The REPs calculated in this work for PCB 105 and 118 (~0.000003) were 10-fold less than the TEF values calculated by the WHO (0.00003, Van den Berg *et al.,* 2006). On the other hand, the REP for PCB 156 obtained in this work (0.0003) was 10-fold more than the value

calculated by the WHO (0.00003, Van den Berg *et al.,* 2006). The agonistic and antagonist study of PCB 105 and PCB 118 showed that both compounds were partial agonists of rat AhR and PCB 105 was shown to be a pure antagonist of human AhR whereas PCB 118 was shown to be a partial agonist. Clemons *et al.* (1998) treated rat H4IIE cells with TCDD in the presence of PCB 105 and PCB 118, and demonstrated a shift of the concentration response curves to the right in comparison to TCDD alone. Clemons *et al.,* (1998) also showed that PCB 77 was partially antagonised by both PCB 105 and PCB 118 in H4IIE cells. Hestermann *et al.* (2000) indicated that PCB 118 may be a partial agonist as opposed to a complete antagonist. The authors also showed that PCB 105 and PCB 128 were competitive antagonists of the AhR. The REPs for PCB 105 in rat H4IIE cells (used to calculate the TEF) ranged from 0.0000075 (Tillitt *et al.,* 1991) to 0.000668 (Sawyer and Safe, 1982). The purity of the compound was >99% in the Tillitt study but was undetermined in the majority of the other studies. As the compound is a very weak agonist, even <1% contamination of a more potent agonist could produce a response. In this study no known potent agonists were found in the PCB 105 stock (Table 2.1). The REPs used to calculate PCB 118 (in rat H4IIE cells) ranged from 0.000002 (Hanberg *et al.,* 1990) to 0.00001 (Bols *et al.,* 1997) in order to create a TEF of 0.00003 (Van den Berg *et al.,* 2006). None of the purities of the PCB 118 stocks used in these studies could be confirmed so the effect of more potent agonists was impossible to calculate. There were no significant impurities found in the PCB 118 stock used in this project. PCB 156 was found to be a pure agonist in rat H4IIE cells and a weak partial agonist in human MCF-7. Clemons *et al.* (1998) also showed that PCB 156 had partial agonistic properties in RTL-W1 rainbow trout liver cells although Hesterman *et al.* (2000) found that PCB 156 had no effect on CYP1A induction in PLHC-1 fish cells. A REP range of 0.000026 (Aarts *et al.,* 1998) to 0.1 (Chen *et al.,* 2004) in rat H4IIE cells was used to calculate the TEF of PCB 156 (Table 4.4; Haws *et al.,* 2006). These REPs from the literature are almost all

higher than the TEF applied to this compound (0.00003; Van den Berg *et al.,* 2006) but fit well with the REP calculated in this project (0.0002; Figure 3.21). The purity of the PCB 156 stocks used to calculate these TEFs were not confirmed which could mean they are also contaminated with more potent dioxin-like HAHs (during synthesis). One interesting point is that the range of REPs calculated for PCB 156, as well as other mono-*ortho*-substituted PCBs (not shown), differ widely between authors compared with the other compounds where TEFs where calculated, showing the difficulty in measuring the potency of these weak agonists.

Method	REP	Study
Evidence of low REP (~0.00003)		
CALUX[a]	0.000026	Aarts *et al.,* 1998
EROD[b]	0.000052	Bols *et al.,* 1997
EROD[c]	0.000054	Tillitt *et al.,* 1991
EROD[a]	0.00007	Schmitz *et al.,* 1995
EROD[c]	0.0000895	Sawyer and Safe, 1982
Evidence of high REP (~0.0003)		
EROD[b]	0.0001	Hanberg *et al.,* 1990
CALUX[d]	0.00014	Brown *et al.,* 2001
EROD[a]	0.0003	Schmitz *et al.,* 1995
EROD[b]	0.1	Chen *et al.,* 2004

Table 4.4: Comparison of the REPs calculated for PCB 156 - All REPs calculated in rat H4IIE cells. Cells were treated for: [a]48 hours, [b]24 hours, [c]72 hours, [d]20 hours. EROD: Ethoxyresorufin-O-deethylation. Luciferase: Luciferase cells. CALUX: Chemical Activated LUciferase gene eXpression.

Assuming the TEF is the best representation of PCB 156, the most likely explanation for the high REP (0.0003) calculated in this study is that it was contaminated with low concentrations of PCB 126 (section 2.1.4) which could have increased the agonistic properties of PCB 156 through additivity. However based on the data from Table 4.4, it is possible to see that the majority of the literature supports a higher REP in the region of ~0.0001.

4.3.5 AZFMHCs are AhR agonists

4.3.5.1 AZ1 is a very potent AhR agonist

The AZFMHCs were previously identified of AhR agonists during a routine drug screening investigation by AstraZeneca. Measurement of the ability of the AZFMHCs to induce CYP1A1 mRNA in rat H4IIE cells showed that all of the compounds were at least medium potency AhR agonists. One of the compounds, AZ1, was shown to be an exceptionally potent inducer, being 5-fold more potent at inducing CYP1A1 RNA compared to TCDD. AZ2, 3 and 4 were shown to be less potent inducers, at least 45-fold less potent than TCDD. None of the AZ compounds demonstrated any antagonistic properties. The ability of AZ1 to induce two other AhR-related metabolism genes, CYP1A2 and CYP1B1, provides strong evidence that the compound does activate the AhR The ability of AZ1 to activate the AhR was not confined to rat cells although both AZ1 and TCDD were ~10-fold less potent at inducing CYP1A1 in human MCF-7 than in rat H4IIE cells. This finding is reminiscent of many other studies which show that the human AhR is less responsive to ligands than is the rat AhR (Budinsky *et al.,* 2006; Xu *et al.,* 2000). However, the results confirm that both substances are potent activators of the AhR in human, and that AZ1 is more potent than TCDD. This is an interesting finding as TCDD is one of the most potent along with 1,2,3,7,8-pentachlorodibenzo-*p*-dioxin and some of the mixed halogenated dibenzo-*p*-dioxins and dibenzofurans investigated in this study. For further analysis of the compound, it would be useful to measure the CYP1A1 protein levels using EROD in order to visualise the whole mechanism of AhR activation by this compound.

4.3.5.2 AZ2, 3 and 4 are medium potency agonists

AZ1 was shown to be a highly potent AhR agonist however the other family members were shown only to be medium potency agonists approximately 100-1000-fold less potent than AZ1. Structurally the most important characteristic for high potency, based on the four

compounds tested, is that there is no group on the R^2 position (section 3.1.3.1). Also, the fact that AZ3 was the least potent compound suggests that the CF_3 group at R^1 is beneficial for high potency. All of the compounds have a very similar structure to alpha-naphthoflavone (α-NF) and β-NF which are also potent ligands of the AhR. α-NF is a potent antagonist but has a strong affinity for the AhR (Gasiewicz and Rucci, 1991; Santostefano *et al.,* 1993) and β-NF has been shown to be a potent agonist of the AhR (Chirulli *et al.,* 2007). The three AZFMHCs were significantly less potent than TCDD (AZ2 = 45-fold less potent, AZ3 = 350-fold less potent and AZ4 = 135-fold less potent than TCDD) and thus only AZ1 was chosen for further investigation.

4.3.5.3 Ligand binding shows AZ1 and TCDD are high affinity ligands

In order to confirm the hypothesis that AZ1 is acting through AhR activation, the ability for AZ1 to compete with TCDD for binding to the AhR was investigated. The K_d and B_{max} for [^{3}H]-TCDD was 1.24 nM and 26.9 fmol/mg, respectively. This data fits well with measurements made by previous authors (using the same [^{3}H]-TCDD) who found the K_d and B_{max} to be 0.27 nM – 1.45 nM and 40 fmol/mg, respectively (Bazzi, 2008; Jiang, 2004). The affinity of AZ1 and TCDD were measured using a ligand binding assay which showed that AZ1 (IC_{50} = 269 pM) had a 14-fold higher affinity for the AhR than TCDD (IC_{50} = 2.11 nM). This compares well with previous findings from other authors using the same [^{3}H]-TCDD and unlabelled TCDD who found the IC_{50} to be 1.65 nM (TCDD; Bazzi, 2008). This shows that the two compounds share the same binding site on the AhR, and proves that AZ1 is agonising the AhR.

4.4 Structure-activity relationships

4.4.1 Affinity vs. Potency

4.4.1.1 Comparison of potency and affinity of HAHs

In this project, only potency data for the HAHs was estimated however investigation of the full mechanism also requires measurement of affinity. The potency data estimated in this study was compared against binding affinity data derived from Bandiera *et al.* (1982, 1984).
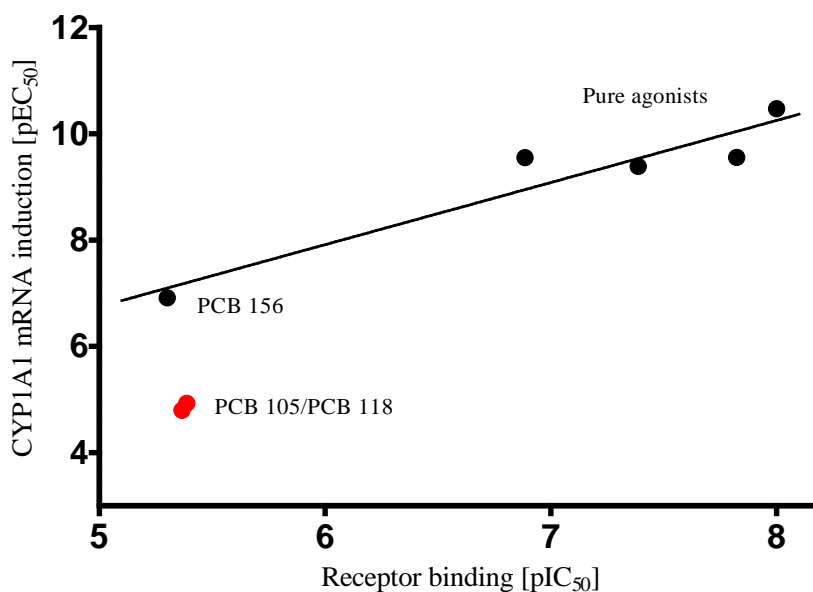
Figure 4.1: CYP1A1 mRNA induction vs. AhR binding in rat – The potency data (mRNA induction) was conducted in this study using rat H4IIE cells and the affinity data was taken from Bandiera *et al.* (1982, 1984). A test group containing the five pure HAH AhR agonists (TCDD, TCDF, PeCDF, PCB 126 and PCB 156) was used to plot the linear trend line. Slope = 1.169, r^2 = 0.901.

Figure 4.1 shows that there is a relationship between binding affinity and potency, demonstrating that as affinity increases, so does the potency. The five potent pure agonists (in rat): TCDD, TCDF, PeCDF, PCB 126 and PCB 156 all have potency related to affinity whereas PCB 105 and PCB 118 do not fit the trend, as they have a low potency despite a reasonably high affinity. This, as discussed early, is most likely due to their antagonist properties (binding to receptor without activating it), leading to a high affinity compared with the potency. The difficulty with this analysis is the lack of data points for

these compounds. PCB 156 fits well with the data despite the fact that it is contaminated with a potentially significant concentration of PCB 126. The purity of the compounds used in the affinity study was not confirmed so they may also be equally contaminated. Only a few researchers have conducted binding affinity experiments on HAHs (Bandiera *et al.,* 1982, 1984; Brown *et al.,* 1994; Poland and Glover, 1977), so one possible piece of further work would be to do binding studies on all of the mixed halogenated compounds in this study to allow a more detailed structure-activity relationship study. Even less work has been conducted on the binding affinity of compounds interacting with the human AhR due to the large quantities of tissue required to conduct the assay. Previous work has shown that human AhR has up to 10-fold lower binding affinity for TCDD than mouse, perhaps partly explaining the difference in the potency of TCDD between the two species (Ema *et al.,* 1994; Harper *et al.,* 1988; Ramadoss and Perdew, 2004). Assuming other rodents have a similar binding affinity for dioxin-like HAHs, this could explain differences (seen here between rat and human) in the potency of these ligands but would require more data on human AhR binding affinity to confirm this statement. Direct comparison of ligand binding to the rat or human AhR may explain the differences seen of ligand potency between rat and human.

4.4.2 Chr compounds

4.4.2.1 Luciferase induction by Chr compounds

The two recombinant AhR-responsive luciferase cell culture models, mouse H1L6.1c2 and human HG2L6.1c3 cells, were used to obtain screening data (Conducted by Prof. Michael Denison; Wall *et al.,* 2012b) on the AhR agonist activity of all of the Chr compounds at a single concentration (10 µM). The results from mouse and human are displayed as direct comparisons with the data normalised to the maximal induction response obtained with TCDD (1 nM for H1L6.1c2 cells and 10 nM for HG2L6.1c3 cells; Figure 4.2A). The results show that none of the compounds were particularly potent agonists especially in the human

cell line. However, Chr-4, 6, 7, 8, 10, 11, 13, 14, 15, 16, 17, 18 and 19 were agonists for the

mouse AhR signalling pathway and Chr-3, 15, 16 and 19 were agonists for the human AhR;

the remaining compounds were inactive as AhR agonists in either cell system.
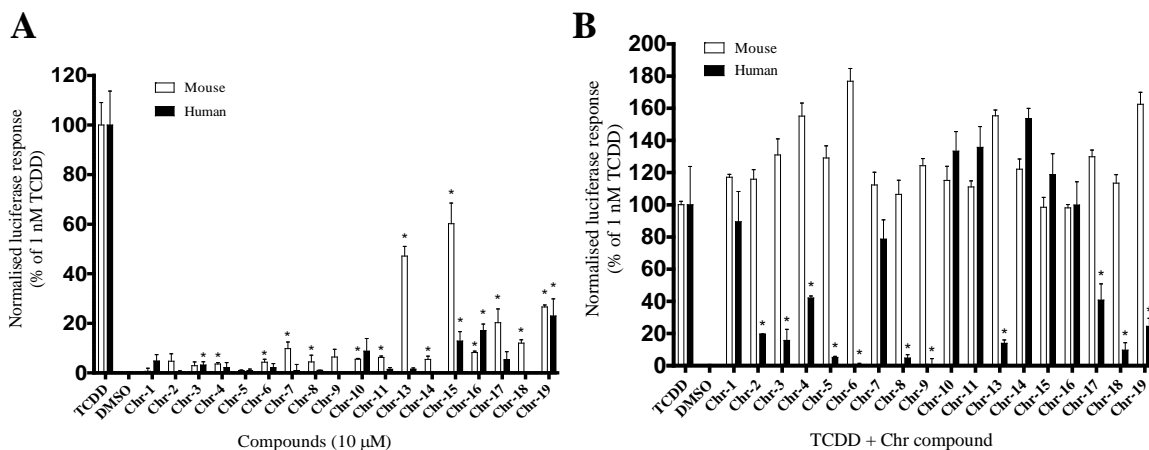
Figure 4.2: AhR agonist and antagonistic activity of 2-amino-isoflavone derivatives in recombinant mouse and human hepatoma cell lines – (A) Mouse H1L6.1c2 and human HG2L6.1c3 cells were incubated with 10 µM Chr compound, TCDD (1 nM for mouse and 10 nM for human) or 0.1% DMSO control for 24 hours. (B) Mouse H1L6.1c2 and human HG2L6.1c3 cells were incubated with 10 µM Chr compound in the presence of TCDD (1 nM for mouse and 10 nM for human cells), TCDD alone or 0.1% DMSO control for 24 hours. Luciferase activity was measured and normalised against TCDD (maximal response). White bars = mouse, black bars = human. Error bars are S.D., n = 3. *Luciferase activity was significantly higher (p-value ≤0.05) than that of DMSO control. The figure was taken from Wall *et al.* (2012b).

To determine the ability of the isoflavones to antagonise mouse and human AhR action, cells

were co-incubated with TCDD (1 nM for mouse H1L6.1c2 and 10 nM for human

HG2L6.1c3) in the absence or presence of 10 µM of the indicated compound and luciferase

activity determined after 24 hours of incubation. The data (Figure 4.2B) shows that while

none of the Chr compounds exerted an antagonistic effect on TCDD dependent activation of

AhR signalling in mouse H1L6.1c2 cells, a large number of the compounds (Chr-2, 3, 4, 5, 6,

8, 9, 13, 17, 18 and 19) antagonised TCDD-dependent induction of luciferase in the human

HG2L6.1c3 cells. These results demonstrate clear species differences in the relative potency

and agonist and/or antagonist activity of these compounds. This reduction of AhR-dependent

transcription of luciferase, when the isoflavones were incubated in the presence of TCDD,

shows that the compounds must have a relatively good affinity for the AhR and that they have very low agonistic efficacy. Comparison of the results in both Figure 4.2A and B suggests that Chr-1 does not interact with the AhR as it neither activates nor inhibits it.

From the luciferase assays, two compounds were selected for further analysis by qRT-PCR to provide a quantitative measure of agonism and antagonism. Chr-13 was shown to be a strong agonist (compared to the other Chr compounds) in mouse H1L6.1c2 cells but a strong antagonist in human HG2L6.1c3 cells, indicating a significant species difference. The second compound selected was Chr-19 which was shown to be a weak agonist in both mouse and human cell lines, but more interestingly was also shown to be an antagonist in the human cell line, thus demonstrating that this compound is a partial agonist in human.

4.4.2.2 Structure activity relationship of Chr compounds

The ability of the compounds to competitively affect the activity of TCDD allowed measurement of the shift in potency of TCDD and hence measurement of their antagonistic effect. The luciferase screening data for Chr-13 matched well with the results obtained through qRT-PCR, however for Chr-19, although qualitatively the same result was obtained there were some discrepancies. The results obtained in the screening data (Figure 4.2) showed that a 10 µM concentration of Chr-19 reduced the response to 10 nM TCDD in human cells by 80% of the maximal response (a 5-fold reduction) whereas when qRT-PCR was used, 10 µM Chr-19 only reduced the response to 10 nM TCDD by 10% (Figure 3.24D). One possibility that could explain these divergent results is that there exist inter-tissue differences in the cell lines that modulate the overall AhR-mediated response for this particular compound, although this remains to be determined. Zhang *et al.* (2003) previously examined AhR activation by a variety of agonists in both HepG2 and MCF-7 cells and while most compounds showed a similar pattern of induction, they also identified several

compounds which exhibited differences in potency between the two cell lines and this must

relate to cell specific differences as the AhR was identical.
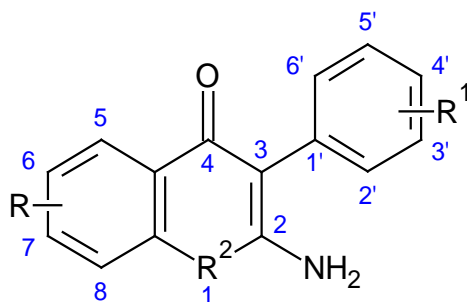
Compound Chr-	R	R^1	R^2
1	H	H	O
2	6-Cl	H	O
3	7-Cl	H	O
4	H	4'-Cl	O
5	6-Cl	4'-Cl	O
6	7-Cl	4'-Cl	O
7	H	4'-OMe	O
8	6-Cl	4'-OMe	O
9	7-Cl	4'-OMe	O
10	H	3',4'-(OMe)$_2$	O
11	6-Cl	3',4'-(OMe)$_2$	O
13	7-OMe	4'-Cl	O
14	7-OMe	3',4'-(OMe)$_2$	O
15	7-Cl	H	NH
16	6-Cl	H	NH
17	7-OMe	H	O
18	7-OMe	4'-OMe	O
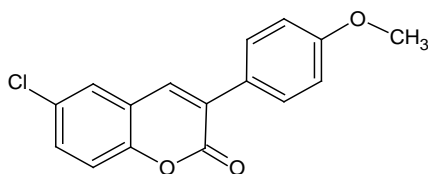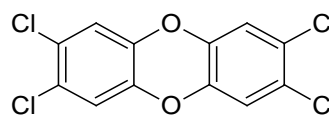
Chr-19   TCDD

Table 4.5: Structures of the 2-amino-isoflavones (2-amino-3-phenylchromen-4-one; Chr) compounds - The structures

were drawn using ChemSketch. Table was taken from Wall *et al.* (2012b).

A basic analysis of the structure-activity relationships, based mainly on the screening data, was conducted. Firstly, Chr-2 and 3 were shown to be human AhR antagonists however, if the ether oxygen (position 1; Table 4.5) was substituted with a secondary amine, such as in Chr-15 and 16, the compounds become agonists in human cells instead. Furthermore, the position of the chlorine atom on these molecules (position 6 or 7) had no effect on the agonistic or antagonist activity of the compounds. This is shown by compounds Chr-5, 8 and 16 which have a chlorine atom on position 7, and Chr-6, 9 and 15 which have a chlorine atom on position 6, yet there is no difference in the ability of these compounds to activate or inhibit the AhR (results were the same for all six compounds).

The data also suggests that a chlorine atom is required somewhere on the molecule (Chr-1 has no effects), although based on the number of compounds tested, the precise location (position 3, 4 or 4') does not seem to affect the compound's properties. The slightly reduced ability of Chr-4 as an antagonist may suggest that there needs to be a chlorine atom on position 6 or 7 in order for it to antagonise completely the AhR at a concentration of 10 µM. The chlorine atoms would provide a high electron density which has been shown to be important for high affinity in similar compounds (Henry *et al.,* 1999).

Chr-13 and 19 are relatively unique in this group of compounds making it difficult to assess what contributes to their species-specific differences in effect. A methoxy group on position 7 is the most likely explanation for why Chr-13 and 17 are agonists in mouse but antagonists in human. Furthermore as discussed earlier the chlorine on position 4' appears to have no effect on AhR binding or activation. The unusual partial agonistic properties of Chr-19 are likely related to the substitution of the amino group on position 2 with a carbonyl group and the removal of the carbonyl group from position 4. If there is a methoxy group on position 3' it appears that the compound will simply not interact significantly with the AhR, as seen in

Chr-10, 11 and 14. Using alpha-naphthoflavone as the backbone structure, Gasiewicz *et al.* (1996) and Henry *et al.* (1999) investigated the effect of chemical substituents on AhR activity. They showed that a methoxy group in the 3' position not only increased affinity for receptor binding (Gasiewicz *et al.,* 1996; Henry *et al.,* 1999), but was very important for antagonist activity (Henry *et al.,* 1999; Lu *et al.,* 1996). The reason for the lack of effect of Chr-1 is unclear as Chr-4 and 7 have antagonistic properties and also have no atom or group on the first benzene ring. Based on the potency of Chr-18 and 19, it would be interesting to test other classes of compounds with similar (AhR binding) structures for instance, chromones and coumarins (such as warfarin).

In terms of AhR agonism, the most potent of the compounds (Chr-13 and 15) were still 10,000-fold less potent than TCDD at activating the AhR and inducing CYP1A1 mRNA. Their agonistic and antagonistic ability suggests they have similar potency to the mono-*ortho*-chlorinated polychlorinated biphenyls (PCBs) such as PCB 105 and PCB 118 (Table 3.3). Isoflavones have been shown to have EC_{50} values in the 10 µM range (Amakura *et al.,* 2003), although more potent isoflavones have been identified. Biochanin A, for example, has a similar structure to Chr-7, but with hydroxyl groups on positions 5 and 7, and it was shown to be only 100-fold less potent than TCDD (Medjakovic and Jungbauer, 2008). Daidzein, an isoflavone which is similar in structure to Chr-18 but with hydroxyl groups on positions 7 and 4' instead of methoxy groups, was shown to be a weak agonist in mouse Hepa1 cells at similar concentrations as Chr-18 (Zhang *et al.,* 2003). Furthermore Zhang *et al.* (2003) also showed that daidzein had no AhR agonistic activity in human MCF-7 or HepG2 cells, similar to Chr-18. Several compounds with flavone and isoflavone structures were tested in human MCF-7 and mouse Hepa1 cells with most of the compounds having no or very limited AhR activity. Similarly, Zhang *et al.* (2003) reported species-specific differences by several flavonoid compounds relative to AhR agonist and antagonist activity.

Quercetin and kaempferol (both flavonols) are the most abundant flavonoids found in the diet and based on EROD analysis, Ciolino *et al.* (1999) reported that quercetin was an AhR agonist and that kaempferol was an antagonist in MCF-7 cells. Several other flavonoid derivatives have also been identified as AhR ligands including galangin, which was shown to act as an AhR antagonist (Ciolino and Yeh, 1999b) and chrysin, shown to be one of the strongest flavonoid agonists. While chrysin is a partial agonist in human cells it produces no antagonistic effects in rat H4IIE cells demonstrating that many compounds based on the flavonoid structure have species-specific differences (Van der Heiden *et al.,* 2007).

4.4.3   Brominated and mixed halogenated dioxin-like HAHs

The addition of bromine had different effects on each of the three groups of compounds (PXDDs, PXDFs and PXBs). A bromine substitution on the dibenzo-*p*-dioxin backbone reduced the potency of the compounds, compared to the compound with Cl at the same position(s), with the exception of 2-B-3,7,8-TriCDD, which may be due to the increase in the size of the molecule. As previously discussed in section 1.2.2, the dibenzo-*p*-dioxin backbone appears to already be the perfect size for high potency compared with dibenzofurans and biphenyls, where an increase in size (substituents i.e. addition of Cl) is required to get ~equivalent potency. Figure 4.3A and B compare the structures of TCDD and 2-B-3,7,8-TriCDD. The bromine atom makes the compound slightly larger and was shown to improve its ability to activate the AhR presumably by having a higher affinity. The substitution of bromine on the dibenzofuran backbone actually increased the potency of the mixed halogenated compounds. One suggestion for this would be that the dibenzofuran backbone is slightly smaller than the dibenzo-*p*-dioxin backbone as it only has one oxygen atom. Increasing the size of the molecule slightly by substituting a chlorine atom for bromine appears to provide a better fit for the AhR ligand binding domain.
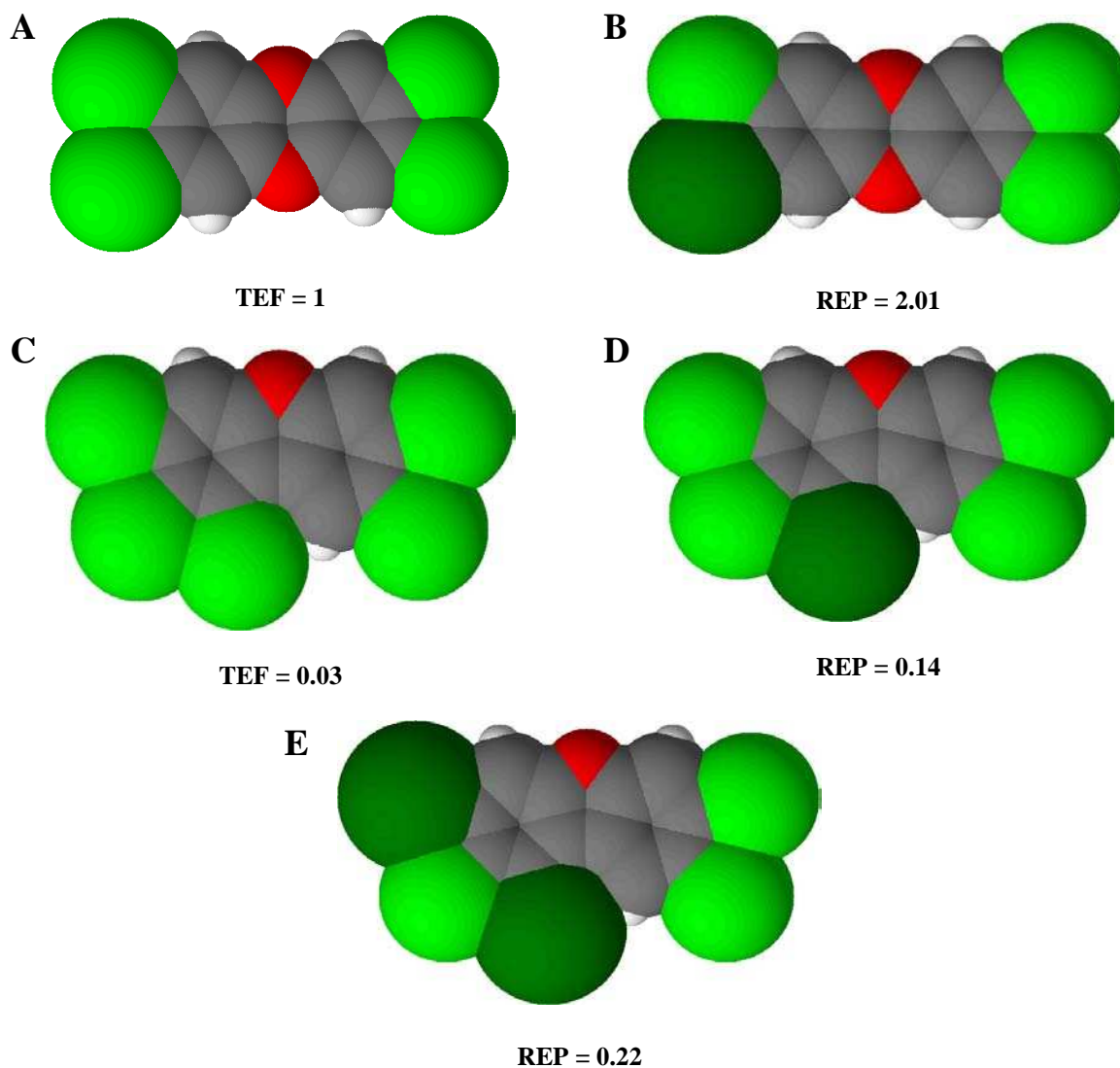
Figure 4.3: The space fill structure of 2,3,7,8-substituted dibenzo-*p*-dioxins and 1,2,3,7,8-substituted dibenzofurans - A) TCDD, B) 2-B-3,7,8-TriCDD, C) 1,2,3,7,8-PeCDF D) 1-B-2,3,7,8-TetraCDF and E) 1,3-DiB-2,7,8-TriCDF. TEFs were taken from Van den Berg *et al.* (2006) and REPs were calculated in this study.

Figure 4.3C, D and E shows the structures of 1,2,3,7,8-substituted dibenzofurans (see also section 1.3.2). Based on the TEF of 1-B-2,3,7,8-TetraCDF (0.03; Van den Berg *et al.,* 2006), 1,2,3,7,8-PeCDF was found to be 3-fold more potent and 1,3-B-2,7,8-TriCDF was found to be 10-fold more potent. Therefore the potency of the compounds employs the following order: 1,2,3,7,8-PeCDF<1-B-2,3,7,8-TetraCDF<1,3-DiB-2,7,8-TriCDF. The substitution of a bromine at position 1 (Table 3.2) increases the potency of the dibenzofuran by 3-fold then a bromine substitution at position 3 increases the potency by a further 3-fold. Further work

would investigate 3-B-1,2,7,8-TetraCDF to see if a single substitution at position 2 or 3 also increases the potency of the compound (by increasing the longitudinal size of the compound). This also appears to be the same for the mixed halogenated PXB 126 congeners, with the bromine making the molecule bigger and thus potentially a better fit for the AhR binding domain. Risk assessment calculation of PBB 126 uses the TEF for PCB 126 however PBB 126 was found to be 3-fold less potent than PCB 126 suggesting a reduced TEF for the compound. The mono-*ortho*-substituted PXBs were generally more potent than their chlorinated congeners showing that the increased size of the compound allows it to bind more effectively to the AhR binding site. PXB 105 was 10-fold and PXB 118 was 100-fold more potent than their purely chlorinated congeners showing than an increase in the size of the compound increases the potency. There are many more mixed halogenated compounds which may also be of similar abundance and potency as their chlorinated counterparts. The main issue there would be what to include and not include in the TEQ calculation. The use of the chlorinated TEFs for the mixed halogenated compounds tested in this work would not be appropriate as in a lot of cases the TEF was 10-fold different from the REP calculated experimentally. Therefore a new range of TEFs are required for these compounds. Further to this it would be interesting to do affinity measurements for all of the mixed halogenated compounds to explore any patterns between the different congeners.

4.4.4 Antagonistic effects of mono-*ortho-substituted* PCBs and PXBs

4.4.4.1 *Structure of partial agonists*

Several mono-*ortho*-substituted PCBs and PXBs were tested in rat and human cell lines and showed that all six of the compounds investigated were partial agonists in rat H4IIE cells with the exception of PCB 156 which was shown to be a pure agonist. There were significant discrepancies between the REPs calculated for PCB 105, PCB 118 and PCB 156 in this paper and those calculated by the WHO consortium. This work suggests that PCB 105 and PCB

118 were 10-fold less potent than previously estimated whereas PCB 156 was 10-fold more potent. In human MCF-7 cells, PCB 118 and PCB 156 were shown to be partial agonists whereas PCB 105 was shown to be a relatively potent antagonist when treated simultaneously with TCDD (although higher concentrations of PCB 105 may have elicited an agonist response in human if tested). A concentration of 3 µM PCB 105 in rat and 10 µM PCB 105 in human reduced the potency of TCDD by 30-fold. Further to this, a concentration of 3 µM PCB 118 in rat and 10 µM PCB 118 in human reduced the potency of TCDD by 10-25-fold. This suggests that the potency of a mixture containing these compounds could be reduced due to competition for binding to the AhR. However binding data and the K_d for these compounds is required to fully characterise their antagonistic properties. Chu *et al.* (2001) assayed TCDD in the presence of a mixture of 13 different PCBs including PCB 118, 156, 105 and 126, which has since been shown by other authors (Chen and Bunce, 2004; Clemons *et al.,* 1998; Suh *et al.,* 2003; Hestermann *et al.,* 2000) to be a mixture of agonists, putative partial agonists and antagonists. They found that when assaying TCDD in the presence of a low concentration of this mixture, the mixture has partial agonistic properties although the data is not conclusive (Chu *et al.,* 2001).

Substitution of one of the chlorine atoms for bromine (either *meta-* or *para-*substituted) increased the length of the compound, which appears to have a significantly large effect on the potency of the compound to activate the AhR (in rat H4IIE cells). This effect was seen for PXB 105/PCB 105 however this substitution appears to have less impact on PXB 156/PCB 156. PCB 156 was shown to have very weak antagonistic properties in human and thus would have a very limited effect on the TEQ. All of the mono-*ortho*-substituted PXBs were shown to be partial antagonists in rat H4IIE cells. A concentration of 1 µM PXB 105 was shown to reduce the potency of TCDD by 200-fold showing that the compound is a more potent antagonist than PCB 105 as a lower concentration had a larger antagonistic effect. A

concentration of 300 nM PXB 118 was shown to reduce the potency of TCDD by 6-fold making it equivalent to PCB 118 in terms of antagonistic potential. PXB 156 was shown to have potent antagonistic properties as a concentration of 100 nM PXB 156 reduced the potency of TCDD by 90-fold showing that the substitution of chlorine for a bromine atom (on position 4') had no effect on the agonistic properties of the compound but had significant effect on the antagonistic potential.

A   **B**

TEF = 0.00003   **REP = 0.00001**
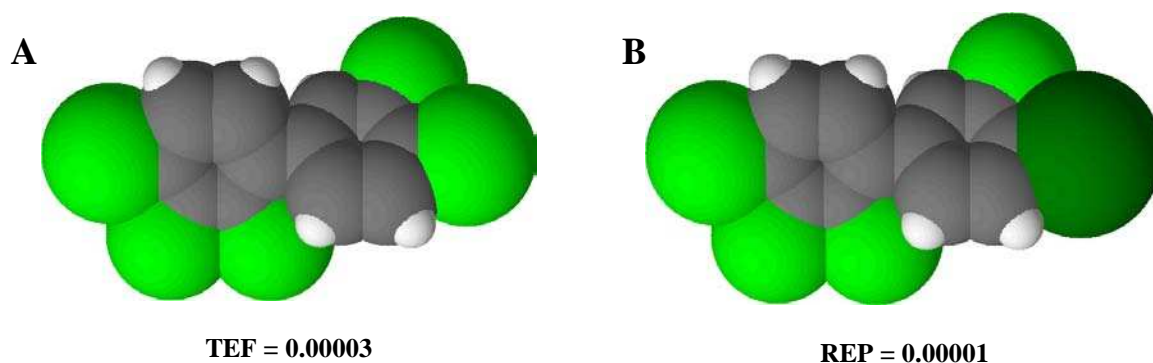
Figure 4.4: The space fill structures of two mono-*ortho-substituted* PXBs - A) PCB 105 and B) PXB 105. The TEF was taken from Van den Berg *et al.* (2006) and the REP was calculated in this study.

Figure 4.4 shows the structures of PCB 105 and PXB 105. Papers that investigate the structure activity relationships of PCBs generally use the same bond lengths for all of the compounds thus removing it as a potential explanation for the partial agonistic properties (Andersson *et al.,* 1997) therefore the only remaining variable is the energy required to rotate between the C-C (between benzene rings). Andersson *et al.* (1997) predicted the internal barrier of rotation (E_{rot}) for all of the PCBs including the ones used in this study. The results showed that only a low E_{rot} was required for the non-*ortho*-substituted PCBs obviously due to the lack of chlorine atoms in the *ortho* positions. On the other hand the mono-*ortho*-substituted PCBs required nearly 3-times as much E_{rot} to rotate in the same way due to the effect of the *ortho* substituted chlorines. This extra energy required to rotate may mean that the molecule is not planar in its most relaxed state but is rather twisted as shown in Figure 4.4. The effect of this twisting of the C-C (between benzene rings) appears be the reason that

these compounds have partial agonistic properties. To fully characterise the mono-*ortho*-substituted PCBs, several different antagonising concentrations of the compounds would be required to do a schild analysis to calculate their K_d.

4.4.4.2 Effect of partial agonists on the TEQ

The TEQ system assumes that all of the compounds undergo additivity whereby all of the TEFs can be added together based on the exposure and potency of that particular compound. However the method does not take into consideration the antagonistic effects of these compounds which may actually reduce the potency of other pure agonists as shown in the antagonism studies in this project (Figure 3.17; Brown *et al.,* 1994; Safe, 1994; Toyoshiba *et al.,* 2004; Walker *et al.,* 2005). As discussed in section 1.4.2.3, several authors recommend adjusted methods which take into consideration these partial agonistic (antagonistic) properties (Howard and Webster, 2009; Howard *et al.,* 2010; Pohjanvirta *et al.,* 1995; Toyoshiba *et al.,* 2004; Walker *et al.,* 2005).

4.5 Species differences

4.5.1 Comparing rat and human AhR

The potency of a variety of AhR agonists was measured in rat and human cells to compare their potency across species. A general finding from this work and from previous literature (Budinsky *et al.,* 2010; Xu *et al.,* 2000) is that these compounds are approximately 10-fold less potent in human cells compared with in rat cells. Figure 4.5 shows the direct comparison of the EC_{50}s calculated in rat and human. TCDD, 2-B-3,7,8-TriCDD and PCB 126 were all found to be ~10-fold more potent in rat than in human however PXB 126B was only ~7-fold more potent in rat, producing a high REP in human cells. The differing potencies are most likely associated with subtle differences in ligand binding domain of the two AhRs (Denison *et al.,* 2002). Comparison of the amino acid composition of the whole AhR amino acid

sequence show some significant differences between the two proteins however it also shows only minor differences in the structure of the ligand binding domains which is not surprising considering the receptors are exposed to the same xenobiotics. A direct comparison of the amino acids making up the ligand binding domains of several species including rat and human has been published previously (Figure 1.3; Burbach *et al.,* 1992; Crews *et al.,* 1988; Hahn *et al.,* 1997). One of the aims of this study was to understand the differences in AhR ligand potency between rat and human. This was investigated by attempting to directly compare between the two AhR proteins as these differences may be due to a variety of reasons such as AhR affinity or be dictated by chaperone proteins.
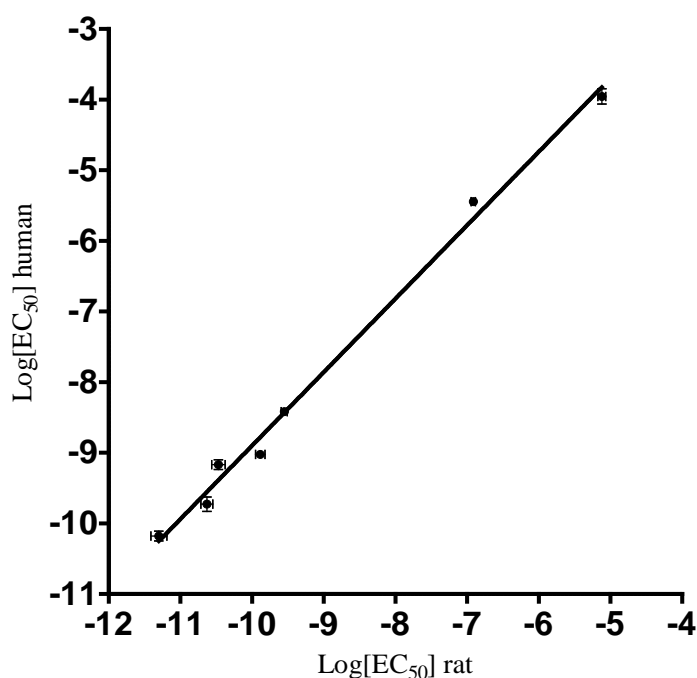
Figure 4.5: Comparison of a variety of AhR agonists in rat and human – Rat and human cells were treated with various concentrations of a variety of compounds to calculate their $EC_{50}s$. The $EC_{50}s$ were then compared. The slope = 1.04 and the $r^2 = 0.993$. Points are the $EC_{50}s \pm$ Standard error. The compounds (left to right) are Chr-19, PCB 156, PCB 126, PCB 126B, TCDD, 2-B-,3,7,8-TriCDD and AZ1.

Figure 4.5 shows that the human EC_{50} was on average 15-fold (7.2-fold – 29.4-fold) more potent than rat for all the compounds shown (based on the equation). The slope was 1.04 and

the r^2 was 0.993 showing that all the compounds shown conform to this conclusion. Even comparing a variety of different compounds, with varying magnitudes of EC_{50}, shows there is a relationship between the potency of the compounds at rat and human AhR.

It is very difficult to compare levels of proteins between rat and human because they may not have same levels of normalisation genes. The levels of CYP1A1 or CYP1A2, which bind to dioxin-like compounds, may have an impact on the overall potency of these compounds in different species. Accurate comparison of these proteins between species may identify a contributing factor of species differences. One possible way of identifying these differences is by measuring the mRNA of these proteins against a large number of normalisation genes as it is difficult even to compare intra-species/inter-tissue levels of normalisation genes as the mRNA/genomic DNA levels can be different.

4.5.2 Expression of AhR in mouse BpRc1 cells

4.5.2.1 Construction of BpRc1 cells

One of the aims of this project was to investigate the species differences of the mechanism of AhR activation between rat and human cell lines. In order to directly compare between the AhR proteins of rat and human it was necessary to measure them without the effects of the different (rat or human) mechanisms of action. For an accurate comparison of the two proteins they would need to be measured with the same back ground mechanism of action to allow direct comparison. There were no issues related to the production of the AhR containing pRevTRE vectors however transfection of the genes into the PT67 cells and infection of the virus into BpRc1 cells gave considerable problems and required several attempts over many months (resulting in only transient expression of AhR in cells). The main issue was that although colonies were selected after antibiotic treatment, the colonies turned out not to contain the vector of interest. This may be due to the vector not fully integrating

into the genomic DNA or simply that the antibiotic was not at a high enough concentration to kill all of the cells which did not contain the vector (resistance gene).

Another consideration was that the His-tag could have been left on as an additional measure of gene translation. There are antibodies available for AhR but they are not specific enough to distinguish between the different species. A His-tag antibody was available and could have been used to identify the infected AhR using western blotting. Alternatively a GFP tag could have been used but this is quite large and may have interfered with the protein folding of the AhR. The 7500fast software uses a threshold to calculate the C_t to compare between samples. The mRNA comparison in Figure 3.36E assumes that the primers and probes for the three AhR genes work at 100% efficiency. The threshold was then set to the same level for all three genes (mouse, rat and human AhR).

4.5.2.2 Comparison of controls for the infected BpRc1 cells

Both Clemons *et al.* (1998) and De Hann *et al.* (1996) calculated an EC_{50} of 140 pM $\pm$ 130 for Hepa1c1c7 cells treated with TCDD. Miller *et al.* (1983), who created the BpRc1 cell line, found that the basal and induced levels of CYP1A1 (AHH) were 10% and 20%, respectively, when treating the cells with 1 nM TCDD for 24 hours. In this study an EC_{50} of 1.65 nM (95% CI = 1.12 nM – 2.44 nM) was calculated which was approximately 10-fold more than literature values in wild-type Hepa1c1c7 cells. 5F 203 was previously measured in rat H4IIE cells by Bazzi *et al.* (2009) who calculated an EC_{50} of 3 µM (95% CI = 1.3 µM – 7.7 µM) in rat H4IIE cells, which was significantly higher than the value calculated in this study (wild-type rat H4IIE cells; 675 nM; 95% CI = 524 nM – 869 nM), and 2 nM (95% CI = 0.9 nM - 5 nM) in human MCF-7 cells which was just higher than the value calculated in this study (wild-type human MCF-7 cells; 1.18 nM; 95% CI = 818 pM – 1.72 nM). The more interesting conclusion of this comparison of 5F 203 between rat and human is that the compound is a relatively weak agonist in rat H4IIE cells but very potent in human MCF-7

cells (almost equal to TCDD). This shows that this compound is a very useful tool when investigating AhR differences between rat and human.

4.5.2.3 BpRc1 rAhR

BpRc1 wild-type cells were infected with a vector containing the rat AhR gene. Although initial infection to produce a double stable cell line was unsuccessful, it was possible to infect cells for use in producing a cell line that transiently expressed rat AhR. Figure 3.34 and Figure 3.35A show that the pRevTRE vector, along with the rat AhR gene, was successfully infected into the cell nucleus. A separate experiment was conducted to show that the rat AhR gene was transcribed. Figure 3.36 shows that there are low levels of rat AhR mRNA, but 4-fold less than the mouse AhR mRNA, which itself was at very low levels compared to wild-type mouse AhR mRNA from Hepa1c1c7 cells. The BpRc1 rAhR cells treated with TCDD did not produce a statistically different EC_{50} from the wild-type BpRc1 cell line. However BpRc1 rAhR cells treated with 5F 203 did produce a response which was not seen in the wild-type cells. This would be substantial proof (three biological replicates with 10 nM TCDD) that the experiment has worked but that the expression of rat AhR was only very low compared with rat H4IIE wild-type cells. Confirmatory *AhR* protein evidence would be needed to substantiate this.

4.5.2.4 BpRc1 hAhR

BpRc1 cells were also infected with pRevTRE containing the human AhR. As with rat, creation of a stably expressing cell line failed but it was possible to infect the cells to produce a cell line that transiently expressed human AhR. Figure 3.34 and Figure 3.35B show that the pRevTRE vector, along with the human AhR gene, was successfully infected into the cell nucleus. To confirm that the human AhR gene was transcribed by the pRevTet-Off vector, measurement of CYP1A1 mRNA was conducted using qRT-PCR (Figure 3.36). The

experiment shows that human AhR was transcribed but only at very low levels (~1%) compared with mouse AhR (which was also at very low levels) and human AhR mRNA from MCF-7 wild-type cells. The BpRc1 hAhR cells were treated with TCDD and 5F 203 but the EC_{50} values for TCDD were the same as for BpRc1 wild-type cells (5F 203 gave no response in either cell line) which shows that the levels of human AhR were not sufficient to have an effect or is non-responsive under these conditions.

4.5.3   Comparison of AhR-related proteins

Although the most likely reason for the experiment not working was that there was not enough rat or human AhR expression in the cell lines, the ability of the mouse chaperone proteins to interact with the rat or human AhR may also have had an impact in the ability of the exogenous AhR to interact with the host mechanism. The similarities of the AhR and Arnt as well as the three chaperone proteins; Hsp90, p23 and XAP2 were compared between rat, human and mouse to see how closely related the proteins were. Table 4.6 shows the similarities between the three species. The values are only estimates based on a direct alignment of the three amino acid sequences.

	AhR	LBD	Arnt	Hsp90	p23	XAP2
Human vs. Mouse	68.7%	86.7%	91.7%	98.8%	98.7%	94.2%
Rat vs. Mouse	86.1%	97.0%	94.1%	99.6%	100%	97.0%
Rat vs. Human	71.2%	85.5%	90.0%	98.9%	98.7%	94.0%

Table 4.6: Amino acid comparison – Comparison of similarities between proteins associated with the AhR activating mechanism based on direct comparison of their amino acid sequences. Gene Ids are shown in Table 2.2. LBD: AhR ligand binding domain, estimated from mouse AhR LBD (Fukunaga *et al.,* 1995).

The similarities between the full AhR amino acid sequences of rat and human were compared against mouse. Human and mouse had only a 68.7% idenity compared with rat and mouse which had an 86.1% identity. Comparison of the mouse LBD with the two other species

showed an even higher homology with 86.7% and 97.0%, for human and rat, respectively. However another important issue was the similarity between the chaperone proteins of rat and human compared with mouse. The Arnt proteins were relatively similar between all three species (90.0 - 94.1% similarity) as were the XAP2 proteins which had a very close homology between all the species (94.0 - 97.0% similarity). Hsp90 was highly conserved between all three species (>98.8%). p23 was also highly conserved between the three species. Rat and mouse shared a 100% similarity compared with human and mouse which had 98.7% similarity. Several researchers have shown the importance of p23 for enhancing the AhR complex (Cox *et al.,* 2004; Kazlauskas *et al.,* 2001; Shetty *et al.,* 2002) however more recent research from Flaveny *et al.* (2009) used p23 null models to show that p23 was not crucial for ligand binding or AhR-related gene expression. It was therefore concluded that none of these chaperone proteins would have an unusually higher effect on the BpRc1 hAhR cell line compared with the rat version. Based on this comparison, the most likely explanation for the failure of this experiment was the lack of DNA successfully transfected into the cell resulting in low human AhR expression. In order to compare the AhRs between rat and human, a new method of comparison is required. The host cell line needs to be AhR null not just AhR deficient to remove background interference.

4.5.4 Alternative method of comparing AhR

Unfortunately the stable infection of BpRc1 cells was unsuccessful, most likely due to the low viral concentrations used in the experiment. Also an issue may be that the gene did not integrate properly with the nucleic DNA. An alternative method could have produced an AhR knockout or even better a gene exchange (Doetschman *et al.,* 1987; Tarutani *et al.,* 1997; Uren *et al.,* 2000; Weiss and Green, 1967). A full knock-out would remove the background levels of AhR activation to allow a higher signal to noise ratio. A gene exchange (knock-out) could be produced by using recombination which would exchange the mouse AhR gene with

an antibiotic resistance gene along with either the rat or human AhR. Recombination would need to occur on both chromosomes to produce a gene exchange.
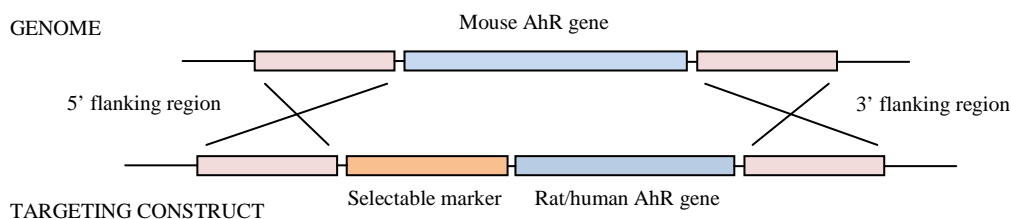
Figure 4.6: Basic example of recombination – gene of interest is cloned into a vector containing the 5' and 3' flanking regions of the gene to be replaced. The vector also contains a selectable marker. Recombination takes place and the gene of interest is integrated into the genome of the mouse cell line and is then selected producing a pure stock.

This would have used a similar method to the one used in this project. Selection would have left mouse cell lines with no mouse AhR, replaced instead with rat or human AhR. There are AhR null mice available (Fernandez-Salguero *et al.,* 1995, 1996; Gonzalez *et al.,* 1995; Lahvis and Bradfield, 1998; Vasquez *et al.,* 2003) so a primary culture could have been conducted as a replacement for the AhR-deficient Tao BpRc1 cell line.

5. Conclusion

A method of quantifying the agonistic and antagonistic properties of various AhR ligands was optimised and applied to a family of potent AhR agonists (AZFMHCs) and a known antagonist, CH223191. This study identified the highest known affinity, high potency ligand of the AhR, AZ1. The compound has been shown to be 5-10-fold more potent than TCDD at inducing CYP1A1 in two species and over several AhR-mediated genes. AZ1 is a synthetic AhR agonist and thus is not of environmental concern (although there is the possibility of occupational exposure; Mackenzie and Brooks, 1998) however it could be a very useful compound to help advance our understanding of the mechanism of AhR activation and provide further insight into the structure-activity relationships. This study also successfully

used Schild regression to characterise the AhR antagonist, CH223191 showing that it is a potent AhR antagonist.

The structure-activity relationships of several families of compounds were investigated to improve our understanding of the requirements for binding and of an AhR ligand to be an agonist or antagonist. Many of the novel 2-amino-isoflavones described in this study were not only active ligands (agonists/antagonists) of the AhR, but they also produce unusual species differences in response. These analyses have shown that even the slightest substitutions in chemical structure can significantly alter not only the potency of the compound but also its antagonistic potential. Both Chr-13 and Chr-19 could be useful tools when investigating the mechanism responsible for ligand-dependent species differences in the activation of the AhR. Perhaps more relevant to risk assessment, the PXDDs investigated in this study were found to have a lower potency than their fully chlorinated congeners whereas the PXDFs and PXBs tested were shown to be of higher potency. Several compounds of notable interest were identified such as 2-B-3,7,8-TriCDD which was found to be 2-fold more potent than TCDD at activating rat and human AhR. 2-B-1,3,7,8-TetraCDD and 2,3-DiB-7,8-DiCDF were also found to be under 2-fold less potent than TCDD demonstrating the potential impact these compounds could have on the total toxicity of a mixture.

This data can now be used for the next generation of TEQ measurement and estimation although further work will be required to decide which compounds should be included in the TEQ as there are several thousand congeners of dioxin-like compounds when including the various mixed halogenated compounds. The potency data, together with occurrence data, should help inform regulators which compounds should be measured in environmental and food samples for purposes of risk assessment which should result in better estimate of our

overall exposure to AhR agonists. With regards to the current WHO TEFs, this study has shown that PCB 105 and PCB 118 are essentially antagonists at all but the highest of concentrations and therefore suggests their TEFs should be decreased. Consideration should be taken regarding the antagonistic properties of the PCBs and PXBs in relation to their ability to reduce the potency of other more potent AhR agonists. The TEF of PCB 156 should be increased to take account of the increased potency (based on previous literature) but care must be taken to measure for any contamination in the stocks of these compounds which may impact the overall potency, before including them in the TEF meta-analysis.

In terms of species differences between rat and human, an estimated 15-fold reduction in the potency of these compounds to activate human AhR was observed in all of the compounds tested in this study. Unfortunately attempts to directly compare between the two AhRs did not fully succeed but the study did demonstrate the potential of the virus-based experiment to work, if the levels of infected exogenous AhR are high enough to have an impact on the cellular response. The study also identified a more promising alternative method which should eliminate the background mouse AhR response allowing a more accurate comparison of the infected AhRs. During this study, 5F 203, was once again shown to be significantly more potent in human (equal to TCDD) than in rat highlighting its usefulness in species comparison.

In conclusion, the data derived in this study will help to improve our overall understanding of the mechanism of AhR activation by environmental pollutants and allow more focused risk assessment on these compounds.

References

Aarts, J.M., Denison, M.S., Cox, M.A., Schalk, M.A., Garrison, P.M., Tullis, K., de Haan, L.H. and Brouwer, A. (1995) Species-specific antagonism of Ah receptor action by 2,2',5,5'-tetrachloro- and 2,2',3,3'4,4'-hexachlorobiphenyl. Eur J Pharmacol 293, 463-474.

Aarts, J.M.M.J.G., Jonas, A., van den Dikkenberg, L.C. and Brouwer, A. (1998) CAFLUX, a simplified version of the CALUX assay for Ah receptor (ant)agonist, based on enhanced green fluorescent protein (EGFP) reporter gene expression. Organohalogen Compd 37, 85-88.

Abbott, P.A., Bonnert, R.V., Caffrey, M.V., Cage, P.A., Cooke, A.J., Donald, D.K., Furber, M., Hill, S. and Withnall, J. (2002) Fused mesoionic heterocycles: synthesis of [1,2,3]triazolo[1,5-a]quinoline, [1,2,3]triazolo[1,5-a]quinazoline, [1,2,3]triazolo[1,5-a]quinoxaline and [1,2,3]triazolo[5,1-c]benzotriazine derivatives. Tetrahedron 58, 3185-3198.

Adachi, J., Mori, Y., Matsui, S., Takigami, H., Fujino, J., Kitagawa, H., Miller, C.A., 3rd, Kato, T., Saeki, K. and Matsuda, T. (2001) Indirubin and indigo are potent aryl hydrocarbon receptor ligands present in human urine. J Biol Chem 276, 31475-31478.

Ahlborg, U.G., Becking, G.C., Birnbaum, L.S., Brouwer, A., Derks, H., Feeley, M., Golor, G., Hanberg, A., Larsen, J.C., Liem, A.K.D., Safe, S.H., Schlatter, C., Waern, F., Younes, M. and Yrjänheikki, E. (1994) Toxic equivalency factors for dioxin-like PCBs: Report on WHO-ECEH and IPCS consultation, December 1993. Chemosphere 28, 1049-1067.

Ahlborg, U.G., Brouwer, A., Fingerhut, M.A., Jacobson, J.L., Jacobson, S.W., Kennedy, S.W., Kettrup, A.A., Koeman, J.H., Poiger, H., Rappe, C., Safe, S.H., Seegal, R.F., Tuomisto, J. and van den Berg, M. (1992) Impact of polychlorinated dibenzo-p-dioxins, dibenzofurans, and biphenyls on human and environmental health, with special emphasis on application of the toxic equivalency factor concept. Eur J Pharmacol 228, 179-199.

Aiello, S., Wells, G., Stone, E.L., Kadri, H., Bazzi, R., Bell, D.R., Stevens, M.F.G., Matthews, C.S., Bradshaw, T.D. and Westwell, A.D. (2008) Synthesis and biological properties of benzothiazole, benzoxazole, and chromen-4-one analogues of the potent antitumor agent 2-(3,4-Dimethoxyphenyl)-5-fluorobenzothiazole (PMX 610, NSC 721648). J Med Chem 51, 5135-5139.

Amakura, Y., Tsutsumi, T., Sasaki, K., Yoshida, T. and Maitani, T. (2003) Screening of the inhibitory effect of vegetable constituents on the aryl hydrocarbon receptor-mediated activity induced by 2,3,7,8-tetrachlorodibenzo-p-dioxin. Biol Pharm Bull 26, 1754-1760.

Andersson, P.L., Haglund, P. and Tysklind, M. (1997) The internal barriers of rotation for the 209 polychlorinated biphenyls. Environ Sci Pollut Res Int 4, 75-81.

Aylward, L.L. and Hays, S.M. (2002) Temporal trends in human TCDD body burden: decreases over three decades and implications for exposure levels. J Expo Anal Environ Epidemiol 12, 319-328.

Backlund, M. and Ingelman-Sundberg, M. (2004) Different structural requirements of the ligand binding domain of the aryl hydrocarbon receptor for high- and low-affinity ligand binding and receptor activation. Mol Pharmacol 65, 416-425.

Bandiera, S., Safe, S. and Okey, A.B. (1982) Binding of polychlorinated biphenyls classified as either phenobarbitone-, 3-methylcholanthrene- or mixed-type inducers to cytosolic Ah receptor. Chem Biol Interact 39, 259-277.

Bandiera, S., Sawyer, T., Romkes, M., Zmudzka, B., Safe, L., Mason, G., Keys, B. and Safe, S. (1984) Polychlorinated dibenzofurans (PCDFs): effects of structure on binding to the 2,3,7,8-TCDD cytosolic receptor protein, AHH induction and toxicity. Toxicology 32, 131-144.

Bazzi, R. (2008) Pharmacological interactions between phenylbenzothiazoles and Aryl hydrocarbon receptor (AhR). PhD thesis, School of Biology, University of Nottingham.

Bazzi, R., Bradshaw, T.D., Rowlands, J.C., Stevens, M.F. and Bell, D.R. (2009) 2-(4-Amino-3-methylphenyl)-5-fluorobenzothiazole is a ligand and shows species-specific partial agonism of the aryl hydrocarbon receptor. Toxicol Appl Pharmacol 237, 102-110.

Behnisch, P.A., Hosoe, K., Brouwer, A. and Sakai, S. (2002) Screening of dioxin-like toxicity equivalents for various matrices with wildtype and recombinant rat hepatoma H4IIE cells. Toxicol Sci 69, 125-130.

Behnisch, P.A., Hosoe, K. and Sakai, S.I. (2001) Bioanalytical screening methods for dioxins and dioxin-like compounds: A review of bioassay/biomarker technology. Environ. Int. 27, 413-439.

Behnisch, P.A., Hosoe, K. and Sakai, S. (2003) Brominated dioxin-like compounds: *in vitro* assessment in comparison to classical dioxin-like compounds and other polyaromatic compounds. Environ Int 29, 861-877.

Bell, D.R., Clode, S., Fan, M.Q., Fernandes, A., Foster, P.M., Jiang, T., Loizou, G., MacNicoll, A., Miller, B.G., Rose, M., Tran, L. and White, S. (2007) Relationships between tissue levels of 2,3,7,8-tetrachlorodibenzo-*p*-dioxin (TCDD), mRNAs, and toxicity in the developing male Wistar(Han) rat. Toxicol Sci 99, 591-604.

Bell, D.R. and Poland, A. (2000) Binding of aryl hydrocarbon receptor (AhR) to AhR-interacting protein. The role of Hsp90. J Biol Chem 275, 36407-36414.

Benedict, W.F., Considine, N., and Nebert, D.W. (1973) Genetic differences in aryl hydrocarbon hydroxylase induction and benzo[a]pyrene-produced tumorigenesis in the mouse. Mol Pharmacol 6, 266-277.

Benedict, W.F., Gielen, J.E., Owens, I.S., Niwa, A. and Bebert, D.W. (1973) Aryl hydrocarbon hydroxylase induction in mammalian liver cell culture. IV. Stimulation of the enzyme activity in established cell lines derived from rat or mouse hepatoma and from normal rat liver. Biochem Pharmacol 22, 2766-2769.

Bertani, G. (1951) A method for detection of mutations, using streptomycin dependence in Escherichia coli. Genetics 36, 598-611.

Bhattacharyya, K.K., Brake, P.B., Eltom, S.E., Otto, S.A. and Jefcoate, C.R. (1995) Identification of a rat adrenal cytochrome P450 active in polycyclic hydrocarbon metabolism as rat CYP1B1. Demonstration of a unique tissue-specific pattern of hormonal and aryl hydrocarbon receptor-linked regulation. J Biol Chem 270, 11595-11602.

Bisson, W.H., Koch, D.C., O'Donnell, E.F., Khalil, S.M., Kerkvliet, N.I., Tanguay, R.L., Abagyan, R. and Kolluri, S.K. (2009) Modeling of the aryl hydrocarbon receptor (AhR) ligand binding domain and its utility in virtual ligand screening to predict new AhR ligands. J Med Chem 52, 5635-5641.

Bjeldanes, L.F., Kim, J.Y., Grose, K.R., Bartholomew, J.C. and Bradfield, C.A. (1991) Aromatic hydrocarbon responsiveness-receptor agonists generated from indole-3-carbinol *in vitro* and *in vivo*: comparisons with 2,3,7,8-tetrachlorodibenzo-*p*-dioxin. Proc Natl Acad Sci USA 88, 9543-9547.

Bols, N.C., Whyte, J.J., Clemons, J.H., Tom, D.J., van den Heuvel, M. and Dixon, D.G. (1997) Use of liver cell lines to develop toxic equivalency factors and to derive toxic equivalent concentrations in environmental samples. In: J.T. Zelikoff (Ed), Ecotoxicology. SOS Publications, Fair Haven. 329–350.

Bradfield, C.A. and Poland, A. (1988) A competitive binding assay for 2,3,7,8-tetrachlorodibenzo-*p*-dioxin and related ligands of the Ah receptor. Mol Pharmacol 34, 682-688.

Brown, M.M., Schneider, U.A., Petrulis, J.R. and Bunce, N.J. (1994) Additive binding of polychlorinated biphenyls and 2,3,7,8-tetrachlorodibenzo-*p*-dioxin to the murine hepatic Ah receptor. Toxicol Appl Pharmacol 129, 243-251.

Budinsky, R.A., LeCluyse, E.L., Ferguson, S.S., Rowlands, J.C. and Simon, T. (2006) Human and rat primary hepatocyte CYP1A1 and 1A2 induction with 2,3,7,8-tetrachlorodibenzo-*p*-dioxin, 2,3,7,8-tetrachlorodibenzofuran, and 2,3,4,7,8-pentachlorodibenzofuran. Toxicol Sci 118, 224-235.

Burbach, K.M., Poland, A. and Bradfield, C.A. (1992) Cloning of the Ah-receptor cDNA reveals a distinctive ligand-activated transcription factor. Proc Natl Acad Sci USA 89, 8185-8189.

Burke, M.D. and Mayer, R.T. (1974) Ethoxyresorufin: direct fluorimetric assay of a microsomal O-dealkylation which is preferentially inducible by 3-methylcholanthrene. Drug Metab Dispos 2, 583-588.

Buters, J.T., Tang, B.K., Pineau, T., Gelboin, H.V., Kimura, S. and Gonzalez, F.J. (1996) Role of CYP1A2 in caffeine pharmacokinetics and metabolism: studies using mice deficient in CYP1A2. Pharmacogenetics 6, 291-296.

Carlstedt-Duke, J.M. (1979) Tissue distribution of the receptor for 2,3,7,8-tetrachlorodibenzo-*p*-dioxin in the rat. Cancer Res 39, 3172-3176.

Carvalhaes, G.K., Brooks, P., Marques, C.G., Azevedo, J.A.T., Machado, M.C.S. and Azevedo, G.C. (2002) Lime as the source of PCDD/F contamination in citrus pulp pellets from Brazil and status of the monitoring program. Chemosphere 46, 1413-1416.

Carver, L.A. and Bradfield, C.A. (1997) Ligand-dependent interaction of the aryl hydrocarbon receptor with a novel immunophilin homolog *in vivo*. J Biol Chem 272, 11452-11456.

Carver, L.A., Hogenesch, J.B. and Bradfield, C.A. (1994a) Tissue specific expression of the rat Ah-receptor and ARNT mRNAs. Nucleic Acids Res 22, 3038-3044.

Carver, L.A., Jackiw, V. and Bradfield, C.A. (1994b) The 90-kDa heat shock protein is essential for Ah receptor signaling in a yeast expression system. J Biol Chem 269, 30109-30112.

Casey, D., Lawless, J. and Wall, P.G. (2010) A tale of two crises: the Belgian and Irish dioxin contamination incidents. Br Food J 112, 1077-1091.

Casper, R.F., Quesne, M., Rogers, I.M., Shirota, T., Jolivet, A., Milgrom, E. and Savouret, J.F. (1999) Resveratrol has antagonist activity on the aryl hydrocarbon receptor: implications for prevention of dioxin toxicity. Mol Pharmacol 56, 784-790.

Chaty, S., Rodius, F., Lanhers, M.C., Burnel, D. and Vasseur, P. (2008) Induction of CYP1A1 in rat liver after ingestion of mussels contaminated by Erika fuel oils. Arch Toxicol 82, 75-80.

Chen, B., Zhong, D. and Monteiro, A. (2006) Comparative genomics and evolution of the HSP90 family of genes across all kingdoms of organisms. BMC Genomics 7, 156-175.

Chen, G. and Bunce, N.J. (2004) Interaction between halogenated aromatic compounds in the Ah receptor signal transduction pathway. Environ Toxicol 19, 480-489.

Chen, G., Konstantinov, A.D., Chittim, B.G., Joyce, E.M., Bols, N.C. and Bunce, N.J. (2001) Synthesis of polybrominated diphenyl ethers and their capacity to induce CYP1A by the Ah receptor mediated pathway. Environ Sci Technol 35, 3749-3756.

Chirulli, V., Marvasi, L., Zaghini, A., Fiorio, R., Longo, V. and Gervasi, P.G. (2007) Inducibility of AhR-regulated CYP genes by beta-naphthoflavone in the liver, lung, kidney and heart of the pig. Toxicology 240, 25-37.

Choi, E.Y., Lee, H., Dingle, R.W., Kim, K.B. and Swanson, H.I. (2012) Development of novel CH223191-based antagonists of the aryl hydrocarbon receptor. Mol Pharmacol 81, 3-11.

Chu, I., Lecavalier, P., Hakansson, H., Yagminas, A., Valli, V.E., Poon, P. and Feeley, M. (2001) Mixture effects of 2,3,7,8-tetrachlorodibenzo-*p*-dioxin and polychlorinated biphenyl congeners in rats. Chemosphere 43, 807-814.

Ciolino, H.P., P.J. Daschner and G.C. Yeh. (1998) Resveratrol inhibits transcription of CYP1A1 *in vitro* by preventing activation of the aryl hydrocarbon receptor. Cancer Res 58, 5707-5712.

Ciolino, H.P., Daschner, P.J. and Yeh, G.C. (1999) Dietary flavonols quercetin and kaempferol are ligands of the aryl hydrocarbon receptor that affect CYP1A1 transcription differentially. Biochem J 340(3), 715-722.

Ciolino, H.P. and Yeh, G.C. (1999a) Inhibition of aryl hydrocarbon-induced cytochrome P-450 1A1 enzyme activity and CYP1A1 expression by resveratrol. Mol Pharmacol 56, 760-767.

Ciolino, H.P. and Yeh, G.C. (1999b) The flavonoid galangin is an inhibitor of CYP1A1 activity and an agonist/antagonist of the aryl hydrocarbon receptor. Br J Cancer 79, 1340-1346.

Clemons, J.H., Dixon, D.G. and Bols, N.C. (1997) Derivation of 2,3,7,8-TCDD toxic equivalent factors (TEFs) for selected dioxins, furans and PCBs with rainbow trout and rat liver cell lines and the influence of exposure time. Chemosphere 34, 1105-1119.

Clemons, J.H., Myers, C.R., Lee, L.E.J., Dixon, D.G. and Bols, N.C. (1998) Induction of cytochrome P4501A by binary mixtures of polychlorinated biphenyls (PCBs) and 2,3,7,8-tetrachlorodibenzo-*p*-dioxin (TCDD) in liver cell lines from rat and trout. Aquat Toxicol 43, 179-194.

Colles, A., Koppen, G., Hanot, V., Nelen, V., Dewolf, M.C., Noel, E., Malisch, R., Kotz, A., Kypke, K., Biot, P., Vinkx, C. and Schoeters, G. (2008) Fourth WHO-coordinated survey of human milk for persistent organic pollutants (POPs): Belgian results. Chemosphere 73, 907-914.

Coumailleau, P., Poellinger, L., Gustafsson, J.A. and Whitelaw, M.L. (1995) Definition of a minimal domain of the dioxin receptor that is associated with Hsp90 and maintains wild type ligand binding affinity and specificity. J Biol Chem 270, 25291-25300.

Coumoul, X., Diry, M., Robillot, C. and Barouki, R. (2001) Differential regulation of cytochrome P450 1A1 and 1B1 by a combination of dioxin and pesticides in the breast tumor cell line MCF-7. Cancer Res 61, 3942-3948.

Cox, M.B. and Miller, C.A., 3rd. (2004) Cooperation of heat shock protein 90 and p23 in aryl hydrocarbon receptor signaling. Cell Stress Chaperon 9, 4-20.

Crews, S.T., Thomas, J.B. and Goodman, C.S. (1988) The Drosophila single-minded gene encodes a nuclear protein with sequence similarity to the per gene product. Cell 52, 143-151.

Darnerud, P.O., Eriksen, G.S., Jóhannesson, T., Larsen, P.B. and Viluksela, M. (2001) Polybrominated diphenyl ethers: occurrence, dietary exposure, and toxicology. Environ Health Perspect 109, 49 - 68.

De Haan, L.H.J., Halfwerk, S., Hovens, S.E.L., De Roos, B., Koeman, J.H. and Brouwer, A. (1996) Inhibition of intercellular communication and induction of ethoxyresorufin-O-deethylase activity by polychlorobiphenyls, -dibenzo-*p*-dioxins and -dibenzofurans in mouse hepa1c1c7 cells. Environ Toxicol Pharmacol 1, 27-37.

Denison, M.S., Fisher, J.M. and Whitlock, J.P., Jr. (1988) The DNA recognition site for the dioxin-Ah receptor complex. Nucleotide sequence and functional analysis. J Biol Chem 263, 17221-17224.

Denison, M.S., Pandini, A., Nagy, S.R., Baldwin, E.P. and Bonati, L. (2002) Ligand binding and activation of the Ah receptor. Chem Biol Interact 141, 3-24.

Denison, M.S. and Whitlock, J.P., Jr. (1995) Xenobiotic-inducible transcription of cytochrome P450 genes. J Biol Chem 270, 18175-18178.

Dere, E., Boverhof, D.R., Burgoon, L.D. and Zacharewski, T.R. (2006) *In vivo-in vitro* toxicogenomic comparison of TCDD-elicited gene expression in Hepa1c1c7 mouse hepatoma cells and C57BL/6 hepatic tissue. BMC Genomics 7, 80.

DeVito, M.J. (2003) The influence of chemical impurity on estimating relative potency factors for PCBs. Organohalogen Compd 65, 288-291.

DeVito, M.J. and Birnbaum, L.S. (1995) The importance of pharmacokinetics in determining the relative potency of 2,3,7,8-tetrachlorodibenzo-*p*-dioxin and 2,3,7,8-tetrachlorodibenzofuran. Fundam Appl Toxicol 24, 145-148.

Diliberto, J.J., Akubue, P.I., Luebke, R.W. and Birnbaum, L.S. (1995) Dose-response relationships of tissue distribution and induction of CYP1A1 and CYP1A2 enzymatic activities following acute exposure to 2,3,7,8-tetrachlorodibenzo-*p*-dioxin (TCDD) in mice. Toxicol Appl Pharmacol 130, 197-208.

Diliberto, J.J., Burgin, D. and Birnbaum, L.S. (1997) Role of CYP1A2 in hepatic sequestration of dioxin: studies using CYP1A2 knock-out mice. Biochem Biophys Res Commun 236, 431-433.

Dixon, B. (2009) Pork problems. Curr Biol 19, R3-4.

Doetschman, T., Gregg, R.G., Maeda, N., Hooper, M.L., Melton, D.W., Thompson, S. and Smithies, O. (1987) Targetted correction of a mutant HPRT gene in mouse embryonic stem cells. Nature 330, 576-578.

Dolwick, K.M., Schmidt, J.V., Carver, L.A., Swanson, H.I. and Bradfield, C.A. (1993) Cloning and expression of a human Ah receptor cDNA. Mol Pharmacol 44, 911-917.

Drahushuk, A.T., McGarrigle, B.P., Tai, H.L., Kitareewan, S., Goldstein, J.A. and Olson, J.R. (1996) Validation of precision-cut liver slices in dynamic organ culture as an *in vitro* model for studying CYP1A1 and CYP1A2 induction. Toxicol Appl Pharmacol 140, 393-403.

Edwards, R.J., Adams, D.A., Watts, P.S., Davies, D.S. and Boobis, A.R. (1998) Development of a comprehensive panel of antibodies against the major xenobiotic metabolising forms of cytochrome P450 in humans. Biochem Pharmacol 56, 377-387.

Ema, M., Ohe, N., Suzuki, M., Mimura, J., Sogawa, K., Ikawa, S. and Fujii-Kuriyama, Y. (1994) Dioxin binding activities of polymorphic forms of mouse and human arylhydrocarbon receptors. J Biol Chem 269, 27337-27343.

European Commission (2001) Communication from the Commission to the council, the European parliament and the economic and social committee. Community strategy for dioxins, furans and polychlorinated biphenyls. 1-31.

European Commission (2002a) Commission recommendation of 4 March 2002 on the reduction of the presence of dioxins, furans and PCBs in feedingstuffs and foodstuffs (2002/201/EC). O J European Union L67, 69-73.

European Commission (2002b) Directive 2002/32/EC of the European parliament and of the council of 7 May 2002 on undesirable substances in animal feed, 1-29.

European Commission (2011) Commission regulation (EU) No 1259/2011 of 2 December 2011 Amending Regulation (EC) No 1881/2006 as regards maximum levels for dioxins, dioxin-like PCBs and non dioxin-like PCBs in foodstuffs. O J European Union L320, 18-23.

Falandysz, J., Rose, M. and Fernandes, A.R. (2012) Mixed poly-brominated/chlorinated biphenyls (PXBs): widespread food and environmental contaminants. Environ Int 44, 118-127.

Fan, M.Q., Bell, A.R., Bell, D.R., Clode, S., Fernandes, A., Foster, P.M., Fry, J.R., Jiang, T., Loizou, G., MacNicoll, A., Miller, B.G., Rose, M., Shaikh-Omar, O., Tran, L. and White, S. (2009) Recombinant expression of aryl hydrocarbon receptor for quantitative ligand-binding analysis. Anal Biochem 384, 279-287.

Fattore, E., Trossvik, C. and Hakansson, H. (2000) Relative potency values derived from hepatic vitamin A reduction in male and female Sprague-Dawley rats following subchronic dietary exposure to individual polychlorinated dibenzo-*p*-dioxin and dibenzofuran congeners and a mixture thereof. Toxicol Appl Pharmacol 165, 184-194.

Fernandes, A., Dicks, P., Mortimer, D., Gem, M., Smith, F., Driffield, M., White, S. and Rose, M. (2008) Brominated and chlorinated dioxins, PCBs and brominated flame retardants in Scottish shellfish: methodology, occurrence and human dietary exposure. Mol Nutr Food Res 52, 238-249.

Fernandes, A.R., Rose, M., Mortimer, D., Carr, M., Panton, S. and Smith, F. (2011) Mixed brominated/chlorinated dibenzo-*p*-dioxins, dibenzofurans and biphenyls: Simultaneous congener-selective determination in food. J Chromatogr A 1218, 9279-9287.

Fernandez-Salguero, P., Pineau, T., Hilbert, D.M., McPhail, T., Lee, S.S., Kimura, S., Nebert, D.W., Rudikoff, S., Ward, J.M. and Gonzalez, F.J. (1995) Immune system impairment and hepatic fibrosis in mice lacking the dioxin-binding Ah receptor. Science 268, 722-726.

Fernandez-Salguero, P.M., Hilbert, D.M., Rudikoff, S., Ward, J.M. and Gonzalez, F.J. (1996) Aryl-hydrocarbon receptor-deficient mice are resistant to 2,3,7,8-tetrachlorodibenzo-*p*-dioxin-induced toxicity. Toxicol Appl Pharmacol 140, 173-179.

Flaveny, C., Perdew, G.H. and Miller, C.A., 3rd. (2009) The Aryl-hydrocarbon receptor does not require the p23 co-chaperone for ligand binding and target gene expression *in vivo*. Toxicol Lett 189, 57-62.

Food Standards Agency (2006a) Brominated chemicals in farmed and wild fish and shellfish and fish oil dietary supplements. Food Survey Information Sheet 04/06.

Food Standards Agency, (2006b) Committee on Toxicity of Chemicals in Food, Consumer Products and the Environment. Statement on organic chlorinated and brominated contaminants in shellfish, farmed and wild fish.

Food Standards Agency, (2006c) Brominated chemicals: UK dietary intakes, Food Surveillance Information Sheet 10/06.

Fried, K. W., Bazzi, R., Levy Lopez, W., Corsten, C., Schramm, K.W., Bell, D.R. and Rozman, K.K. (2007) Relationship between aryl hydrocarbon receptor-affinity and the induction of EROD activity by 2,3,7,8-tetrachlorinated phenothiazine and derivatives. Toxicol Appl Pharmacol 224, 147-155.

Fukunaga, B.N., Probst, M.R., Reisz-Porszasz, S. and Hankinson, O. (1995) Identification of functional domains of the aryl hydrocarbon receptor. J Biol Chem 270, 29270-29278.

Garrison, P.M., Tullis, K., Aarts, J.M., Brouwer, A., Giesy, J.P. and Denison, M.S. (1996) Species-specific recombinant cell lines as bioassay systems for the detection of 2,3,7,8-tetrachlorodibenzo-*p*-dioxin-like chemicals. Fundam Appl Toxicol 30, 194-203.

Gasiewicz, T.A., Kende, A.S., Rucci, G., Whitney, B. and Jeff Willey, J. (1996) Analysis of structural requirements for Ah receptor antagonist activity: Ellipticines, flavones, and related compounds. Biochem Pharmacol 52, 1787-1803.

Gasiewicz, T.A. and Rucci, G. (1991) Alpha-naphthoflavone acts as an antagonist of 2,3,7,8-tetrachlorodibenzo-*p*-dioxin by forming an inactive complex with the Ah receptor. Mol Pharmacol 40, 607-612.

Gonzalez, F.J. and Fernandez-Salguero, P. (1998) The Aryl hydrocarbon receptor. Drug Metab Dispos 26, 1194-1198.

Gonzalez, F.J., Fernandez-Salguero, P., Lee, S.S., Pineau, T. and Ward, J.M. (1995) Xenobiotic receptor knockout mice. Toxicol Lett 82-83, 117-121.

Gonzalez, F.J., Fernandez-Salguero, P. and Ward, J.M. (1996) The role of the aryl hydrocarbon receptor in animal development, physiological homeostasis and toxicity of TCDD. J Toxicol Sci 21, 273-277.

Gu, Y.Z., Hogenesch, J.B. and Bradfield, C.A. (2000) The PAS superfamily: sensors of environmental and developmental signals. Annu Rev Pharmacol Toxicol 40, 519-561.

Guengerich, F.P. (1991) Reactions and significance of cytochrome P-450 enzymes. J Biol Chem 266, 10019-10022.

Gupta, B.N., Vos, J.G., Moore, J.A., Zinkl, J.G. and Bullock, B.C. (1973) Pathologic effects of 2,3,7,8-tetrachlorodibenzo-*p*-dioxin in laboratory animals. Environ Health Perspect 5, 125-140.

Hahn, M.E. (1998) The aryl hydrocarbon receptor: a comparative perspective. Comp Biochem Physiol C Pharmacol Toxicol Endocrinol 121, 23-53.

Hahn, M.E., Karchner, S.I., Shapiro, M.A. and Perera, S.A. (1997) Molecular evolution of two vertebrate aryl hydrocarbon (dioxin) receptors (AHR1 and AHR2) and the PAS family. Proc Natl Acad Sci USA 94, 13743-13748.

Hamm, J.T., Chen, C.-Y. and Birnbaum, L.S. (2003) A mixture of dioxins, furans, and non-*ortho* pcbs based upon consensus toxic equivalency factors produces dioxin-like reproductive effects. Toxicol Sci 74, 182-191.

Han, D., Nagy, S.R. and Denison, M.S. (2004) Comparison of recombinant cell bioassays for the detection of Ah receptor agonists. Biofactors 20, 11-22.

Hanberg, A., Wærn, F., Asplund, L., Haglund, E. and Safe, S. (1990) Swedish dioxin survey: Determination of 2,3,7,8-TCDD toxic equivalent factors for some polychlorinated biphenyls and naphthalenes using biological tests. Chemosphere 20, 1161-1164.

Hankinson, O. (1979) Single-step selection of clones of a mouse hepatoma line deficient in aryl hydrocarbon hydroxylase. Proc Natl Acad Sci USA 76, 373-376.

Hankinson, O. (1994) The role of the aryl hydrocarbon receptor nuclear translocator protein in aryl hydrocarbon receptor action. Trends Endocrinol Metab 5, 240-244.

Hankinson, O. (1995) The aryl hydrocarbon receptor complex. Annu Rev Pharmacol Toxicol 35, 307-340.

Harper, P.A., Golas, C.L. and Okey, A.B. (1988) Characterization of the Ah receptor and aryl hydrocarbon hydroxylase induction by 2,3,7,8-tetrachlorodibenzo-*p*-dioxin and benz(a)anthracene in the human A431 squamous cell carcinoma line. Cancer Res 48, 2388-2395.

Haws, L.C., Su, S.H., Harris, M., Devito, M.J., Walker, N.J., Farland, W.H., Finley, B. and Birnbaum, L.S. (2006) Development of a refined database of mammalian relative potency estimates for dioxin-like compounds. Toxicol Sci 89, 4-30.

Head, J.A. and Kennedy, S.W. (2007) Differential expression, induction, and stability of CYP1A4 and CYP1A5 mRNA in chicken and herring gull embryo hepatocytes. Comp Biochem Physiol C Toxicol Pharmacol 145, 617-624.

Helaly, A. (2011) Expression of the Caenorhabditis elegans aryl hydrocarbon receptor ligand binding domain. PhD thesis, School of Biology, University of Nottingham, Nottingham.

Richard Wall

Hellemans, J., G. Mortier, A.D. Paepe, F. Speleman and J. Vandesompele. (2007) QbasePlus relative quantification framework and software for management and automated analysis of real-time quantitative PCR data. Genome Biology 8, 1-14.

Hemming, H., Bager, Y., Flodström, S., Nordgren, I., Kronevi, T., Ahlborg, U.G. and Wärngård, L. (1995) Liver tumour promoting activity of 3,4,5,3',4'-pentachlorobiphenyl and its interaction with 2,3,7,8-tetrachlorodibenzo-*p*-dioxin. Eur J Pharmacol 292, 241-249.

Henry, E.C., Kende, A.S., Rucci, G., Totleben, M.J., Willey, J.J., Dertinger, S.D., Pollenz, R.S., Jones, J.P. and Gasiewicz, T.A. (1999) Flavone antagonists bind competitively with 2,3,7,8-tetrachlorodibenzo-*p*-dioxin (TCDD) to the aryl hydrocarbon receptor but inhibit nuclear uptake and transformation. Mol Pharmacol 55, 716-725.

Hestermann, E.V., Stegeman, J.J. and Hahn, M.E. (2000) Relative contributions of affinity and intrinsic efficacy to aryl hydrocarbon receptor ligand potency. Toxicol Appl Pharmacol 168, 160-172.

Hilscherova, K., Kannan, K., Kang, Y.S., Holoubek, I., Machala, M., Masunaga, S., Nakanishi, J. and Giesy, J.P. (2001) Characterization of dioxin-like activity of sediments from a Czech river basin. Environ Toxicol Chem 20, 2768-2777.

Hord, N.G. and Perdew, G.H. (1994) Physicochemical and immunocytochemical analysis of the aryl hydrocarbon receptor nuclear translocator: characterization of two monoclonal antibodies to the aryl hydrocarbon receptor nuclear translocator. Mol Pharmacol 46, 618-626.

Howard, G.J., Schlezinger, J.J., Hahn, M.E. and Webster, T.F. (2010) Generalized concentration addition predicts joint effects of aryl hydrocarbon receptor agonists with partial agonists and competitive antagonists. Environ health perspect 118, 666-672.

Howard, G.J. and Webster, T.F. (2009) Generalized concentration addition: a method for examining mixtures containing partial agonists. J Theor Biol 259, 469-477.

Hu, W., Sorrentino, C., Denison, M.S., Kolaja, K. and Fielden, M.R. (2007) Induction of CYP1A1 is a nonspecific biomarker of aryl hydrocarbon receptor activation: results of large scale screening of pharmaceuticals and toxicants *in vivo* and *in vitro*. Mol Pharmacol 71, 1475-1486.

Huff, J. (1992) 2,3,7,8-TCDD: A potent and complete carcinogen in experimental animals. Chemosphere 25, 173-176.

Hutchinson, I., Chua, M.-S., Browne, H.L., Trapani, V., Bradshaw, T.D., Westwell, A.D. and Stevens, M.F.G. (2001) Antitumor benzothiazoles. 14.1 Synthesis and *in vitro* biological properties of fluorinated 2-(4-Aminophenyl)benzothiazoles. J Med Chem 44, 1446-1455.

Hutchinson, I., Jennings, S.A., Vishnuvajjala, B.R., Westwell, A.D. and Stevens, M.F.G. (2002) Antitumor Benzothiazoles. 16.1 Synthesis and Pharmaceutical Properties of Antitumor 2-(4-Aminophenyl)benzothiazole Amino Acid Prodrugs. J Med Chem 45, 744-747.

Huwe, J.K. and Larsen, G.L. (2005) Polychlorinated dioxins, furans, and biphenyls, and polybrominated diphenyl ethers in a U.S. meat market basket and estimates of dietary intake. Environ Sci Technol 39, 5606-5611.

Ikeya, K., Jaiswal, A.K., Owens, R.A., Jones, J.E., Nebert, D.W. and Kimura, S. (1989) Human CYP1A2: sequence, gene structure, comparison with the mouse and rat orthologous gene, and differences in liver 1A2 mRNA expression. Mol Endocrinol 3, 1399-1408.

Inouye, K., Shinkyo, R., Takita, T., Ohta, M. and Sakaki, T. (2002) Metabolism of polychlorinated dibenzo-p-dioxins (PCDDs) by human cytochrome P450-dependent monooxygenase systems. J Agric Food Chem 50, 5496-5502.

Iwanari, M., Nakajima, M., Kizu, R., Hayakawa, K. and Yokoi, T. (2002) Induction of CYP1A1, CYP1A2, and CYP1B1 mRNAs by nitropolycyclic aromatic hydrocarbons in various human tissue-derived cells: chemical-, cytochrome P450 isoform-, and cell-specific differences. Arch Toxicol 76, 287-298.

Jacobs, M.N., Dickins, M. and Lewis, D.F. (2003) Homology modelling of the nuclear receptors: human oestrogen receptorbeta (hERbeta), the human pregnane-X-receptor (PXR), the Ah receptor (AhR) and the constitutive androstane receptor (CAR) ligand binding domains from the human oestrogen receptor alpha (hERalpha) crystal structure, and the human peroxisome proliferator activated receptor alpha (PPARalpha) ligand binding domain from the human PPARgamma crystal structure. J Steroid Biochem Mol Biol 84, 117-132.

Jenkinson, D.H., Barnard, E.A., Hoyer, D., Humphrey, P.P.A., Leff P. and Shankley, N.P. (1995) International union of pharmacology committee on receptor nomenclature and drug classification (ix) recommendations on terms and symbols in quantitative pharmacology. ASPET 47, 255-266.

Jiang, T. (2004) Characterisation of recombinant aryl hydrocarbon receptor ligand binding domain. PhD thesis, School of Biology, University of Nottingham, Nottingham.

Jiang, T., Bell, D.R., Clode, S., Fan, M.Q., Fernandes, A., Foster, P.M., Loizou, G., MacNicoll, A., Miller, B.G., Rose, M., Tran, L. and White, S. (2009) A truncation in the aryl hydrocarbon receptor of the CRL:WI(Han) rat does not affect the developmental toxicity of TCDD. Toxicol Sci 107, 512-521.

Johnson, C.W., Williams, W.C., Copeland, C.B., DeVito, M.J. and Smialowicz, R.J. (2000) Sensitivity of the SRBC PFC assay versus ELISA for detection of immunosuppression by TCDD and TCDD-like congeners. Toxicology 156, 1-11.

Kalantzi, O.I., Martin, F.L., Thomas, G.O., Alcock, R.E., Tang, H.R., Drury, S.C., Carmichael, P.L., Nicholson, J.K. and Jones, K.C. (2004) Different levels of polybrominated diphenyl ethers (PBDEs) and chlorinated compounds in breast milk from two U.K. Regions. Environ Health Perspect 112, 1085-1091.

Kazlauskas, A., Poellinger, L. and Pongratz, I. (1999) Evidence that the co-chaperone p23 regulates ligand responsiveness of the dioxin (Aryl hydrocarbon) receptor. J Biol Chem 274, 13519-13524.

Kenakin, T.P. (1997) Pharmacologic Analysis of Drug-Receptor Interaction, Lippincott-Raven Publishers, USA.

Kennedy, J., Delaney, L., Hudson, E.M., McGloin, A. and Wall, P.G. Public perceptions of the dioxin incident in Irish pork. J Risk Res 13, 937-949.

Kennedy, S.W., Lorenzen, A., James, C.A. and Collins, B.T. (1993) Ethoxyresorufin-O-deethylase and porphyrin analysis in chicken embryo hepatocyte cultures with a fluorescence multiwell plate reader. Anal Biochem 211, 102-112.

Kim, S.H., Henry, E.C., Kim, D.K., Kim, Y.H., Shin, K.J., Han, M.S., Lee, T.G., Kang, J.K., Gasiewicz, T.A., Ryu, S.H. and Suh, P.G. (2006) Novel compound 2-methyl-2H-pyrazole-3-carboxylic acid (2-methyl-4-o-tolylazo-phenyl)-amide (CH223191) prevents 2,3,7,8-TCDD-induced toxicity by antagonizing the aryl hydrocarbon receptor. Mol Pharmacol 69, 1871-1878.

Koistinen, J., Sanderson, J.T., Giesy, J.P., Nevalainen, T. and Paasivirta, J. (1996) Ethoxyresorufin-O-deethylase induction potency of polychlorinated diphenyl ethers in H4IIE rat hepatoma cells. Environ Toxicol Chem 15, 2028-2034.

Krishnan, V. and Safe, S. (1993) Polychlorinated biphenyls (PCBs), dibenzo-p-dioxins (PCDDs), and dibenzofurans (PCDFs) as antiestrogens in MCF-7 human breast cancer cells: quantitative structure-activity relationships. Toxicol Appl Pharmacol 120, 55-61.

Kuratsune, M., Yoshimura, T., Matsuzaka, J. and Yamaguchi, A. (1972) Epidemiologic study on Yusho, a Poisoning Caused by Ingestion of Rice Oil Contaminated with a Commercial Brand of Polychlorinated Biphenyls. Environ Health Perspect 1, 119-128.

Lahvis, G.P. and Bradfield, C.A. (1998) Ahr null alleles: distinctive or different? Biochem Pharmacol 56, 781-787.

Laupeze, B., Amiot, L., Sparfel, L., Le Ferrec, E., Fauchet, R. and Fardel, O. (2002) Polycyclic aromatic hydrocarbons affect functional differentiation and maturation of human monocyte-derived dendritic cells. J Immunol 168, 2652-2658.

Lewis, D.F., Lake, B.G., George, S.G., Dickins, M., Eddershaw, P.J., Tarbit, M.H., Beresford, A.P., Goldfarb, P.S. and Guengerich, F.P. (1999) Molecular modelling of CYP1 family enzymes CYP1A1, CYP1A2, CYP1A6 and CYP1B1 based on sequence homology with CYP102. Toxicology 139, 53-79.

Li, W., Wu, W.Z., Schramm, K.W., Xu, Y. and Kettrup, A. (1999) Toxicity of mixtures of polychlorinated dibenzo-p-dioxins, dibenzofurans, and biphenyls determined by dose-response curve analysis. Bull Environ Contam Toxicol 62, 539-546.

Liehr, J.G. and Ricci, M.J. (1996) 4-Hydroxylation of estrogens as marker of human mammary tumors. Proc Natl Acad Sci USA 93, 3294-3296.

Lin, T.-M., Ko, K., Moore, R.W., Simanainen, U., Oberley, T.D. and Peterson, R.E. (2002) Effects of Aryl hydrocarbon receptor null mutation and in utero and lactational 2,3,7,8-tetrachlorodibenzo-*p*-dioxin exposure on prostate and seminal vesicle development in C57BL/6 Mice. Toxicol Sci 68, 479-487.

Lo Piparo, E., Koehler, K., Chana, A. and Benfenati, E. (2006) Virtual screening for aryl hydrocarbon receptor binding prediction. J Med Chem 49, 5702-5709.

Loaiza-Perez, A.I., Trapani, V., Hose, C., Singh, S.S., Trepel, J.B., Stevens, M.F.G., Bradshaw, T.D. and Sausville, E.A. (2002) Aryl hydrocarbon receptor mediates sensitivity of MCF-7 breast cancer cells to antitumor agent 2-(4-amino-3-methylphenyl) benzothiazole. Mol Pharmacol 61, 13-19.

Lorber, M. (2002) A pharmacokinetic model for estimating exposure of Americans to dioxin-like compounds in the past, present, and future. Sci Total Environ 288, 81-95.

Lu, Y.-F., Santostefano, M., Cunningham, B.D.M., Threadgill, M.D. and Safe, S. (1996) Substituted flavones as aryl hydrocarbon (Ah) receptor agonists and antagonists. Biochem Pharmacol 51, 1077-1087.

Ma, Q. and Whitlock, J.P., Jr. (1997) A novel cytoplasmic protein that interacts with the Ah receptor, contains tetratricopeptide repeat motifs, and augments the transcriptional response to 2,3,7,8-tetrachlorodibenzo-*p*-dioxin. J Biol Chem 272, 8878-8884.

Mackenzie, A.R. and Brooks, S. (1998) Chemical Safety - New Chloracnegens. Chem Eng News 76, 8.

Mann, P.C. (1997) Selected lesions of dioxin in laboratory rodents. Toxicol Pathol 25, 72-79.

Manz, A., Berger, J., Dwyer, J.H., Flesch-Janys, D., Nagel, S. and Waltsgott, H. (1991) Cancer mortality among workers in chemical plant contaminated with dioxin. Lancet 338, 959-964.

Martignoni, M., Groothuis, G.M. and de Kanter, R. (2006) Species differences between mouse, rat, dog, monkey and human CYP-mediated drug metabolism, inhibition and induction. Expert Opin Drug Metab Toxicol 2, 875-894.

Mason, G., Sawyer, T., Keys, B., Bandiera, S., Romkes, M., Piskorska-Pliszczynska, J., Zmudzka, B. and Safe, S. (1985) Polychlorinated dibenzofurans (PCDFs): correlation between *in vivo* and *in vitro* structure-activity relationships. Toxicology 37, 1-12.

Max, S.R. and Silbergeld, E.K. (1987) Skeletal muscle glucocorticoid receptor and glutamine synthetase activity in the wasting syndrome in rats treated with 2,3,7,8-tetrachlorodibenzo-*p*-dioxin. Toxicol Appl Pharmacol 87, 523-527.

NATO/CCMS (1988a) Pilot Study on International Information Exchange on Dioxins and Related Compounds: International Toxicity Equivalency Factor (I -TEF) Method of Risk Assessment for Complex Mixtures of Dioxins and Related Compounds. North Atlantic Treaty Organization, Committee on the Challenges of Modern Society, Report Number 176, August, 1988.

NATO/CCMS (1988b) Pilot Study on International Information Exchange on Dioxins and Related Compounds: Scientific Bases for the Development of the International Toxicity Equivalency Factor (I-TEF) Method of Risk Assessment for Complex Mixtures of Dioxins and Related Compounds. North Atlantic Treaty Organization, Committee on the Challenges of Modern Society, Report Number 178, December, 1988.

McFadyen, M.C., McLeod, H.L., Jackson, F.C., Melvin, W.T., Doehmer, J. and Murray, G.I. (2001) Cytochrome P450 CYP1B1 protein expression: a novel mechanism of anticancer drug resistance. Biochem Pharmacol 62, 207-212.

Medjakovic, S. and Jungbauer, A. (2008) Red clover isoflavones biochanin A and formononetin are potent ligands of the human aryl hydrocarbon receptor. The Journal of Steroid Biochemistry and Molecular Biology 108, 171-177.

Meyer, B.K., Pray-Grant, M.G., Vanden Heuvel, J.P. and Perdew, G.H. (1998) Hepatitis B virus X-associated protein 2 is a subunit of the unliganded aryl hydrocarbon receptor core complex and exhibits transcriptional enhancer activity. Mol Cell Biol 18, 978-988.

Miller, A.G., Israel, D. and Whitlock, J.P., Jr. (1983) Biochemical and genetic analysis of variant mouse hepatoma cells defective in the induction of benzo(a)pyrene-metabolizing enzyme activity. J Biol Chem 258, 3523-3527.

Murk, A.J., Legler, J., Denison, M.S., Giesy, J.P., van de Guchte, C. and Brouwer, A. (1996) Chemical-activated luciferase gene expression (CALUX): a novel *in vitro* bioassay for Ah receptor active compounds in sediments and pore water. Fundam Appl Toxicol 33, 149-160.

Murray, G.I., Melvin, W.T., Greenlee, W.F. and Burke, M.D. (2001) Regulation, function, and tissue-specific expression of cytochrome P450 CYP1B1. Annu Rev Pharmacol Toxicol 41, 297-316.

NTP (National Toxicology Program) TR-520 (2006) NTP technical report on the toxicology and carcinogenesis studies of 3,3',4,4',5-pentachlorobiphenyl (PCB 126) in female harlan sprague-dawley rat (gavage studies).

NTP (National Toxicology Program) TR-521 (2006) NTP technical report on the toxicology and carcinogenesis studies of 2,3,7,8-tetrachlorodibenzo-*p*-dioxin (TCDD) in female harlan sprague-dawley rat (gavage studies).

NTP (National Toxicology Program) TR-525 (2006) NTP technical report on the toxicology and carcinogenesis studies of 2,3,4,7,8-pentachlorodibenzofuran (PeCDF) in female harlan sprague-dawley rat (gavage studies).

NTP (National Toxicology Program) TR-526 (2006) NTP technical report on the toxicology and carcinogenesis studies of a mixture of 2,3,7,8-tetrachlorodibenzo-*p*-dioxin (TCDD), 2,3,4,7,8-pentachlorodibenzofuran (PeCDF) and 3,3',4,4',5-pentachlorobiphenyl (PCB 126) in female harlan sprague-dawley rat (gavage studies).

Nebert, D.W., Dalton, T.P., Okey, A.B. and Gonzalez, F.J. (2004) Role of aryl hydrocarbon receptor-mediated induction of the CYP1 enzymes in environmental toxicity and cancer. J Biol Chem 279, 23847-23850.

Nebert, D.W., Eisen, H.J., Negishi, M., Lang, M.A., Hjelmeland, L.M. and Okey, A.B. (1981) Genetic mechanisms controlling the induction of polysubstrate monooxygenase (P-450) activities. Annu Rev Pharmacol Toxicol 21, 431-462.

Nebert, D.W. and Gelboin, H.V. (1969) The *in vivo* and *in vitro* induction of aryl hydrocarbon hydroxylase in mammalian cells of different species, tissues, strains, and developmental and hormonal states. Arch Biochem Biophys 134, 76-89.

Nebert, D.W. and Gonzalez, F.J. (1987) P450 genes: structure, evolution, and regulation. Annu Rev Biochem 56, 945-993.

Nebert, D.W., Roe, A.L., Dieter, M.Z., Solis, W.A., Yang, Y. and Dalton, T.P. (2000) Role of the aromatic hydrocarbon receptor and [Ah] gene battery in the oxidative stress response, cell cycle control, and apoptosis. Biochem Pharmacol 59, 65-85.

Nelson, D.R., Koymans, L., Kamataki, T., Stegeman, J.J., Feyereisen, R., Waxman, D.J., Waterman, M.R., Gotoh, O., Coon, M.J., Estabrook, R.W., Gunsalus, I.C. and Nebert, D.W. (1996) P450 superfamily: update on new sequences, gene mapping, accession numbers and nomenclature. Pharmacogenetics 6, 1-42.

Ohta, S., Okumura, T., Nishimura, H., Nakao, T., Shimizu, Y., Ochiai, F., Aozasa, O. and Miyata, H. (2004.) Levels of PBDEs, TBBPA, TBPs, PCDD/Fs PxDD/Fs and PBDD/Fs in human milk of nursing women and dairy milk products in Japan. Organohalog Comp 66, 2891.

Okey, A.B., Riddick, D.S. and Harper, P.A. (1994) Molecular biology of the aromatic hydrocarbon (dioxin) receptor. Trends Pharmacol Sci 15, 226-232.

Olsman, H., Engwall, M., Kammann, U., Klempt, M., Otte, J., Bavel, B. and Hollert, H. (2007) Relative differences in aryl hydrocarbon receptor-mediated response for 18 polybrominated and mixed halogenated dibenzo-*p*-dioxins and -furans in cell lines from four different species. Environ Toxicol Chem 26, 2448-2454.

Olson, J.R., McGarrigle, B.P., Gigliotti, P.J., Kumar, S. and McReynolds, J.H. (1994) Hepatic uptake and metabolism of 2,3,7,8-tetrachlorodibenzo-*p*-dioxin and 2,3,7,8-tetrachlorodibenzofuran. Fundam Appl Toxicol 22, 631-640.

Pandini, A., Denison, M.S., Song, Y., Soshilov, A.A. and Bonati, L. (2007) Structural and functional characterization of the aryl hydrocarbon receptor ligand binding domain by homology modeling and mutational analysis. Biochem 46, 696-708.

Pang, S., Cao, J.Q., Katz, B.H., Hayes, C.L., Sutter, T.R. and Spink, D.C. (1999) Inductive and inhibitory effects of non-*ortho*-substituted polychlorinated biphenyls on estrogen metabolism and human cytochromes P450 1A1 and 1B1. Biochem Pharmacol 58, 29-38.

Papke, O. (1998) PCDD/PCDF: human background data for Germany, a 10-year experience. Environ Health Perspect 106 Suppl 2, 723-731.

Perdew, G.H. (1988) Association of the Ah receptor with the 90-kDa heat shock protein. J Biol Chem 263, 13802-13805.

Peters, A.K., van Londen, K., Bergman, Ã., Bohonowych, J., Denison, M.S., van den Berg, M. and Sanderson, J.T. (2004) Effects of Polybrominated Diphenyl Ethers on Basal and TCDD-Induced Ethoxyresorufin Activity and Cytochrome P450-1A1 Expression in MCF-7, HepG2, and H4IIE Cells. Toxicol Sci 82, 488-496.

Petkov, P.I., Rowlands, J.C., Budinsky, R., Zhao, B., Denison, M.S. and Mekenyan, O. (2010) Mechanism-based common reactivity pattern (COREPA) modelling of aryl hydrocarbon receptor binding affinity. SAR QSAR Environ Res 21, 187-214.

Petrulis, J.R. and Perdew, G.H. (2002) The role of chaperone proteins in the aryl hydrocarbon receptor core complex. Chem Biol Interact 141, 25-40.

Petrulis, J.R. and Bunce, N.J. (1999) Competitive inhibition by inducer as a confounding factor in the use of the ethoxyresorufin-O-deethylase (EROD) assay to estimate exposure to dioxin-like compounds. Toxicol Lett 105, 251-260.

Phelan, D., Winter, G.M., Rogers, W.J., Lam, J.C. and Denison, M.S. (1998) Activation of the Ah receptor signal transduction pathway by bilirubin and biliverdin. Arch Biochem Biophys 357, 155-163.

Pirkle, J.L., Wolfe, W.H., Patterson, D.G., Needham, L.L., Michalek, J.E., Miner, J.C., Peterson, M.R. and Phillips, D.L. (1989) Estimates of the half-life of 2,3,7,8-tetrachlorodibenzo-*p*-dioxin in Vietnam Veterans of Operation Ranch Hand. J Toxicol Environ Health 27, 165-171.

Pluess, N., Poiger, H., Hohbach, C. and Schlatter, C. (1988) Subchronic toxicity of some chlorinated dibenzofurans (PCDFs) and a mixture of PCDFs and chlorinated dibenzodioxins (PCDDs) in rats. Chemosphere 17, 973-984.

Pohjanvirta, R. and Tuomisto, J. (1994) Short-term toxicity of 2,3,7,8-tetrachlorodibenzo-*p*-dioxin in laboratory animals: effects, mechanisms, and animal models. Pharmacol Rev 46, 483-549.

Pohjanvirta, R., Unkila, M., Linden, J., Tuomisto, J.T. and Tuomisto, J. (1995) Toxic equivalency factors do not predict the acute toxicities of dioxins in rats. Eur J Pharmacol 293, 341-353.

Poiger, H. and Schlatter, C. (1986) Pharmaco kinetics of 2,3,7,8-TCDD in man. Chemosphere 15, 1489-1494.

Poland, A. and Glover, E. (1973) 2,3,7,8-Tetrachlorodibenzo-*p*-dioxin: a potent inducer of -aminolevulinic acid synthetase. Science 179, 476-477.

Poland, A., Glover, E. and Kende, A.S. (1976) Stereospecific, high affinity binding of 2,3,7,8-tetrachlorodibenzo-*p*-dioxin by hepatic cytosol. Evidence that the binding species is receptor for induction of aryl hydrocarbon hydroxylase. J Biol Chem 251, 4936-4946.

Poland, A. and Glover, E. (1977) Chlorinated biphenyl induction of aryl hydrocarbon hydroxylase activity: a study of the structure-activity relationship. Mol Pharmacol 13, 924-938.

Poland, A. and Knutson, J.C. (1982) 2,3,7,8-Tetrachlorodibenzo-*p*-dioxin and related halogenated aromatic hydrocarbons: Examination of the mechanism of toxicity. Ann. Rev. Pharmacol. Toxicol. 22, 517-554.

Polder, A., Gabrielsen, G.W., Odland, J.O., Savinova, T.N., Tkachev, A., Loken, K.B. and Skaare, J.U. (2008a) Spatial and temporal changes of chlorinated pesticides, PCBs, dioxins (PCDDs/PCDFs) and brominated flame retardants in human breast milk from Northern Russia. Sci Total Environ 391, 41-54.

Polder, A., Thomsen, C., Lindstrom, G., Loken, K.B. and Skaare, J.U. (2008b) Levels and temporal trends of chlorinated pesticides, polychlorinated biphenyls and brominated flame retardants in individual human breast milk samples from Northern and Southern Norway. Chemosphere 73, 14-23.

Procopio, M., Lahm, A., Tramontano, A., Bonati, L. and Pitea, D. (2002) A model for recognition of polychlorinated dibenzo-*p*-dioxins by the aryl hydrocarbon receptor. Eur J Biochem 269, 13-18.

Quezada, E., Delogu, G., Picciau, C., Santana, L., Podda, G., Borges, F., Garcia-Morales, V., Vina, D. and Orallo, F. (2010) Synthesis and vasorelaxant and platelet antiaggregatory activities of a new series of 6-halo-3-phenylcoumarins. Molecules 15, 270-279.

Ramadoss, P. and Perdew, G.H. (2004) Use of 2-azido-3-[125I]iodo-7,8-dibromodibenzo-*p*-dioxin as a probe to determine the relative ligand affinity of human versus mouse aryl hydrocarbon receptor in cultured cells. Mol Pharmacol 66, 129-136.

Riddick, D.S., Y. Huang, P.A. Harper and A.B. Okey. (1994) 2,3,7,8-Tetrachlorodibenzo-*p*-dioxin versus 3-methylcholanthrene: comparative studies of Ah receptor binding, transformation, and induction of CYP1A1. J Bio Chem 269, 12118-12128.

Safe, S.H. (1986) Comparative toxicology and mechanism of action of polychlorinated dibenzo-*p*-dioxins and dibenzofurans. Annu Rev Pharmacol Toxicol 26, 371-399.

Safe, S.H. (1990) Polychlorinated biphenyls (PCBs), dibenzo-*p*-dioxins (PCDDs), dibenzofurans (PCDFs), and related compounds: environmental and mechanistic considerations which support the development of toxic equivalency factors (TEFs). Crit Rev Toxicol 21, 51-88.

Safe, S.H. (1994) Polychlorinated biphenyls (PCBs): environmental impact, biochemical and toxic responses, and implications for risk assessment. Crit Rev Toxicol 24, 87-149.

Samara, F., Gullett, B.K., Harrison, R.O., Chu, A. and Clark, G.C. (2009) Determination of relative assay response factors for toxic chlorinated and brominated dioxins/furans using an enzyme immunoassay (EIA) and a chemically-activated luciferase gene expression cell bioassay (CALUX). Environ Int 35, 588-593.

Sambrook, J., Fritsch, E. F. and Maniatis, T. (1989) *Molecular Cloning: A Laboratory Manual*, Cold Spring Press, Cold Spring Harbor, NY.

Sanderson, J.T., Aarts, J.M.M.J.G., Brouwer, A., Froese, K.L., Denison, M.S. and Giesy, J.P. (1996) Comparison of Ah Receptor-Mediated Luciferase and Ethoxyresorufin-O-deethylase Induction in H4IIE Cells: Implications for Their Use as Bioanalytical Tools for the Detection of Polyhalogenated Aromatic Hydrocarbons. Toxicol Appl Pharmacol 137, 316-325.

Santostefano, M., Merchant, M., Arellano, L., Morrison, V., Denison, M.S. and Safe, S. (1993) Alpha-Naphthoflavone-induced CYP1A1 gene expression and cytosolic aryl hydrocarbon receptor transformation. Mol Pharmacol 43, 200-206.

Santostefano, M.J., Ross, D.G., Savas, U., Jefcoate, C.R. and Birnbaum, L.S. (1997) Differential time-course and dose-response relationships of TCDD-induced CYP1B1, CYP1A1, and CYP1A2 proteins in rats. Biochem Biophys Res Commun 233, 20-24.

Sawyer, T. and Safe, S. (1982) PCB isomers and congeners: induction of aryl hydrocarbon hydroxylase and ethoxyresorufin O-deethylase enzyme activities in rat hepatoma cells. Toxicol Lett 13, 87-93.

Sawyer, T.W., Vatcher, A.D. and Safe, S. (1984) Comparative aryl hydrocarbon hydroxylase induction activities of commercial PCBs in Wistar rats and rat hepatoma H-4-II E cells in culture. Chemosphere 13, 695-701.

Scerri, L., Zaki, I. and Millard, L.G. (1995) Severe halogen acne due to a trifluoromethylpyrazole derivative and its resistance to isotretinoin. Brit J Dermatol 132, 144-148.

Schecter, A. (1994) Dioxins and health, Plenum Publishing Co., N.Y.

Schmidt, J.V., Su, G.H., Reddy, J.K., Simon, M.C. and Bradfield, C.A. (1996) Characterization of a murine Ahr null allele: involvement of the Ah receptor in hepatic growth and development. Proc Natl Acad Sci 93, 6731-6736.

Schmitz, H.J., Hagenmaier, A., Hagenmaier, H.P., Bock, K.W. and Schrenk, D. (1995) Potency of mixtures of polychlorinated biphenyls as inducers of dioxin receptor-regulated CYP1A activity in rat hepatocytes and H4IIE cells. Toxicology 99, 47-54.

Schulz, K.H. (1968) Clinical picture and etiology of chloracne. Arbeitsmed Socialmed Arbeitshyg 8, 25-29.

Schweikl, H., Taylor, J.A., Kitareewan, S., Linko, P., Nagorney, D. and Goldstein, J.A. (1993) Expression of CYP1A1 and CYP1A2 genes in human liver. Pharmacogenetics 3, 239-249.

Shen, H., Han, J., Tie, X., Xu, W., Ren, Y. and Ye, C. (2009) Polychlorinated dibenzo-*p*-dioxins/furans and polychlorinated biphenyls in human adipose tissue from Zhejiang Province, China. Chemosphere 74, 384-388.

Shetty, P.V., Bhagwat, B.Y. and Chan, W.K. (2003) p23 enhances the formation of the aryl hydrocarbon receptor-DNA complex. Biochem Pharmacol 65, 941-948.

Shinkyo, R., Sakaki, T., Ohta, M. and Inouye, K. (2003) Metabolic pathways of dioxin by CYP1A1: species difference between rat and human CYP1A subfamily in the metabolism of dioxins. Arch Biochem Biophys 409, 180-187.

Silkworth, J.B., Koganti, A., Illouz, K., Possolo, A., Zhao, M. and Hamilton, S.B. (2005) Comparison of TCDD and PCB CYP1A induction sensitivities in fresh hepatocytes from human donors, sprague-dawley rats, and rhesus monkeys and HepG2 cells. Toxicol Sci 87, 508-519.

Southworth, D.R. and Agard, D.A. (2008) Species-dependent ensembles of conserved conformational states define the Hsp90 chaperone ATPase cycle. Mol Cell 32, 631-640.

Stohs, S.J. and Hassoun, E.A. (2011) Dioxin-Activated AhR: Toxic responses and the induction of oxidative stress. In: Pohjanvirta, R. (Ed), The Ah receptor in biology and toxicology, John Wiley & Sons, Inc., pp. 229-244.

Suh, J., Kang, J.S., Yang, K.H. and Kaminski, N.E. (2003) Antagonism of aryl hydrocarbon receptor-dependent induction of CYP1A1 and inhibition of IgM expression by di-*ortho*-substituted polychlorinated biphenyls. Toxicol Appl Pharmacol 187, 11-21.

Sutter, T.R., Tang, Y.M., Hayes, C.L., Wo, Y.Y., Jabs, E.W., Li, X., Yin, H., Cody, C.W. and Greenlee, W.F. (1994) Complete cDNA sequence of a human dioxin-inducible mRNA identifies a new gene subfamily of cytochrome P450 that maps to chromosome 2. J Biol Chem 269, 13092-13099.

Takagi, A, Hirose, A., Hirubayushi, Y., Kaneko, T., Ema, M. and Kanno, J. (2003) Assessment of the cleft palate induction by seven PCDD/F congeners in the mouse fetus Organohalogen compd 64, 336-338

Tarutani, M., Itami, S., Okabe, M., Ikawa, M., Tezuka, T., Yoshikawa, K., Kinoshita, T. and Takeda, J. (1997) Tissue-specific knockout of the mouse Pig-a gene reveals important roles for GPI-anchored proteins in skin development. Proc Natl Acad Sci USA 94, 7400-7405.

Taylor, B.L. and Zhulin, I.B. (1999) PAS Domains: Internal sensors of oxygen, Redox potential, and light. Microbiol Molecul Bio Rev 63, 479-506.

Theelen, R.M.C., Liem, A.K.D., Slob, W. and Van Wijnen, J.H. (1993) Intake of 2,3,7,8 chlorine substituted dioxins, furans, and planar PCBs from food in the Netherlands: Median and distribution. Chemosphere 27, 1625-1635.

Tillitt, D.E., Ankley, G.T., Verbrugge, D.A., Giesy, J.P., Ludwig, J.P. and Kubiak, T.J. (1991) H4IIE rat hepatoma cell bioassay-derived 2,3,7,8-tetrachlorodibenzo-*p*-dioxin equivalents in colonial fish-eating waterbird eggs from the Great Lakes. Arch Environ Contam Toxicol 21, 91-101.

Tindall, J.P. (1985) Chloracne and chloracnegens. J Am Acad Dermatol 13, 539-558.

Toyoshiba, H., Walker, N.J., Bailer, A.J. and Portier, C.J. (2004) Evaluation of toxic equivalency factors for induction of cytochromes P450 CYP1A1 and CYP1A2 enzyme activity by dioxin-like compounds. Toxicol Appl Pharmacol 194, 156-168.

Uren, A.G., Wong, L., Pakusch, M., Fowler, K.J., Burrows, F.J., Vaux, D.L. and Choo, K.H. (2000) Survivin and the inner centromere protein INCENP show similar cell-cycle localization and gene knockout phenotype. Curr Biol 10, 1319-1328.

Van Birgelen, A.P., Van der Kolk, J., Fase, K.M., Bol, I., Poiger, H., Brouwer, A. and Van den Berg, M. (1994) Toxic potency of 3,3',4,4',5-pentachlorobiphenyl relative to and in combination with 2,3,7,8-tetrachlorodibenzo-*p*-dioxin in a subchronic feeding study in the rat. Toxicol Appl Pharmacol 127, 209-221.

Van den Berg, M., Birnbaum, L., Bosveld, A.T., Brunstrom, B., Cook, P., Feeley, M., Giesy, J.P., Hanberg, A., Hasegawa, R., Kennedy, S.W., Kubiak, T., Larsen, J.C., van Leeuwen, F.X., Liem, A.K., Nolt, C., Peterson, R.E., Poellinger, L., Safe, S., Schrenk, D., Tillitt, D., Tysklind, M., Younes, M., Waern, F. and Zacharewski, T. (1998) Toxic equivalency factors (TEFs) for PCBs, PCDDs, PCDFs for humans and wildlife. Environ Health Perspect 106, 775-792.

Van den Berg, M., Birnbaum, L.S., Denison, M., DeVito, M., Farland, W., Feeley, M., Fiedler, H., Hakansson, H., Hanberg, A., Haws, L., Rose, M., Safe, S., Schrenk, D., Tohyama, C., Tritscher, A., Tuomisto, J., Tysklind, M., Walker, N. and Peterson, R.E. (2006) The 2005 World Health Organization reevaluation of human and Mammalian toxic equivalency factors for dioxins and dioxin-like compounds. Toxicol Sci 93, 223-241.

Van der Heiden, E., Bechoux, N., Sergent, T., Schneider, Y.J., Muller, M., Maghuin-Rogister, G. and Scippo, M.L. (2007) Aryl hydrocarbon receptor-mediated agonist/antagonist/synergic activities of food polyphenols are species- and tissue-dependent. Organohalogen Compd. 69, 365-368.

Van Duursen, M.B., Sanderson, J.T., van der Bruggen, M., van der Linden, J. and van den Berg, M. (2003) Effects of several dioxin-like compounds on estrogen metabolism in the malignant MCF-7 and nontumorigenic MCF-10A human mammary epithelial cell lines. Toxicol Appl Pharmacol 190, 241-250.

Van Larebeke, N., Hens, L., Schepens, P., Covaci, A., Baeyens, J., Everaert, K., Bernheim, J.L., Vlietinck, R. and De Poorter, G. (2001) The Belgian PCB and dioxin incident of January-June 1999: exposure data and potential impact on health. Environ Health Perspect 109, 265-273.

Vanden Heuvel, J.P., Clark, G.C., Kohn, M.C., Tritscher, A.M., Greenlee, W.F., Lucier, G.W. and Bell, D.A. (1994) Dioxin-responsive genes: examination of dose-response relationships using quantitative reverse transcriptase-polymerase chain reaction. Cancer Res 54, 62-68.

Vanden Heuvel, J.P. and Lucier, G. (1993) Environmental toxicology of polychlorinated dibenzo-*p*-dioxins and polychlorinated dibenzofurans. Environ Health Perspect 100, 189-200.

Vandesompele, J., De Preter, K., Pattyn, F., Poppe, B., Van Roy, N., De Paepe, A. and Speleman, F. (2002) Accurate normalization of real-time quantitative RT-PCR data by geometric averaging of multiple internal control genes. Genome Biol 3(7): 1-12.

Vasquez, A., Atallah-Yunes, N., Smith, F.C., You, X., Chase, S.E., Silverstone, A.E. and Vikstrom, K.L. (2003) A role for the aryl hydrocarbon receptor in cardiac physiology and function as demonstrated by AhR knockout mice. Cardiovasc Toxicol 3, 153-163.

Veldhoen, M., Hirota, K., Christensen, J., O'Garra, A. and Stockinger, B. (2009) Natural agonists for aryl hydrocarbon receptor in culture medium are essential for optimal differentiation of Th17 T cells. J Exp Med 206, 43-49.

Villeneuve, D., DeVita, W.M. and Crunkilton, R.L. (1998) Identification of cytochrome P4501A inducers in complex mixtures of polycyclic aromatic hydrocarbons. In: Little, E.E., Greenberg, B.M. and DeLonay, A.J. (Ed), Environmental Toxicology and Risk Assessment. ASTM International.

Vos, J.G., Moore, J.A. and Zinkl, J.G. (1974) Toxicity of 2,3,7,8-tetrachlorodibenzo-*p*-dioxin (TCDD) in C57B1/6 mice. Toxicol Appl Pharmacol 29, 229-241.

Wærn, F., Flodström, S., Busk, L., Kronevi, T., Nordgren, I. and Ahlborg, U.G. (1991) Relative Liver Tumour Promoting Activity and Toxicity of some Polychlorinated Dibenzo-*p*-dioxin- and Dibenzofuran-Congeners in Female Sprague-Dawley Rats. Pharmacol Toxicol 69, 450-458.

Wahl, M., Lahni, B., Guenther, R., Kuch, B., Yang, L., Straehle, U., Strack, S. and Weiss, C. (2008) A technical mixture of 2,2',4,4'-tetrabromo diphenyl ether (BDE47) and brominated furans triggers aryl hydrocarbon receptor (AhR) mediated gene expression and toxicity. Chemosphere 73, 209-215.

Walker, M.K., Cook, P.M., Butterworth, B.C., Zabel, E.W. and Peterson, R.E. (1996) Potency of a complex mixture of polychlorinated dibenzo-*p*-dioxin, dibenzofuran, and biphenyl congeners compared to 2,3,7,8-tetrachlorodibenzo-*p*-dioxin in causing fish early life stage mortality. Fundam Appl Toxicol 30, 178-186.

Walker, N.J., Crockett, P.W., Nyska, A., Brix, A.E., Jokinen, M.P., Sells, D.M., Hailey, J.R., Easterling, M., Haseman, J.K., Yin, M., Wyde, M.E., Bucher, J.R. and Portier, C.J. (2005) Dose-Additive Carcinogenicity of a Defined Mixture of "Dioxin-like Compounds". Environ health perspect 113(1) 43-48.

Walker, N.J., Crofts, F.G., Li, Y., Lax, S.F., Hayes, C.L., Strickland, P.T., Lucier, G.W. and Sutter, T.R. (1998) Induction and localization of cytochrome P450 1B1 (CYP1B1) protein in the livers of TCDD-treated rats: detection using polyclonal antibodies raised to histidine-tagged fusion proteins produced and purified from bacteria. Carcinogenesis 19, 395-402.

Walker, N.J., Portier, C.J., Lax, S.F., Crofts, F.G., Li, Y., Lucier, G.W. and Sutter, T.R. (1999) Characterization of the dose-response of CYP1B1, CYP1A1, and CYP1A2 in the liver of female Sprague-Dawley rats following chronic exposure to 2,3,7,8-tetrachlorodibenzo-*p*-dioxin. Toxicol Appl Pharmacol 154, 279-286.

Wall, R.J. (2008) Testing for partial agonism of the aryl hydrocarbon receptor. MRes thesis, School of Biology, University of Nottingham, Nottingham.

Wall, R.J., Fernandes, A., Rose, M., Rowlands, J.C., Bell, D.R. and Mellor, I.R. (2012a) Fused mesoionic heterocyclic compounds are a new class of Aryl hydrocarbon receptor agonist of exceptional potency, Toxicology, Submitted.

Wall, R.J., He, G., Denison, M.S., Congiu, C., Onnis, V., Fernandes, A., Bell, D.R., Rose, M., Rowlands, J.C., Balboni, G. and Mellor, I.R. (2012b) Novel 2-amino-isoflavones exhibit aryl hydrocarbon receptor agonist or antagonist activity in a species/cell-specific context. Toxicology 297, 26-33.

Waller, C.L. and McKinney, J.D. (1995) Three-dimensional quantitative structure-activity relationships of dioxins and dioxin-like compounds: model validation and Ah receptor characterization. Chem Res Toxicol 8, 847-858.

Weber, H., Lamb, J.C., Harris, M.W. and Moore, J.A. (1984) Teratogenicity of 2,3,7,8-tetrachlorodibenzofuran (TCDF) in mice. Toxicol Lett 20, 183-188.

Weiss, M.C. and Green, H. (1967) Human-mouse hybrid cell lines containing partial complements of human chromosomes and functioning human genes. Proc Natl Acad Sci USA 58, 1104-1111.

Whitlock, J.P., Jr. (1999) Induction of cytochrome P4501A1. Annu Rev Pharmacol Toxicol 39, 103-125.

Whyte, J.J., Schmitt, C.J. and Tillitt, D.E. (2004) The H4IIE cell bioassay as an indicator of dioxin-like chemicals in wildlife and the environment. Crit Rev Toxicol 34, 1-83.

Wiebel, F.J., Wegenke, M. and Kiefer, F. (1996) Bioassay for determining 2,3,7,8-tetrachlorodibenzo-p-dioxin equivalents (TEs) in human hepatoma Hepg2 cells. Toxicol Lett 88, 335-338.

Wu, Q., Ohsako, S., Baba, T., Miyamoto, K. and Tohyama, C. (2002) Effects of 2,3,7,8-tetrachlorodibenzo-p-dioxin (TCDD) on preimplantation mouse embryos. Toxicology 174, 119-129.

Xu, L., Li, A.P., Kaminski, D.L. and Ruh, M.F. (2000) 2,3,7,8 Tetrachlorodibenzo-p-dioxin induction of cytochrome P4501A in cultured rat and human hepatocytes. Chem Biol Interact 124, 173-189.

Yamamoto, J., Ihara, K., Nakayama, H., Hikino, S., Satoh, K., Kubo, N., Iida, T., Fujii, Y. and Hara, T. (2004) Characteristic expression of aryl hydrocarbon receptor repressor gene in human tissues: organ-specific distribution and variable induction patterns in mononuclear cells. Life Sci 74, 1039-1049.

Yoshimura, T. (2003) Yusho in Japan. Ind Health 41, 139-148.

Zeiger, M., Haag, R., Hockel, J., Schrenk, D. and Schmitz, H.J. (2001) Inducing effects of dioxin-like polychlorinated biphenyls on CYP1A in the human hepatoblastoma cell line HepG2, the rat hepatoma cell line H4IIE, and rat primary hepatocytes: comparison of relative potencies. Toxicol Sci 63, 65-73.

Zhang, S., Qin, C. and Safe, S.H. (2003) Flavonoids as aryl hydrocarbon receptor agonists/antagonists: effects of structure and cell context. Environ Health Perspect 111, 1877-1882.

Zhao, B., Baston, D.S., Khan, E., Sorrentino, C. and Denison, M.S. (2010) Enhancing the response of CALUX and CAFLUX cell bioassays for quantitative detection of dioxin-like compounds. Sci China Chem 53, 1010-1016.

Zhao, B., Degroot, D.E., Hayashi, A., He, G. and Denison, M.S. (2010) CH223191 is a ligand-selective antagonist of the Ah (Dioxin) receptor. Toxicol Sci 117, 393-403.